1-26-2011 12:00 AM

Development of an Active Elbow Motion Simulator and Coordinate Systems to Evaluate Kinematics in Multiple Positions

Louis M. Ferreira, *The University of Western Ontario*

Supervisor: Dr. James Johnson, *The University of Western Ontario*

A thesis submitted in partial fulfillment of the requirements for the Doctor of Philosophy degree in Biomedical Engineering

DEVELOPMENT OF AN ACTIVE ELBOW MOTION SIMULATOR AND COORDINATE SYSTEMS TO EVALUATE KINEMATICS IN MULTIPLE POSITIONS

(Spine Title: DEVELOPMENT OF A MULTI-POSITION ELBOW MOTION SIMULATOR)

(Thesis format: Integrated Article)

by

Louis Miguel Ferreira

Graduate Program
in
Biomedical Engineering

A thesis submitted in partial fulfillment
of the requirements for the degree of
Doctor of Philosophy

School of Graduate and Postdoctoral Studies
The University of Western Ontario
London, Ontario, Canada

THE UNIVERSITY OF WESTERN ONTARIO
SCHOOL OF GRADUATE AND POSTDOCTORAL STUDIES

CERTIFICATE OF EXAMINATION

Supervisor	Examiners
_____ Dr. James Johnson	_____ Dr. Timothy Bryant
	_____ Dr. Thomas Jenkyn
Co-Supervisor	_____ Dr. Rajni Patel
_____ Dr. Graham King	_____ Dr. Anand Singh

The thesis by

Louis Miguel Ferreira

entitled:

Development of an Active Elbow Motion Simulator and Coordinate Systems to Evaluate Kinematics in Multiple Positions

is accepted in partial fulfillment
of the requirements for the degree of
Doctor of Philosophy

Date_____ _____
Chair of the Thesis Examination Board

ABSTRACT

Elbow disorders are common as a consequence of both traumatic and degenerative conditions. Relative to disorders of the lower limb, there is comparatively little evidence to direct the treatment of many elbow disorders. Biomechanical studies are required to develop and validate the optimal treatment of elbow disorders prior to their application in patients. Clinically relevant simulation of elbow motion in the laboratory can be a powerful tool to advance our knowledge of elbow disorders.

This work was undertaken with the rationale that simulation and quantification of elbow motion could be improved significantly. This treatise includes the development and evaluation of an *in-vitro* elbow motion simulator which, with the humerus horizontally positioned, is the first to achieve active flexion and extension in a vertical plane. Additionally, it is capable of operating in the vertical, varus and valgus positions, and while maintaining full forearm pronation or supination.

The simulator controller employs a Cascade PID configuration with feedforward transfer functions, which achieves unified control of flexion angle and muscle tension for multiple muscles. Feedback of the elbow joint angle and muscle tension is utilized to achieve closed-loop control. A performance evaluation in a full series of specimens clearly demonstrated that the actual joint angle is not more than 5˚ removed from the desired setpoint during flexion or extension in any position.

Also, a new method for creating upper extremity bone segment coordinate systems which are derived from elbow flexion and forearm rotation was developed and tested. This produced joint kinematics with significantly less inter-subject variability than traditional anatomy-derived coordinate systems. This minimally-invasive method also provides increased statistical power for laboratory based studies and may prove useful for clinical applications.

The new simulation techniques developed herein were applied to an *in-vitro* investigation of olecranon fracture repair with clinical significance. This study revealed valuable insights into a common repair procedure. This was made possible by the previously unattainable measurements that these new techniques now provide.

These developments will assist surgeons and other investigators in the design and

evaluation of treatments for elbow disorders, and contribute to the betterment of patient care.

KEYWORDS:

Elbow motion, active simulation, biomechanics, kinematics, coordinate systems.

CO-AUTHORSHIP STATEMENTS

Chapter 1: Louis Ferreira – sole author

Chapter 2: Louis Ferreira – developed controller, study design, supervised data collection, statistical analysis, wrote manuscript
James Johnson – study design, reviewed manuscript
Graham King – study design, reviewed manuscript

Chapter 3: Louis Ferreira – developed controller, study design, supervised data collection, statistical analysis, wrote manuscript
Bashar Alolabi – specimen preparation, data collection
Alia Grey – data collection
Graham King – reviewed manuscript
James Johnson – study design, reviewed manuscript

Chapter 4: Louis Ferreira – developed coordinate system method, study design, data collection, statistical analysis, wrote manuscript
J Pollock – specimen preparation
James Brownhill – data collection
Graham King – reviewed manuscript
James Johnson – reviewed manuscript

Chapter 5: Louis Ferreira – study design, supervised data collection, statistical analysis, wrote manuscript
Timothy Bell – study analysis, performed surgeries, supervised data collection
James Johnson – study design, reviewed manuscript
Graham King – study design, reviewed manuscript

Chapter 6: Louis Ferreira – sole author

ACKNOWLEDGEMENTS

First and foremost, I am pleased to thank my supervisors, Dr. James Johnson and Dr. Graham King, for their extensive contributions to my work and training. Much more than their professional advice and insight, I am deeply appreciative of their steady character, which instilled a sense of stability throughout this long endeavour. Their support and encouragement kept me focused, and their guidance kept me on track.

To the HULC students whom I've known over the years. I thank all of them for their friendship and for the positive environment that they created. Always social communal lunches were sometimes the only pleasant break in an otherwise bleak day of data analysis. They also served as my travel companions on conference trips, which I always looked forward to, and were made much more memorable by their presence.

Thanks to the surgical residents and clinicians at St. Joseph's, for lending their expertise in preparing specimens for simulation, and performing the surgeries for the investigations that comprise much of this work. Specifically, Dr. Bashar Alolabi, Dr. Timothy Bell, Dr. J Pollock, and Dr. Marlis Sabo. Your eagerness to help and your tireless and professional attitudes were inspirational.

I owe a debt of gratitude to Dr. Yves Bureau who patiently and attentively advised me on my statistical analyses. His instruction inspired in me a genuine interest in what continues to be my least favourite subject – a true love/hate relationship.

I would also like to thank The University of Western Ontario for providing me with the funding for tuition through its Educational Assistance Plan, which encourages its employees to continue their professional growth through continued education.

Aos meus pais: Agradeço-vos por seu amor e incentivo, e por seu apoio quando eu lutava como um estudante. E também por sua ajuda incansável durante todos os meus empreendimentos.

To Cheryl: The six years that this work has taken me, has often taken from our time together. It's seen us go from close companions to a married couple. In that time, your support for me never wavered. I'm glad to have this thesis behind me, and I'm excited about our future together. I only hope that you'll understand when it turns out that I'm not ready to start taking care of myself any time soon☺

CONTENTS

LIST OF CHARTS

LIST OF FIGURES

ABBREVIATIONS, SYMBOLS AND NOMENCLATURE

AC/DC ..... alternating electrical current / direct electrical current

aSDA ..... average screw displacement axis

c_x ..... "x" component of position vector

c_y ..... "y" component of position vector

c_z ..... "z" component of position vector

DOF ..... degrees-of-freedom

dp ..... differential change in muscle/tendon position p

dθ ..... differential change in joint angle θ

HULC ..... Hand and Upper Limb Centre

Hz ..... Herts (unit of frequency)

IE ..... magnitude of internal-external joint rotation

MOSE ..... Multiple Orientation Simulator for the Elbow

P ..... position vector

p ..... muscle/tendon position

PID ..... proportional integral derivative

PPC ..... proportional pressure controller

psi ..... pounds per square inch (unit of pressure)

R ..... rotation matrix

r_{01} ..... component of rotation matrix from 0^{th} row and 1^{st} column

SD ..... standard deviation

SDA ..... screw displacement axis

T ..... transformation matrix

${}^{ref}_{body}T$ ..... transformation of body wrt ref (reference)

t ..... time

t_{trans} ..... transition time

VV ..... magnitude of varus-valgus angulation or joint laxity

wrt ..... with respect to, meaning relative to a reference frame

X ..... magnitude of translation along the "x" coordinate direction

Y ..... magnitude of translation along the “y” coordinate direction

Z ..... magnitude of translation along the “z” coordinate direction

θ ..... angle of rotation

ΔPosition ..... change in position

ΔTension ..... change in tension

^ ..... over a vector label denotes a unit vector

º ..... degrees (unit of rotation)

± ..... plus or minus; prefixes magnitude of one standard deviation

Δ ..... (delta) indicating change

→ ..... between items; denotes sequence of execution in direction of arrow

CHAPTER 1 – INTRODUCTION

OVERVIEW: *This chapter begins with a synopsis of elbow joint anatomy and biomechanics, followed by an overview and comparative discussion of two common joint motion simulation techniques: in-vitro vs. in-silico. Previously developed in-vitro simulators presented in the literature are described. Issues concerning the preparation and integrity of cadaveric tissues are then discussed, followed by an examination of spatial coordinate systems and the measurement and analysis of elbow joint motion. This chapter concludes with the rationale for performing this work, and the objectives and hypotheses.*

1.1 ELBOW ANATOMY

Anatomy of the elbow which is pertinent to this discussion includes all structures which govern and affect elbow motion. There are three classes of such anatomy: osteology (bony structures), ligaments, and musculature.

1.1.1 OSTEOLOGY

The elbow's osseous anatomy consists of three bones: the humerus, radius, and ulna. Three articulations are formed between those bones: the ulnohumeral, radiohumeral, and proximal radioulnar articulations (Figure 1.1). These articulations allow for simultaneous elbow flexion-extension and forearm rotation (pronation-supination) motions. The axis of rotation for flexion-extension passes through the centers of the capitellum and trochlea (Figure 1.2) (Morrey, 2000). It is angled an average of 6-8° valgus with respect to the medial-lateral axis of the humerus.

1.1.1.1 Humerus

The humerus is the long bone of the upper arm which forms articulations with the shoulder and elbow joints. The distal humerus has a large, and complexly contoured, cartilaginous surface (Figure 1.3). The distal surface is all articular, but rather than

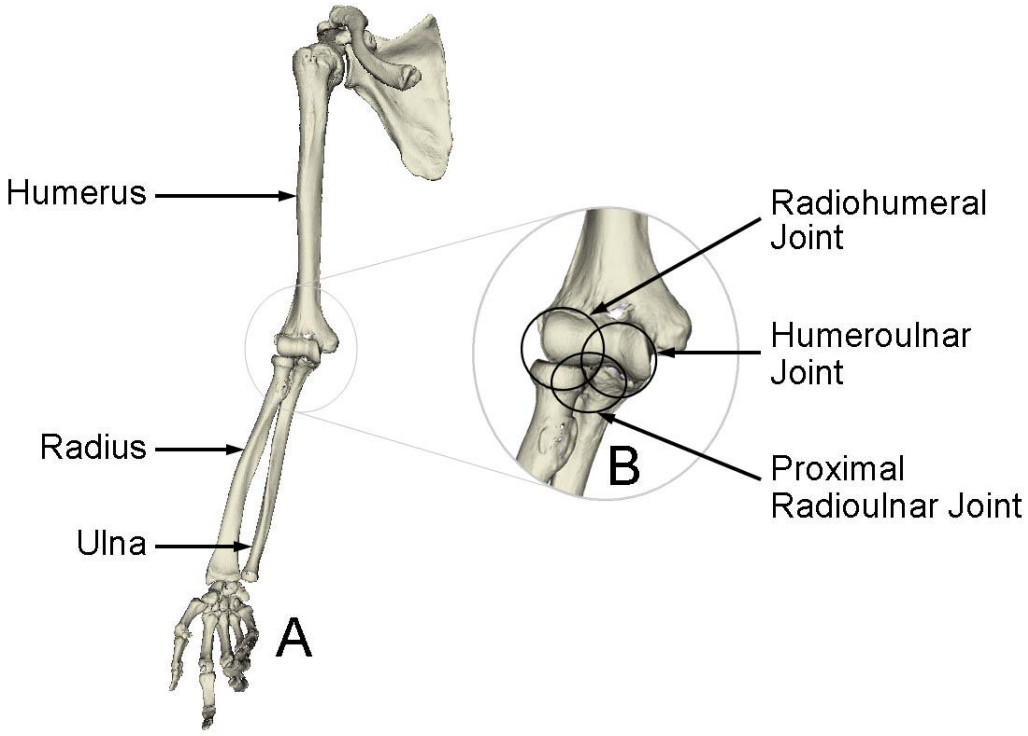

Figure 1.1: Osteotology of the Elbow

(A) The entire upper extremity (right arm shown). The elbow joint is comprised of the articulations between the humerus, radius, and ulna. (B) The three articulations are the radiohumeral (or radiocapitellar) joint, the humeroulnar (or ulnohumeral) joint, and the proximal radioulnar joint.

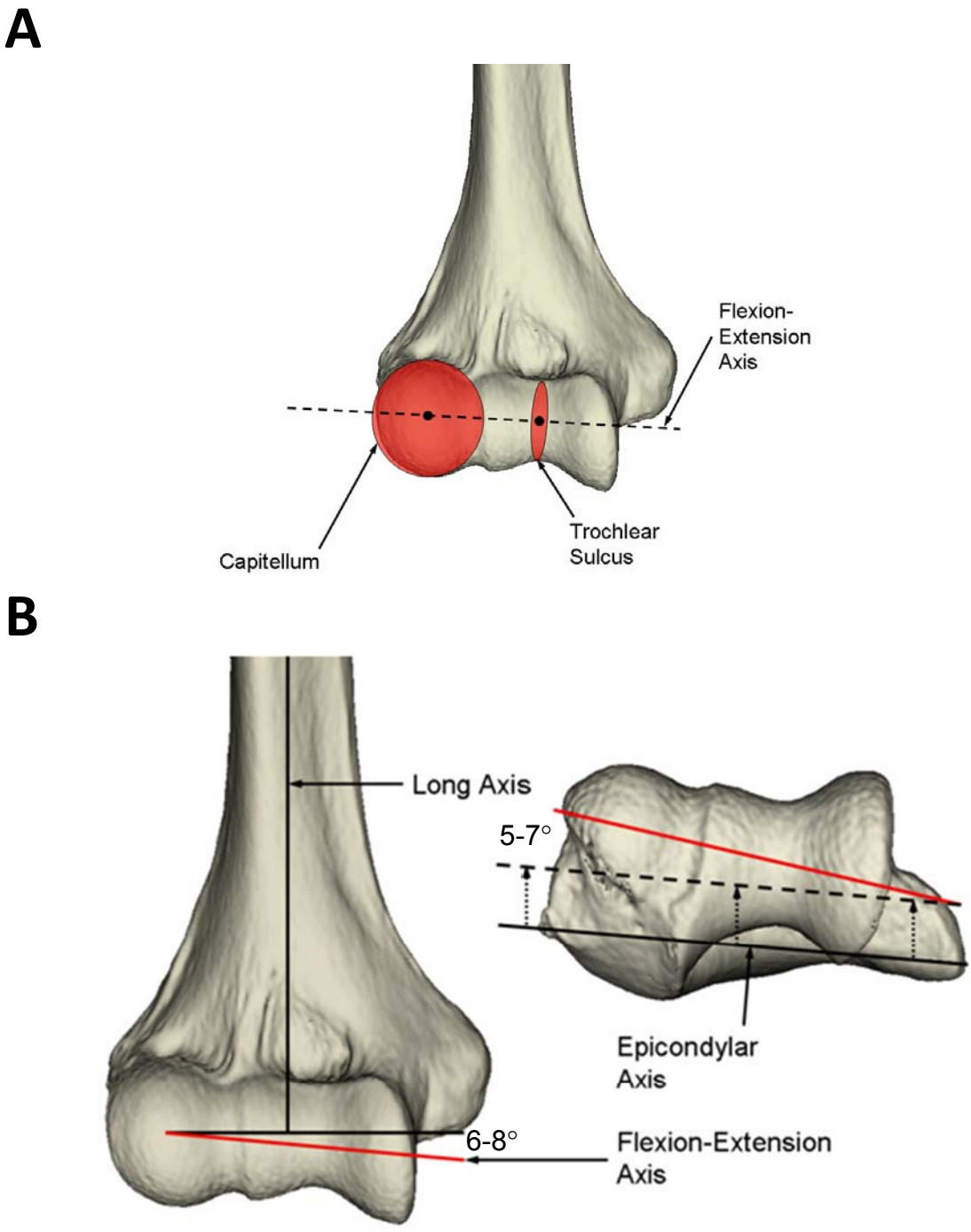

Figure 1.2: Flexion-Extension Axis of the Elbow Joint

(A) The flexion-extension axis (FEA) passes through the center of the capitellum and the center of the trochlear sulcus. (B) The FEA is both 6-8° valgus and 5-7° internally rotated with respect to the humerus. Right arm shown.

forming one joint, this complex geometry allows for two distinct joint rotations (Flexion-extension and pronation-supination). The medial, spool-shaped surface, is the trochlea, which articulates with the greater sigmoid notch of the ulna, and is covered by 300° of articular cartilage (Morrey, 2000; Shiba *et al*., 1988). This surface provides the articular bearing for flexion-extension motion. The trochlear sulcus is a smaller diameter waist in the middle of the trochlea, and forms a track which keeps the greater sigmoid notch of the ulna centered. Laterally, the capitellum is a nearly spherical structure, which articulates with the concave dish of the radial head. It is covered by approximately 180° of articular cartilage, and provides the bearing for both elbow flexion-extension and forearm rotation (pronation-supination). Two extra-articular bony outcroppings, called the medial and lateral epicondyles, serve as attachment sites for the medial and lateral collateral ligaments, and for the muscles of the forearm and hand (Morrey, 2000).

1.1.1.2 Radius

At its most proximal aspect, the radial head has a nearly spherical concave articular surface called the radial dish. The radial dish is entirely covered with cartilage and articulates with the capitellum to allow for forearm rotation (pronation-supination). The cylindrical perimeter of the radial head is covered with 240° of articular cartilage that articulates with the lesser sigmoid notch of the proximal ulna to form the proximal radioulnar joint (PRUJ). The anterolateral portion does not articulate with the ulna and is devoid of articular cartilage, which coincides with the approximate 180° range of forearm rotation. The radial tubercle is a bony outcropping distal to the radial head, which serves as the insertion of the biceps tendon (Figure 1.4) (Morrey, 2000).

1.1.1.3 Ulna

The proximal ulna has two articular surfaces: the greater and lesser sigmoid notches. The guiding ridge of the greater sigmoid notch fits into the track of the trochlear sulcus of the distal humerus. It is angled 30° posteriorly, and is terminated by the olecranon process posteriorly, and by the coronoid process anteriorly. The lesser sigmoid notch is the ulnar half of the proximal radioulnar joint (PRUJ), and has 60-80° of articular cartilage. The PRUJ has a theoretical 180° range of rotation (Morrey, 2000).

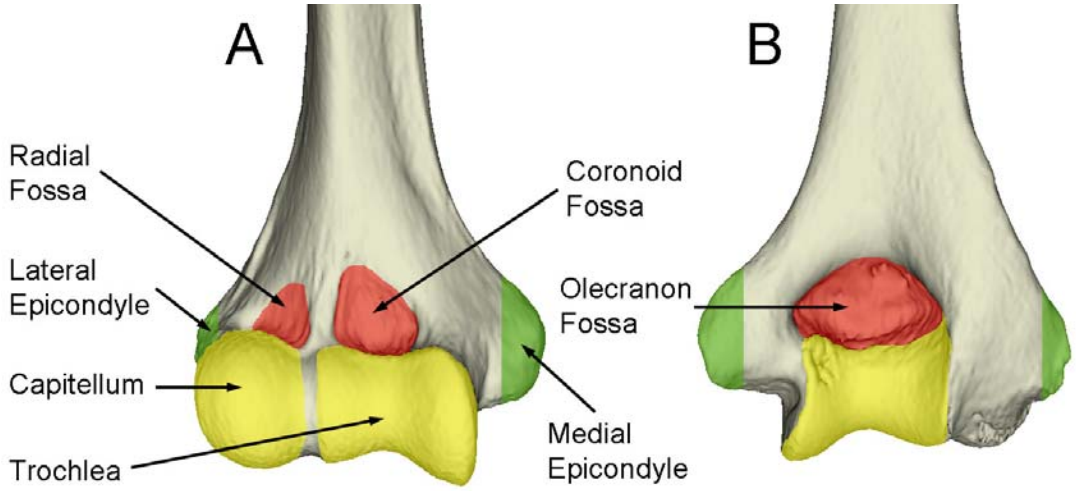

Figure 1.3: Osteology of the Distal Humerus

(A) Anterior view and (B) Posterior view (right arm). The articular surface consists of two parts, the capitellum (lateral, in yellow) and the trochlea (medial, in yellow). The three fossae (red) are depressions which accommodate the radial head and coronoid at full flexion, and the olecranon prominences at full extension. The epicondyles serve as attachments for the collateral ligaments, and as origins for various muscles that act distally in the forearm and hand (green).

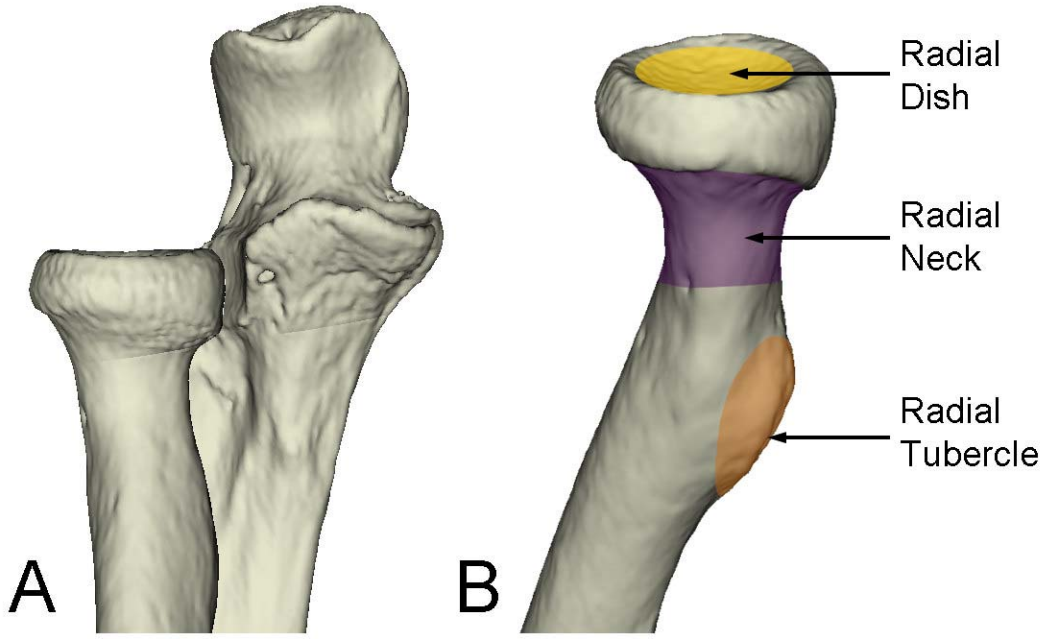

Figure 1.4: Osteology of the Proximal Radius

(A) Anterior view of the radius and ulna in their correct anatomical relationship (right arm). (B) The proximal radius consists of the radial head, neck, and tubercle. The radial head has two articulations. The radial dish (yellow) articulates with the capitellum. The cylindrical rim around the radial head articulates with the lesser sigmoid notch of the proximal ulna. The radial head and neck (purple) are angled approximately 15˚ to the long axis of the radial shaft. The radial tubercle (orange) is the insertion of the biceps tendon.

The coronoid and olecranon processes engage their corresponding fossae on the distal humerus at full flexion and extension respectively (Figure 1.5).

1.1.2 LIGAMENTS

Two major ligamentous structures, the medial and lateral collateral ligaments, contribute to primary stabilization of the elbow. The medial collateral ligament has three components: the anterior, posterior, and transverse bundles. The anterior and posterior bundles originate from the medial epicondyle of the humerus. Their ulnar attachments are much broader. The anterior bundle attaches to the sublime tubercle on the coronoid process. The posterior bundle, though less defined, attaches more posteriorly along the medial aspect of the proximal ulna. The transverse bundle attaches to the ulna only, and currently has no known function (Figure 1.6) (Morrey, 2000).

The lateral collateral ligament has four components. The lateral ulnar collateral ligament (LUCL) originates from the lateral epicondyle of the humerus, coincident with the flexion-extension axis, and attaches to the crista supinatorum tubercle of the ulna. It also blends with the annular ligament, which wraps around the radial head and neck and attaches to the anterior and posterior rims of the lesser sigmoid notch. The radial collateral ligament (RCL) originates from the lateral epicondyle and also blends with the annular ligament. A variable accessory collateral ligament is sometimes described, which originates from the crista supinatorum and blends with the annular ligament (Figure 1.6) (Morrey, 2000).

The collateral ligaments each consist of collagen bundles which provide stability in various directions. Each bundle has fibres which are orientated according to the primary tensile direction for which the bundle offers stability. The bundles themselves are heterogeneous structures composed of a combination of collagen and elastin. Ligaments are viscoelastic (Ohman *et al.*, 2009) which makes their mechanical behaviour dependent on the direction of tension and also on loading rate.

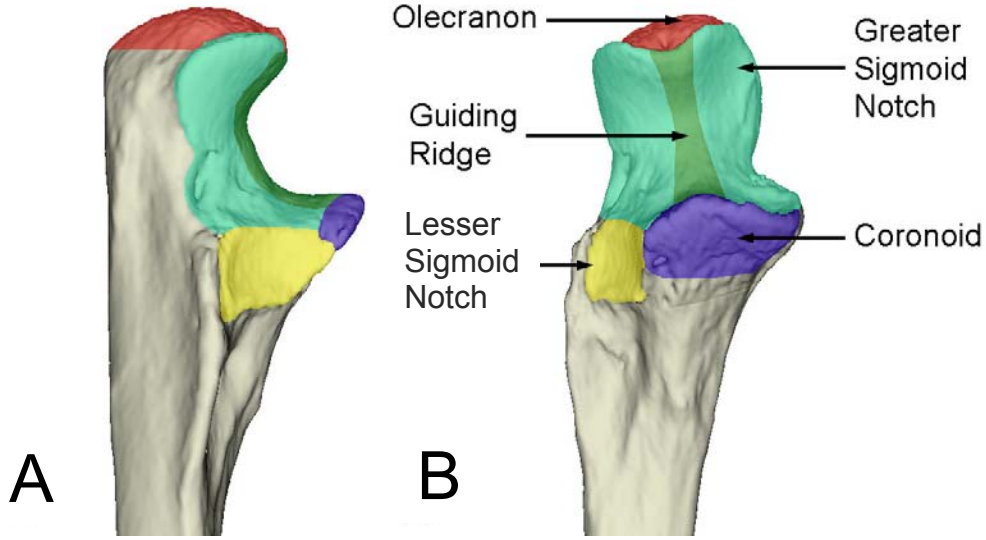

Figure 1.5: Osteology of the Proximal Ulna

(A) Lateral view of the proximal ulna. (B) The proximal ulna consists of the olecranon process, greater and lesser sigmoid notches, and the coronoid. The olecranon process (red) is the insertion of the triceps tendon. The greater sigmoid notch (green) articulates with the humeral trochlea. The coronoid process (purple) forms the anterior prominence of the guiding ridge of the greater sigmoid notch. The lesser sigmoid notch (yellow) articulates with the radial head to form the proximal radioulnar joint. Right arm shown.

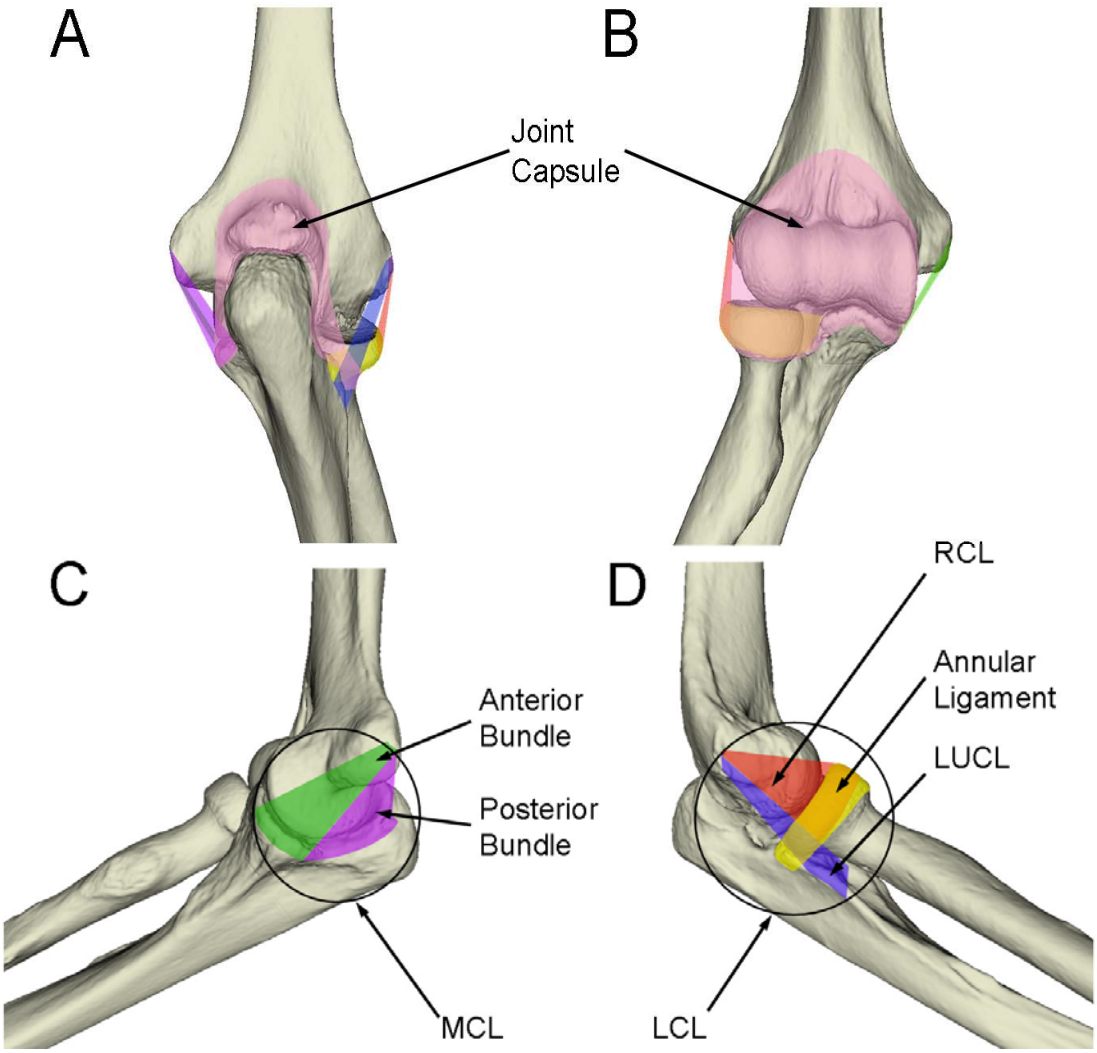

Figure 1.6: Ligaments and Capsule of the Elbow

(A) Posterior view and (B) Anterior view of elbow ligaments and joint capsule. The elbow capsule attaches around the elbow joints (pink). (C) The medial collateral ligament (MCL) has two important components: the anterior bundle (green), and the posterior bundle (purple). (D) The lateral collateral ligament (LCL) consists of the radial collateral ligament (RCL, red), the lateral ulnar collateral ligament (LUCL, blue), and the annular ligament (yellow). Right arm shown.

1.1.3 ELBOW JOINT CAPSULE

The three articulations of the elbow are encapsulated by a single soft tissue structure called the elbow joint capsule. The capsule attaches superiorly of the distal humeral articulations, and encapsulates the radial head, neck, and coronoid process anteriorly. Posteriorly, the capsule attaches around the perimeter of the olecranon process of the ulna, and encloses the olecranon fossa on the humerus (Morrey, 2000). The capsular tissue integrates with the elbow joint's ligamentous structures, giving the impression of a thickening of the capsule medially and laterally (Figure 1.6). The capsule is a broadly encompassing, non-directional structure with regions being taut or slack depending on the position of the elbow, offering stability in the presence of varying directions of joint load. The anterior capsule is taut in extension and the posterior capsule in flexion (King *et al.*, 1993b).

1.1.4 MUSCULATURE

Several muscles originate from the distal humerus and cross the elbow joint before inserting on the forearm and hand (Currier, 1972; Morrey, 2000). These muscles produce elbow flexion-extension, forearm pronation-supination, and flexion-extension of the wrist and fingers (Figure 1.7).

1.1.4.1 Flexors

Three muscles cross the elbow joint to generate a flexion moment (brachialis, biceps brachii, and brachioradialis). The brachialis originates from the anterior surface of the distal humerus and its insertion occupies both the base of the coronoid and the ulnar tuberosity. The biceps brachii has two origins, from which its name is derived (Latin: bi-ceps, meaning "two heads"). Both heads originate at the scapula; the long head at the superior glenoid tubercle, and the short head at the coracoid process. The two heads converge distally to form a single tendon which inserts at the bicipital tuberosity of the proximal radius. Due to its large cross section and insertion on the medial aspect of the radius, the biceps brachii is a strong forearm supinator, and thus contributes greatest to

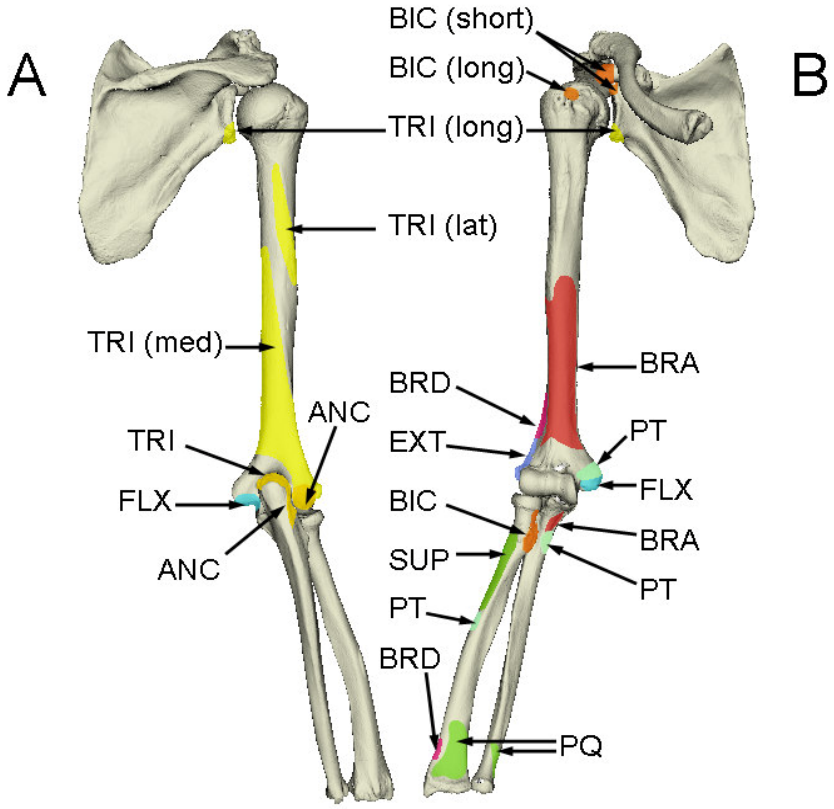

Figure 1.7: Muscles Crossing the Elbow Joint

(A) Posterior view and (B) Anterior view (right arm). Triceps (TRI) is the primary elbow extensor. Biceps brachii (BIC), brachialis (BRA), and brachioradialis (BRD) are major elbow flexors. Biceps brachii and supinator (SUP) supinate the forearm, while pronator teres (PT) and pronator quadratus (PQ) generate pronation. EXT and FLX are the common extensor and flexor tendon origins, respectively.

the elbow flexion moment when the forearm is supinated. The brachioradialis originates from the lateral supracondylar ridge of the humerus between the triceps and brachialis, and inserts distally at the radial styloid (Morrey, 2000). Though it has the longest moment arm of the flexors, it also has the smallest cross section, thus making the brachioradialis the weakest of the three flexor muscles (An *et al*., 1981; Murray *et al*., 1995; Pigeon *et al*., 1996).

1.1.4.2 Extensors

The elbow extension moment is generated principally by a single muscle, the triceps. As its name implies, it has three heads. The long head originates from the scapula at the infraglenoid tubercle. The lateral head originates on the lateral intermuscular septum and humerus. The medial head originates broadly from the posteromedial humeral shaft and medial intermuscular septum. All three heads merge to form a single large tendon that inserts at the olecranon process of the ulna (Morrey, 2000).

1.1.4.3 Pronators

Two muscles generate a pronation moment of the forearm (pronator teres and pronator quadratus). The pronator teres has two origins, one at the medial epicondyle is the common flexor-pronator origin. The other is at the coronoid process of the ulna. The muscle passes beneath the brachioradialis to its insertion between the middle and proximal thirds of the radius. It is a strong pronator, and also contributes slightly to the flexion moment. The pronator quadratus is a short, flat muscle that originates at the distal ulna and inserts at the distal radius, running transversely to the forearm on the volar aspect. It is a weak pronator but also provides stability through compression of the distal radioulnar joint (Gordon *et al*., 2004; Morrey, 2000).

1.1.4.4 Supinators

Two muscles generate a supination moment of the forearm (biceps brachii and supinator). Due to its large cross section and insertion on the medial aspect of the radius, the biceps brachii is a strong forearm supinator. The supinator originates on the anterolateral aspect of the lateral epicondyle, the lateral collateral ligament, and the crista supinatorum of the ulna. It then wraps laterally around the proximal ulna to its broad

insertion on the posterior aspect of the proximal radius (Morrey, 2000). The supinator is not as strong as the biceps brachii, but its location is mechanically advantageous for generating a supination moment. Also due to its isolated function, the supinator can be active throughout the flexion range.

1.2 ELBOW KINEMATICS & BIOMECHANICS

1.2.1 KINEMATICS

The flexion-extension axis of the elbow is located anterior to the humeral shaft. As mentioned previously, is defined as an axis through the centers of the capitellum and the trochlear sulcus (Amis *et al.*, 1979b). A full range of flexion for most subjects is approximately from 0° (full extension) to 145° (Figure 1.8A) (Morrey, 2000). Many subjects can obtain some hyperextension, which is indicated by a negative flexion angle. The actual flexion range attainable for a subject can be affected by the bulk of soft tissue present, prior disease or trauma, and the ligamentous laxity of the individual. Generally, four principal positions of flexion-extension are simulated (Figure 1.9).

With respect to forearm rotation, the ulna remains stationary while the radius pronates and supinates around it. However the motion of the radius is not purely circumferential about the ulna. Rather, the distal radius encircles the distal ulna, while the proximal radius pivots about its own center. Thus the radius crosses the ulna volarly in full pronation. A normal subject can obtain 150-160° of forearm rotation (Figure 1.8B) (Morrey, 2000).

In addition to the principal motions of the elbow articulations (*i.e.* flexion and forearm rotation), the bones of the forearm are also known to exhibit coupled motion patterns. The proximal ulna rotates with respect to the humerus. Pronation causes the ulna to internally rotate, while supination produces external rotation. The radius also moves proximally with pronation and distally with supination, as well as showing movement within the sagittal plane (Morrey, 2000).

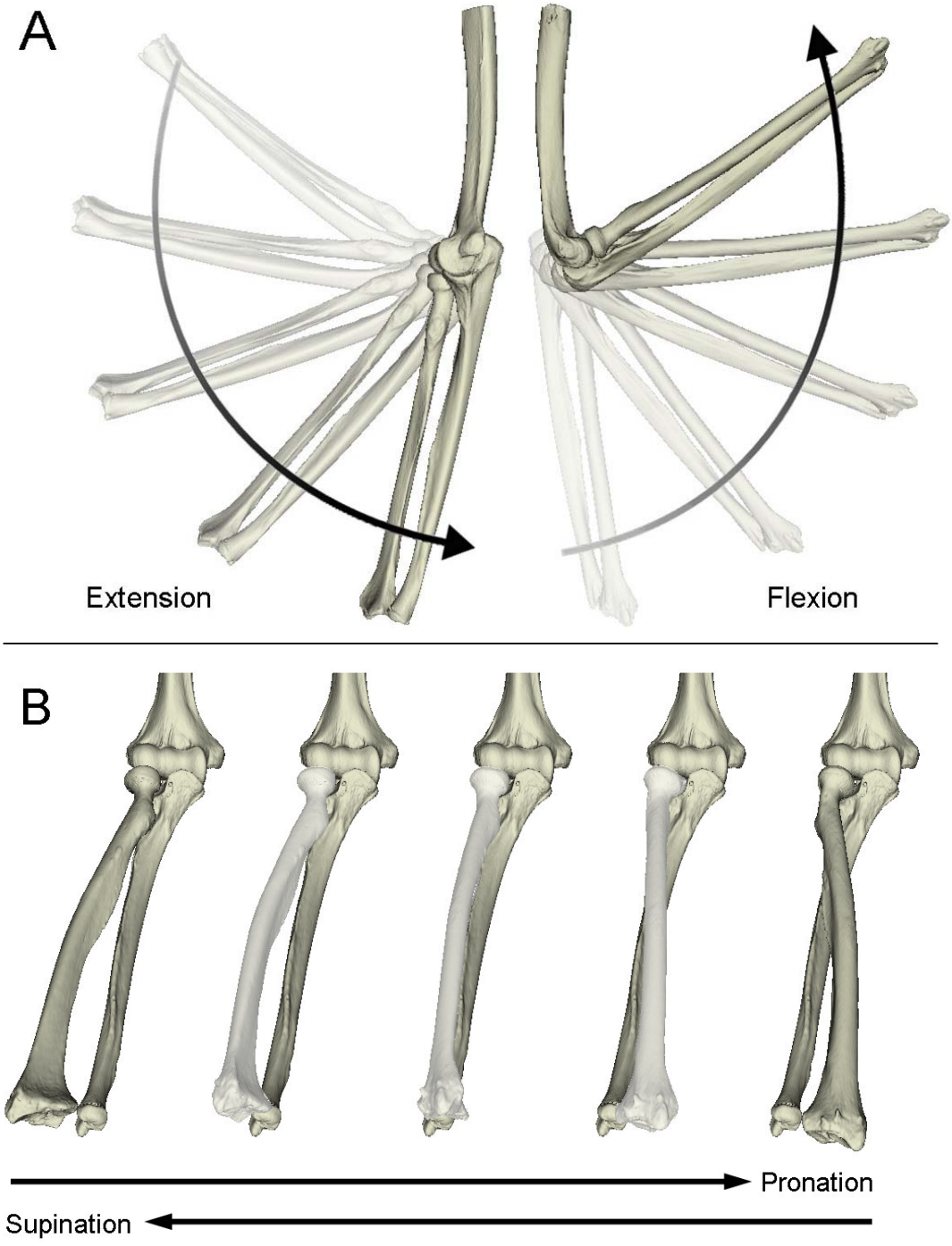

Figure 1.8: Elbow Motions

(A) Lateral view. The elbow is capable of an average of 145˚ of flexion. (B) Anterior view. The radius rotates around the ulna an average of 160˚ of rotation. Right arm shown.

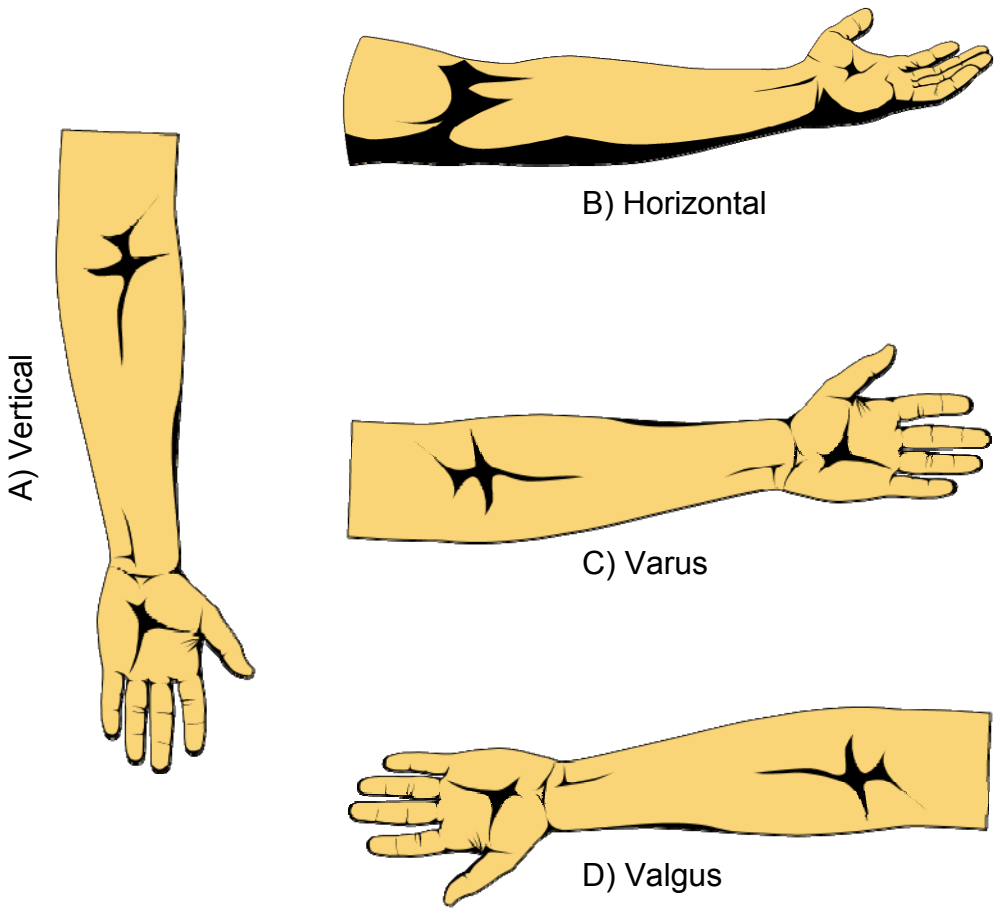

Figure 1.9: Positions of Upper Extremity Motion Testing

Studying elbow flexion-extension with the gravity load vector in the (A) vertical, (B) horizontal, (C) varus, and (D) valgus positions, provides us with kinematic data in four principal functional positions. Left arm shown.

1.2.2 STABILITY

Elbow stability is dependent on ligamentous, osseous (the interlocking shape of the articulations) and dynamic (muscular) stabilizers (Morrey and An, 1983; King *et al*., 1993c). The articular surfaces of the elbow are highly congruent. This osseous geometry contributes to the relatively high degree of stability enjoyed by the elbow, compared to some other major joints such as the knee and shoulder. Both static and dynamic stabilizers contribute to the overall stability of the elbow.

1.2.2.1 Static Stabilizers

A major source of stability is the congruency between the articular surfaces of the three joints that make up the elbow. The greater sigmoid notch conforms closely to the curvature and complex contours of the trochlea, which when reduced, provides a smooth hinge with resistance to medial-lateral and anterior-posterior translations.

The coronoid and olecranon processes at the terminals of the greater sigmoid notch, are osseous features which provide stability under certain conditions. The coronoid process anteriorly acts as a buttress when it engages the coronoid fossa at full flexion. This prevents posterior subluxation of the ulna on the humerus. It also serves as an important ligamentous attachment (see below). The olecranon process posteriorly contributes to varus and valgus angular stability when it engages the olecranon fossa at full extension.

The anterior band of the medial collateral ligament provides primary stability against valgus loads. It attaches to the sublime tubercle of the coronoid process anteriorly. In the absence of a functional medial collateral ligament, compression of the radiocapitellar joint acts as an important secondary stabilizer under valgus loading. The lateral collateral ligament complex has several stabilizing functions. The annular ligament stabilizes the proximal radioulnar joint, while the LUCL and RCL prevent varus instability and posterolateral rotatory instability. The anterior capsule of the elbow also provides a stabilizing effect, especially at full extension, where it resists hyperextension of the elbow (Morrey, 2000).

1.2.2.2 Dynamic Stabilizers

All the muscles that cross the elbow joint provide dynamic stability. Muscle activation compresses and reduces the three elbow joints, causing their articular surfaces to conform and their proper function to be realized. The common extensor origin and the flexor-pronator origin also have a role in stabilizing the elbow that is not fully clarified. However, instability does correlate with the extent of injury to one or both of these muscular origins (Morrey, 2000).

1.3 ELBOW JOINT KINEMATICS

Kinematics is the branch of classical mechanics that describes the motion of bodies (objects) without consideration of the forces that cause the motion. Numerous studies have used joint motion kinematics as a means to quantify the biomechanical characteristics of the elbow in both *in-vivo* and *in-vitro* models. The importance of the collateral ligaments as elbow joint stabilizers have been evaluated in terms of varus-valgus elbow laxity (Morrey and An, 1983; Olsen *et al*., 1996a; Sojbjerg *et al*., 1987b; Dunning *et al*., 2001b; King *et al*., 1993b). Others have measured the contribution of partial and total elbow joint implants to varus-valgus and internal-external rotation pathways of the ulna relative to the humerus(An, 2005; Itoi *et al*., 1994; King *et al*., 1994; King *et al*., 1999; O'Driscoll *et al*., 1992a; Pomianowski *et al*., 2001a; Stokdijk *et al*., 2003). Kinematic measurements have been used to design and evaluate implant designs and also surgical interventions and repairs. Conditions which cause non-physiological joint motion pathways can lead to osteoarthritis or undue ligament and muscle strain. Malalignment of the osseous articulations can also cause regions of bone to become shielded from normal compressive forces, which can lead to bone weakening and bone loss due to resorption. In the case of joint implants; malalignment of implant components to native joint rotation axes or articular surfaces can also be revealed by changes in joint motion (Itoi *et al*., 1994; King *et al*., 1993a; O'Driscoll *et al*., 1992a; Schuind *et al*., 1995; An, 2005; Morrey and An, 1983; Olsen *et al*., 1996a; Sojbjerg *et al*., 1987b). In general, much can be learned by quantifying elbow joint motion.

1.3.1 MOTION TRACKING METHODS

A variety of technologies and techniques have been employed to measure and record *in-vitro* joint motion. Mechanical linkages attached to bone segments can measure joint rotations. These can be employed as rotary variable transducers, or rotary (shaft) encoders. It is difficult to accurately align these devices to the joint rotation axes, and any misalignment results in an underestimation of the actual joint rotation. It is possible to measure translations with linkages as well. However, 6DOF (6 degrees of freedom) measurements would require six linkages with six transducers for each bone of interest.

Biplane Fluoroscopy and Roentgen Stereophotogrammetric Analysis (RSA) has been used to record 6DOF joint motion (Li *et al*., 2008; Hanson *et al*., 2006). While traditional RSA techniques require impaction of small spherical metal beads into the surface of bones, new model-based registration techniques do not (Bey *et al*., 2006; de Bruin *et al*., 2008). The common use of biplane fluoroscopy in clinical diagnostics and surgical navigation, also makes it well suited for some *in-vitro* investigations. However, the bulk and cost of the equipment and the use of radiation make it difficult to justify its generalized use for *in-vitro* joint motion studies.

Dynamic 6DOF spatial tracking devices are available in a few forms that are easily categorized by the physics they employ. These are sonic, optical and electromagnetic. Sonic trackers (usually ultrasonic) can suffer from signal blocking and interference. Accuracies are generally in the range of 2-3 mm RMS, and sonic reflection from walls and objects can be problematic (Welch, 2002).

Optical trackers use cameras to measure the position of optical targets in their view. The position and orientation of an object containing at least three targets can be measured. However, the targets must remain visible by the cameras at all times. Occlusion of the targets by objects, people, or even other targets can be problematic in some applications. Also, optical targets generally have a limit on their viewable angular range. This means that even without occlusion, a target can be rotated only so much before the cameras can no longer measure its location. Types of optical targets are: active, passive, and pattern. Active targets emit light (usually infrared) which the cameras

"see". They are often wired for power and synchronization, but can be wireless with battery power, though this means a much larger active target. Passive targets have retro-reflective surfaces which reflect light (usually infrared) that is emitted from the cameras. Their retro-reflective property ensures that the light emitted from each camera is reflected back to the camera so that the location of the target can be "seen". Since every passive target in the field of view is illuminated, objects are generally identified by having different geometric configurations of passive targets. This can lead to large collections of passive targets compared to active targets which can be identified by illumination sequence. The location of both active and passive targets are measured according to their centroid, and thus they represent single points, which is why an object needs at least three of them to be located in space. Pattern targets generally are high-contrast (usually black and white) patterns or 2D bar codes which are imaged in the viewable spectrum. Targets are distinguished by their unique patterns. Pattern recognition algorithms identify the targets and track their position and orientation. The pattern origin can be defined arbitrarily.

Electromagnetic trackers employ a field transmitter which generates an electromagnetic field in the working volume (Figure 1.10). Generally, the transmitter has three independent field coils, one for each global coordinate axis $Tr_{(X, Y, Z)}$. Receivers, much smaller than the transmitter, also contain three independent coils, one for each axis of the receiver's local coordinate system. The receiver's coils act as antennas in the transmitted field. These trackers do not suffer from target occlusion and the receivers are generally quite small, making this modality easy to implement. However, sources of electromagnetic noise and induced eddy currents in metallic objects can interfere with their measurements (Welch, 2002).

At the time of this writing, there are two dominant spatial tracking modalities: electromagnetic and optical. In the fields of *in-vivo* gate kinematics, optical tracking with passive retro-reflective targets and an array of cameras is the predominant setup. Passive retro-reflective targets are light and wireless, allowing freedom of movement for a subject. Since cameras can acquire all passive targets in a single frame, this provides for very fast frame rates, which is necessary if recording rapid gate motions.

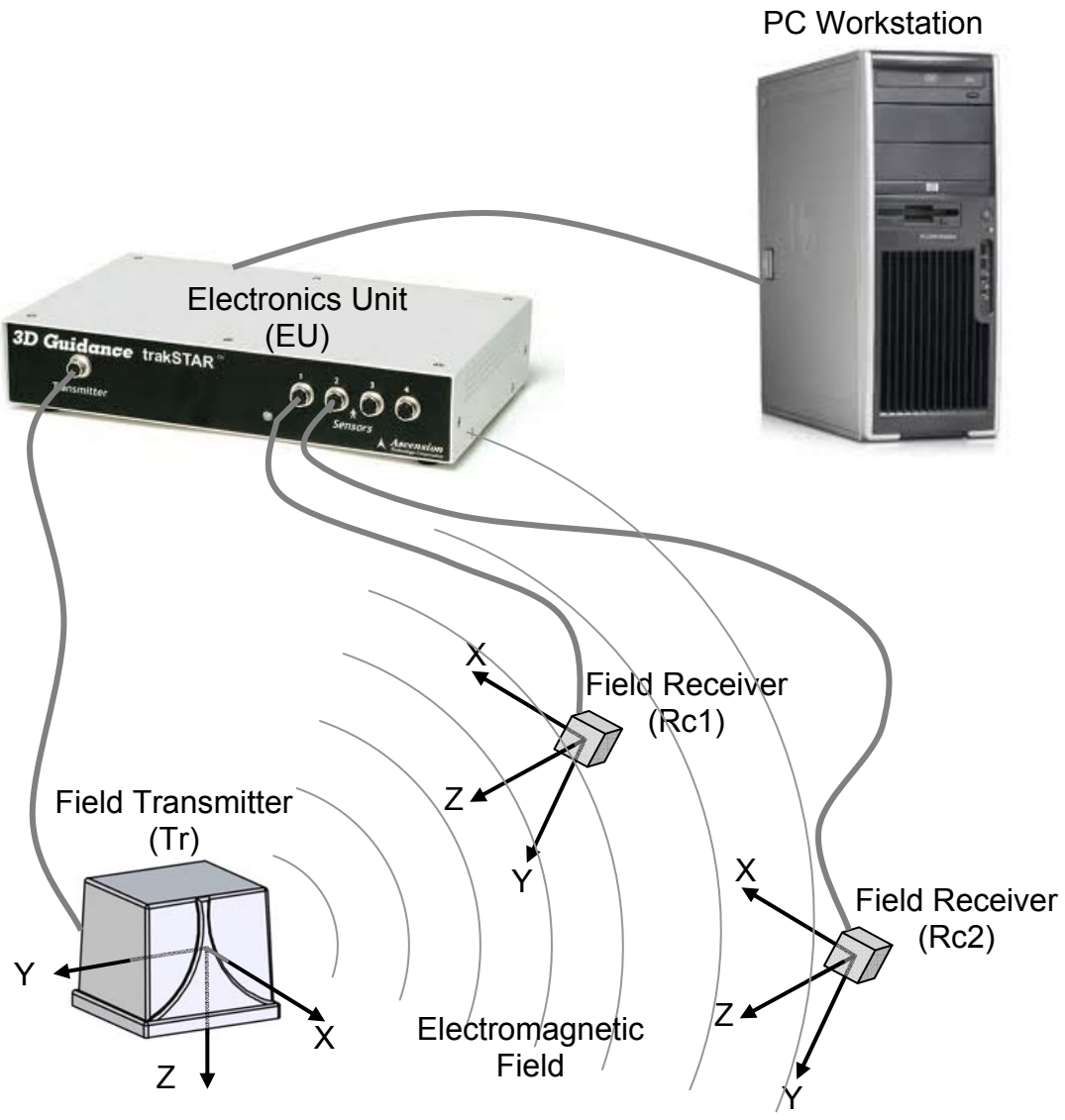

Figure 1.10: Electromagnetic Tracking System

The transmitter (Tr) emits an electromagnetic field from each of its three coordinate coils. Each field induces currents in the antennae of any receivers (Rc) within range. The electronics unit (EU) measures the induced currents and interprets their relative magnitudes as positions and rotations of the receiver relative to the transmitter. trakSTAR™ (Ascension Technologies Inc., Burlington, VT) shown.

For *in-vitro* study applications such as those described in this work, both electromagnetic and optical trackers enjoy a similar amount of acceptance. All the data presented herein was collected using either a Flock of Birds® or trakSTAR® from Ascension Technologies Corp. (Burlington, VT) electromagnetic tracker. More recently, the Optotrak Certus® (Northern Digital Inc., Waterloo, ON) has been used for motion data collection and computer-navigated orthopaedic surgical protocols. The Certus is the most accurate 6DOF tracker available, and its position measurements are more reliable than electromagnetic trackers when there are accompanying rotations. However, due to the various positions in which this simulator can perform elbow flexion, occlusion of optical targets is a major limitation of the Certus system. Thus, electromagnetic tracking remains a practical choice for *in-vitro* studies of this nature.

1.3.2 ORTHONORMAL BASIS

A vector space is created from an orthonormal basis. That is a set of mutually perpendicular vectors of magnitude one. These are the vectors that define the Cartesian coordinate directions in which kinematic descriptors will be quantified. Vector spaces will henceforth be referred to as coordinate systems. These can be thought of as being global or local (body-specific). Body-specific coordinate systems allow the 6DOF location and orientation of a body to be quantified in space (the global system) or relative to other bodies (Figure 1.11). Any orthonormal coordinate system is easily created by first defining two vectors, then by calculating the vector cross product between them which gives a third vector that is perpendicular to both of the initial vectors.

Another cross product can be calculated using the third vector and either of the first two vectors to produce a vector that is again perpendicular to both input vectors. Since the input vectors are already perpendicular to each other from the first cross product, then we now have three mutually perpendicular vectors. Normalizing their magnitudes produces an orthonormal basis. For this to be useful as a coordinate system, a coordinate origin must be defined. The origin of the global vector space is simply (0, 0, 0). The origin of a local coordinate system is what describes that body's location in the global vector space.

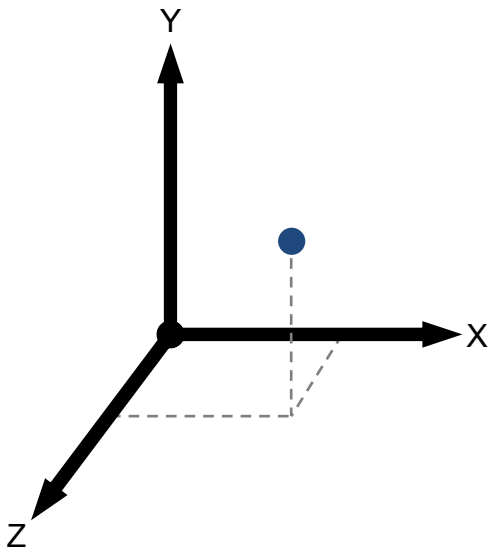

Figure 1.11: Orthonormal Basis

Three mutually perpendicular unit vectors form an orthonormal basis or coordinate system. The location (blue dot) is defined in terms of components along the three axes (x, y, z).

The simplest body is a particle, represented by a point and assumed to have negligible dimensions. A particle requires three quantities to specify its location in 3D space relative to a reference coordinate system. Thus, the location of a particle can be described by translations in three principal coordinate directions (x, y, z), and is said to have 3DOF degrees of freedom. Because a particle has negligible dimensions, pure rotation of the particle is not described, since the result of a rotated point leads to the same point. The next level of complexity in kinematics describes the motion of bodies with non-negligible dimensions. Such a body can be thought of as a collection of particles that are fixed relative to each other - whose relative positions are time invariant.

These collections of particles are referred to as rigid bodies. A rigid body can undergo translations and rotations (Figure 1.12). As with a particle, the location of a rigid body can be quantified by translations in the three Cartesian coordinate directions (*i.e.* x, y, z). Since a rigid body has non-zero dimensions, its location is defined to a point fixed relative to the rigid body, which corresponds to the center of its local coordinate system. Then the orientation of the rigid body can be quantified by three rotations about the coordinate axes of the reference coordinate system. Thus, an unconstrained rigid body is said to have 6DOF.

1.3.3 BONE SEGMENT COORDINATE SYSTEMS

In order to quantify elbow kinematics, a coordinate system must be created for each bone segment of interest. The coordinate system is made up of three orthonormal vectors and the position vector of an origin point. Since this work includes only motion of the ulna relative to the humerus, coordinate systems for only those bone segments will be defined (Figure 1.13). The direction and position vectors of each bone are all relative to the coordinate system of the receiver attached to the bone. Thus, these local bone coordinate systems become fixed (constant); invariant in both time and space as long as the receivers remain rigidly fixed to their corresponding bone segments.

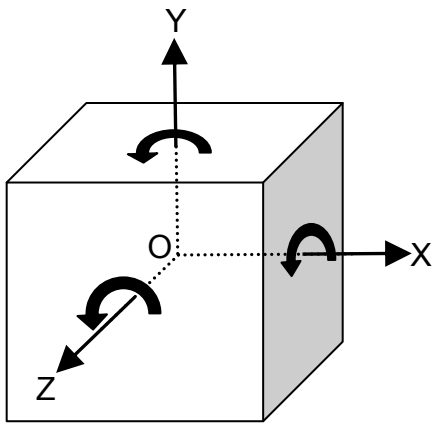

Figure 1.12: Rigid Body Pose

Three linear translations along coordinate axes (x, y, z) and three rotations about those axes. These six degrees of freedom (DOF) completely define the pose (location and orientation) of the rigid body (object). Shown is the trivial case where the rigid body coordinate system is coincident with the global coordinate system. The general case will be described later.

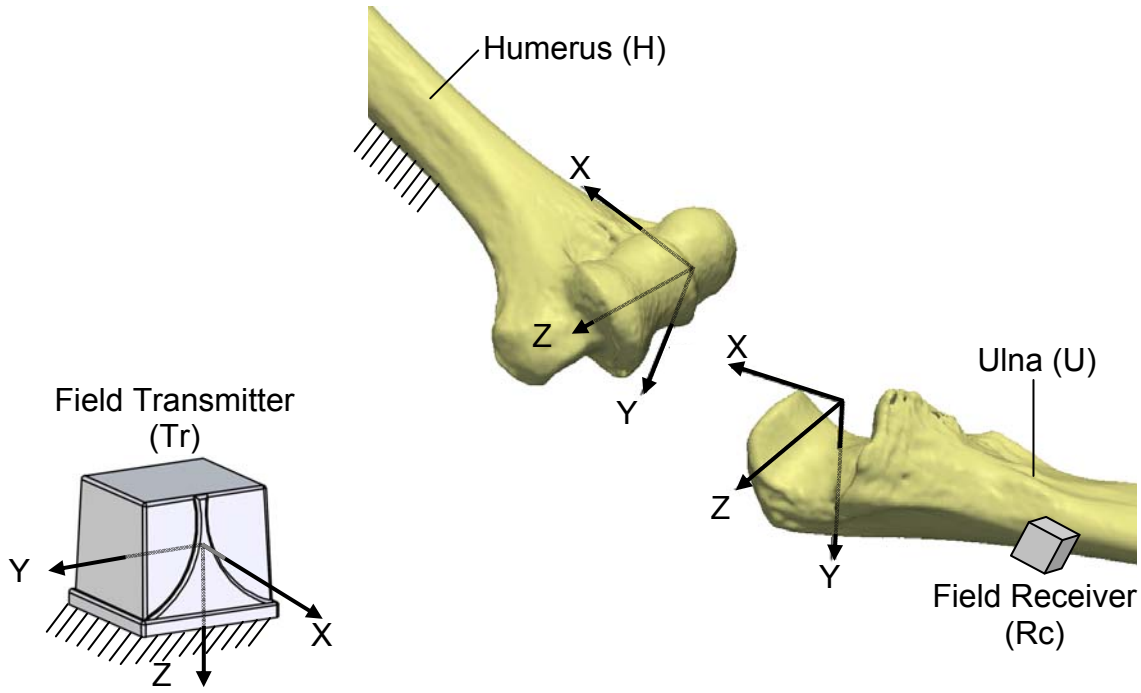

Figure 1.13: Bone Fixed Local Coordinate Systems

The humerus is rigidly mounted relative to the transmitter and the humeral coordinate system is created relative to the transmitter. The ulnar coordinate system is created relative to its corresponding field receiver. By convention, the +X and +Z axes point proximally and medially, respectively, for both bones. To maintain a right hand rotation convention, the +Y axis points anteriorly for a right arm and posteriorly for a left. The origins of the coordinate systems correspond to the joint rotation center. Left arm shown.

1.3.3.1 Anatomy-Derived Coordinate Systems

A common method for creating the direction and position vectors is by using a digitizing stylus probe. A field receiver is mounted to a stylus probe, whose tip position vector is known relative to the receiver. The stylus is used to probe the surface of the bones, while the receiver pose transforms are recorded. The surface of the bone relative to the bone's reference receiver is calculated using the known stylus tip position vector. This method is called "digitizing". Surface digitization can also be performed using non-contact methods such as laser scanners. Bony features that are digitized include the articular surfaces and landmarks that can describe the long axes. The usual intent is to digitize bony features that describe the flexion axis and long axis, so that the resulting fixed coordinate systems are aligned with the functional axes of the bones (Wu *et al.*, 2005). These are referred to as Anatomy-Derived CS (Coordinate Systems).

Although Anatomy-Derived CS have enjoyed widespread use in biomechanics research; they also have significant limitations. Anatomy-Derived CS are based on the precept that joint function follows from joint form (Brownhill *et al.*, 2006). However, in the case of the elbow; the anatomy-derived flexion axis has been found to deviate systematically from the axis about which the ulna rotates (Brownhill *et al.*, 2006). This is likely due to the fact that elbow motion is not only a function of its articulations, but also includes contributions from muscle activity, as well as guiding support from the capsule and ligaments.

1.3.3.2 Motion-Derived Coordinate Systems

Another method for creating bone fixed coordinate systems is by using joint motion recordings. By analyzing the joint motions, the flexion and forearm rotation axes can be calculated. These are often referred to as helical or Screw Displacement Axes (SDAs), and they have been shown to accurately represent the rotation axes of flexion and forearm rotation. By using these rotation axes and their intersection, bone fixed coordinate systems can be created as per (Ferreira *et al.*, 2010) and described in Chapter 4 of this dissertation.

1.3.4 COORDINATE TRANSFORMATIONS

Before meaningful and clinically relevant joint kinematic data can be interpreted, they must first be calculated from the pose (position and orientation) records collected by the spatial tracking system. Each pose record represents a time frame of positions and orientations of each spatial tracker target with respect to the tracker's origin. The tracker's origin can be the center of an electromagnetic field transmitter, a camera or system of cameras, or any object or abstract locale, depending on the spatial tracking modality. Thus, coordinate transformations are needed to convert this data into joint kinematic data.

1.3.4.1 The Transformation Matrix

Coordinate systems will be represented numerically with transformation matrices. A transformation matrix T, is a 4 by 4 (16 element) array of real numbers (Figure 1.14). It is composed of three parts: a 3 by 3 (9 element) rotation matrix R, a translation vector c, and the last row [0, 0, 0, 1]. The rotation matrix, is itself composed of three parts: the three orthonormal direction vectors (x, y, z). The unit direction vectors of the body's local coordinate system are inserted vertically into the rotation matrix portion of the array. This syntax ensures that the matrix represents the transformation of the body relative to its reference coordinate system (Figure 1.12). It is worth noting that the horizontal rows of the rotation matrix represent the orientation of the reference system relative to the body, which is equal to the result of the inverse operation. Therefore, the transpose of the rotation matrix is equal to its inverse. This is a convenient property because the transpose operation is much less computationally expensive than matrix inversion.

The last row [0, 0, 0, 1] of the transformation matrix ensures that the direction vectors and position vector are all represented in homogeneous coordinates. Homogeneous coordinates are a system of coordinates used in projective geometry much like Cartesian coordinates are used in Euclidean geometry. The reason for using transformation matrices in homogeneous coordinates is that they ensure simpler and more symmetric formulas.

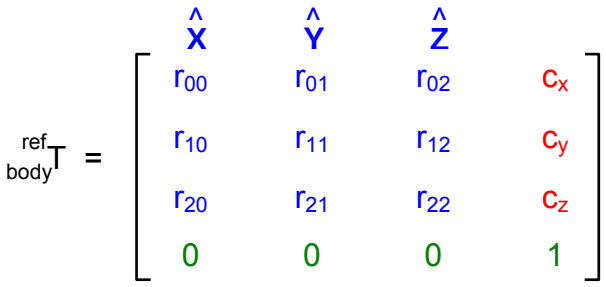

Figure 1.14: The Transformation Matrix

The transformation matrix is denoted by an upper case T. The preceding subscript and superscript represent the rigid body and its reference coordinate systems respectively. The rotation matrix (blue) portion is composed of the three orthonormal vectors of a rigid body's local coordinate system described in the space of a reference coordinate system, and represents the rigid body's orientation relative to that reference coordinate system. The position vector (red) represents the location of the rigid body relative to the reference coordinate system. The last row on the bottom (green) facilitates matrix operations.

In this work, we are dealing with rigid bones. Thus, we will use only translation and rotation operations, which result in rigid body transformations. Thus, a rigid body will always have the same size, shape and aspect ratio before and after the transformation is applied. The orthonormality of the direction vectors in the rotation matrix portion is the property that limits transformations to rigid body rotation only. This is the reason for using the orthonormal basis for all coordinate systems.

1.3.4.2 Transformation Chain

A typical setup for data collection is one where a receiver is mounted on the ulna and the humerus is rigidly mounted relative to the transmitter (Figure 1.13). During motion recording, raw pose data for the receiver is recorded relative to the field transmitter. The pose data is represented in the form of transformation matrices. Where ${}^{Tr}_{Rc}T$ represents the pose of the ulnar receiver relative to the field transmitter. ${}^{Tr}_{H}T$ and ${}^{Rc}_{U}T$ represent the pose of the humerus and ulna relative to the transmitter and receiver, respectively. The following sequence shows the matrix multiplications needed to generate ${}^{H}_{U}T$, which represents the transform of the ulna into the humerus' coordinate system.

$$ {}^{H}_{Tr}T \; {}^{Tr}_{Rc}T \; {}^{Rc}_{U}T = {}^{H}_{U}T \qquad \text{(Eq. 1.1)} $$

Notice that the preceding subscript and superscript of adjacent transforms are equal, meaning that those transforms involve a common body or coordinate system. By writing the equation in this way, the common intermediate body "cancels out", leaving a transform of the remaining bodies. Using this logic, it is possible to automate this process.

The transformation chain can easily be expanded to include more moving bodies, or deeper reference bodies. The above transform represents the ulna relative to the humerus, but one can easy add other anatomical structures such as the radius and hand, simply by appending a T matrix for each bone segment to the end of the chain. The same can be done at the beginning of the chain if one wants to include the scapula, the trunk, and other related structures.

1.3.5 EULER ANGLES

The Euler angle method is commonly used to quantify joint kinematics. Euler angles describe the attitude of a body with an ordered sequence of rotations about the body's local coordinate axes (Craig, 1989; Karduna *et al*., 2000; Small *et al*., 1992; Woltring, 1991). The change in attitude of a body (*i.e.* ulna) from an initial orientation that is coincident with a reference frame (*i.e.* humerus) to any subsequent position is fully described by defining three angles termed (yaw, pitch, roll). These angles describe rotations about the bone-fixed axes of the Z, Y and X axes of the ulna respectively. The rotation angles are applied in sequence and the order of that sequence is important.

Since the rotation angles are referenced with respect to the body's own axes, as the body is rotated, the axes of subsequent rotations get moved by rotations earlier in the sequence. The rotation sequence representing ulnar motion is Z→Y→X in the ulna's own reference frame. Since the ulnar reference frame is moving, this means that after the rotation sequence is applied, the first rotation will have occurred about the humeral Z axis, and the last rotation about the final location of the ulnar X axis. In the final orientation, the second rotation appears to have occurred about an arbitrary axis which is generally no longer coincident with any of the humeral or ulnar axes. The axis of the second rotation was called the "line of nodes" by Euler (Goldstein H., 1950) because it contains the two orbital nodes which represent the intersections of conceptual orbital arc paths within the first and third rotation planes. Grood and Suntay termed it the "floating axis" (Grood and Suntay, 1983) because it is not fixed to the rigid body as are the X, Y, Z axes, which makes its location (observed globally) dependent on the magnitude of the first rotation angle.

A limitation of the Euler angle method is the special case of "gimbal lock". Without disregarding the name, details regarding the analogy between the Euler rotation sequence and a physical set of gimbals will not be discussed here. It will suffice to point out that if the second rotation in the sequence is equal to 90º, then the last rotation axis will become collinear with the first. In this special case, there is no longer a distinct axis about which to execute the last rotation, and one degree of freedom is lost. Due to

numerical precision of computers, rotations near 90º will also exhibit symptoms due to gimbal lock. We avoid this problem by choosing a rotation sequence that cannot lead to a second rotation of 90º. In the elbow, this is accomplished by defining a direction perpendicular to the elbow flexion axis as the second Euler rotation axis. Functionally, the ulna can achieve a flexion angle of 90º, but rotation about the anterior-posterior axis of the ulna is limited by ligamentous stabilizers. Only a catastrophically disrupted and dislocated elbow could achieve a rotation near 90º about this axis.

1.3.6 JOINT MOTION PATHWAYS

Kinematic descriptors are necessary to quantify joint motions in ways that are clinically relevant. To facilitate this, it is useful to align the local bone segment coordinate system with relevant anatomical or functional axes, such as the bone's long axis or flexion axis. This alignment is crucial if the Euler angle descriptions are to be accurate. The bone local coordinate system provides the axes for Euler rotations. Thus, misalignment between the coordinate system and the functional axes of the joint will cause a component of one joint rotation to be falsely interpreted as contributing to another rotation of interest, and concurrently, a component of the joint rotation of interest will be lost (Piazza and Cavanagh, 2000). This is because the coordinate misalignment will cause a rotation about a true functional axis to be represented by more than one coordinate rotation, thus being divided into smaller components.

It is useful to consider descriptors of joint motion as a function of the flexion angle. This allows us to quantify and clinically interpret kinematics of the elbow joint throughout its functional range. In accordance with the bone segment coordinate systems defined above, the $Z \rightarrow Y \rightarrow X$ Euler rotation sequence corresponds to: flexion angle→varus angle→internal rotation of the ulna relative to the humerus. Varus angle and internal rotation are examples of joint motion descriptors. These and others are defined in the following sections.

1.3.6.1 Varus-Valgus Angulation and Joint Laxity

An elbow joint motion of clinical interest is the varus or valgus angle of the ulna relative to the humerus (Figure 1.15A). If the ulnar and humeral coordinate systems are coincident, then varus-valgus (VV) angulation is the adducted-abducted (toward-away from body) angular deviation of the ulnar long axis from the humeral sagittal plane about the anterior-posterior axis of the ulna. Since this is not about a rotation axis of the elbow, it is useful as a measure of elbow function in the evaluation of the integrity of osseous and soft tissue stabilizers. Thus VV angulation serves as a very common kinematic descriptor of elbow performance as a function of flexion angle.

Elbow joint laxity is another important descriptor of joint function. Varus-valgus laxity is quantified as the difference in the varus and valgus angles between the varus and valgus gravity loaded positions (Figure 1.9). It is essentially a measure of how loose the joint is, or how effective the joint stabilizers are.

1.3.6.2 Internal-External Rotation

Internal or external rotation of the ulna relative to the humerus is another useful kinematic descriptor of elbow function. Internal-External (IE) rotation is defined as ulnar rotation about its own long axis (Figure 1.15B) – not to be confused with forearm rotation (radius about the ulna). IE rotation is not an articular degree of freedom, though some degree of ulnohumeral IE rotation does occur normally. Thus, the degree of IE rotation can also be used to evaluate the condition of osseous and soft tissue stabilizers.

1.3.6.3 Joint Translations

Linear movement of the ulna relative to the humerus is described as translations of the ulnar local coordinate origin along the coordinate axes of the humeral coordinate system. This is another reason why it is important to align coordinate axes with relevant anatomical directions. Using the coordinate definitions, ulnar translations in the X, Y and Z directions (Figure 1.13) represent proximal, anterior/posterior (right arm/left arm), and medial translations respectively, relative to the humerus (Figure 1.15C).

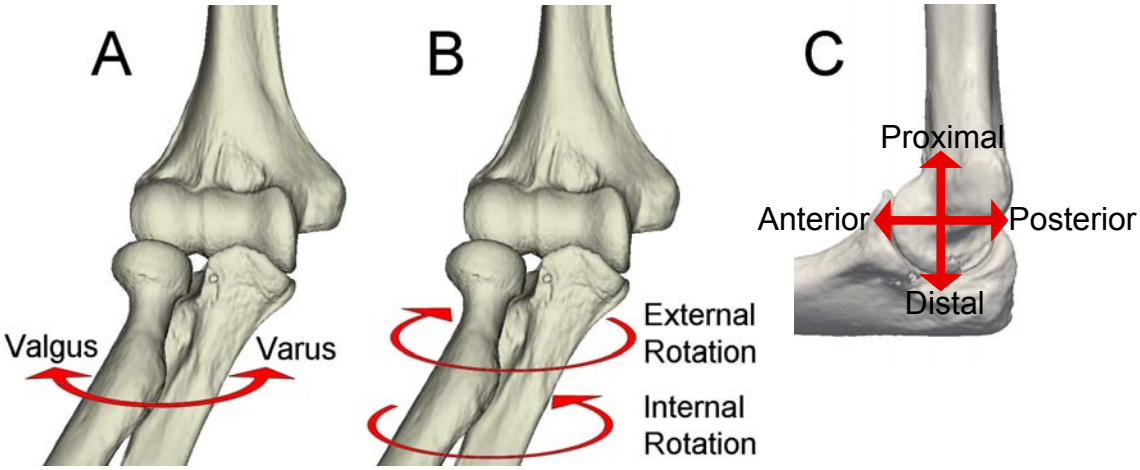

Figure 1.15: Elbow Kinematics

These are the kinematic descriptors of elbow motion. (A) Varus-valgus (VV) angulation. (B) Internal-external (IE) rotations. (C) Proximal-Distal, Medial (out of page), Lateral (into page), and Anterior-Posterior translations. Right arm shown.

1.4 SIMULATING ELBOW JOINT MOTION

Elbow joint motion that occurs naturally *in vivo* can be studied through simulation. Although no method of joint simulation has yet been developed which is a perfect elbow joint analog, there is still a strong scientific rationale for employing simulations. Simulation allows investigators to isolate and control various aspects of a specimen and its environment, and in so doing to create a more understandable or analyzable system. For example surgical procedures and implants can be tested and optimized using simulators, prior to their application in patients. Furthermore, many studies cannot be performed *in vivo* due to issues of safety and practicality.

Testing devices and simulators (if defined as systems which aim to model joint motion and loading) have been developed to mimic joint motion and loading for various activities. None of the presently available devices can fully model *in-vivo* loading. However, they do provide a useful basis to compare various rehabilitation protocols and surgical procedures.

As regards the elbow, there are four principal positions of the upper extremity in which flexion-extension is generally simulated. These are the vertical (gravity dependent), horizontal, varus and valgus positions (Figure 1.9). Testing in all four of these positions covers a broad range of externally applied moments that are experienced by the elbow during normal use.

In-vitro joint simulators have been developed to mimic kinematics and loading in the laboratory for various motions. While modeling the *in-vivo* state is difficult to achieve, these devices are useful in order to design and evaluate rehabilitation protocols, surgical procedures, implants, and to increase the knowledge base pertaining to physiological movement. With respect to elbow simulators, only a few systems have been reported. Most of these have simulated forces in the major muscles crossing the joint while testing in static elbow positions, or while an investigator flexed the arm passively.

1.4.1 *IN-SILICO* VERSUS *IN-VITRO* ELBOW JOINT SIMULATION

Simulation of elbow motion can be performed virtually (*in-silico*) using computer models, or physically with cadaveric specimens (*in-vitro*) by using specialized devices to move the specimen and record the characteristics of its motion (*i.e.* kinematics). Each method of simulation has its advantages and challenges.

The clear advantage of *in-silico* simulation is that virtual anatomical models can be an inexpensive and readily reusable source of specimens, while avoiding the challenges and expense of maintaining a biohazard test facility. Virtual models, allow investigators to control and adjust every variable that the model is designed to account for, which makes them valuable for a variety of studies. However, as with all virtual simulators, *in-silico* models of elbow joint motion must incorporate many assumptions and simplifications of anatomical functions and properties in order to successfully execute the simulations (Klein *et al.*, 2007). These simplifications are not due to a lack of computing power. Rather they are necessary in order to compensate for the complexities of the elbow as a system of interacting muscles, bones, and other soft tissues with complex and still incompletely understood mechanical properties. For instance, consider the capsuloligamentous and tendinous structures previously described in Sections 1.1.2 Ligaments and 1.1.3 Elbow Joint Capsule. These tissues have complex geometries with constituent components that offer stability in multiple and varying directions. Their mechanical performance is rate dependent due to viscoelastic properties, and their degree of stabilization is direction dependent due to heterogeneous material composition (Quapp and Weiss, 1998). These are compound structures – having a number of sub-bundles – with complex and variable geometries.

In-silico models must incorporate numerous assumptions in order to compensate for an incomplete knowledge of the tissues involved. For example, ligament properties are often considered identical to that of tendons for the purpose of modeling mechanical properties (Benjamin *et al*., 2002; Cooper and Misol, 1970; Evans *et al*., 1990). This is despite considerable evidence that ligaments and tendons have significantly different compositions and mechanical behaviours (Scutt *et al*., 2008; Zschabitz, 2005).

Furthermore, the properties of tendons are not completely understood. In measuring patellar tendon properties *in vivo*, (Couppe *et al.*, 2009) noted that studies based on cross-sectional designs, such as theirs and many others, have inherent limitations which leave them at risk of type II errors (Couppe *et al.*, 2009). The main reason given was the wide variation in tendon mechanical properties among the population (Magnusson *et al.*, 2001). Effects related to aging are also inconclusive due to disagreement in the literature; with some experiments suggesting that tendon compliance increases, others that it decreases, and yet others that it remains unchanged with age (Carroll *et al*., 2008; Couppe *et al*., 2009; Karamanidis and Arampatzis, 2006; Kubo *et al*., 2003; Kubo *et al*., 2007a; Kubo *et al*., 2007b; Mademli *et al*., 2008; Mian *et al*., 2007; Morse *et al*., 2005; Onambele *et al*., 2006).

These deficits in the current knowledge base necessitate compromises when modeling each discrete structure (*i.e.* ligament, tendon, muscle, etc.). However, elbow function involves complex interaction among many such structures, and this interaction of incompletely defined mechanical properties may compound modelling errors.

The advantage of *in-vitro* simulation is that the unknowns discussed above concerning tissue properties and mechanical behaviours, and the complex interactions among the various tissues can be left to function as they normally would *in vivo*. Also, using specimens selected from the actual human population automatically incorporates the wide variations in osseous anatomy, ligament and tendon properties (Ohman *et al.*, 2009) that occur among individuals.

Furthermore, certain studies must be performed on real tissue. For example, the results from evaluating surgical repairs are more realistic when those repairs are performed *in vitro*, because there are normal variations in outcomes that are caused by the practical aspects of surgery. Variables such as surgeon performance, variations in tissue properties and others are nearly impossible to model. If the performance of a surgical repair is being evaluated, then the hands-on nature of that repair must be present in the study protocol if a proper evaluation is to be achieved. If the evaluation includes measurements of motion or internal forces, then *in-vitro* simulation is the only option. Further, it is worth noting that the accuracy of *in-silico* simulations has most often been

evaluated using *in-vitro* experiments (Baldwin *et al*., 2009; Halloran *et al*., 2005; Laz *et al*., 2006; Mommersteeg *et al*., 1996; Sathasivam and Walker, 1997; Patil *et al*., 2003; Saikko and Calonius, 2002). Thus, the future of *in-silico* models is dependent on the continued development of *in-vitro* simulators. Until the day comes when virtual models achieve near perfect simulations of elbow joint function, there will be a need for *in-vitro* simulation, since it is logical that the perfect *in-silico* model may one day be validated by the perfect *in-vitro* simulator.

1.4.2 PASSIVE MOTION SIMULATORS

Elbow joint function can be simulated with passive motion, in which an investigator manually moves the forearm through a range of motion, while dependent variables such as kinematics or joint forces are measured. For *in-vitro* tests, this method can be used with or without simulated muscle forces. This technique has implications to post-trauma and post-surgical rehabilitation protocols, in which therapists employ passive motions to help patients regain elbow function.

One of the first passive simulators included a handle mounted to the ulna by which an investigator manually moved the forearm (Sojbjerg *et al*., 1987a; Sojbjerg *et al*., 1987b). The handle was instrumented with strain gauges in order to measure the applied moments, allowing the investigator to apply a varus-valgus or internal-external moment to the forearm while passively flexing or extending the elbow. Sojbjerg *et al.* investigated the contribution of the radial head and annular ligament (Sojbjerg *et al.*, 1987b) and the medial collateral ligament to the stability of the elbow (Sojbjerg *et al.*, 1987a). This device formed the basis for several more investigations into elbow stability following radial head excision and ligament disruption (Olsen *et al*., 1994; Olsen *et al*., 1998; Olsen *et al*., 1996b; Jensen *et al*., 1999).

Stokdijk *et al.* (2003) fixed the humerus to a rigid frame, and employed manual passive elbow flexion. An electromagnetic tracking system recorded ulnohumeral motion, and SDAs were used to evaluate total elbow replacement in a cadaveric model (Stokdijk *et al.*, 2003).

A simulator first reported by Morrey *et al.* (1991), simulated muscle forces with

static weights applied to the tendons of the brachialis, biceps and triceps muscles. These forces were 5% of the maximum potential force for those muscles and less than the physiologic forces needed to move the joint. They were only intended to stabilize the joint, as this can improve joint congruity and likely produce more physiologically accurate kinematics *in-vitro.* Elbow flexion was still generated manually by an investigator. The humeral mount allowed axial rotation of the humerus, which was used to model varus and valgus gravity loaded flexion (Figure 1.9) (Morrey *et al.*, 1991). Subsequently, several elbow studies utilized this simulator (O'Driscoll *et al*., 1992a; O'Driscoll *et al*., 1992b; Itoi *et al*., 1994; King *et al*., 1993a; Pomianowski *et al*., 2001a; Pomianowski *et al*., 2001b).

Another passive motion simulator used a DC electric motor and pulley aligned with the flexion axis, which applied an external force directly to the bones of the forearm in order to generate elbow flexion. Static weights were applied to the biceps, brachialis and triceps muscles, in order to simulate muscle loads, as with the above passive simulator. This system was used in conjunction with an electromagnetic tracking system to quantify ulnohumeral passive motion kinematics with SDAs (Screw Displacement Axes) (Bottlang *et al*., 2000a; Bottlang *et al*., 2000b). While the motion generated by this device is not performed manually, it is also not representative of *in-vivo* active motion, since the moments causing rotation about the flexion axis are not generated by tension loads crossing the elbow joint, in a manner consistent with physiological muscle activation. Rather, this form of simulation can be described as automated passive motion. The advantages of this over manual passive simulation are improved repeatability and constant angular joint rotation (Bottlang *et al.*, 2000b).

Another automated passive simulator used stepper motors to apply external loads directly to the humerus and forearm. Four stepper motors applied three orthogonal joint translations, and forearm rotation. Flexion angle was preset and the apparatus allowed free varus-valgus angulation. This device was used to evaluate elbow joint stability under various conditions (Deutch *et al*., 2003b; Deutch *et al*., 2003a; Deutch *et al*., 2003c; Jensen *et al*., 2003).

Some passive simulators use static joint angles while applying known loads or

joint torques, or known displacements in order to quantify joint stability. These represent a type of stop-and-go method of modeling elbow joint kinematics (Seiber *et al*., 2009; Fern *et al*., 2009; Hull *et al*., 2005). With these, static muscle loads can also be simulated (Fern *et al*., 2009; Hull *et al*., 2005). However, there are limitations in interpreting these measurements as being joint kinematics, since "kinematics" would suggest that the joint is actually moving. Passively moving the joint to various flexion angles and fixing it in place while taking kinematic measurements may not account for all the subtle and changing tissue interactions.

Passive motion with simulated muscle loads, whether manual or automated, produces a muscle loading model that is a balanced static system of loads. However, *in-vivo* active motion is clearly a system not in equilibrium, but rather a dynamic unbalanced system of loads, which generates the flexion-extension moment about the elbow flexion axis. Thus, *in-vitro* passive motion is not a complete and physiologically accurate model by which to simulate *in-vivo* motion.

1.4.3 ACTIVE MOTION SIMULATORS

In order for an *in-vitro* simulator to be categorized as active, it must produce flexion-extension in a sense that is representative of *in-vivo* motion. Thus, the flexion-extension moment generated about the elbow flexion axis must be developed from forces crossing the elbow joint. This can only be achieved by loading the muscles described in section 1.1.4. Simulating muscle activation to generate elbow flexion-extension has benefits. Balanced loading of the triceps, biceps and brachialis has been demonstrated to significantly stabilize the intact elbow in *in-vitro* studies (King *et al.*, 1994). Simulated variable muscle loading has also been shown to have an important stabilizing effect on the intact elbow (Johnson *et al.*, 2000). This stabilizing effect is even more evident following transection of primary stabilizers such as the MCL or LCL (Armstrong *et al*., 2000; Dunning *et al*., 2001b).

It is incumbent on the designers to employ muscle forces that are consistent with muscle effort during *in-vivo* motion. However, this is not a trivial problem. Unknown muscle and joint contact forces outnumber the equilibrium equations, resulting in an

indeterminate problem. One method of obtaining *in-vivo* muscle activation data is through the use of EMG (Electromyography) and muscle cross-sectional area (Funk *et al*., 1987; Johnson *et al*., 2000; Amis *et al*., 1979a). This produces a measure of muscle effort (load) during certain motions, which can then be applied in *in-vitro* studies. Another method is called mathematical optimization, which resolves the indeterminacy by minimizing muscle load and joint compression force (Kaufman *et al*., 1991; Vigouroux *et al*., 2007; Erdemir *et al*., 2007; Tsirakos *et al*., 1997; Raikova, 1996). This algorithm can be calculated before *in-vitro* testing, or applied in real-time.

Between 1995 and 2001, active motion simulators could be roughly grouped into two categories: Load-control or position-control devices. The category, to which an active simulator belonged, could be determined by the type of actuators that were primarily used to load the muscles in order to produce joint motion. Actuators also fall into those same two categories. By the basic nature of its design, an actuator can produce either a desired and controlled load or position, but not both. Load-control actuators include pistons or rotary actuators, which are driven by pneumatic, hydraulic or electromechanical solenoids. The force generated is proportional to the fluid pressure applied to the chamber (pneumatic and hydraulic), or the electrical current applied to the voice-coil (solenoid) and distraction (electromechanical). Thus, load-control actuators function in an analog sense. Their output is a function of a physical variable, such as pressure or electrical current, which is continuous in time.

Position-control actuators include stepper or servo motors. Typical servos give a rotary (angular) output. Linear types are common as well, using a screw thread or a linear motor to produce linear motion. Three basic types of servo motors are used in modern servo systems: AC servo motors, based on induction motor designs; DC servo motors, based on dc motor designs; and AC brushless servo motors, based on synchronous motor designs.

The configuration of windings and stators of these devices are such that application of a continuous electrical current “locks” the rotor in one position. The term “continuous” does not imply constant amplitude, as in the case of an AC motor which converts sinusoidal amplitude of an input voltage into shaft rotation. Rather, stepper and

servo motors achieve position control by energizing their complex windings using current control amplifiers. The intended rotor position is specified through an input command signal from the user or controlling application.

Simulated active elbow flexion in the vertical position (Figure 1.9A) has been reported (Dunning *et al*., 2003; Johnson *et al*., 2000; Dunning *et al*., 2001a; Rath, 1997). Major muscle groups for flexion were brachialis, biceps and triceps. The brachialis muscle was deemed the 'prime mover' for flexion and its movement was position-controlled using a PID (Proportional Integral Derivative) algorithm. A load cell was interposed in-line with the brachialis cable. This provided brachialis muscle force feedback, which was used to apportion muscle loads to the remaining muscles of interest. Those muscle loads were calculated as a ratio of the brachialis load, as determined by EMG and muscle cross-sectional area (Funk *et al*., 1987; Johnson *et al*., 2000; Amis *et al*., 1979a). This simulator, with its "prime mover" control scheme, was well suited for gravity dependent vertical flexion. In this position, the gravity vector resists flexion and thus provides a stabilizing effect by maintaining tension on the agonist muscles of flexion (Biceps, Brachialis and Brachioradialis), thus requiring little control for the antagonist (*i.e.* Triceps). However, it did not have the ability to perform horizontal, varus or valgus elbow flexion (Figure 1.9B,C,D).

Madey *et al.* reported an active elbow motion simulator that applied a flexion moment via a cable that was directly attached to the ulna 150 mm distal to the epicondyles (Madey *et al.*, 2000). The cable was actuated with a DC motor and static weights simulated Brachialis and Triceps loads. While flexion-extension was generated by loads crossing the elbow joint, this system did not model muscle loads in a physiologically accurate manner. The motion actuation cable was attached to the ulna in a location inconsistent with any flexor muscle, and Biceps was not simulated at all. Thus the loads crossing the elbow joint, and the resulting kinematics, cannot be representative of *in-vivo* conditions. In those respects, this device is more consistent with an automated passive method described in 1.4.2 above.

Some previously reported simulators have also achieved active flexion by using actuators to simulate active muscle loads (Kuxhaus *et al*., 2009; Kuxhaus, 2008;

Schimoler, 2008). Of these, the most advanced is the AGH elbow simulator, which derives its name from the Allegheny General Hospital (AGH) in Pittsburgh, PA. While not yet capable of horizontal flexion-extension, it has achieved some success in the varus and valgus positions. The AGH control scheme was based on the Dunning *et al.* (2003) simulator, which used displacement-control for the brachialis, dubbed the 'prime mover' of flexion, and all other muscles were load-controlled, including the triceps for antagonism. Schimoler *et al.* modified this control scheme by switching the 'prime mover' to triceps when brachialis load falls below a user-defined minimum. This causes triceps to drive the flexion angle down when it surpasses the desired setpoint. Other muscles (*i.e.* biceps and pronator teres) are load-controlled. Of course, the AGH is still a 'prime mover' simulator in principle, since it follows the paradigm that one muscle should be driven with displacement-control, while the rest are load-controlled as determined by some load transfer functions.

The efficacy of the 'prime mover' paradigm for the future of active elbow simulation will be discussed in Chapter 3, in the context of the challenges facing active flexion-extension in the horizontal, varus and valgus positions.

1.5 THESIS RATIONALE

The assessment of joint kinematics and stability in the laboratory is essential to gain an improved understanding of joint function and aberrations that occur with injury or disease. Moreover, *in-vitro* testing allows treatment options to be evaluated and optimized prior to application in patients. *In-vitro* simulation of elbow motion has not enjoyed significant development, especially in positions other than vertical (gravity dependent). Thus, as research and development in elbow implants and surgical repair/reconstruction procedures continues, it does so with an incomplete – and at times perhaps inadequate – understanding of elbow function.

By studying elbow motion in the four principal positions, important information regarding joint kinematics and dynamics, including soft tissue loads, can be deduced for a variety of common upper extremity activities. However, no system has been developed

that is capable of generating active elbow flexion and extension with the arm oriented in the horizontal, valgus and varus positions (Figure 1.9B,C,D). Thus, the effects of simulated muscle activation on elbow joint laxity and kinematic pathways in these positions are unknown. Furthermore, the appropriateness of passive flexion with regard to accurately modeling physiological motion remains unknown. This indicates a lingering deficit in our understanding of elbow joint motion. The deficit may lie in the degree to which we are able to generate physiologically representative motion in an *in-vitro* model, or to create reliable reference frames with which to accurately measure and evaluate that motion. Since reliability of coordinate reference frames is essential to get reliable kinematic data, the methods by which bone segment coordinate systems are generated must also be investigated. Advancements in both of these concepts are presented in this work.

1.6 OBJECTIVES AND HYPOTHESES

The objectives of this treatise were to develop a testing system with coordinate system refinements for the *in-vitro* study of elbow disorders, and to evaluate its performance for a clinically relevant surgical problem. The clinical model used for this evaluation was one of comminuted olecranon fracture with associated bone loss. This was done in a study comparing two surgical repair techniques for triceps reattachment following simulated olecranon excision.

The specific objectives of the research were:

1. To develop a set of transfer functions, using muscle tension and flexion angle feedback for control of muscle tension, in order to achieve active elbow flexion in the varus, valgus and horizontal positions, and to evaluate its repeatability in comparison to passive simulation.
2. To develop an algorithm capable of simultaneous muscle tension and flexion angle control (tension/flexion controller) for multiple muscles, using closed-loop feedback of actuator force and flexion angle, and feedforward control elements.

3. To develop a system (hardware and software) capable of real-time execution of the simultaneous tension/flexion controller, for multiple muscles while recording muscle forces and motion data as a function of elbow flexion angle.
4. To achieve constant elbow flexion and extension rate control in the varus, valgus and horizontal positions using the new active simulator.
5. To develop elbow coordinate systems generated from elbow joint motion, and to evaluate their inter-subject variability in comparison to traditional anatomy-derived coordinate systems.
6. To use the elbow motion simulator and motion-derived coordinate systems developed in this work, in an *in-vitro* study to evaluate the performance of two techniques of triceps repairs following simulated olecranon excisions.

The hypotheses of this work were:

1. *In-vitro* elbow flexion can be achieved in the varus, valgus and horizontal positions using muscle tension and flexion angle feedback with transfer functions for control of muscle tension.
2. Sufficiently fast and accurate control to an accuracy of 1 N of muscle tension can be achieved using servo-motors for actuation and instrumented motor mounts for tension input.
3. A constant flexion-extension rate of 10 °/s can be achieved with no more than 5º RMS error in the vertical, varus, valgus and horizontal positions using the above controller.
4. Motion-derived coordinate systems can be generated from elbow motions, and these produce kinematic pathways with less inter-subject variability when compared to the anatomy-derived coordinate systems.
5. The elbow motion simulator and motion-derived coordinate systems developed in this work will be effective in comparing two techniques of triceps repair following olecranon fracture/excision.

1.7 THESIS OVERVIEW

Chapter 2 presents an open-loop flexion controller based on transfer functions for the vertical, varus, valgus and horizontal positions. The transfer functions output muscle tensions and use inputs from load transducers and the flexion angle calculated from elbow motions measured by a 6DOF electromagnetic tracking system. There is one transfer function for each muscle and for each flexion position. The performance of the controller is evaluated in terms of its repeatability in achieving a consistent valgus joint pathway, and its performance is compared to that of passive simulation.

Chapter 3 describes the development of a closed-loop controller that is capable of simultaneous muscle tension and flexion angle control, using a single algorithm in all four positions: vertical, varus, valgus and horizontal. The controller uses flexion angle and muscle tension feedback from multiple muscles, and includes several extra-controller feedforward transfer functions. Hardware and software implementation is described with references to additional developmental material in the appendices, along with several discussions of hardware and software issues related to achieving real-time performance. In a full series of specimens, the controller is evaluated in terms of achieving a constant flexion rate, and its performance is compared to that of passive simulation.

Chapter 4 presents a method for creating ulnar and humeral bone segment coordinate systems from elbow motion data. It is found that, besides providing a minimally invasive method, motion-derived coordinate systems produce less inter-subject variability in kinematics data, compared to anatomy-derived coordinate systems.

Chapter 5 presents the new elbow joint motion simulator and motion-based coordinate system method in the application of an *in-vitro* clinical study. Anterior and posterior triceps repairs following simulated olecranon excision are evaluated and compared. By using the new methods presented in this work, new data (active motion simulated in varus, valgus and horizontal) and improved data (reduced inter-subject variability) will be used by investigators to improve patient care.

Chapter 6 provides a discussion of this treatise work, as well as conclusions and future directions for this research.

1.8 REFERENCES

Amis A A, Dowson D, Wright V. Muscle strengths and musculoskeletal geometry of the upper limb. Engineering in Medicine 1979a; (8): 41-48.

Amis A A, Dowson D, Wright V, Miller J H. The derivation of elbow joint forces, and their relation to prosthesis design. J Med Eng Technol 1979b; (3): 229-234.

An K N. Kinematics and constraint of total elbow arthroplasty. J Shoulder Elbow Surg 2005; (14): 168S-173S.

An K N, Hui F C, Morrey B F, Linscheid R L, Chao E Y. Muscles across the elbow joint: a biomechanical analysis. J Biomech 1981; (14): 659-669.

Armstrong A D, Dunning C E, Faber K J, Duck T R, Johnson J A, King G J. Rehabilitation of the medial collateral ligament-deficient elbow: an in vitro biomechanical study. J Hand Surg [Am] 2000; (25): 1051-1057.

Baldwin M A, Clary C, Maletsky L P, Rullkoetter P J. Verification of predicted specimen-specific natural and implanted patellofemoral kinematics during simulated deep knee bend. J Biomech 2009; (42): 2341-2348.

Benjamin M, Kumai T, Milz S, Boszczyk B M, Boszczyk A A, Ralphs J R. The skeletal attachment of tendons--tendon "entheses". Comp Biochem Physiol A Mol Integr Physiol 2002; (133): 931-945.

Bey M J, Zauel R, Brock S K, Tashman S. Validation of a new model-based tracking technique for measuring three-dimensional, in vivo glenohumeral joint kinematics. J Biomech Eng 2006; (128): 604-609.

Bottlang M, Madey S M, Steyers C M, Marsh J L, Brown T D. Assessment of elbow joint kinematics in passive motion by electromagnetic motion tracking. J Orthop Res 2000a; (18): 195-202.

Bottlang M, O'Rourke M R, Madey S M, Steyers C M, Marsh J L, Brown T D. Radiographic determinants of the elbow rotation axis: experimental identification and quantitative validation. J Orthop Res 2000b; (18): 821-828.

Brownhill J R, Furukawa K, Faber K J, Johnson J A, King G J. Surgeon accuracy in the selection of the flexion-extension axis of the elbow: an in vitro study. J Shoulder Elbow Surg 2006; (15): 451-456.

Carroll C C, Dickinson J M, Haus J M, Lee G A, Hollon C J, Aagaard P, Magnusson S P, Trappe T A. Influence of aging on the in vivo properties of human patellar tendon. J Appl Physiol 2008; (105): 1907-1915.

Cooper R R, Misol S. Tendon and ligament insertion. A light and electron microscopic study. J Bone Joint Surg Am 1970; (52): 1-20.

Couppe C, Hansen P, Kongsgaard M, Kovanen V, Suetta C, Aagaard P, Kjaer M, Magnusson S P. Mechanical properties and collagen cross-linking of the patellar tendon in old and young men. J Appl Physiol 2009; (107): 880-886.

Craig J J. Introduction to Robotics Mechanics & Control. Addison-Wesley Publishing Company, Massachusets 1989.

Currier D P. Maximal isometric tension of the elbow extensors at varied positions. 2. Assessment of extensor components by quantitative electromyography. Phys Ther 1972; (52): 1265-1276.

de Bruin P W, Kaptein B L, Stoel B C, Reiber J H, Rozing P M, Valstar E R. Image-based RSA: Roentgen stereophotogrammetric analysis based on 2D-3D image registration. J Biomech 2008; (41): 155-164.

Deutch S R, Jensen S L, Olsen B S, Sneppen O. Elbow joint stability in relation to forced external rotation: An experimental study of the osseous constraint. J Shoulder Elbow Surg 2003a; (12): 287-292.

Deutch S R, Jensen S L, Tyrdal S, Olsen B S, Sneppen O. Elbow joint stability following experimental osteoligamentous injury and reconstruction. J Shoulder Elbow Surg 2003b; (12): 466-471.

Deutch S R, Olsen B S, Jensen S L, Tyrdal S, Sneppen O. Ligamentous and capsular restraints to experimental posterior elbow joint dislocation. Scand J Med Sci Sports 2003c; (13): 311-316.

Dunning C E, Duck T R, King G J, Johnson J A. Simulated active control produces repeatable motion pathways of the elbow in an in vitro testing system. J Biomech 2001a; (34): 1039-1048.

Dunning C E, Gordon K D, King G J, Johnson J A. Development of a motion-controlled in vitro elbow testing system. J Orthop Res 2003; (21): 405-411.

Dunning C E, Zarzour Z D, Patterson S D, Johnson J A, King G J. Ligamentous stabilizers against posterolateral rotatory instability of the elbow. J Bone Joint Surg Am 2001b; (83-A): 1823-1828.

Erdemir A, McLean S, Herzog W, van den Bogert A J. Model-based estimation of muscle forces exerted during movements. Clin Biomech (Bristol , Avon) 2007; (22): 131-154.

Evans E J, Benjamin M, Pemberton D J. Fibrocartilage in the attachment zones of the quadriceps tendon and patellar ligament of man. J Anat 1990; (171): 155-162.

Fern S E, Owen J R, Ordyna N J, Wayne J S, Boardman N D, III. Complex varus elbow instability: a terrible triad model. J Shoulder Elbow Surg 2009; (18): 269-274.

Ferreira L M, King G J, Johnson J A. Motion-derived coordinate systems reduce inter-subject variability of elbow flexion kinematics. J Orthop Res 2010.

Funk D A, An K N, Morrey B F, Daube J R. Electromyographic analysis of muscles across the elbow joint. J Orthop Res 1987; (5): 529-538.

Goldstein H. Classical Mechanics. Addison-Wesley, Massechusetts 1950.

Gordon K D, Pardo R D, Johnson J A, King G J, Miller T A. Electromyographic activity and strength during maximum isometric pronation and supination efforts in healthy adults. J Orthop Res 2004; (22): 208-213.

Grood E S, Suntay W J. A joint coordinate system for the clinical description of three-dimensional motions: application to the knee. J Biomech Eng 1983; (105): 136-144.

Halloran J P, Petrella A J, Rullkoetter P J. Explicit finite element modeling of total knee replacement mechanics. J Biomech 2005; (38): 323-331.

Hanson G R, Suggs J F, Freiberg A A, Durbhakula S, Li G. Investigation of in vivo 6DOF total knee arthoplasty kinematics using a dual orthogonal fluoroscopic system. J Orthop Res 2006; (24): 974-981.

Hull J R, Owen J R, Fern S E, Wayne J S, Boardman N D, III. Role of the coronoid process in varus osteoarticular stability of the elbow. J Shoulder Elbow Surg 2005; (14): 441-446.

Itoi E, King G J, Neibur G L, Morrey B F, An K N. Malrotation of the humeral component of the capitellocondylar total elbow replacement is not the sole cause of dislocation. J Orthop Res 1994; (12): 665-671.

Jensen S L, Deutch S R, Olsen B S, Sojbjerg J O, Sneppen O. Laxity of the elbow after experimental excision of the radial head and division of the medial collateral ligament. Efficacy of ligament repair and radial head prosthetic replacement: a cadaver study. J Bone Joint Surg Br 2003; (85): 1006-1010.

Jensen S L, Olsen B S, Sojbjerg J O. Elbow joint kinematics after excision of the radial head. J Shoulder Elbow Surg 1999; (8): 238-241.

Johnson J A, Rath D A, Dunning C E, Roth S E, King G J. Simulation of elbow and forearm motion in vitro using a load controlled testing apparatus. J Biomech 2000; (33): 635-639.

Karamanidis K, Arampatzis A. Mechanical and morphological properties of human quadriceps femoris and triceps surae muscle-tendon unit in relation to aging and running. J Biomech 2006; (39): 406-417.

Karduna A R, McClure P W, Michener L A. Scapular kinematics: effects of altering the Euler angle sequence of rotations. J Biomech 2000; (33): 1063-1068.

Kaufman K R, An K N, Litchy W J, Morrey B F, Chao E Y. Dynamic joint forces during knee isokinetic exercise. Am J Sports Med 1991; (19): 305-316.

King G J, Itoi E, Niebur G L, Morrey B F, An K N. Motion and laxity of the capitellocondylar total elbow prosthesis. J Bone Joint Surg Am 1994; (76): 1000-1008.

King G J, Itoi E, Risung F, Niebur G L, Morrey B F, An K N. Kinematic and stability of the Norway elbow. A cadaveric study. Acta Orthop Scand 1993a; (64): 657-663.

King G J, Morrey B F, An K N. Stabilizers of the Elbow. Journal of Shoulder and Elbow Surgery 1993b; (2): 165-174.

King G J, Morrey B F, An K N. Stabilizers of the elbow. J Shoulder Elbow Surg 1993c; (2): 165-171.

King G J, Zarzour Z D, Rath D A, Dunning C E, Patterson S D, Johnson J A. Metallic radial head arthroplasty improves valgus stability of the elbow. Clin Orthop Relat Res 1999;114-125.

Klein H, Koopman H F, van der Helm F C, Prose L P, Veeger H E. Morphological muscle and joint parameters for musculoskeletal modelling of the lower extremity. Clin Biomech (Bristol , Avon) 2007; (22): 239-247.

Kubo K, Ishida Y, Komuro T, Tsunoda N, Kanehisa H, Fukunaga T. Age-related differences in the force generation capabilities and tendon extensibilities of knee extensors and plantar flexors in men. J Gerontol A Biol Sci Med Sci 2007a; (62): 1252-1258.

Kubo K, Kanehisa H, Miyatani M, Tachi M, Fukunaga T. Effect of low-load resistance training on the tendon properties in middle-aged and elderly women. Acta Physiol Scand 2003; (178): 25-32.

Kubo K, Morimoto M, Komuro T, Tsunoda N, Kanehisa H, Fukunaga T. Age-related differences in the properties of the plantar flexor muscles and tendons. Med Sci Sports Exerc 2007b; (39): 541-547.

Kuxhaus L, Schimoler P J, Vipperman J S, Miller M C. Validation of a Feedback-Controlled Elbow Simulator Design: Elbow Muscle Moment Arm Measurement. Journal of Medical Devices 2009; (3).

Kuxhaus L. Development Of A Feedback-Controlled Elbow Simulator: Design Validation And Clinical Application. 2008.
University of Pittsburgh .
Ref Type: Thesis/Dissertation

Laz P J, Pal S, Halloran J P, Petrella A J, Rullkoetter P J. Probabilistic finite element prediction of knee wear simulator mechanics. J Biomech 2006; (39): 2303-2310.

Li G, Van de Velde S K, Bingham J T. Validation of a non-invasive fluoroscopic imaging technique for the measurement of dynamic knee joint motion. J Biomech 2008; (41): 1616-1622.

Mademli L, Arampatzis A, Walsh M. Age-related effect of static and cyclic loadings on the strain-force curve of the vastus lateralis tendon and aponeurosis. J Biomech Eng 2008; (130): 011007.

Madey S M, Bottlang M, Steyers C M, Marsh J L, Brown T D. Hinged external fixation of the elbow: optimal axis alignment to minimize motion resistance. J Orthop Trauma 2000; (14): 41-47.

Magnusson S P, Aagaard P, Dyhre-Poulsen P, Kjaer M. Load-displacement properties of the human triceps surae aponeurosis in vivo. J Physiol 2001; (531): 277-288.

Mian O S, Thom J M, Ardigo L P, Minetti A E, Narici M V. Gastrocnemius muscle-tendon behaviour during walking in young and older adults. Acta Physiol (Oxf) 2007; (189): 57-65.

Mommersteeg T J, Huiskes R, Blankevoort L, Kooloos J G, Kauer J M, Maathuis P G. A global verification study of a quasi-static knee model with multi-bundle ligaments. J Biomech 1996; (29): 1659-1664.

Morrey B F. The Elbow and Its Disorders. W. B. Saunders Company, Philadelphia 2000.

Morrey B F, An K N. Articular and ligamentous contributions to the stability of the elbow joint. Am J Sports Med 1983; (11): 315-319.

Morrey B F, Tanaka S, An K N. Valgus stability of the elbow. A definition of primary and secondary constraints. Clin Orthop Relat Res 1991;187-195.

Morse C I, Thom J M, Birch K M, Narici M V. Tendon elongation influences the amplitude of interpolated doublets in the assessment of activation in elderly men. J Appl Physiol 2005; (98): 221-226.

Murray W M, Delp S L, Buchanan T S. Variation of muscle moment arms with elbow and forearm position. J Biomech 1995; (28): 513-525.

O'Driscoll S W, An K N, Korinek S, Morrey B F. Kinematics of semi-constrained total elbow arthroplasty. J Bone Joint Surg Br 1992a; (74): 297-299.

O'Driscoll S W, Morrey B F, Korinek S, An K N. Elbow subluxation and dislocation. A spectrum of instability. Clin Orthop Relat Res 1992b;186-197.

Ohman C, Baleani M, Viceconti M. Repeatability of experimental procedures to determine mechanical behaviour of ligaments. Acta Bioeng Biomech 2009; (11): 19-23.

Olsen B S, Sojbjerg J O, Dalstra M, Sneppen O. Kinematics of the lateral ligamentous constraints of the elbow joint. J Shoulder Elbow Surg 1996a; (5): 333-341.

Olsen B S, Sojbjerg J O, Nielsen K K, Vaesel M T, Dalstra M, Sneppen O. Elbow joint instability: A kinematic model. J Shoulder Elbow 1994; (3): 143-150.

Olsen B S, Sojbjerg J O, Nielsen K K, Vaesel M T, Dalstra M, Sneppen O. Posterolateral elbow joint instability: the basic kinematics. J Shoulder Elbow Surg 1998; (7): 19-29.

Olsen B S, Vaesel M T, Sojbjerg J O, Helmig P, Sneppen O. Lateral collateral ligament of the elbow joint: anatomy and kinematics. J Shoulder Elbow Surg 1996b; (5): 103-112.

Onambele G L, Narici M V, Maganaris C N. Calf muscle-tendon properties and postural balance in old age. J Appl Physiol 2006; (100): 2048-2056.

Patil S, Bergula A, Chen P C, Colwell C W, Jr., D'Lima D D. Polyethylene wear and acetabular component orientation. J Bone Joint Surg Am 2003; (85-A Suppl 4): 56-63.

Piazza S J, Cavanagh P R. Measurement of the screw-home motion of the knee is sensitive to errors in axis alignment. J Biomech 2000; (33): 1029-1034.

Pigeon P, Yahia L, Feldman A G. Moment arms and lengths of human upper limb muscles as functions of joint angles. J Biomech 1996; (29): 1365-1370.

Pomianowski S, Morrey B F, Neale P G, Park M J, O'Driscoll S W, An K N. Contribution of monoblock and bipolar radial head prostheses to valgus stability of the elbow. J Bone Joint Surg Am 2001a; (83-A): 1829-1834.

Pomianowski S, O'Driscoll S W, Neale P G, Park M J, Morrey B F, An K N. The effect of forearm rotation on laxity and stability of the elbow. Clin Biomech (Bristol , Avon) 2001b; (16): 401-407.

Quapp K M, Weiss J A. Material characterization of human medial collateral ligament. J Biomech Eng 1998; (120): 757-763.

Raikova R. A model of the flexion-extension motion in the elbow joint some problems concerning muscle forces modelling and computation. J Biomech 1996; (29): 763-772.

Rath DA. Design and development of an elbow loading apparatus and determination of elbow kinematics. 1997. The University of Western Ontario.
Ref Type: Thesis/Dissertation

Saikko V, Calonius O. Slide track analysis of the relative motion between femoral head and acetabular cup in walking and in hip simulators. J Biomech 2002; (35): 455-464.

Sathasivam S, Walker P S. A computer model with surface friction for the prediction of total knee kinematics. J Biomech 1997; (30): 177-184.

Schimoler PJ. Design Of A Control System For An Elbow Joint Motion Simulator. 2008. University of Pittsburgh .
Ref Type: Thesis/Dissertation

Schuind F, O'Driscoll S, Korinek S, An K N, Morrey B F. Loose-hinge total elbow arthroplasty. An experimental study of the effects of implant alignment on three-dimensional elbow kinematics. J Arthroplasty 1995; (10): 670-678.

Scutt N, Rolf C, Scutt A. Tissue specific characteristics of cells isolated from human and rat tendons and ligaments. J Orthop Surg 2008; (3): 32.

Seiber K, Gupta R, McGarry M H, Safran M R, Lee T Q. The role of the elbow musculature, forearm rotation, and elbow flexion in elbow stability: an in vitro study. J Shoulder Elbow Surg 2009; (18): 260-268.

Shiba R, Sorbie C, Siu D W, Bryant J T, Cooke T D, Wevers H W. Geometry of the humeroulnar joint. J Orthop Res 1988; (6): 897-906.

Small C F, Bryant J T, Pichora D R. Rationalization of kinematic descriptors for three-dimensional hand and finger motion. J Biomed Eng 1992; (14): 133-141.

Sojbjerg J O, Ovesen J, Gundorf C E. The stability of the elbow following excision of the radial head and transection of the annular ligament. An experimental study. Arch Orthop Trauma Surg 1987a; (106): 248-250.

Sojbjerg J O, Ovesen J, Nielsen S. Experimental elbow instability after transection of the medial collateral ligament. Clin Orthop Relat Res 1987b;186-190.

Stokdijk M, Nagels J, Garling E H, Rozing P M. The kinematic elbow axis as a parameter to evaluate total elbow replacement: A cadaver study of the iBP elbow system. J Shoulder Elbow Surg 2003; (12): 63-68.

Tsirakos D, Baltzopoulos V, Bartlett R. Inverse optimization: functional and physiological considerations related to the force-sharing problem. Crit Rev Biomed Eng 1997; (25): 371-407.

Vigouroux L, Quaine F, Labarre-Vila A, Amarantini D, Moutet F. Using EMG data to constrain optimization procedure improves finger tendon tension estimations during static fingertip force production. J Biomech 2007; (40): 2846-2856.

Welch G. Motion Tracking: No Silver Bullet, but a Respectable Arsenal. IEEE computer graphics and applications 2002; (22): 24-38.

Woltring H J. Representation and calculation of 3-D joint movement. Human Movement Science 1991; (10): 603-616.

Wu G, van der Helm F C, Veeger H E, Makhsous M, Van Roy P, Anglin C, Nagels J, Karduna A R, McQuade K, Wang X, Werner F W, Buchholz B. ISB recommendation on definitions of joint coordinate systems of various joints for the reporting of human joint motion--Part II: shoulder, elbow, wrist and hand. J Biomech 2005; (38): 981-992.

Zschabitz A. [Structure and behavior of tendons and ligaments]. Orthopade 2005; (34): 516-525.

CHAPTER 2 – DEVELOPMENT OF AN ACTIVE ELBOW FLEXION SIMULATOR TO EVALUATE JOINT KINEMATICS WITH THE HUMERUS IN THE HORIZONTAL POSITION

OVERVIEW: *In-vitro simulation of active joint motion is useful to evaluate rehabilitation protocols and surgical procedures in the laboratory prior to their application in patients. To date, simulated active elbow flexion has been reliably achieved and well established only in the vertical position (humerus vertical with hand down). This chapter presents a development and performance evaluation of a new elbow motion simulator capable of active flexion in the vertical, varus, valgus and horizontal positions. Muscle loading and motion control was achieved via a combination of motors and actuators attached to relevant tendons. Simulated active flexion was compared to passive flexion in terms of repeatability, motion pathways and joint laxity. The joint kinematics of active flexion were significantly more repeatable than passive flexion ($p < 0.05$). Active flexion reduced varus-valgus joint laxity by 29% (supinated $p < 0.05$) and 26% (pronated $p < 0.05$) compared to passive flexion. Greater repeatability of simulated active flexion suggests that this mode of in-vitro testing should increase statistical power and decrease required sample sizes.*[1]

1) A version of this work has been published: Ferreira LM, Johnson JA, King GJW. Development of an Active Elbow Flexion Simulator to Evaluate Joint Kinematics with the Humerus in the Horizontal Position. *Journal of Biomechanics*, 2010 Aug 10;43(11):2114-9. (See Appendix E.1)

2.1 INTRODUCTION

Joint simulators have been developed to mimic kinematics and loading in the laboratory for various motions. While modelling the *in-vivo* state is difficult to achieve, these devices are useful in order to design and evaluate rehabilitation protocols, surgical procedures, implants, and to increase the knowledge base pertaining to physiological movement. With respect to elbow flexion, only a few systems have been reported. Most of these have simulated muscle forces in the major muscles crossing the joint while testing in static elbow positions, or while an investigator flexed the arm passively (Itoi *et al*., 1994; King *et al*., 1993; O'Driscoll *et al*., 1992; Pomianowski *et al*., 2001b; Pomianowski *et al*., 2001a; Olsen *et al*., 1998; Morrey *et al*., 1991; Baratz *et al*., 1996; Seiber *et al*., 2009).

The upper extremity is often placed in one of four principal positions when simulating elbow flexion in vitro. These are the vertical, horizontal, valgus, and varus positions (Figure 2.1). Isolating elbow motion in each of these discrete positions permits the modeling and understanding of kinematics and loading experienced during *in-vivo* flexion.

The weight of the forearm generates a moment about the elbow which resists the moments generated by the muscles controlling flexion. The resistance moment depends on the distance of the forearm's center of mass to the elbow joint, and is a function of flexion angle and gravity load direction (*i.e.* vertical, horizontal, valgus, varus). Simulated active elbow flexion in the vertical position has been extensively reported in the literature (Dunning *et al*., 2003; Johnson *et al*., 2000). In this position, the gravity-assisted load resists flexion, and thus provides a stabilizing effect by maintaining tension on the agonist muscles of flexion (Biceps, Brachialis and Brachioradialis), thus requiring little control for the antagonists (*i.e.* Triceps).

Simulated active flexion has been achieved by loading relevant muscles using pneumatic or hydraulic actuators, or via motor control (Bottlang *et al*., 2000; Sojbjerg *et al*., 1987b; Sojbjerg *et al*., 1987a; Kuxhaus *et al*., 2009; Tanaka *et al*., 1998).

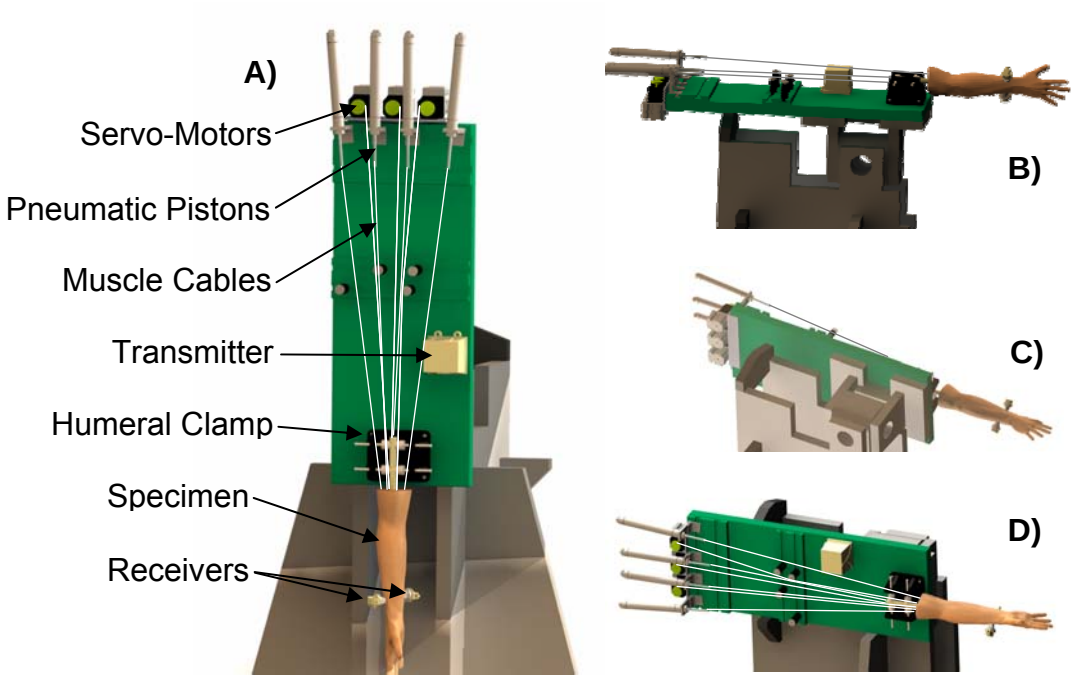

Figure 2.1: Elbow Motion Simulator

The simulator is shown in the (A) Vertical, (B) Horizontal, (C) Varus, and (D) Valgus positions. Specimens were mounted in a humeral clamp. A 6DOF tracker transmitter was fixed relative to the humerus and two receivers mounted to the ulna and radius. Various muscle tendons were sutured to stainless steel cables, which were then connected to servo-motors and pneumatic pistons. Computer control produced simulated active flexion using flexion angle feedback from the tracker. Right arm shown.

Most of these systems have been able to produce highly reproducible flexion in the vertical position, and some success has been achieved in the varus and valgus loaded positions as well. However, no system has been developed that is capable of generating active flexion in the horizontal, valgus and varus positions. Thus, the effects of simulated muscle activation on elbow joint laxity and kinematic pathways in these positions has not been reported. Furthermore, the appropriateness of passive flexion with regard to accurately modeling physiological motion remains unknown.

Hence, the objective of this study was to develop and test a new elbow motion and loading system capable of generating repeatable active elbow flexion for the vertical, horizontal, valgus and varus positions. It was hypothesized that *in-vitro* elbow flexion can be achieved in these positions using muscle tension and flexion angle feedback with transfer functions for control of muscle tension. Simulated active flexion was compared to passive flexion for repeatability, elbow joint laxity and kinematic pathways.

2.2 METHODS

Four previously frozen cadaveric upper extremities (67 ± 5 years, 2 male), amputated at the mid-humeral level, were mounted with a humeral clamp in a testing apparatus which was capable of positioning the arm in the vertical, horizontal, valgus and varus positions (Figure 2.1) (Johnson *et al.*, 2000). Sutures were secured to the distal tendons of the wrist flexors (flexor carpi ulnaris and flexor carpi radialis), wrist extensors (extensor carpi ulnaris and extensor carpi radialis longus), Brachioradialis, Pronator Teres, Supinator, Biceps, Brachialis and Triceps. The supinator origin was simulated using a suture anchor placed at the centre of the attachment point on the radial tuberosity. The suture was passed through an interosseous tunnel in the ulnar canal and exited the proximal aspect of the olecranon. Physiological lines of action for the tendons were maintained with suture alignment guides. The tendon sutures were transitioned to stainless steel cables which were connected to mechanical actuators. Tissues were kept moist with normal saline irrigation during dissections and by suturing the skin closed throughout testing. The skin incision was sutured using similar techniques which are

employed clinically, so as to closely replicate its condition prior to the incision, and to avoid interference with muscle lines of action.

The Brachialis, Biceps and Triceps were simulated by actuating servo-motors (SM2315, Animatics Corp., CA). Load feedback for these modeled muscles was measured with strain-gauge instrumented motor mounts. The remaining muscles were simulated by pneumatic pistons (Bimba Co., IL). Elbow kinematics and flexion angle were quantified from the real-time 6DOF (6 degree of freedom) pose readings of an electromagnetic tracking system (manufacturer-specified accuracy: 1.8 mm, 0.5º RMS) (Flock of Birds, Ascension Technology, VT) via a receiver fixed to the ulna (Johnson *et al*., 2000; King *et al*., 1999; Milne *et al*., 1996). The tracker's transmitter (global coordinate reference) was fixed on the simulator with respect to the humerus.

Each active flexion trial had one muscle designated as the "prime mover", which moved according to a predefined motion profile in order to produce a near constant flexion rate. This motion profile was created by first performing a flexion trial in the vertical position with a constant "prime mover" motor velocity, while recording the motor position feedback and the elbow flexion angle feedback. The inverse of the recorded flexion angle *vs*. motor position relationship produces a non-linear motor position curve corresponding to a linear flexion angle progression. This motor position curve was then sent to the prime mover motor to be "replayed" for each flexion trial. Since the recorded motion profile remained the same for each specimen throughout the protocol, the controller did not account for real-time changes, and thus the flexion rate was termed "near constant".

The remaining agonist muscles of flexion (other than the prime mover) were load-controlled as a function of prime mover load, or position-controlled as a function of flexion angle. Real-time flexion angle and prime mover tension were used as inputs to the transfer function of each muscle. The control protocols (Table 2.1) evolved from those of a previously reported vertical flexion simulator which employed muscle loading ratios derived from EMG and muscle cross-sectional area (Amis *et al*., 1979; Funk *et al*., 1987; Johnson *et al*., 2000). Defining the flexion angle as 0º at full extension and increasing as elbow flexion progresses, the following is a brief description of the control protocols in

Table 2.1. In the horizontal position, the secondary flexion agonist (Biceps or Brachialis) tension was reduced logarithmically after 60º flexion to avoid uncontrolled forearm acceleration. In the varus and valgus positions, Triceps antagonist tension was required to maintain extension at the beginning of flexion. Since the supinator suture/cable was routed out the proximal olecranon to maintain the line-of-action, supinator tension also contributed as an antagonist to flexion. Thus for supinated flexion, Triceps antagonist was reduced to compensate. Pronator teres and supinator were tensioned at 30-40 N as needed to produce pronated or supinated flexion respectively, except in the vertical position where supinator was not used due to sufficient supination from Biceps. Wrist flexors and extensors were tensioned to 10 N each in order to maintain neutral wrist flexion. Since the muscle moment arms involved in flexion are also affected by the forearm rotation angle (Ettema *et al*., 1998; Kuxhaus *et al*., 2009), separate control protocols were developed for pronated and supinated flexion. These protocols are summarized in Table 2.1.

Passive flexion trials were also performed on each specimen. The investigator held the specimen by the wrist while manually flexing the elbow. In the vertical position, the investigator caused flexion by lifting the specimen at the wrist while attempting not to impose any undue varus-valgus angulations. In the varus and valgus positions, the wrist was gripped lightly and the specimen was allowed to follow the gravity-loaded pathway. In the horizontal position, the wrist and hand were gripped lightly and flexion was manually produced in a similar manner as in the vertical position. The hand was supported in the horizontal position in order to prevent it from falling after 90º of elbow flexion.

Anatomic coordinate reference systems for each bone were established by digitizing appropriate osseous landmarks following the completion of testing (Rath, 1997). Kinematic data was transformed into these anatomic coordinate systems, permitting direct measurements of the motion of the ulna relative to the humerus (*i.e.* varus-valgus flexion pathways).

A)

	Flexion Position			
	Vertical	Horizontal	Valgus	Varus
Brachialis (BR)	PM	PM	PM	PM
Biceps	52%BR	θ≤60˚: 39%BR θ>60˚: -log10(θ)	52%BR	52%BR
Brachioradialis	40%BR	40%BR	40%BR	40%BR
Triceps	15 N	θ≤90˚: 15 N θ>90˚: 5 mm/s	15 N	30 N
Pronator Teres	30-40 N	30-40 N	30-40 N	30-40 N
Supinator	0 N	0 N	0 N	0 N

B)

	Flexion Position			
	Vertical	Horizontal	Valgus	Varus
Brachialis (BR)	PM	PM	52%BI	52%BI
Biceps (BI)	52%BR	θ≤60˚:100%BR θ>60˚: -log10(θ)	PM	PM
Brachioradialis	29%BR	29%BR	38%BI	38%BI
Triceps	15 N	θ≤90˚: 15 N θ>90˚: 5 mm/s	15 N	30 N
Pronator Teres	0 N	0 N	0 N	0 N
Supinator	30-40 N	30-40 N	30-40 N	30-40 N

Table 2.1: Flexion Control Transfer Functions

During (A) pronated and (B) supinated flexion, the prime mover (PM) was position-controlled. Other muscle loads were a percentage of PM, a fixed load, or a fixed velocity. In the horizontal position, Biceps and Triceps control was also a function of flexion angle (θ). Flexion angle (θ) is defined as 0º at full extension and increasing as elbow flexion progresses. These muscle loading ratios and absolute loads evolved from those of a previously reported vertical flexion simulator which employed muscle loading ratios derived from EMG and muscle cross-sectional area (Amis *et al*., 1979; Funk *et al*., 1987; Johnson *et al*., 2000).

Five trials of simulated active and passive flexion were performed in each of the vertical, horizontal, valgus and varus positions. Elbow kinematics were quantified as valgus angle versus flexion angle. Varus-valgus laxity of the elbow was quantified as the difference in valgus angulation with the arm oriented in the varus and valgus positions. Average laxity for a flexion trial was calculated as the varus-valgus laxity throughout the flexion range at 2º flexion increments. Repeatability was calculated as the standard deviation of the valgus angle throughout the flexion range for five trials at 2º flexion increments (Johnson *et al*., 2000). Statistical analysis consisted of a two-way analysis of variance and pair-wise comparison procedure using SPSS 17.0 (SPSS Inc., Chicago, IL). Independent variables were simulation method (active *vs*. passive) and flexion angle.

2.3 RESULTS

Active flexion was more repeatable than passive in the pronated and supinated vertical and valgus positions, as well as the supinated horizontal position ($p < 0.05$) (Figure 2.2). There was no statistically significant difference in repeatability for pronated horizontal flexion ($p = 0.07$), or in the varus position for either pronated ($p = 0.8$) or supinated ($p = 0.3$) flexion.

The difference between kinematics in the varus and valgus positions (*i.e.* joint laxity) was less for active than passive flexion in both the pronated and supinated positions ($p < 0.05$) (Figure 2.3). Average varus-valgus joint laxity in pronation was 5.9 ± 1.2° for active flexion and 7.6 ± 2.1° for passive flexion. Average varus-valgus joint laxity in supination was 6.1 ± 1.8° for active flexion and 8.6 ± 2.5° for passive flexion. This corresponded to a reduction in joint laxity of 26% for pronated and 29% for supinated flexion when using active flexion.

Active flexion resisted gravity loading more than passive in the pronated and supinated valgus positions, and in the supinated varus position ($p < 0.05$) (Figure 2.3). There was no difference between active and passive flexion in the pronated varus position ($p = 0.08$).

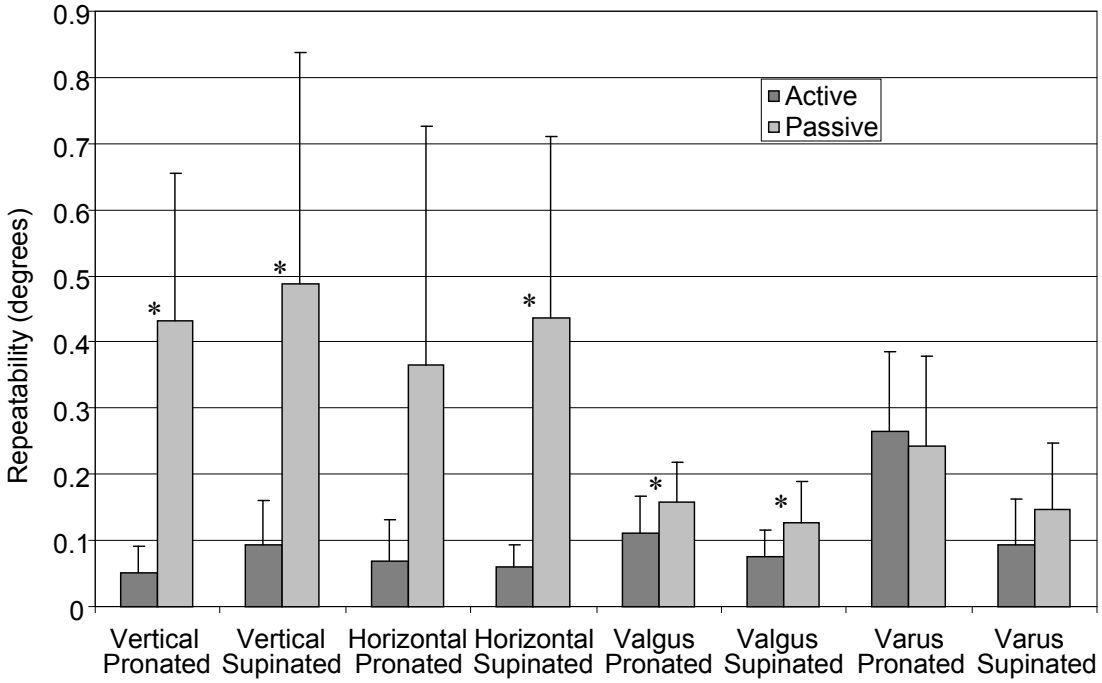

Figure 2.2: Repeatability of Valgus Angulation

Five trials of active and passive flexion were performed. The mean standard deviation of the valgus angle of four specimens was calculated throughout the flexion range. Bars represent 1 standard deviation. Active flexion was more repeatable than passive in the pronated and supinated vertical and valgus positions, as well as the supinated horizontal position *($p < 0.05$).

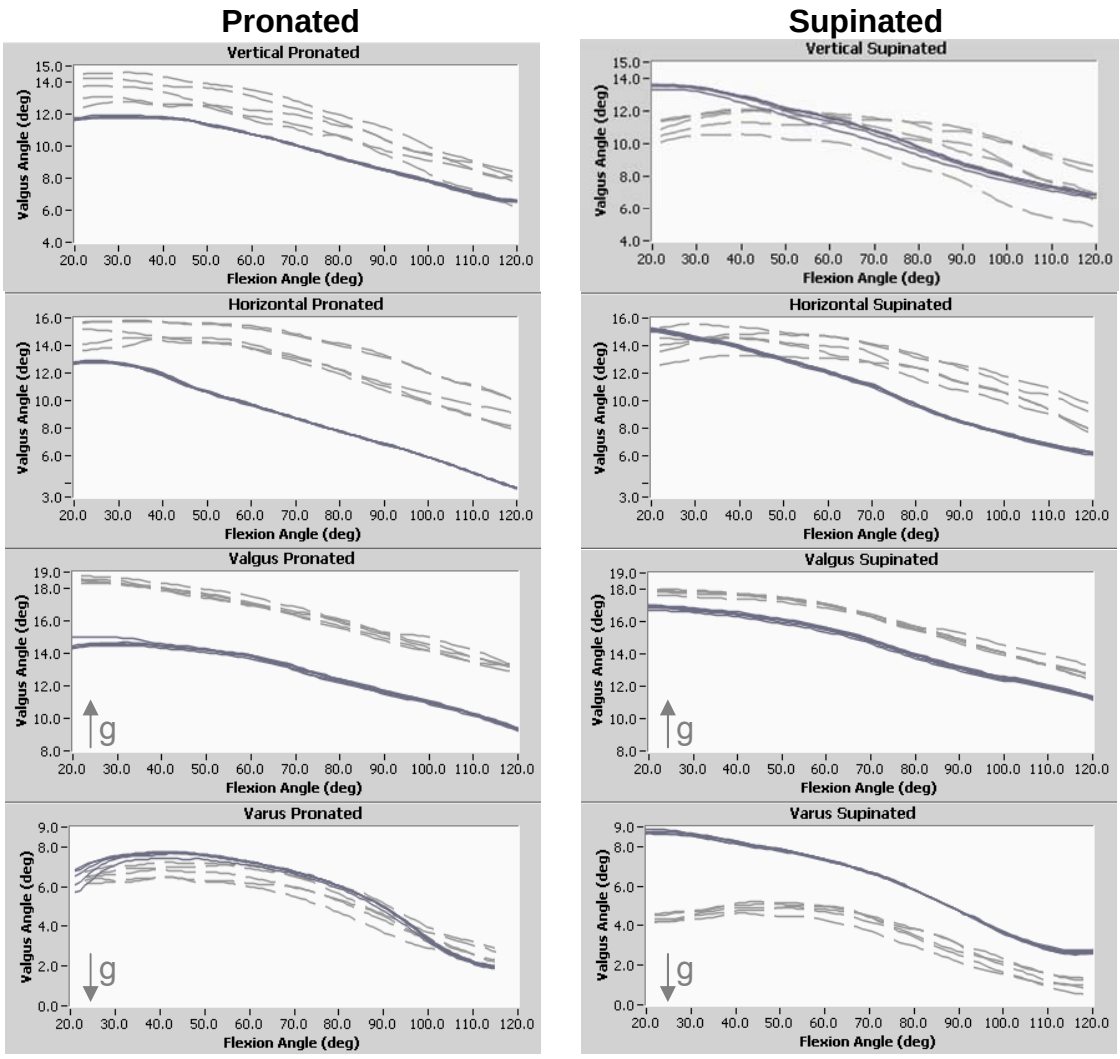

Figure 2.3: Valgus Angle Pathways

Five trials of valgus pathways for active (solid) and passive (dashed) flexion are shown for one specimen. Active flexion resisted gravity loading more than passive flexion in the pronated and supinated valgus positions, and in the supinated varus position ($p < 0.05$). There was no difference between active and passive flexion in the pronated varus position ($p = 0.08$). The difference between kinematics in the varus and valgus positions (*i.e.* joint laxity) was less for active than passive flexion ($p < 0.05$). The g denotes the gravity load direction.

2.4 DISCUSSION

Performance of the current simulator in the vertical position agrees with similar previous studies, which showed that flexion kinematics in the vertical position are significantly different for active versus passive flexion, and that active flexion is more repeatable than passive (Dunning *et al*., 2001; Johnson *et al*., 2000). Active flexion was also more repeatable than passive flexion for the valgus, vertical and supinated horizontal positions. There was no difference in the varus or pronated horizontal positions. The difference in repeatability of active *vs*. passive flexion was also less pronounced in the valgus position. This is likely because the kinematic pathways in the varus and valgus positions are largely limited by osseous and ligamentous constraints. In these positions, passive flexion would be expected to be guided by these constraints, thus producing a repeatable flexion pathway. By contrast, in the horizontal and vertical positions, passive flexion would not be subjected to substantial valgus or varus constraints, relying primarily on the investigator's input.

Greater repeatability of simulated active flexion suggests that this mode of *in-vitro* testing should reduce the standard error of kinematic dependent variables in biomechanics investigations, and thus increase statistical power and decrease required sample sizes. This is consistent with investigations of statistical methods in biomechanics which emphasize "a need to make every reasonable attempt to control and minimize within-subject variability." (Bates *et al*., 1992; Dufek *et al*., 1995).

In the horizontal, varus and valgus positions, the challenge of generating active flexion is due to the relationship between the resistance moment and muscle moment arms. In the varus and valgus positions, the carrying angle changes with flexion angle (Van Roy *et al*., 2005). Thus, the gravity load vector in these positions causes the resistance moment to sometimes tend toward elbow extension. Therefore, muscle load control must shift to the antagonist (Triceps) muscle throughout varus or valgus flexion. However, in these positions, the gravity load vector is perpendicular to the flexion plane,

and so the component of gravity load contributing to generate the resistance moment is relatively small compared to the muscle moments.

Generating active flexion in the horizontal position is a markedly greater challenge. At full extension, the resistance moment is at its greatest because the gravity load vector through the forearm's center of mass is furthest from the elbow joint. Also at full extension, the agonist muscle moment arms are at their shortest (Kuxhaus *et al*., 2009; Pigeon *et al*., 1996; An *et al*., 1981; Ettema *et al*., 1998). This creates a "worst case scenario" in terms of mechanical advantage to initiate flexion. As flexion progresses, the resistance moment decreases in an exponential fashion to zero at 90º, where the resistance moment arm is zero. Hence, the control system must be able to quickly reduce the high agonist loads to prevent the forearm from accelerating. But if the agonist loads are decreased too rapidly, then the forearm will fall back toward extension due to the resistance moment. Flexion control is challenged further by reversal of the resistance moment past 90º, where Triceps takes over as the primary flexion controller, and the "worst case scenario" shifts toward full flexion. In contrast, in the vertical position the resistance moment is lowest at full extension and thus eases the initiation of flexion. Also the resistance moment is greatest at 90º, just where the agonist muscle moment arms are also at their maximum (Kuxhaus *et al*., 2009; Pigeon *et al*., 1996; An *et al*., 1981; Ettema *et al*., 1998).

Muscle loads are relatively lower in the vertical, varus and valgus positions, which allows the muscle/tendon complexes to be more compliant and to absorb rapid changes in actuator velocities. In contrast, horizontal flexion with a highly dynamic resistance moment, is an inverted pendulum balancing problem, and is made more difficult by the increased muscle tensions which cause the muscle/tendon complexes to become less compliant, making a more rigid system. Thus, any inadequacies of the controller (*i.e.* under- or over-compensating efforts) are much less tolerated because the highly tensioned muscles efficiently transmit changes in loads, converting them into rapid accelerations which can quickly destabilize the system.

The advantage of active flexion in the varus and valgus positions was more apparent in terms of kinematic pathway and joint laxity. In these positions, simulated

muscle activation caused the arms to track at less than the laxity limits of the collateral ligaments, and thus most certainly relieved some of the stresses on these stabilizing structures. This decrease in varus-valgus joint laxity can be attributed to the simulated muscle loads overcoming the relatively large varus and valgus moments produced by gravity loading of the forearm. Thus, active flexion clearly outperforms passive flexion in these positions, suggesting that muscle tension compresses the articular surfaces of the elbow, increasing osseous stability, or alternatively guides the elbow motion pathways directly.

In the varus position with pronation, active flexion provided no significant resistance to gravity load compared to passive flexion. This may have been due to differences between the pronated and supinated flexion control protocols. In order to achieve forearm pronation, 30-40 N were applied to the Pronator Teres. The Pronator Teres has been found to cause significant elbow varus movement, relieving valgus stresses (Lin *et al*., 2007; Udall *et al*., 2009). This further validates our results, which show that in all positions, the actively flexed arm tracked in less valgus when pronated than when supinated.

A previously reported vertical flexion simulator employed muscle loading ratios derived from EMG and muscle cross-sectional area (Amis *et al*., 1979; Funk *et al*., 1987; Johnson *et al*., 2000). These ratios were the basis for the current controller. However, there is a lack of EMG data in the literature for flexion in the varus, valgus and horizontal positions. Furthermore, and as discussed, these positions reveal and amplify any inadequacies of the control protocol or assumptions in the elbow flexion model, which are otherwise well tolerated in the vertical position. Thus the control protocols of Table 2.1 evolved from those of the original vertical simulator by addressing the various aspects of flexion in each position on an individual basis. As a result, the control protocols were developed in an iterative process. Future development should include further studies of EMG activity in all the principle flexion positions in order to refine the control protocols.

Little data exists with respect to physiologic motion pathways or *in-vivo* control of muscle forces, particularly for the different anatomical positions simulated in the current investigation. Hence, this limits our ability to compare *in-vitro* pathways with

those which might occur *in-vivo*. Still, the kinematic pathways reported herein are similar to those documented by other investigators, and display the characteristic decreasing valgus angle with increasing flexion angle (Van Roy *et al*., 2005). Furthermore the passive and active mean kinematic pathways were similar in shape, again supporting the clinical relevance of this approach. The high repeatability of the simulator motion pathways suggests that it should be useful for laboratory based studies of non-surgical and surgical treatments for elbow disorders.

2.5 ACKNOWLEDGEMENTS

Funding for this research was provided by the Canadian Institute for Health Research (CIHR).

2.6 REFERENCES

Amis A A, Dowson D, Wright V, Miller J H. The derivation of elbow joint forces, and their relation to prosthesis design. J Med Eng Technol 1979; (3): 229-234.

An K N, Hui F C, Morrey B F, Linscheid R L, Chao E Y. Muscles across the elbow joint: a biomechanical analysis. J Biomech 1981; (14): 659-669.

Baratz M E, Des Jardins J D, Anderson D D, Imbriglia J E. Displaced intra-articular fractures of the distal radius: The effect of fracture displacement on contract stresses in a cadaver model. The Journal of Hand Surgery 1996; (21): 183-188.

Bates B T, Dufek J S, Davis H P. The effect of trial size on statistical power. Med Sci Sports Exerc 1992; (24): 1059-1065.

Bottlang M, O'Rourke M R, Madey S M, Steyers C M, Marsh J L, Brown T D. Radiographic determinants of the elbow rotation axis: experimental identification and quantitative validation. J Orthop Res 2000; (18): 821-828.

Dufek J S, Bates B T, Davis H P. The effect of trial size and variability on statistical power. Med Sci Sports Exerc 1995; (27): 288-295.

Dunning C E, Duck T R, King G J, Johnson J A. Simulated active control produces repeatable motion pathways of the elbow in an in vitro testing system. J Biomech 2001; (34): 1039-1048.

Dunning C E, Gordon K D, King G J, Johnson J A. Development of a motion-controlled in vitro elbow testing system. J Orthop Res 2003; (21): 405-411.

Ettema G, Styles G, Kippers V. The Moment Arms of 23 Muscle Segments of the Upper Limb With Varying Elbow and Forearm Positions: Implications for Motor Control. Human Movement Science 1998; (17): 201-220.

Funk D A, An K N, Morrey B F, Daube J R. Electromyographic analysis of muscles across the elbow joint. J Orthop Res 1987; (5): 529-538.

Itoi E, King G J, Neibur G L, Morrey B F, An K N. Malrotation of the humeral component of the capitellocondylar total elbow replacement is not the sole cause of dislocation. J Orthop Res 1994; (12): 665-671.

Johnson J A, Rath D A, Dunning C E, Roth S E, King G J. Simulation of elbow and forearm motion in vitro using a load controlled testing apparatus. J Biomech 2000; (33): 635-639.

King G J, Itoi E, Risung F, Niebur G L, Morrey B F, An K N. Kinematic and stability of the Norway elbow. A cadaveric study. Acta Orthop Scand 1993; (64): 657-663.

King G J, Zarzour Z D, Rath D A, Dunning C E, Patterson S D, Johnson J A. Metallic radial head arthroplasty improves valgus stability of the elbow. Clin Orthop 1999; (114-25.).

Kuxhaus L, Schimoler P J, Vipperman J S, Miller M C. Validation of a Feedback-Controlled Elbow Simulator Design: Elbow Muscle Moment Arm Measurement. Journal of Medical Devices 2009; (3).

Lin F, Kohli N, Perlmutter S, Lim D, Nuber G W, Makhsous M. Muscle contribution to elbow joint valgus stability. J Shoulder Elbow Surg 2007; (16): 795-802.

Milne A D, Chess D G, Johnson J A, King G J. Accuracy of an electromagnetic tracking device: a study of the optimal range and metal interference. J Biomech 1996; (29): 791-793.

Morrey B F, Tanaka S, An K N. Valgus stability of the elbow. A definition of primary and secondary constraints. Clin Orthop Relat Res 1991;187-195.

O'Driscoll S W, An K N, Korinek S, Morrey B F. Kinematics of semi-constrained total elbow arthroplasty. J Bone Joint Surg Br 1992; (74): 297-299.

Olsen B S, Sojbjerg J O, Nielsen K K, Vaesel M T, Dalstra M, Sneppen O. Posterolateral elbow joint instability: the basic kinematics. J Shoulder Elbow Surg 1998; (7): 19-29.

Pigeon P, Yahia L, Feldman A G. Moment arms and lengths of human upper limb muscles as functions of joint angles. J Biomech 1996; (29): 1365-1370.

Pomianowski S, Morrey B F, Neale P G, Park M J, O'Driscoll S W, An K N. Contribution of monoblock and bipolar radial head prostheses to valgus stability of the elbow. J Bone Joint Surg Am 2001a; (83-A): 1829-1834.

Pomianowski S, O'Driscoll S W, Neale P G, Park M J, Morrey B F, An K N. The effect of forearm rotation on laxity and stability of the elbow. Clin Biomech (Bristol , Avon) 2001b; (16): 401-407.

Rath DA. Design and development of an elbow loading apparatus and determination of elbow kinematics. 1997. The University of Western Ontario.
Ref Type: Thesis/Dissertation

Seiber K, Gupta R, McGarry M H, Safran M R, Lee T Q. The role of the elbow musculature, forearm rotation, and elbow flexion in elbow stability: an in vitro study. J Shoulder Elbow Surg 2009; (18): 260-268.

Sojbjerg J O, Ovesen J, Gundorf C E. The stability of the elbow following excision of the radial head and transection of the annular ligament. An experimental study. Arch Orthop Trauma Surg 1987a; (106): 248-250.

Sojbjerg J O, Ovesen J, Nielsen S. Experimental elbow instability after transection of the medial collateral ligament. Clin Orthop 1987b; (186-90.).

Tanaka S, An K N, Morrey B F. Kinematics and Laxity of Ulnohumeral Joint Under Valgus-Varus Stress. Journal of Musculoskeletal Research 1998; (2): 45-54.

Udall J H, Fitzpatrick M J, McGarry M H, Leba T B, Lee T Q. Effects of flexor-pronator muscle loading on valgus stability of the elbow with an intact, stretched, and resected medial ulnar collateral ligament. J Shoulder Elbow Surg 2009; (18): 773-778.

Van Roy P, Baeyens J P, Fauvart D, Lanssiers R, Clarijs J P. Arthro-kinematics of the elbow: study of the carrying angle. Ergonomics 2005; (48): 1645-1656.

CHAPTER 3 – THE DEVELOPMENT AND VALIDATION OF A NOVEL CONTROLLER FOR UNIFIED CONTROL OF JOINT ANGLE AND MUSCLE TENSION FOR AN ELBOW MOTION SIMULATOR

OVERVIEW: *This chapter details the design and development of a real-time control loop which governs elbow joint angle using both feedback from joint angle and muscle tension. Process models for feedforward control are also presented. The feedback controller was implemented as a Cascade Proportional-Integral-Derivative (PID) design in which a primary PID loop controls joint angle by affecting the setpoint of a nested secondary PID loop which controls muscle tension. Tension was controlled for three major muscles simulated simultaneously using servo-motors. The controller's ability to follow a desired joint angle (setpoint) curve was evaluated in seven cadaveric arms for all four testing positions with the forearm in both pronation and supination. The largest absolute angular error was 5.3 ± 2.4º for flexion, and 4.5 ± 2.8º for extension. For any individual specimen, the largest error was 9.4º for flexion and 13.3º for extension. RMS errors for flexion were all less than 3.0º except for vertical pronated flexion (4.1º). RMS errors for extension were 1.7-4.1º, except for valgus supinated flexion (5.1º). The controller was able to accurately follow the setpoint curve at a flexion-extension rate of 10º/s, and in all positions.*[1]

1) This work in being prepared for submission to *The Journal of Biomechanics*.

3.1 INTRODUCTION

Producing flexion-extension using an elbow motion simulator with the humerus in horizontal positions presents considerable challenges which are not present in the vertical position. These challenges were discussed by Ferreira and co-workers (2010) (Chapter 2). The flexion controller developed and employed for that study was the first capable of simulating the full range of active elbow flexion in all positions, and with superior repeatability and less joint laxity than passive flexion. Testing demonstrated that simulated active flexion outperforms passive flexion as a mode of *in-vitro* testing by reducing the standard error of kinematic dependent variables. This has the benefit of increasing statistical power and decreasing required sample sizes.

Some previously reported simulators from the Allegheny General Hospital (AGH) in Pittsburgh have achieved active flexion by loading relevant muscles (Kuxhaus *et al.*, 2009; Kuxhaus, 2008; Schimoler, 2008). While not yet capable of horizontal flexion-extension, the AGH control scheme was based on a previous simulator, which used displacement-control for the brachialis, dubbed the 'prime mover of flexion', and all other muscles were load-controlled (Dunning *et al.*, 2001; Dunning *et al.*, 2003). This simulator was designed primarily for vertical flexion, and in his thesis dissertation, Schimoler (2008) correctly noted the shortcoming of the brachialis 'prime mover' in positions other than vertical. Their solution for the AGH simulator was to switch the prime mover to the triceps when the brachialis load fell below a user-defined minimum, which caused triceps to pull the joint angle down when it surpassed the desired setpoint. Of course, the AGH is still a 'prime mover' simulator in principle, as it follows the paradigm that one muscle should be driven with displacement-control, while the rest are load-controlled as determined by some load transfer functions. While the AGH simulator has had some success in the varus and valgus positions, special challenges in the horizontal position may preclude the use of 'prime mover' control, which also puts into question its suitability for the varus and valgus positions. Furthermore, in their investigation of simulator performance, Dunning *et al.* (2003) also noted that switching

the prime mover from brachialis to biceps had no apparent effect on performance (Dunning *et al.*, 2003). This would seem to suggest that the 'prime mover' method might not be the best elbow motion model.

The control protocols described by Ferreira *et al*. (2010) (Chapter 2) evolved from those of the original vertical position simulator (Dunning *et al.*, 2003), by addressing the various aspects of flexion in each of the four principle positions on an individual basis. As a result, those transfer functions lacked a certain refinement and unifying mathematical approach for elbow flexion in general. This controller was highly repeatable and produced a reduction in joint laxity compared to passive flexion. Real-time flexion angle was used as an input to the controller's transfer functions, but not employed as feedback for error correction. Furthermore, its performance in producing elbow extension was not explored, nor was its performance in generating a constant elbow flexion rate.

It would seem necessary to control muscle tension as well as joint angle if the simulator is to replicate *in-vivo* motion. At least, this would be consistent with physiological joint motor control. However, previous simulator designs have not merged the control of these processes. Furthermore, a joint angle that is controlled by simulated muscle activation is not as responsive as muscle tension. This is because joint angle is indirectly affected by muscle tension/distraction, due to both tissue stretching and muscle antagonism. In light of the foregoing, it was postulated that a Cascade PID control design could merge control of muscle tension and elbow flexion-extension while taking advantage of the differences in responsiveness between the two processes.

The purpose of this study was to develop a closed-loop controller which incorporated joint angle and muscle tension feedback into a unified Cascade PID design for simultaneous control of flexion-extension and muscle tension for multiple muscles. The complete simulator equipped with this new controller was termed the Hand and Upper Limb Centre Multiple Orientation Simulator for the Elbow (HULC MOSE), henceforth referred to as MOSE. The ability of MOSE to follow a constant angular setpoint rate during flexion and extension was then evaluated using cadaveric specimens. The hypothesis was that a constant flexion-extension rate of 10º/s can be achieved with

no more than 5º RMS error in the vertical, varus, valgus and horizontal positions using this controller.

3.2 METHODS

Biceps, brachialis and triceps were actuated using servo-motors (SmartMotor™ SM2315, Animatics, Santa Clara, CA). Joint angle feedback was provided by an electromagnetic tracking system (trakSTAR®, Ascension Technology Corp., Burlington, VT). Muscle tension feedback was provided by custom strain-gauge instrumented motor mounts for each of the servo-motors, as per Appendix B. The various aspects of the controller software, as described in detail in Sections 3.2.1-7 ahead, were programmed using LabVIEW® (National Instruments Inc., Austin, TX).

As with some previously reported simulators, the system presented here uses PID (Proportional Integral Derivative) control to govern the elbow flexion-extension process. This uses the current joint angle (process variable) to determine the difference (error) between the desired angle (setpoint) and the current joint angle. The PID output (process output) acts to minimize that error, also referred to as closed-loop feedback control.

Unlike previous simulators, the controller for this system simultaneously controls muscle tension for biceps, brachialis and triceps. It does this with a controller configuration referred to as a Cascade PID design. Feedforward transfer functions are also integrated into the controller, which provide *a-priori* process adjustments. The following sections describe the major controller elements.

3.2.1 CASCADE PID CONTROLLER WITH FEEDFORWARD TRANSFER FUNCTIONS

The process to be controlled is a combination of two sequential processes (***i.e.*** joint angle and muscle tension). These processes have different response characteristics, and so cannot be governed by a single controller (Patranabis, 1996). The muscle tension process has influence over the joint angle process, and so muscle tension feedback is required for closed-loop control of this process. Moreover, the muscle tension process has very fast process dynamics. For these reasons, a Cascade PID configuration (Figure 3.1)

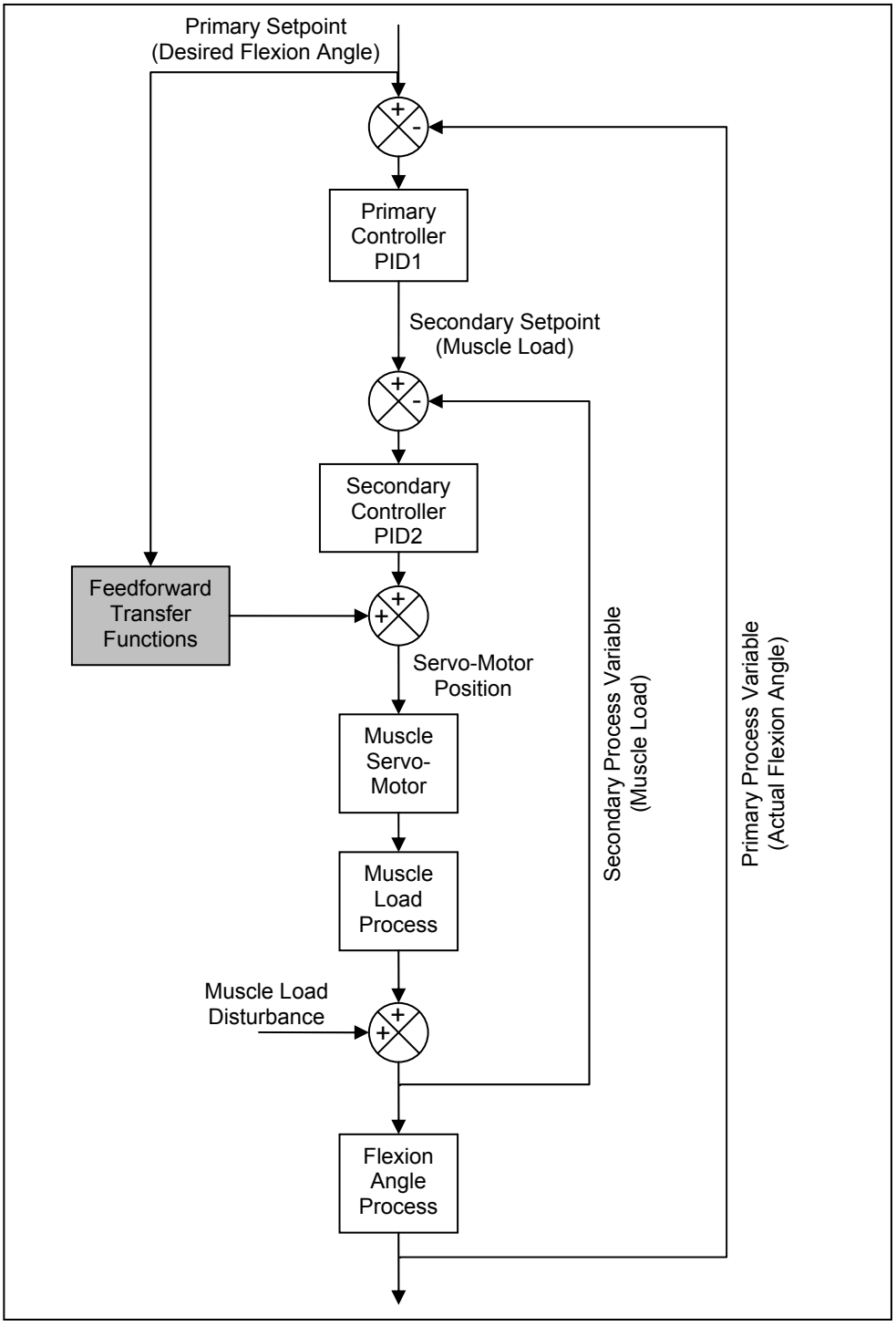

Figure 3.1: Cascade PID Controller with Feedforward Control

Controller output is dominated by the feedforward control output. The PID controller makes fine adjustments to correct errors in the process variable from the desired setpoint.

was selected (Erickson and Hedrick, 1999). The overall controller includes both feedforward and feedback control. The purpose of feedback control is to reduce the error in the process variable. The feedforward transfer function consists of a sum of partial functions which provide the controller with *a-priori* knowledge of the process in the form of a mathematical model.

The Cascade PID design controls joint angle (primary process) with an outer loop (PID1), while muscle tension (secondary process) is controlled by a nested inner loop (PID2) (Blevins and Nixon, 2011). Feedforward transfer functions provide *a-priori* anticipatory action, while the PID controllers react to process errors and work to minimize them (Leigh, 1987b).

3.2.2 CASCADE PID WITH MULTIPLE MUSCLES

Tension in the brachialis, biceps brachii and triceps muscles were controlled with separate secondary PID2 loops (Figure 3.2). By having distinct tension controllers for each muscle, flexor and extensor controllers can individually adjust motor displacement in order to find the tension that satisfies the joint angle setpoint. Since flexors and triceps have opposite effects on joint angle, the sign of the triceps ΔTension is reversed.

The secondary nested PID loop for tension control was implemented as a subroutine with scalable input/output arrays for the tension-controlled muscles. Scalability allows the controller to automatically adjust to the desired number of tension-controlled muscles.

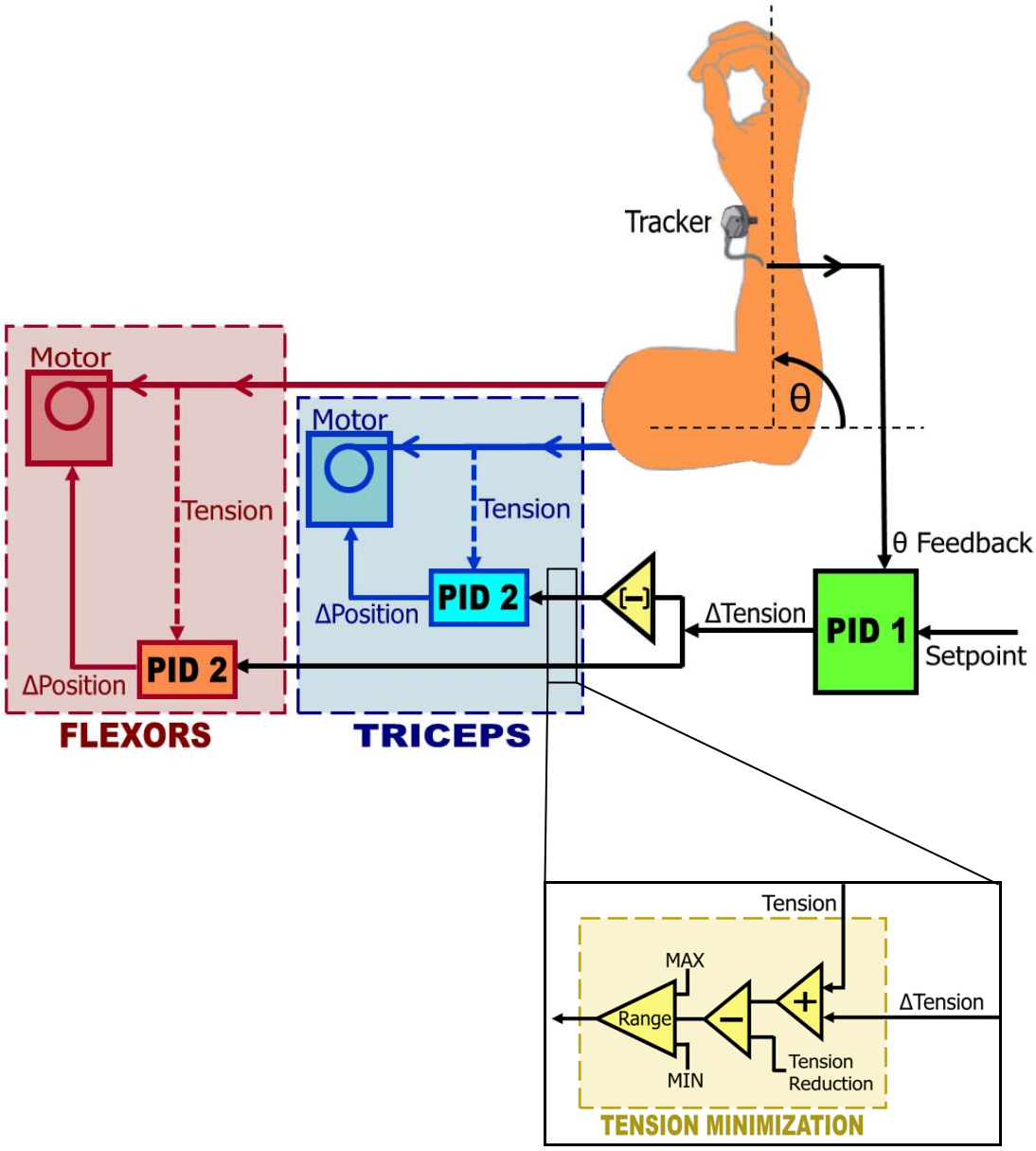

Figure 3.2: Cascade PID Joint Angle Controller

Each muscle has a dedicated PID2 controller. Tension setpoint from the PID1 output can be apportioned in any desired ratio to the setpoint inputs of each PID2 muscle controller. Tension minimization is achieved by subtracting a tension reduction amount from the PID setpoint input of each PID2 controller. Right arm shown.

3.2.3 SETPOINT FEEDFORWARD RATE RESPONSE

The output of the muscle/tendon rate function was used as a feedforward control element to anticipate the needs of the muscle/tendon actuator as a function of the current joint angle. The rate of change of the joint angle setpoint input was used to increase motor speed (*i.e.* tendon speed) in anticipation of the increased muscle forces needed to prevent the actual joint angle from falling behind the rapidly changing setpoint input. This anticipatory rate response was modeled as tendon position parallel to the humerus as a function of joint angle. Using a flexor tendon as an example, the relationship between muscle/tendon position p and joint angle θ was determined. With the assumptions that the muscle/tendon line of action remains parallel to the humerus, and that the tendon attachment is a single point at constant distance r from the elbow joint, the relationship is:

$$p = r - r\cos(\theta) \qquad \text{(Eq. 3.1)}$$

The rate of change of muscle/tendon position $dp/d\theta$ can be calculated from the derivative of the muscle/tendon position function:

$$dp/d\theta = d(r - r\cos(\theta))/d\theta = r\sin(\theta) \qquad \text{(Eq. 3.2)}$$

When the outputs of this function and the PID controller are summed, the rate function becomes the dominant control element. In this way, the rate response output becomes the dominant component of the motor displacement command, and the PID component plays a correctional role, which is consistent with feedforward control (Blevins and Nixon, 2011).

3.2.4 MUSCLE TENSION MINIMIZATION

Tension in the muscles must be high enough to maintain joint angle control, but should be minimized in order to achieve an efficient level of work. The controller minimizes muscle tension by applying negative pressure on the muscle tension setpoint of the nested PID2 motor controller. This is achieved by subtracting a tension reduction

amount from the tension setpoint input (Figure 3.2). A tension reduction value of at least 1 N is applied. However in some cases, such as a heavy or long arm, rapid (more aggressive) tension minimization can reduce the requirements on the PID controller. Thus when necessary, 2 N of tension reduction are applied. The circumstances depend on the position of the arm with respect to the gravity vector, and the joint angle. These are listed in Table 3.1.

	Brachialis	Biceps Brachii	Triceps
Vertical	0º to 0º (never)	0º to 0º (never)	-∞º to ∞º (always)
Horizontal	105º to ∞º (late flexion)	105º to ∞º (late flexion)	-∞º to 75º (early flexion)
Varus	-∞º to 120º (all but full flexion)	-∞º to 120º (all but full flexion)	0º to 0º (never)
Valgus	0º to 0º (never)	0º to 0º (never)	-∞º to 120º (all but full flexion)

Table 3.1: Ranges of Rapid Tension Minimization

Tension minimization is increased from 1 N to 2 N in certain flexion ranges as a function of joint angle, and depending on simulator position. The settings which define the ranges of rapid tension minimization are shown, along with descriptions in parentheses.

3.2.5 PRONATION AND SUPINATION

The muscle forces needed to maintain forearm pronation and supination moments were determined using muscle force ratios, as in previous studies (Dunning *et al.*, 2001; Dunning *et al.*, 2003; Ferreira *et al.*, 2010). Since flexors are composed of two muscles (*i.e.* brachialis and biceps brachii), the flexors ΔTension input from the PID1 process must be divided between these muscles. Since biceps is a strong supinator, the total load for flexors must be divided between biceps and brachialis in order to maintain pronation or supination during flexion. The ratio of this division was based on EMG (*i.e.* muscle activity) data and muscle cross-sectional area (Amis *et al.*, 1979; Funk *et al.*, 1987), and ratios from Chapter 2 (Ferreira *et al.*, 2010) Table 3.2.

	Vertical	Horizontal	Valgus	Varus
Pronated	0.52	0.39	0.52	0.52
Supinated	0.52	1.00	1.92	1.92

Table 3.2: Biceps Brachii/Brachialis Muscle Tension Ratios
Shown are the ratios of biceps brachii to brachialis loads for flexion and extension as a function of simulator position and forearm rotation.

The ratios of Table 3.2 are only meant to maintain full pronation or supination during flexion-extension, in conjunction with the pronator and supinator muscles. This ratio control forms a component of the feedforward transfer function (Erickson and Hedrick, 1999). The sum total of the flexor tensions is governed by the flexion control loop PID1. Load ratios for other muscles such as brachioradialis were the same as in Chapter 2.

3.2.6 JOINT ANGLE SETPOINT

A setpoint versus time transfer function is pre-calculated and stored so that the calculation process does not impact real-time performance. This function represents a linear function with slope equal to the desired joint angle rate. The current desired joint angle as a function of time is used as the controller's PID1 setpoint. Since different arms have different ranges of full extension to full flexion, the current elbow joint angle is

automatically used as the start angle.

A curved toe-in region with gradually increasing slope is used to accelerate to the 10º/s flexion rate. This curved region ends with a slope of 10º/s to transition smoothly into the linear setpoint ramp. Thus, the exponential function $\exp(t)$ is used because its value at time t is equal to its slope at time t.

$$\exp(t) = d(\exp(t))/dt \qquad \text{(Eq. 3.3)}$$

This is achieved by first calculating the transition time t_{trans} where the curves will be stitched together. The transition will occur where the value of the exponential function is equal to the desired rate (*i.e.* slope of the setpoint ramp):

$$\exp(t_{trans}) = rate \qquad \text{(Eq. 3.4)}$$

The transition time t_{trans} is calculated as the natural logarithm of the desired rate:

$$t_{trans} = \exp^{-1}(t_{trans}) = \ln(rate) \qquad \text{(Eq. 3.5)}$$

Since $\exp(t) = 1$ at $t = 0$s, this means that all curves start at a rate of 1º/s for 1s, then transition smoothly into the linear ramp at the desired rate. However, this causes a discontinuity of +1º at the start of flexion. This is dealt with by inserting a 1º/s straight ramp for 1s before the exp curve (Figure 3.3). This uses the property that the slope of the exp function at t=1 is 1º/s. Thus, a smooth transition occurs from the initial straight ramp, and the transition to the final ramp is maintained at the convenient slope value. The transition time to the final ramp occurs at t=ln(rate)+1. This also ensures that all flexion curves start at a rate of 1º/s for 1s.

Discrete values are generated from the setpoint *vs.* time transfer function. These are stored in a lookup table indexed by time with interpolated values for fractional time indices. Since interpolation is used, only the endpoints of the straight ramp portions of the setpoint function are stored in the lookup table, which reduces the required memory.

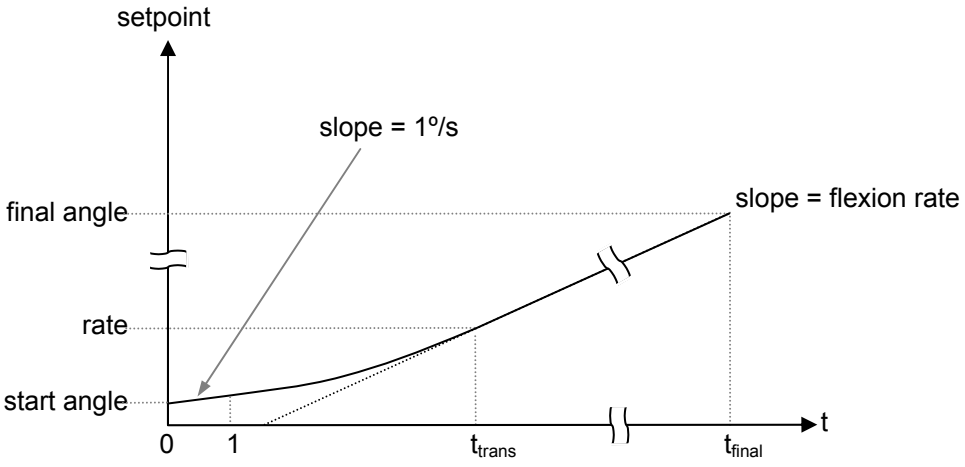

Figure 3.3: Joint Angle Setpoint *vs.* Time

The joint angle setpoint is started gradually by an initial linear ramp at 1º/s for 1s which transitions smoothly into an exponential curve region at $t = 1$s. A smooth transition is made at $t = t_{trans}$ to a linear curve with a 10º/s slope.

3.2.7 SUMMARY OF CONTROLLER IMPLEMENTATION

The elements of the overall MOSE controller, which were developed in Sections 3.2.1-5 above, were integrated into the simulator, as well as the joint angle setpoint generator of Section 3.2.6 above. The continuous functions of the setpoint feedforward rate response (Section 3.2.3), and the setpoint curve itself (Section 3.2.6), were discritized into lookup tables and indexed by joint angle in 0.1˚ increments. The results were looked up by joint angle in real-time with interpolation for intermediate angles. Since interpolation is used, only the endpoints of the straight ramp portion of the setpoint curve were stored in the lookup table, which greatly reduces the required memory. The use of lookup tables avoided the need to calculate continuous functions with each iteration, which reduced processor load and aided in maintaining real-time performance.

The Cascade PID design allows the desired joint angle to affect the muscle tension control loop, which affects the joint angle control loop process variable. This is analogous to *in-vivo* control, in which muscle activation is adjusted to achieve the desired joint angle as determined from proprioceptive feedback from the articulation, and muscle tension is minimized on the basis of stretch receptors in the muscle-tendon unit. An elbow model function is used to implement feedforward control, which provides the main controller action. This leaves the PID elements of the controller to correct for process errors, which is typically the strength of PID control. Thus, the proactive action the feedforward transfer function avoids large process errors, which would result in PID over-corrections.

3.3 EXPERIMENTAL EVALUATION

Performance of the MOSE Cascade PID Controller was evaluated in an *in-vitro* study of seven upper extremities. Specimens were previously frozen (78 ± 7 years, all male), and amputated at the mid-humeral level. Each specimen was mounted with a humeral clamp in the Elbow Motion Simulator (Figure 3.4). Sutures were secured to the distal tendons of the wrist flexors (flexor carpi ulnaris and flexor carpi radialis), wrist extensors (extensor carpi ulnaris and extensor carpi radialis longus), brachioradialis,

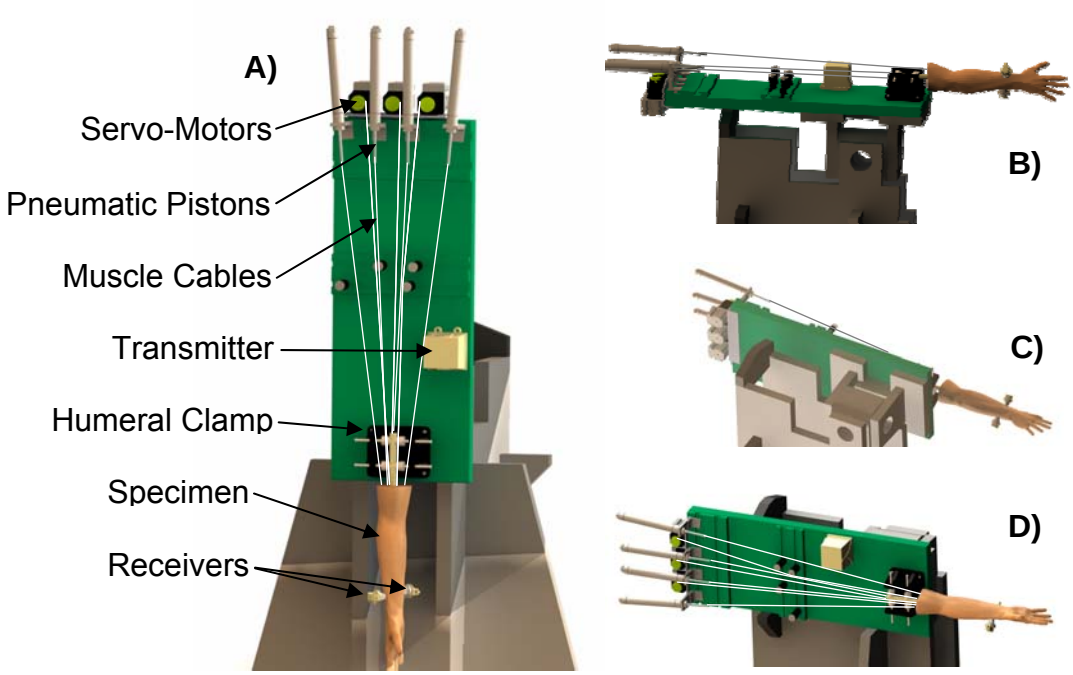

Figure 3.4: Elbow Motion Simulator

The simulator is shown in the (A) Vertical, (B) Horizontal, (C) Varus, and (D) Valgus positions. Specimens were mounted in a humeral clamp. A 6DOF tracker transmitter was fixed relative to the humerus and two receivers mounted to the ulna and radius. Various muscle tendons were sutured to stainless steel cables, which were then connected to servo-motors and pneumatic pistons. Computer control produced simulated active flexion using joint angle feedback from the tracker. Right arm shown.

pronator teres and supinator using a locking Krackow technique (Howard *et al.*, 1997). The supinator origin was simulated using a suture anchor placed at the centre of the attachment point on the radial tuberosity. The suture was passed through an interosseous tunnel in the ulnar canal and exited the proximal aspect of the olecranon. The sutures were transitioned to stainless steel cables which were connected to pneumatic actuators. Guides were mounted on the bones to replicate native muscle moment arms. Alignment guides between the specimen and actuators ensured that the sutures followed physiologic lines of action. Alignment guides for the pronator teres and wrist flexors were located on the medial epicondyle. The wrist extensors guide was on the lateral epicondyle, and the brachioradialis guide was on the supracondylar ridge. Biceps brachii, brachialis and triceps were sutured using heavy braided Dacron® line with the same Krackow technique, and attached to servo-motors via alignment guides.

Simulated active flexion and extension were performed in the vertical, horizontal, varus, and valgus positions, with the forearm maintained in pronation and supination. The rate of flexion was set to 10º/s. Joint angle feedback for motion control, and elbow joint kinematics were collected using an electromagnetic tracking system (trakSTAR®, Ascension Technology Corp., Burlington, VT), by rigidly fixing the humerus relative to the transmitter and mounting a receiver on the ulna. Joint motion kinematics were calculated from the 6DOF pose output of the tracking system.

The error of the actual joint angle compared to the desired setpoint angle was evaluated in the 10-120º flexion range using continuous tracker output. Error was quantified in terms of absolute error as a function of joint angle, and also as RMS (root mean square) error for the entire flexion range. This was done for flexion and extension in all four positions.

3.4 RESULTS

The Cascade PID Controller performed well under all testing conditions. There were no major impediments to flexion-extension, even in the horizontal position which was expected to be the most challenging. No failures occurred due to controller action.

The RMS (root mean square) error of the joint angle controller is shown for each testing condition during flexion (Table 3.3) and extension (Table 3.4). The average (N=7) actual joint angle as a function of the desired joint angle is shown for all tested positions in Figures 3.5 through 3.8. The average (N=7) absolute joint angle error as a function of the desired joint angle is shown for all tested positions in Figures 3.9 through 3.12.

During flexion, the largest absolute errors of 5.2 ± 2.4º and 5.3 ± 2.4º occurred at 115º of flexion in the pronated vertical position (Figure 3.9A), and at 21º of flexion in the supinated horizontal position (Figure 3.10B), respectively. The largest error during flexion for any individual specimen was 9.4º, which also occurred at 21º of flexion for the same condition.

During extension, the largest absolute error of 4.5 ± 2.8º occurred at 106º of extension in the pronated vertical position (Figure 3.11A). The largest error during extension for any individual specimen was 13.3º, which occurred at 25º of flexion for supinated extension in the horizontal position (Figure 3.12B).

Position	Pronated Flexion	Supinated Flexion
Vertical	4.1	1.9
Horizontal	2.7	2.9
Varus	2.8	2.5
Valgus	2.9	2.2

Table 3.3: Joint Angle Root Mean Square Error for Flexion

The RMS (root mean square) error of the joint angle controller throughout the 10-120º flexion range for pronated and supinated flexion.

Position	Pronated Extension	Supinated Extension
Vertical	4.1	1.7
Horizontal	3.0	2.7
Varus	3.8	2.3
Valgus	3.5	5.1

Table 3.4: Joint Angle Root Mean Square Error for Extension

The RMS (root mean square) error of the joint angle controller throughout the 120-10º extension range for pronated and supinated extension.

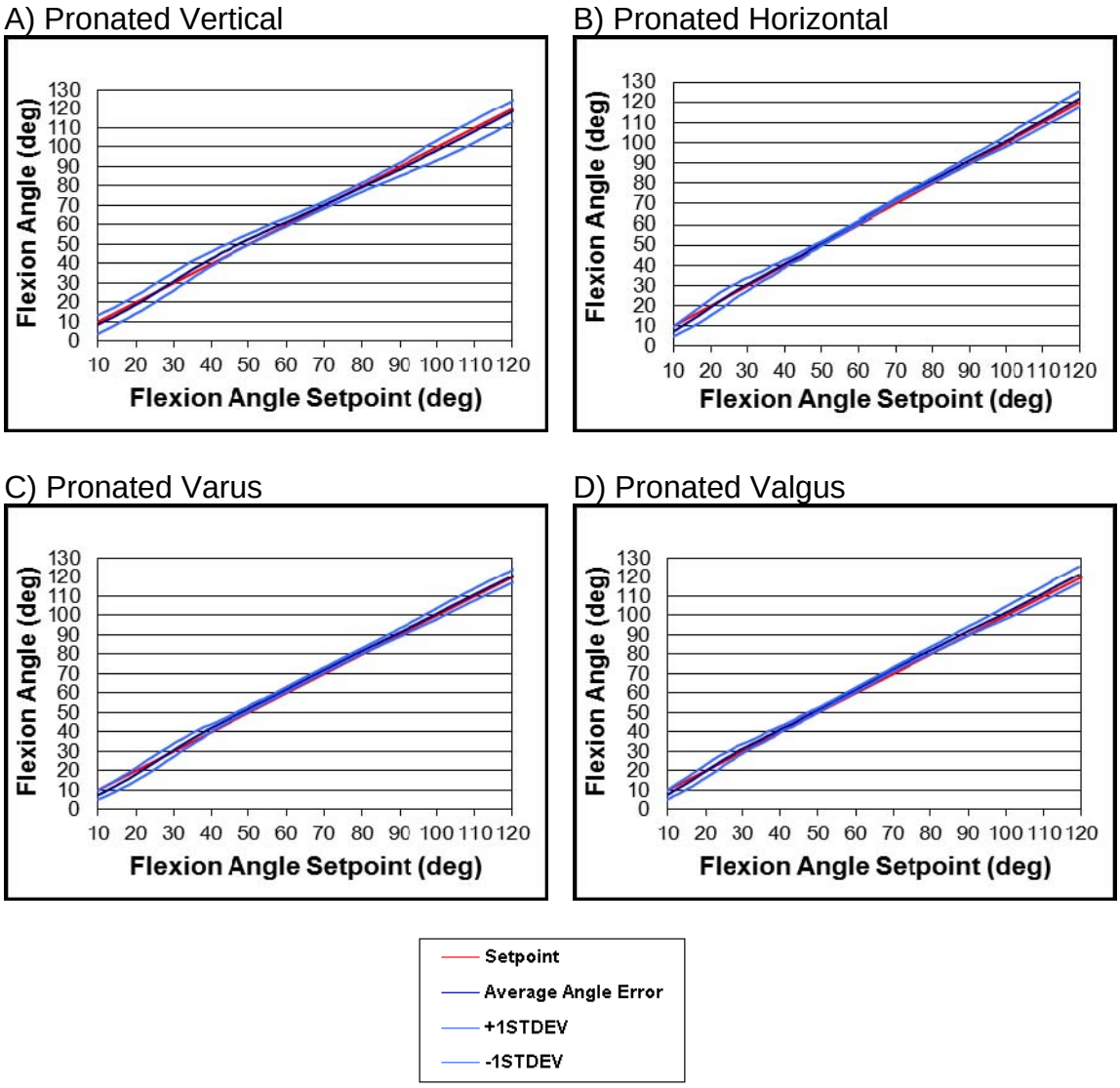

Figure 3.5: Joint angle Performance for Pronated Flexion

Actual joint angle compared to the joint angle setpoint curve for pronated flexion in the (A) vertical, (B) horizontal, (C) varus, and (D) valgus positions. Average ± one standard deviation of seven specimens are shown.

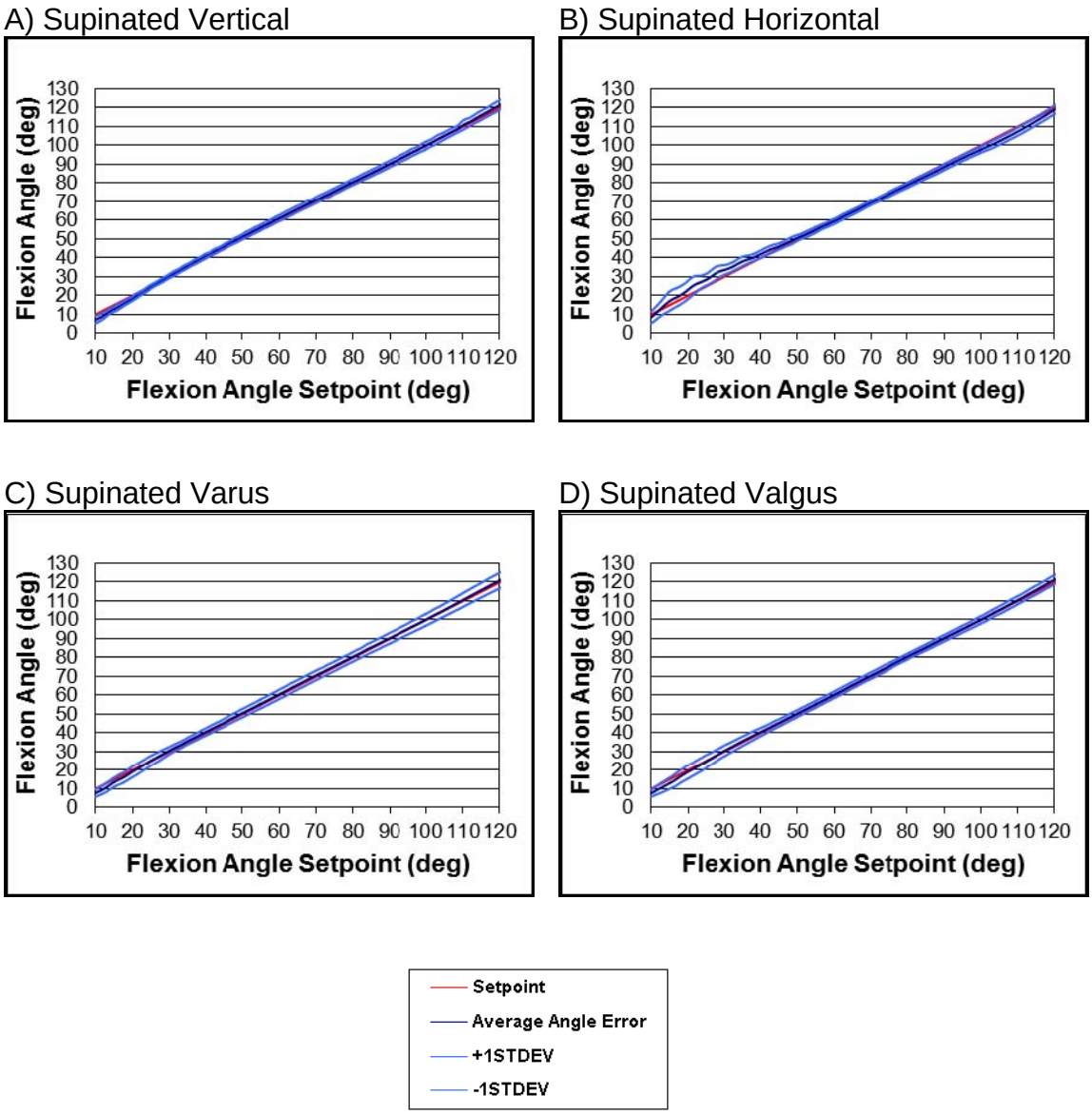

Figure 3.6: Joint angle Performance for Supinated Flexion

Actual joint angle compared to joint angle setpoint curve for supinated flexion in the (A) vertical, (B) horizontal, (C) varus, and (D) valgus positions. Average ± one standard deviation of seven specimens are shown.

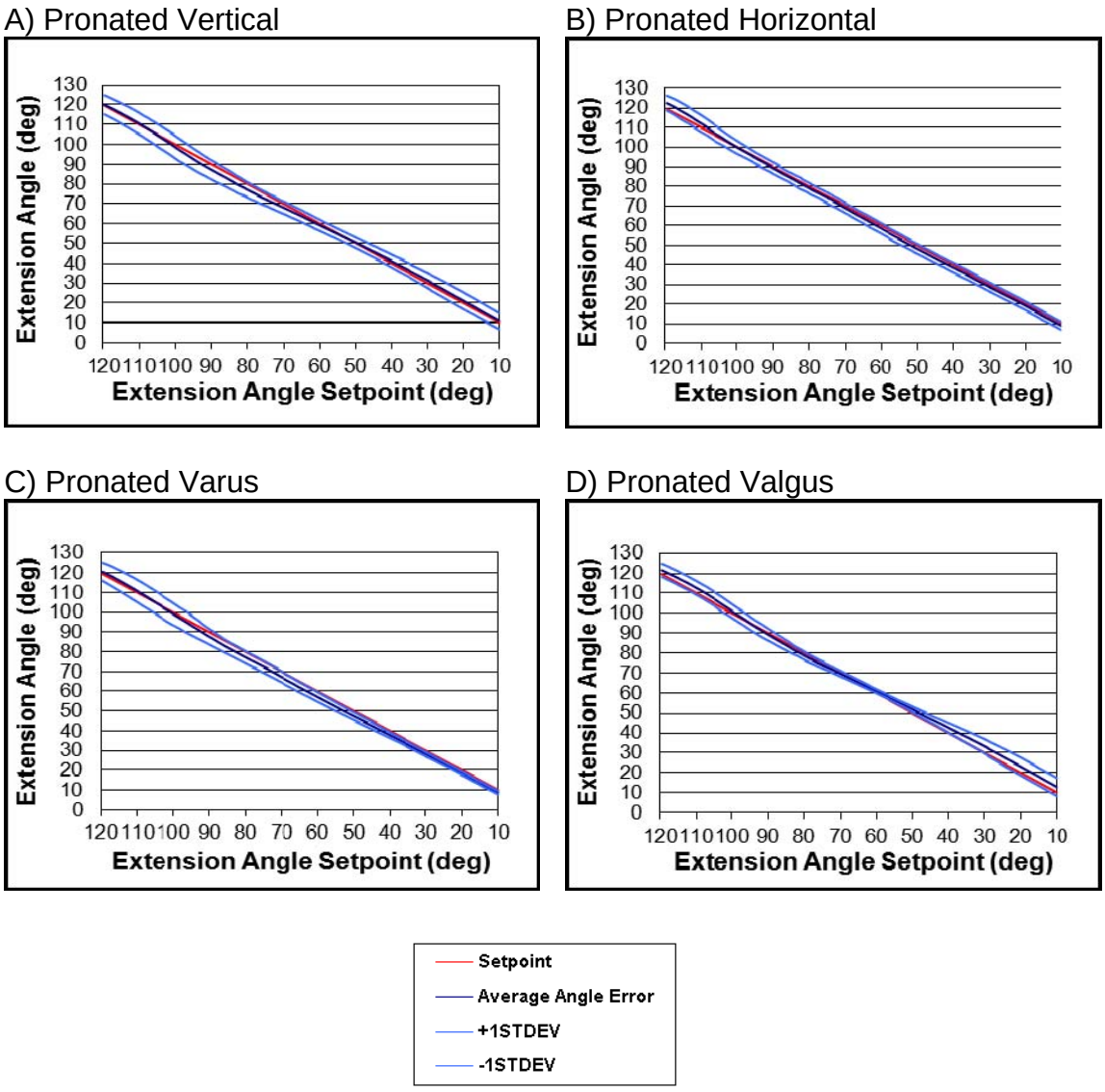

Figure 3.7: Joint angle Performance for Pronated Extension

Actual joint angle compared to the joint angle setpoint curve for pronated extension in the (A) vertical, (B) horizontal, (C) varus, and (D) valgus positions. Average ± one standard deviation of seven specimens are shown.

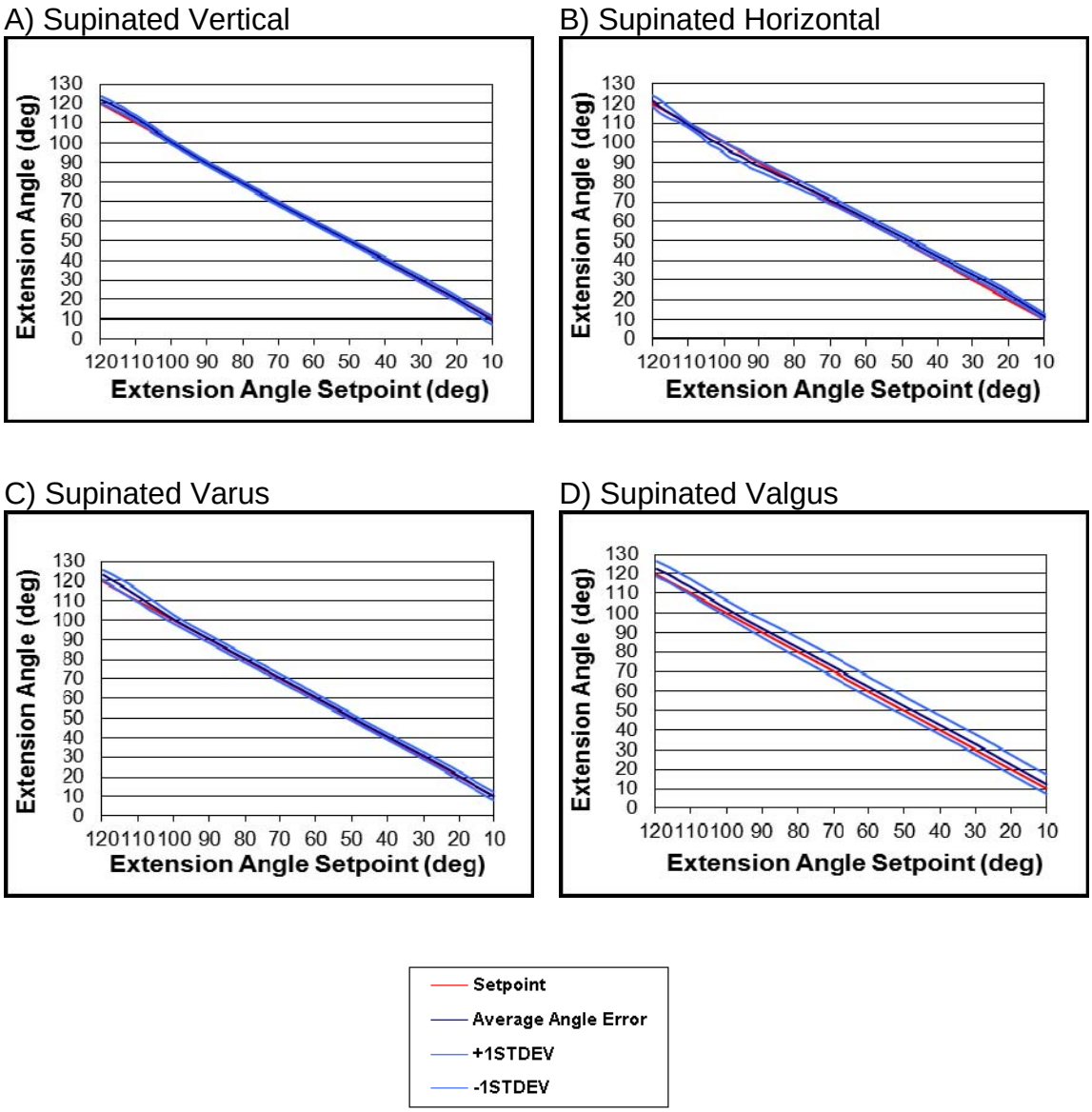

Figure 3.8: Joint angle Performance for Supinated Extension

Actual joint angle compared to the joint angle setpoint curve for supinated extension in the (A) vertical, (B) horizontal, (C) varus, and (D) valgus positions. Average ± one standard deviation of seven specimens are shown.

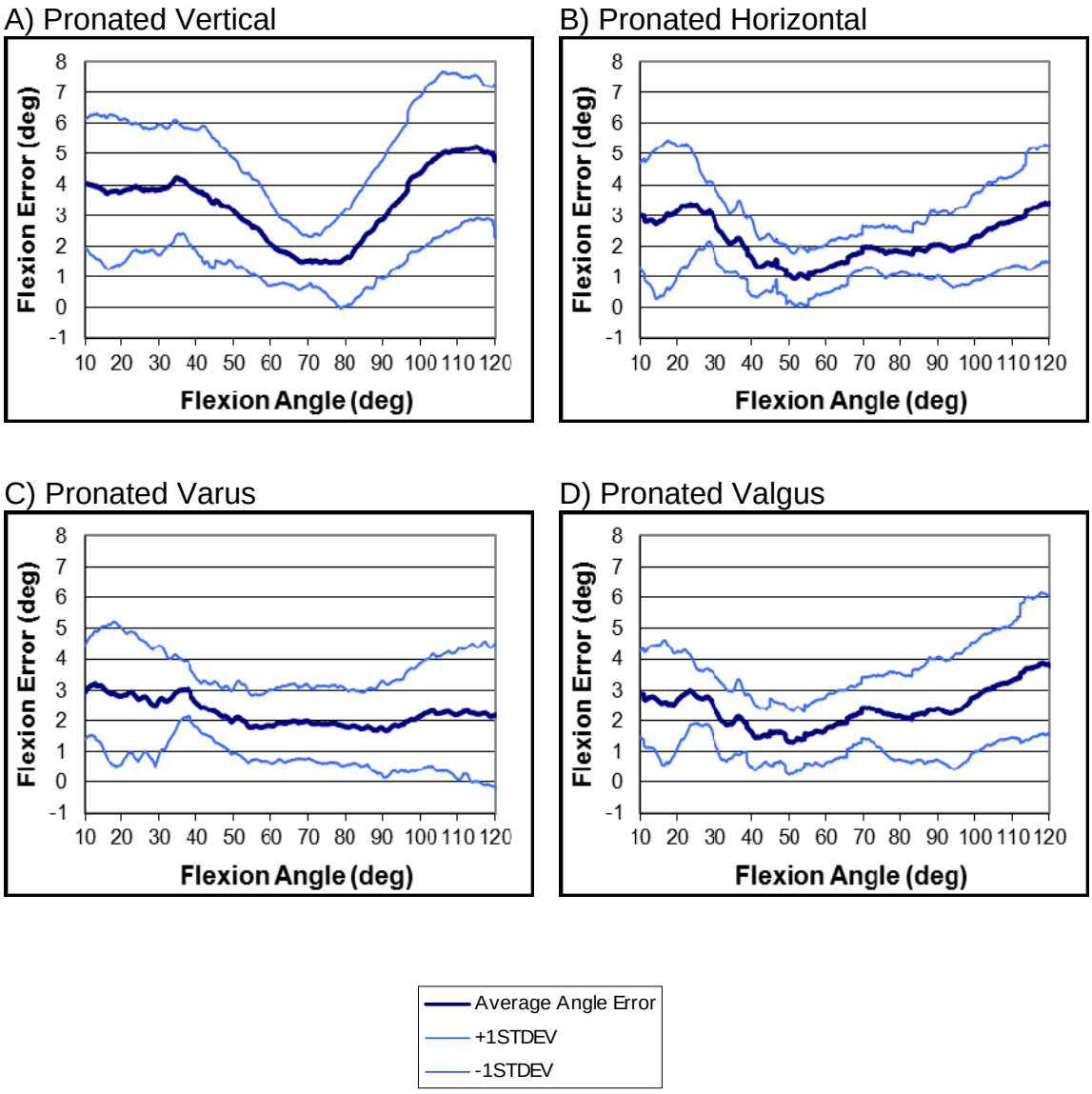

Figure 3.9: Absolute Joint angle Error for Pronated Flexion

The absolute difference between the actual joint angle and the joint angle setpoint curves for pronated flexion in the (A) vertical, (B) horizontal, (C) varus, and (D) valgus positions. Average ± one standard deviation of seven specimens are shown.

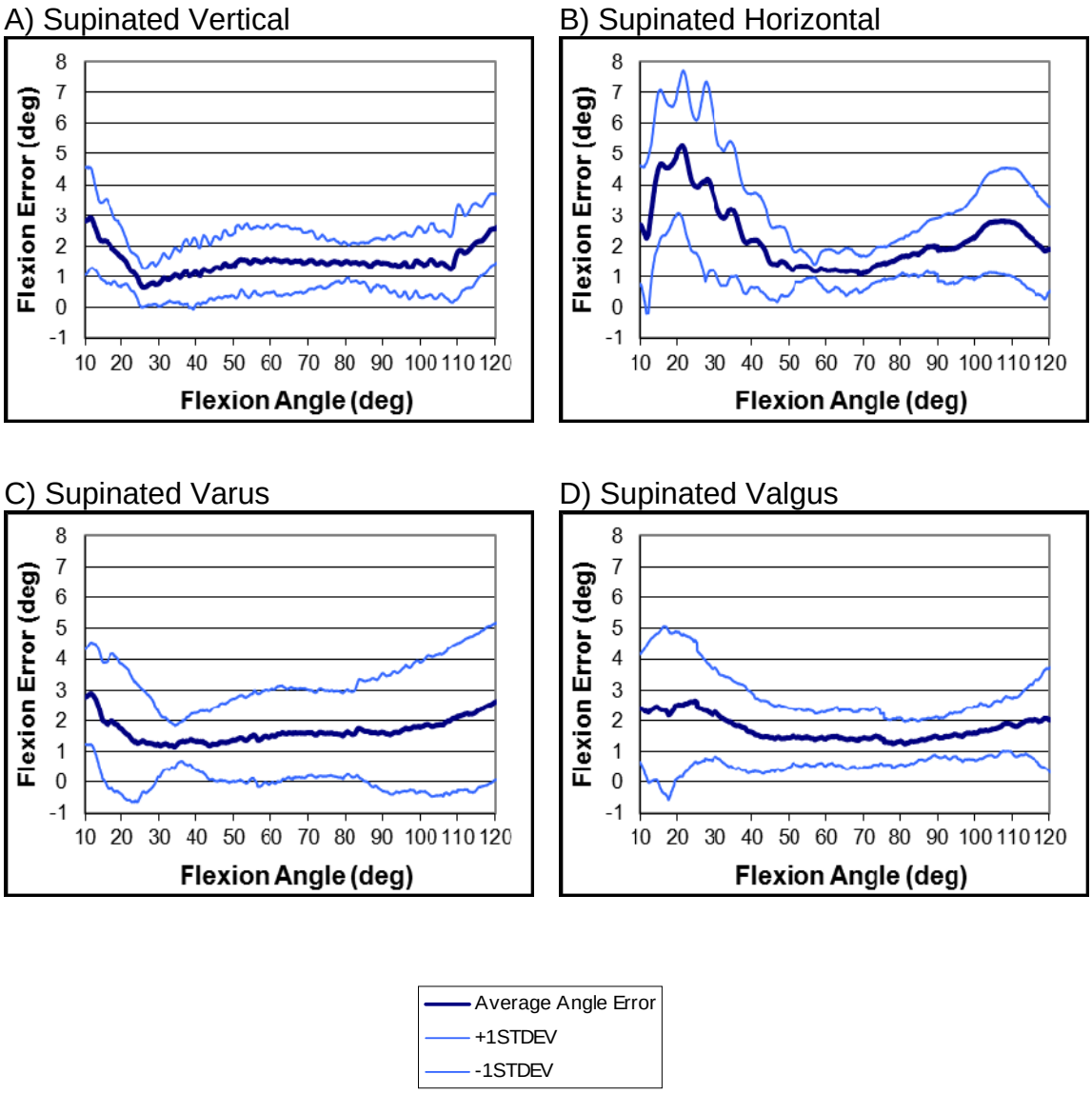

Figure 3.10: Absolute Joint angle Error for Supinated Flexion

The absolute difference between the actual joint angle and the joint angle setpoint curves for supinated flexion in the (A) vertical, (B) horizontal, (C) varus, and (D) valgus positions. Average ± one standard deviation of seven specimens are shown.

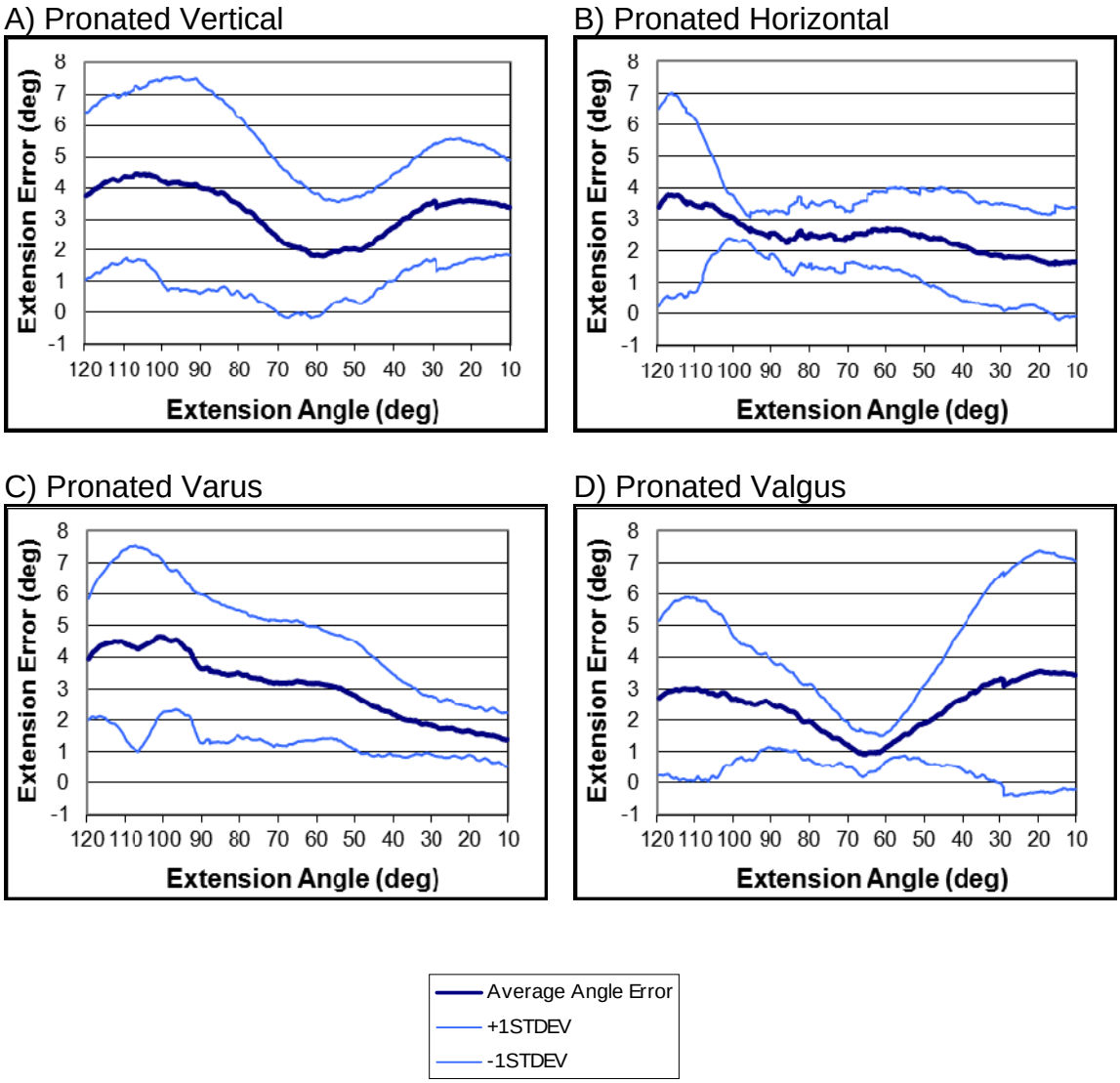

Figure 3.11: Absolute Joint angle Error for Pronated Extension

The absolute difference between the actual joint angle and the joint angle setpoint curves for pronated extension in the (A) vertical, (B) horizontal, (C) varus, and (D) valgus positions. Average ± one standard deviation of seven specimens are shown.

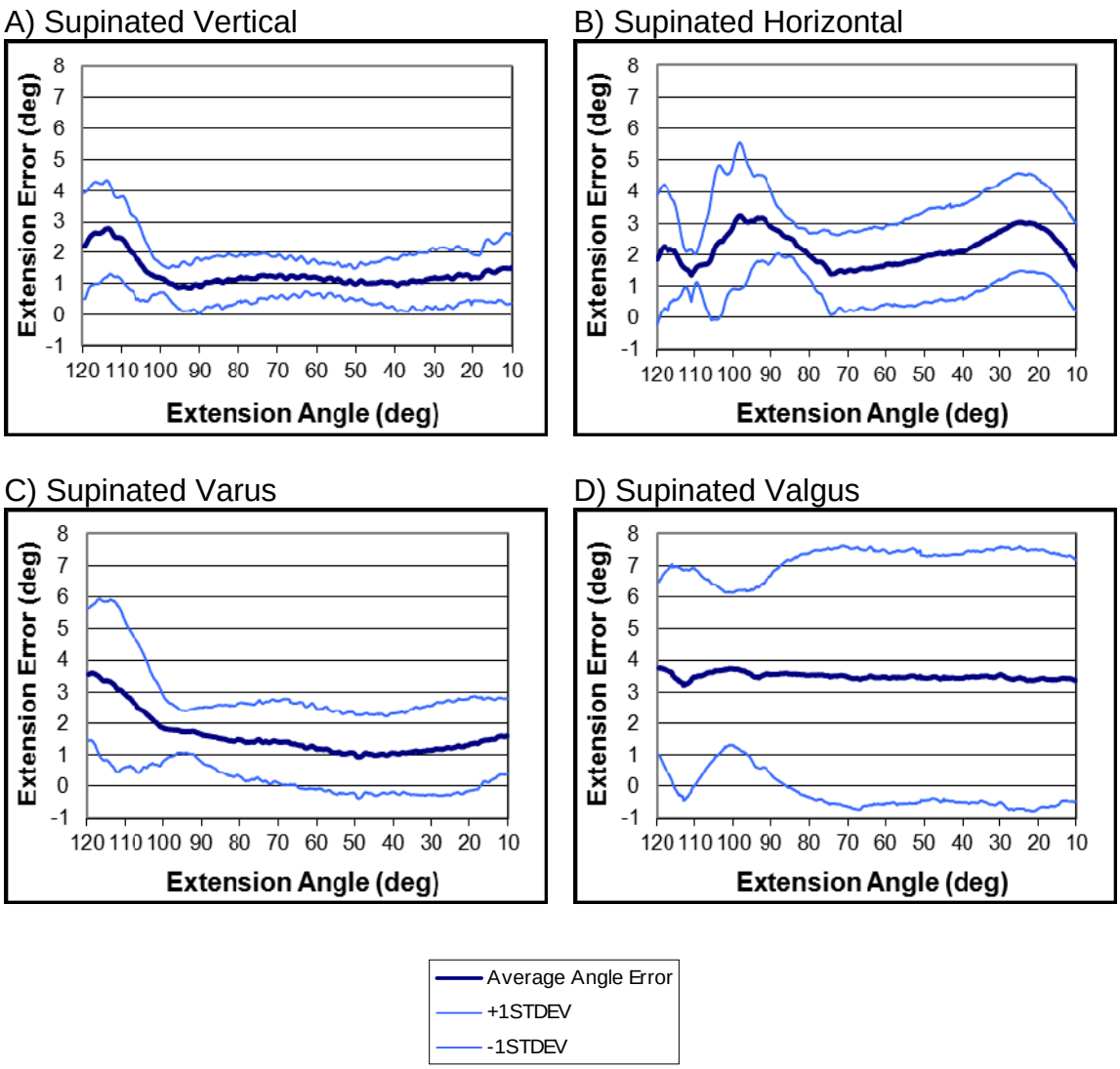

Figure 3.12: Absolute Joint angle Error for Supinated Extension

The absolute difference between the actual joint angle and the joint angle setpoint curves for supinated extension in the (A) vertical, (B) horizontal, (C) varus, and (D) valgus positions. Average ± one standard deviation of seven specimens are shown.

3.5 DISCUSSION

The new MOSE controller was able to reliably perform and control pronated and supinated elbow flexion and extension in the vertical, horizontal, varus and valgus positions. The actual joint angle followed the desired setpoint very closely with low errors overall. Also, there were no apparent signs of overly aggressive error corrections, or that control of the arm could become unstable. This was indicated by the fact that the PID process outputs never saturated, indicating that PID correction effort was never at maximum potential.

RMS errors for the entire motion range were generally less than 3.0º for flexion and supinated extension. RMS error was higher (4.1º) for pronated flexion and extension in the vertical position. Vertical elbow motion requires relatively high flexor loads. Since biceps brachii is a strong supinator, high biceps loads also serve to produce full forearm supination during supinated vertical flexion. In contrast, during pronated flexion, biceps loads are lower in order to allow pronator teres to pronate the forearm. It is possible that the larger imbalance between brachialis and biceps loads, or the reduced contribution from biceps during pronated vertical flexion, may be a greater challenge for the flexion controller. Further tuning of the controller may ameliorate this problem, but it is not likely to be resolved without specifically addressing forearm rotation.

A notable exception is supinated extension in the valgus position (Figure 3.12). Error was relatively low (~3.5º) and constant throughout extension, but standard deviations were exceptionally high (~4.0º) from 70-10º of elbow extension. This is also evidenced by the RMS error of 5.1º for the whole extension range, which is the highest of all the test conditions. The reason for this inconsistently large inter-subject variability may be due to a loss of articular congruity caused by the valgus gravity load. It is unclear why there is an additional local peak in variability near 110º. Pronated valgus extension has a similar level of variability near the endpoints of flexion-extension, but variability is quite low in the mid-region (Figure 3.11). These large levels of variability did not occur for flexion, neither pronated nor supinated (Figures 3.9 and 3.10). Clearly, the increased

activation of flexors is the reason, perhaps improving joint congruity in this position.

Some oscillatory behaviour was measured for supinated horizontal flexion in the 10-50º range (Figure 3.10B). This is precisely where the greatest challenges to flexion were expected. The fact that it did not occur for pronated horizontal flexion is likely due to the greater biceps effort during supinated flexion. Since the servo-motor displacements of the biceps and brachialis tension controllers are not linked, it may be that the similar efforts from these simulated muscles causes the majority of forearm weight to alternate between the two sides and, under some conditions, to develop an oscillatory pattern. The addition of some controller logic to govern the relative displacements of these muscles may be helpful. It is interesting to note that these oscillations were primarily seen in three specimens. These donors were among the tallest in the group and two had the lowest BMIs (Body Mass Index). The greater counter flexion moment generated by longer specimens would certainly require greater flexor loads, and that any controller corrections would thusly be greater. It may be that these larger loads, together with the relatively low mass of some specimens, may cause over-corrections. Thus, further refinement is needed to resolve this issue. Oscillations to a much lesser degree were also noted throughout supinated vertical flexion, though this was apparent only in the absolute joint angle error (Figure 3.10A). These occurred in all seven specimens.

As described previously, the horizontal position is the most challenging for achieving smooth and constant flexion rate control due to gravitational effects. Therefore, much of the simulator's development was done for this position. Although the varus and valgus positions have similar characteristics with the horizontal, they are not as extreme. This is evident in the performance curves, which are better for varus and valgus than for horizontal. The design goal of the current controller was to achieve flexion in these three positions, however, it could benefit from some refinement specific to the vertical position. Tuning the controller in each of the four flexion positions, in order to obtain separate PID parameters, may refine the simulator's performance in the vertical position.

In general, average absolute error and standard deviations were greater near full flexion and extension. This is likely due to the increase in the counter-moment as the forearm becomes more horizontal in these regions. Since the same PID parameters were

used for all specimens, and since the mass of the system is generally a factor in PID tuning, it is likely that custom tuning to produce specimen-specific PID parameters would reduce this error. The decision to use common PID parameters in this study, which were previously determined, was intended to reduce set up time by avoiding a complex tuning routine for each specimen. Thus, the option to obtain specimen-specific PID parameters and feedforward functions could be considered for future studies with this simulator.

It is notable that performance at 90º of flexion was quite good, even in the horizontal position where the forearm acts as an inverted pendulum. This indicates that while further improvements are needed, the cascade PID design of the current controller is an appropriate model for elbow flexion-extension.

A previous elbow flexion simulator from our laboratory, which used the 'prime mover' paradigm, was designed primarily for vertical flexion (Dunning *et al.*, 2003). In testing the accuracy of their 'prime mover' actuator to follow the setpoint, lower RMS error was noted during supinated as compared to pronated flexion in the vertical position. This is in agreement with the results of the current study, in which RMS error of the joint angle setpoint was lower during vertical supinated flexion, and in general, for supinated flexion in all positions. Dunning *et al.* (2003) also found that their RMS actuator error was less for pronated varus than for pronated vertical loaded flexion, and that the opposite was true between the valgus and vertical positions during supinated flexion. This is also consistent with the results for flexion (Table 3.3). In contrast, the simulator by Dunning *et al.* (2003) failed to produce flexion for the supinated varus and pronated valgus conditions, whereas the current simulator in this investigation was able to operate in those conditions with no apparent difficulty. Dunning *et al.* also noted that "The [increased] scatter observed in the velocity data … can be attributed to a number of factors, including differences in arm geometries since, strictly speaking, [their] model controlled the rate of tendon displacement as opposed to flexion angle versus time." This was one of the design goals of the current investigation. As the new Cascade PID controller is able to control joint angle with closed-loop feedback, error minimization is applied directly through muscle tension adjustments. In this way, the joint angle is directly controlled.

In evaluating the performance of their AGH simulator, Schimoler *et al.* (2008) reported average flexion-extension error of less than 0.20º with standard deviations generally less than 1.50º, though most of their errors were much smaller – average 0.00º with standard deviations less than 0.50º. Though the AGH simulator is capable of flexion extension in the vertical, varus and valgus position, they did not specify which position generated those results. These exceptionally low errors may in part be explained by the testing model and data processing methods employed. They used a sinusoidal setpoint alternating between 45º and 135º of flexion-extension. Data was collected once the controller attained a steady sinusoidal reaction pattern to the setpoint waveform it was following. Thus the region near full extension, which was expected and found to be one of the more challenging, was not modeled in the AGH evaluation. Moreover, errors during the initial start-up, generally where PID performance is worst, were not considered. Also, it is apparent that the average error they reported was not the average of absolute errors (*i.e.* magnitude of disagreement between controller and setpoint), but rather the averaged signed error. This would have led to positive and negative errors cancelling each other, which may explain the incredibly small average error magnitudes. This is also evidenced by their maximum errors of 4-8º, which are actually in agreement with the results of the controller presented here. Furthermore, the sinusoidal setpoint model used by the AGH simulator would have coerced alternating errors because the actual joint angle always lagged the setpoint, thus systematically causing positive and negative errors of similar magnitudes, leading to such small average errors.

Before calculating the error, Schimoler *et al.* (2008) subtracted the system delay from the measurement, effectively causing a phase shift in the data. The authors reasoned that without this phase correction, "It would have introduced a DC bias to the error because the system constantly lagged a certain number of degrees behind the reference [setpoint angle]." However, lag in the process variable of a closed-loop controller is generally seen as a deficiency in the actuators' force or displacement output, or an improper tuning process leading to inappropriate PID parameters. It is understandable, but expected that lag would occur in regions of acceleration (*i.e.* flexion-extension endpoints or rapid changes in setpoint velocity), but a proper PID controller would be

expected to correct the lag. Failure to do so implies insufficient Integral control in the PID parameters. It is the Integral control portion of the PID controller which should eliminate residual steady-state error. Since PID controllers can fall into an oscillatory pattern as a consequence of improper parameter tuning or insufficient controller capacity, it would seem that the use of a sinusoidal setpoint would not allow conclusive determination of the controller's ability to minimize elbow joint angle error.

These potential study weaknesses were not present in this investigation. The performance of the new Cascade controller was evaluated throughout a flexion range that was common to all ten specimens tested. Rather than cycling the joint angle, measurements were recorded from the first run of each condition. This tested the simulator's ability to quickly bring the joint angle under control.

Muscle tension control is a very fast process (small time constant), as determined in Appendix B, making muscle tension control responsive and relatively easy to tune. In comparison, elbow flexion is a much slower process (large time constant), making PID parameters difficult to tune and control prone to large joint angle errors. The elbow flexion-extension process is slower to react to changes in PID output because elbow joint angle is indirectly affected by muscle tension; both tissue elasticity and muscle antagonism can cause the joint angle process to lag. The Cascade PID design takes advantage of this difference between the rates of processes dynamics. Furthermore, muscle tension has influence over joint angle, which is a requirement for Cascade PID control. The Cascade configuration is also well suited for multiple secondary processes, which was implemented as tension control for the biceps, brachialis and triceps muscles in this application. Thus, the Cascade configuration would seem to be a logical model, and analogous to *in-vivo* motor control.

In an agonist-antagonist model, the elbow is essentially a cable mechanism with three major cables; two flexors (*i.e.* brachialis and biceps brachii), and one extensor (*i.e.* triceps). As with cables, muscles can influence the joint angle process only through tension. Thus, left unchecked, tension can only accumulate in such a system. This was addressed by the tension minimization routine, which successfully lowered tension while

the Cascade PID with feedforward controller maintained sufficient muscle tension to govern the elbow joint angle process.

A strength of the MOSE controller in this investigation is the use of elbow joint angle feedback, which allows the use of PID error correction. Obtaining joint angle feedback from the same tracking system used to collect kinematics data, rather than from another dedicated transducer, reduces hardware complexity. Another strength is the Cascade PID design of the controller. Unlike the muscle tension process, which has negligibly little lag (Appendix B), the joint angle process has relatively greater lag because changes in muscle tension do not directly affect the joint angle. Tissue stretching and the interaction between agonists and antagonists increase the flexion process time constant. Moreover, the spatial transformations needed to calculate the joint angle, and the native report rate of the tracker itself, all detract from real-time control. The Cascade PID control design actually makes use of the disparity between the muscle tension and joint angle process time constants, and allows the use of the well established form of PID control for this application (Leigh, 1987a; Blevins and Nixon, 2011). This allows errors in the muscle tension process to be corrected before they affect the elbow joint angle process (Bequette, 2003).

The use of PID control for error correction is also a strength. Simulators that employ only feedforward control without feedback for error correction assume that the mathematical model or process measurements that define the feedforward transfer function perfectly describe the behaviour of the process variable. But inevitably, errors in the models or imprecise measurements in the data will impact performance of the feedforward controller. Additionally, the models or measurements that the feedforward controller is based on, do not account for potential disturbances to the process variable. Once the control signal has been sent to the process variable, it can no longer be adjusted.

Feedforward control is still an integral part of this controller, and its integration with the Cascade PID design counts as a study strength. Furthermore, using feedforward together with feedback does not influence the stability of the feedback loop because feedforward does not introduce new process dynamics into the loop (Bequette, 2003). Stroeve (1997) deduced that, by considering its inherent lags and speeds of movement,

the body must combine feedforward and feedback control (Stroeve, 1997). It may be interesting to note that in his thesis dissertation, Schimoler 2008, recalling Stroeve's conclusions, predicted that "the next step in joint motion simulator evolution may be the introduction of feedforward models within closed-loop feedback control."

Another study strength was that all four principal positions were evaluated, as well as flexion and extension with both pronated and supinated forearm rotations, thus making the results of this controller very relevant to investigations of upper extremity motion.

There were limitations in this study. Cadaveric specimens of advanced age were used, the tissue properties of which may not be entirely representative of the population. The only setpoint tested was a straight ramp at a relatively slow rate of 10º/s. Thus, the errors calculated herein may not apply for faster and more complex motion patterns.

In summary, this work develops and validates a new motion controller for an elbow motion simulator capable of generating *in-vitro* flexion and extension. The MOSE controller incorporates joint angle and muscle force feedback and feedforward transfer functions, as well as a cascade PID architecture, which is capable of simultaneously controlling joint angle and muscle tension for multiple muscles. This novel control scheme can achieve smooth and accurate pronated or supinated flexion and extension with the arm in the vertical, horizontal, varus and valgus positions. The HULC MOSE is the first reported active motion simulator capable of all these motions for *in-vitro* studies.

The active kinematic data that can be collected from the HULC MOSE will allow for new *in-vitro* studies to better understand elbow disorders and to develop new treatments. Load cells could also be added to the osseous anatomy in order to study elbow flexion dynamics which would further advance the modelling of elbow function for virtual simulations. Thus, MOSE is a valuable platform for future studies of the elbow which would not otherwise have been possible. Chapter 5 presents such a clinical study. A better understanding of elbow disorders can only benefit patients in the future.

3.6 REFERENCES

Amis A A, Dowson D, Wright V. Muscle strengths and musculoskeletal geometry of the upper limb. Engineering in Medicine 1979; (8): 41-48.

Bequette W. Combined Feed-Forward and Cascade. In: Process control: modeling, design, and simulation. New Jersey: Prentice Hall, 2003; 330-333.

Blevins T, Nixon M. Cascade Control. In: Control Loop Foundation: Batch and Continuous Processes. International Society of Automation, 2011; 260-267.

Dunning C E, Duck T R, King G J, Johnson J A. Simulated active control produces repeatable motion pathways of the elbow in an in vitro testing system. J Biomech 2001; (34): 1039-1048.

Dunning C E, Gordon K D, King G J, Johnson J A. Development of a motion-controlled in vitro elbow testing system. J Orthop Res 2003; (21): 405-411.

Erickson K, Hedrick J. Enhancements to Single-Loop Regulatory Control. In: Plantwide process control. John Wiley & Sons Inc., 1999; 213-219.

Ferreira L M, Johnson J A, King G J. Development of an active elbow flexion simulator to evaluate joint kinematics with the humerus in the horizontal position. J Biomech 2010; (43): 2114-2119.

Funk D A, An K N, Morrey B F, Daube J R. Electromyographic analysis of muscles across the elbow joint. J Orthop Res 1987; (5): 529-538.

Howard R F, Ondrovic L, Greenwald D P. Biomechanical analysis of four-strand extensor tendon repair techniques. J Hand Surg Am 1997; (22): 838-842.

Kuxhaus L, Schimoler P J, Vipperman J S, Miller M C. Validation of a Feedback-Controlled Elbow Simulator Design: Elbow Muscle Moment Arm Measurement. Journal of Medical Devices 2009; (3).

Kuxhaus L. Development Of A Feedback-Controlled Elbow Simulator: Design Validation And Clinical Application. 2008.
University of Pittsburgh .
Ref Type: Thesis/Dissertation

Leigh J. Cascade control. In: Applied control theory. London, UK: Peter Peregrinus Ltd., 1987a; 77.

Leigh J. Feedforward control. In: Applied control theory. London, UK: Peter Peregrinus Ltd., 1987b; 77-78.

Patranabis D. Cascade Control. In: Principles of Process Control. Tata McGraw-Hill, 1996; 2nd: 182-191.

Schimoler PJ. DESIGN OF A CONTROL SYSTEM FOR AN ELBOW JOINT MOTION SIMULATOR. 2008. University of Pittsburgh .
Ref Type: Thesis/Dissertation

Stroeve S. A learning feedback and feedforward neuromuscular control model for two degrees of freedom human arm movements. Human Movement Science 1997; (16): 621-651.

CHAPTER 4 – MOTION-DERIVED COORDINATE SYSTEMS REDUCE INTER-SUBJECT VARIABILITY OF ELBOW FLEXION KINEMATICS

OVERVIEW: *The selection of a joint coordinate system affects the outcome of motion pathways. This chapter described the development of coordinate systems for the ulna and humerus which are generated from upper extremity motion. These Motion-Derived CS (Coordinate Systems) were compared to traditional Anatomy-Derived CS created using surface digitizations of anatomical features. Within-subject repeatability of creating Motion-Derived CS was quantified. In-vitro elbow flexion was generated in the vertical (gravity dependent) position using an active upper extremity motion simulator. Kinematic pathways of those motions were calculated in terms of valgus angulation and internal rotation of the ulna relative to the humerus, using both coordinate systems. The method of creating Motion-Derived CS was highly repeatable - less than 0.5 mm and 1º for all coordinate directions measured. Inter-subject variability of active flexion pathways was reduced with Motion-Derived CS compared to Anatomy-Derived CS ($p < 0.05$). The decrease in inter-subject kinematic variability when using Motion-Derived CS may increase the statistical power of biomechanical studies and allow for reduced sample sizes. This minimally invasive method, which also determines the elbow flexion and forearm rotation axes and centre of the capitellum, may also be applicable in computer-navigated surgery of the upper limb.*[1]

1) A version of this work has been published: Ferreira LM, King GJW, Johnson JA. Motion-Derived Coordinate Systems Reduce Inter-Subject Variability of Elbow Flexion Kinematics. *Journal of Orthopaedic Research*. In Press. 2010. (See Appendix E.2)

4.1 INTRODUCTION

Anatomically relevant coordinate systems are widely used in biomechanics research and have found some applications in orthopaedic surgical procedures such as navigated joint arthroplasty. With respect to the elbow, coordinate systems for the ulna and humerus are often derived solely from surface digitizations of specific osseous anatomical features (King *et al.*, 1999; Morrey *et al.*, 1991).

In 2005, the International Society of Biomechanics (ISB) expressed the need for standardized bone segment Coordinate Systems (CS) and proposed definitions of various coordinate systems including the elbow. These were primarily based on osseous anatomy, and thus came with characteristic caveats with respect to accuracy and repeatability. The ISB acknowledged that "it cannot be assured that the [humerus and forearm] Z axis is equal to the joint rotation axis" and that "the numerical and practical inaccuracies in defining the lateral and medial epicondyles may swamp the accuracy of [the coordinate system] definition" (Wu *et al.*, 2005).

A consequence of coordinate system misalignment with the elbow flexion axis is kinematic crosstalk. This occurs when a component of one joint rotation is falsely interpreted as contributing to another rotation of interest, and concurrently, a component of the joint rotation of interest is lost (Piazza and Cavanagh, 2000). Such misalignments in knee joint coordinate systems have been shown to cause erroneous abduction angle and external rotation measurements (Blankevoort *et al.*, 1988; Piazza and Cavanagh, 2000).

In order to address the inaccuracies associated with precisely locating anatomical features such as the humeral epicondyles, some investigators have used digitizations of the articular anatomy to calculate the elbow flexion axis. Specifically, sphere fits of the capitellum and radial head, and circle fits of the trochlear sulcus and greater sigmoid notch articulations have been employed to calculate the geometric centers of these articular structures, which are then used to approximate the flexion axis (King *et al.*, 1999). The theory behind geometric centre fitting is that elbow function follows from

elbow joint form. Brownhill *et al.* (2006) investigated the variability of producing a flexion axis using geometric fitting, compared to manual selection of the epicondyles according to the ISB definition. The error in the surgeons' selections resulted in frontal plane angles ranging from 6.3º varus to 9.6º valgus, and coronal plane angles ranging from 8.3º internal to 10.2º external rotation (Brownhill *et al.*, 2006). In another study by Brownhill *et al.* (2009), a circle fit of the greater sigmoid notch was found to produce an accurate flexion axis (Brownhill *et al.*, 2009).

The flexion axis can also be calculated directly from motion data using methods developed from Screw Theory (Ball, 1876). In particular, the helical axis, also known as Screw Displacement Axis (SDA), method has been widely reported in the biomechanics literature and shown to accurately determine the true elbow flexion axis (Bottlang *et al.*, 2000; Duck *et al.*, 2003; Duck *et al.*, 2004; Veeger and Yu, 1996). It has also been shown that the SDA method can be used to calculate the forearm rotation axis, and that it intersects with the flexion axis SDA at the radiocapitellar joint (Veeger and Yu, 1996). This provides a convenient way to locate the origin of a CS. Potentially, these characteristics could be used to create coordinate systems based on motion of the upper extremity, hereafter referred to as Motion-Derived CS.

There has been much development in Motion-Derived CS for the knee and hip, which have been shown to be more reproducible, and to generate more accurate kinematics than Anatomy-Derived CS (Besier *et al.*, 2003; Gamage and Lasenby, 2002; Schache *et al.*, 2006; Schwartz and Rozumalski, 2005). Much less progress on this front has been made in the upper extremity. To our knowledge, no Motion-Derived axis technique for the upper extremity has been reported which can generate complete coordinate systems for the ulna and humerus for the determination of ulno-humeral (viz. Elbow) kinematics. While a single axis is sufficient for alignment purposes, only a complete Cartesian coordinate system provides the information necessary for full 6DOF measurements and navigation. Thus, the aim of this study was to develop anatomically relevant ulnar and humeral CS derived from the SDAs of passive elbow flexion and forearm rotation.

Other joint applications may exist, and procedures such as joint arthroplasty or reconstruction might benefit from accurate alignment facilitated by a reference CS. Any joint with nearly intersecting rotation axes might be a candidate for a Motion-Derived CS method. A CS for the wrist might be generated using rotation axes of forearm rotation and wrist flexion. The shoulder's humeral rotation axis and abduction or forward flexion axis might be suitable, and similarly for the hip. The screw home mechanism of the knee, or possibly the femoral rotation axis, may provide a suitable intersection with the knee flexion axis to make such a CS.

The Humeral and Ulnar Motion-Derived CS developed in this study were compared to traditional Anatomy-Derived CS created from manual surface digitizations of anatomical features. It was hypothesized that the Motion-Derived CS would produce kinematic pathways with less inter-subject variability when compared to the Anatomy-Derived CS.

4.2 METHODS

Specimen Preparation and Biomechanical Testing

Ten previously fresh-frozen cadaveric upper extremities, amputated at mid humerus (mean age: 65 ± 11, 5 male, 8 left), were mounted using a humeral clamp on the MOSE simulation system in the vertical (gravity dependent) position (arm vertical with hand toward the ground) (Dunning *et al.*, 2001; Dunning *et al.*, 2003). An electromagnetic tracking system was used to record 6DOF pose data (Flock of Birds, Ascension Technologies Inc., VT, USA). Tracking system receivers (henceforth referred to as trackers) were rigidly fixed to the ulna and radius. The transmitter was mounted to the base of the simulator so as to rigidly fix it relative to the humerus. The simulator used computer-controlled servo-motors and pneumatic actuators that were connected to tendons via sutures and braided steel cables (Dunning *et al.*, 2001; Dunning *et al.*, 2003). The controlling algorithm used closed loop control of muscle loads and flexion angle to generate simulated active flexion.

For the purpose of creating Motion-Derived CS, an investigator manually produced unloaded forearm rotation and elbow flexion while the tracking system recorded the motion. This passive motion was performed in the following sequence: Beginning at full pronated extension, the forearm was fully supinated, then the elbow was flexed to full flexion, followed by full forearm pronation. The same investigator performed this passive motion for every specimen.

Creating Anatomy-Derived Joint Coordinate Systems

Following all flexion trials, the elbow and wrist were disarticulated in order to digitize the articular anatomy. The digitizations were performed using a tracker-mounted stylus. From the digitized surface data, coordinate systems for the humerus and ulna were created as described in previous studies (Figure 4.1) (King *et al.*, 1999). These will henceforth be referred to as Anatomy-Derived CS.

For the Humeral Anatomy-Derived CS (Figure 4.1A), the anatomy digitized was the capitellum, trochlear sulcus, and the circumference about the mid-diaphysis of the humeral shaft. The capitellum was sphere fit in a least squares sense to calculate its center. The trochlear sulcus was collapsed onto a best fit plane to produce a 2D arc, which was then circle fit in a least squares sense to calculate its center. The +Z axis (directed medially) was defined from the center of the capitellum to the center of the trochlear sulcus, and formed the flexion axis. The mid-diaphyseal circumference of the humeral shaft was circle fit to calculate its center. The long axis was defined from the bisector of the capitellum and trochlear centers to the humeral shaft center. The +Y axis was made perpendicular to the Z axis and the long axis. This +Y axis was directed anteriorly for a right arm and posteriorly for a left arm. The +X axis (directed proximally) was made perpendicular to the Y and Z axes. The origin of the humeral coordinate system was taken to be the center of the capitellum.

For the Ulnar Anatomy-Derived CS (Figure 4.1B), the anatomy digitized was the greater sigmoid notch and distal ulnar styloid. The greater sigmoid notch was circle fit to calculate its center. As described above, the greater sigmoid notch was collapsed onto a best fit plane. The normal vector of the plane, located at the center of the arc, provided

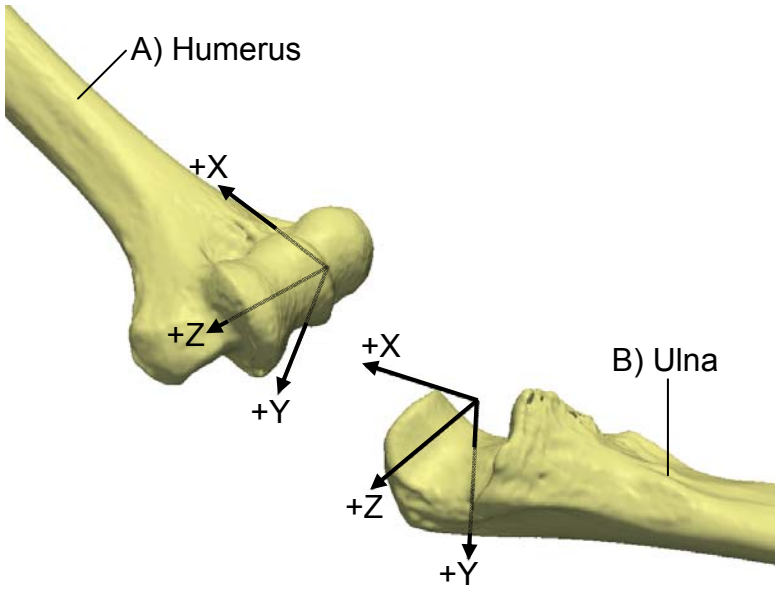

Figure 4.1: Joint Coordinate Systems

Joint Coordinate Systems (CS) for (A) the Humerus and (B) the Ulna. The origins and vector directions coincide for both the motion-derived and anatomy-derived CS. Left arm shown.

the ulnar flexion axis, and defined as the +Z axis (directed medially). The long axis was defined by a line from the distal ulnar styloid to the center of the greater sigmoid notch. The +Y axis was made perpendicular to the Z axis and long axis. This +Y axis was directed anteriorly for a right arm and posteriorly for a left arm. The +X axis (directed proximally) was made perpendicular to the Y and Z axes. The origin of the ulnar coordinate system was taken to be the center of the greater sigmoid notch.

Creating Motion-Derived Joint Coordinate Systems

SDAs (Figure 4.2) were created from the passive motion sequence described above, using the SDA algorithm described by Beggs (1983) (Beggs, 1983). The SDA algorithm generates many "instantaneous" SDAs (iSDAs), each one corresponding to a rotation between two frames of motion. The algorithm is sensitive to small rotations, and thus consecutive motion frames must be separated by at least 5º of joint rotation in order to avoid many outlier iSDAs (Bottlang *et al.*, 1998; Duck *et al.*, 2004). The average SDA was calculated for both elbow flexion and forearm rotation. For clarity, the average SDA will henceforth be referred to simply as the SDA. The elbow flexion SDA was calculated using motion of the ulna relative to the humerus. The forearm rotation SDA was calculated using motion of the radius relative to the ulna. These SDAs were used to create coordinate systems for the ulna and humerus which will henceforth be referred to as Motion-Derived CS.

For the Humeral Motion-Derived CS (Figure 4.1A), the elbow flexion SDA formed the +Z axis. The forearm rotation SDA was transformed from the ulna tracker to the global space (in same space with the Z axis). The +Y axis was made perpendicular to the Z axis and forearm rotation SDA. The +Y was directed anteriorly for a right arm and posteriorly for a left arm. The +X axis (directed proximally) was made perpendicular to the Y and Z axes. The origin was defined as the nearest intersection of the flexion SDA and forearm rotation SDA. The shortest distance between the two SDA vectors was less than 1 mm for most specimens and corresponds to the center of the radiocapitellar joint.

For the Ulnar Motion-Derived CS (Figure 4.1B), the flexion SDA was calculated from motion of the humerus relative to the ulna. A point on the ridge of the greater

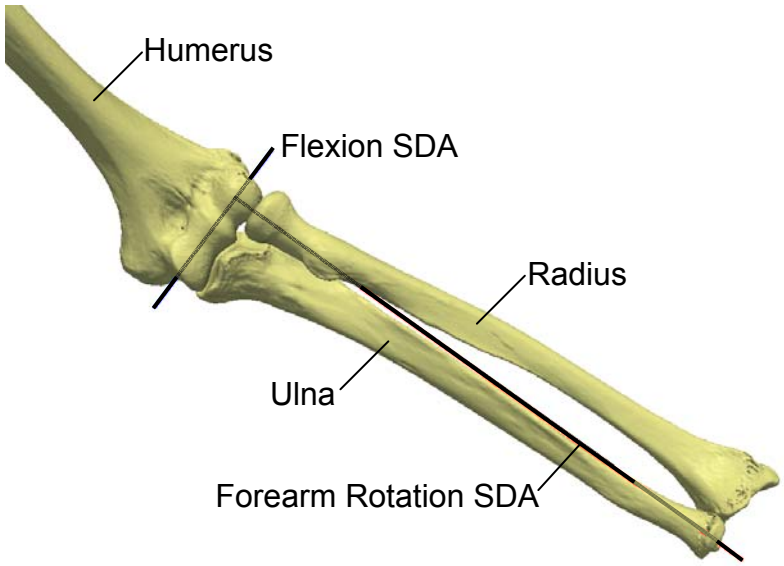

Figure 4.2: Elbow Flexion and Forearm Rotation SDAs

The SDAs tend to intersect at the center of the radiocapitellar articulation. Left arm shown.

sigmoid notch, half way between the coronoid tip and olecranon tip, was automatically extracted from the digitized trace of the greater sigmoid notch. The perpendicular projection of this point onto the flexion SDA resulted in a point corresponding to the center of the greater sigmoid notch, and was defined as the origin. Another point was digitized over the skin near the distal ulnar styloid, and projected perpendicularly onto the forearm rotation SDA. These two points defined the +X axis directed proximally. The +Y axis was made perpendicular to the flexion SDA and the X axis, and was directed anteriorly for a right arm and posteriorly for a left. The +Z axis (directed medially) was made perpendicular to the X and Y axes. Use of the anatomical landmark on the greater sigmoid notch was done in order to achieve a Motion-Derived CS consistent with the Anatomy-Derived CS, in order to facilitate a direct comparison.

Kinematic Outcomes and Statistical Analyses

Elbow flexion kinematics as a function of flexion angle were calculated for each simulated active flexion trial using an Euler analysis (Dunning *et al.*, 2001; Dunning *et al.*, 2003; King *et al.*, 1999). Kinematic dependent variables were valgus angulation and internal rotation of the ulna relative to the humerus (An *et al.*, 1984; Dunning *et al.*, 2001; King *et al.*, 1999).

Five specimens were randomly selected to evaluate the within-subject repeatability of generating Motion-Derived CS. Repeatability was calculated as the standard deviation of 5 repeated trials, and averaged over 5 specimens. This was evaluated for varus-valgus angle, internal-external rotation, anterior-posterior and proximal-distal positions of the CS relative to its corresponding bone segment. The measurements were made relative to the tracker coordinate systems, as their locations on the bones were constant throughout the 5 trials.

Once all trials were completed, the specimens were disarticulated and digitized as described above, and flexion kinematics were calculated using both Anatomy-Derived and Motion-Derived CS. This produced two sets of kinematic pathways, both of which originated from the same tracker motion data. Thus in all comparisons, the only difference was the type of CS in which the kinematics were calculated.

Inter-subject variability was calculated as the difference of the kinematic measure (*i.e.* valgus angle or internal rotation) for each specimen relative to the average of the 10 specimens. This was calculated at every 1° increment of flexion, resulting in the difference from the mean as a function of flexion angle. Statistical analysis consisted of a two-way repeated-measures ANOVA (analysis of variance) to investigate the effect of flexion angle and coordinate system type on inter-subject variability using SPSS 17.0 (SPSS Inc., Chicago, Il). Inter-subject variability was also studied using a box plot analysis. These analyses were performed over a flexion range of 20° to 120°.

4.3 RESULTS

The within-subject repeatability of generating Motion-Derived CS was less than 0.5 mm and 1º in all measured coordinate directions for the humerus and ulna (Table 4.1).

Inter-subject variability of valgus angulation kinematics (Figure 4.3A) was 1.0 ± 0.8° when using Motion-Derived CS, which was significantly less than the 3.8 ± 2.7° calculated using Anatomy-Derived CS ($p < 0.05$). Inter-subject variability of internal ulnar rotation kinematics (Figure 4.3B) was 1.8 ± 1.6° when using Motion-Derived CS, which was also less than the 6.6 ± 5.7° calculated using Anatomy-Derived CS ($p < 0.05$).

Inter-subject variability of kinematic pathway was analyzed using box plots. The median, min, max, first quartile, third quartile, and inner fences are shown for valgus angulation (Figure 4.4A) and internal rotation (Figure 4.4B). All corresponding features of the box plots were less for Motion-Derived than for Anatomy-Derived CS. For valgus angulation, the median values were 0.8° and 3.4°, and the maximum values were 3.3° and 9.2°, for Motion-Derived and Anatomy-Derived CS respectively. For internal rotation, the median values were 1.2° and 4.8°, and the maximum values were 5.9° and 21.6°, for Motion-Derived and Anatomy-Derived CS respectively.

Measurement Direction	Humerus	Ulna
Varus-Valgus Angle (deg)	0.36	0.46
Internal-External Rotation (deg)	0.72	0.64
Proximal-Distal Position (mm)	0.39	0.29
Anterior-Posterior Position (mm)	0.39	0.36

Table 4.1: Within-Subject Repeatability of Generating Motion-Derived CS
Standard deviation of 5 repeated trials averaged over 5 specimens.

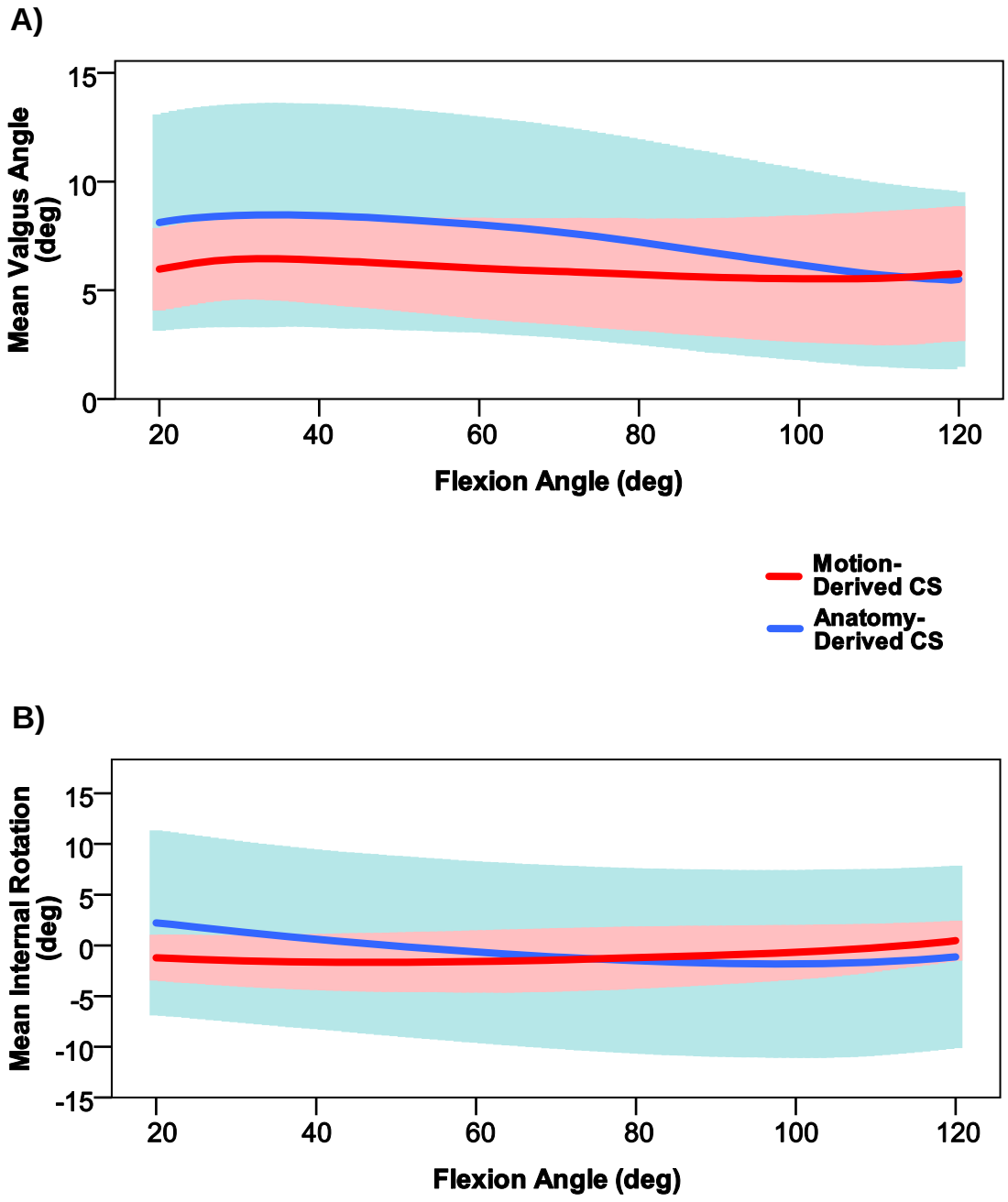

Figure 4.3: Kinematic Pathways

Kinematic pathways of (A) valgus angulation and (B) internal rotation were calculated using Motion-Derived (red) and Anatomy-Derived (blue) CS. Ulna relative to the humerus as a function of flexion angle. Solid lines represent the mean of 10 specimens. Translucent areas represent +/-1SD.

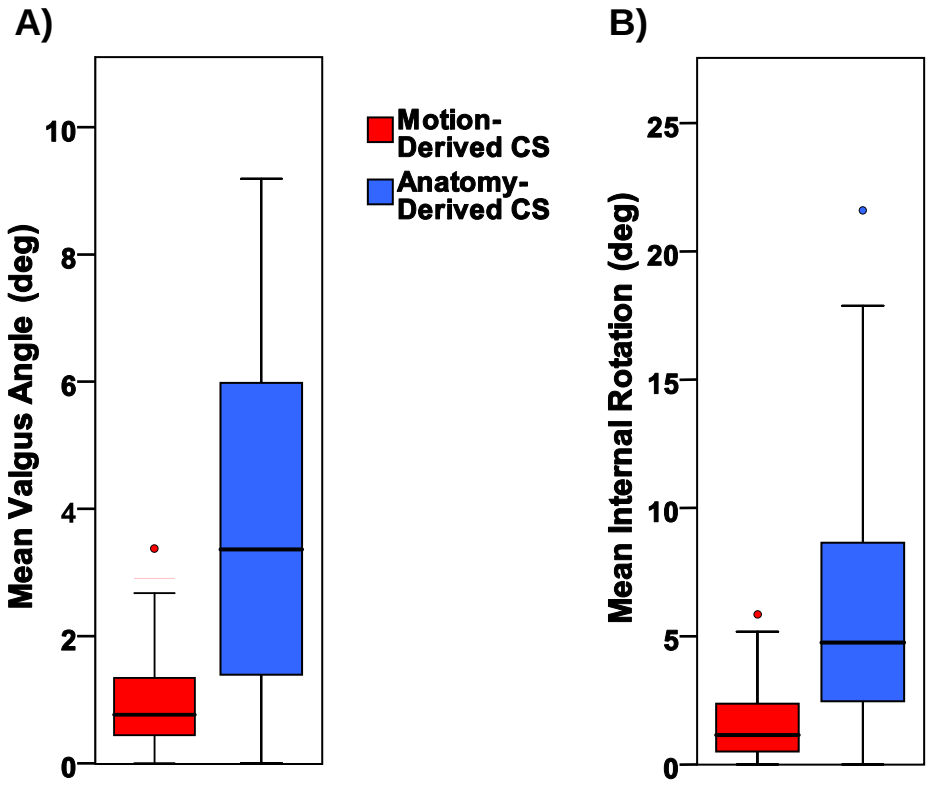

Figure 4.4: Inter-Subject Variability

Inter-subject variability of (A) valgus angulation and (B) internal rotation were calculated using Motion-Derived (red) and Anatomy-Derived (blue) CS. Ulna relative to the humerus. Shown are the median, minimum, maximum, first quartile, third quartile, and inner fences of 10 specimens over a flexion range of 20° to 120°.

4.4 DISCUSSION

The Motion-Derived CS for the humerus and ulna were highly repeatable. Moreover, they produced kinematic pathways with less variability among specimens. Doro *et al.* (2008) presented similar findings in the knee using a commercially available knee navigation system (Doro *et al.*, 2008). The greater variability among elbows calculated using Anatomy-Derived CS suggests that much of the kinematic variability observed between specimens can be largely attributable to differences in anatomy which do not coincide with joint motion patterns. Therefore, the use of Motion-Derived CS may increase the signal to noise ratio in measurements by reducing the standard error of kinematic dependent variables, thereby potentially increasing the statistical power of biomechanical studies and allow for reduced sample sizes.

The obvious appeal of using Motion-Derived CS is to avoid the disruption of soft tissues in order to digitize anatomical features, and also to avoid relying on the accuracy of manually selecting these features. The Anatomy-Derived method is prone to geometric imprecision and human error (Brownhill *et al.*, 2006), and in applications such as registration, requires direct access to a significant amount of bony anatomy, thus precluding this technique for *in-vivo* studies and reducing its efficacy in orthopaedic procedures.

The origin of the Ulnar Motion-Derived CS was partly based on a digitized point. Thus, it must be conceded that the ideal of a fully Motion-Derived CS was compromised by employing an anatomical landmark. Alternatively, a fully Motion-Derived origin can be employed where the Motion-Derived Humeral origin is projected onto the flexion SDA, then shifted anywhere along that axis. To confirm this, all kinematic angles and positions were also calculated with a projected Humeral origin located 2 cm medial along the flexion axis, and used as the Ulnar origin. These calculations were made using the same raw data collected from the N=10 specimens, but with no statistical analysis. These produced identical results, which is logical since the location of the CS along the flexion

axis would not be expected to influence the off-axis measurements that were evaluated in this study.

The objective of this study was, first and foremost, to determine which coordinate system method is less variable between subjects. The approach was taken where Motion-Derived features, such as rotational centers and axes, were consistent with the Anatomy-Derived method. This conscious compromise put the onus on the Motion-Derived method to be compared against an established Anatomy-Derived method. Since the Motion-Derived Ulnar CS did not entirely conform to the Motion-Derived ideal, then to what extent did it detract from the ideal? The digitized point was projected onto the ulnar flexion SDA to determine the location of the origin along the flexion axis. Since the flexion SDA was entirely Motion-Derived, any error from the digitization process could only influence the medial-lateral position of the origin along the flexion axis. The radial location was still entirely Motion-Derived.

Similarly, the X axis of the Ulnar Motion-Derived CS was based on two digitized points. The origin can be fully Motion-Derived as described above. This leaves the over the skin digitization of the distal ulnar styloid, which is readily palpable and does not detract from a minimally invasive paradigm. However, where a fully Motion-Derived CS is desired, the Y axis can be defined perpendicular to the flexion and forearm rotation SDAs. Then the flexion SDA forms the Z axis, with the X axis perpendicular to the Y and Z axes. Though this could conceivably affect the flexion angle calculation, it was found that both methods produced virtually identical results. It is also possible to create a Motion-Derived CS for the radius. Such a coordinate system might have its origin at the center of the radio-capitellar joint, and use the flexion and forearm rotation SDAs in a similar manner as presented in this work.

The efficacy of this method in joints other than the elbow will depend on the repeatability of rotation axes and the intersection of those axes. Where only one body segment CS is desired, it is not necessary for both rotation axes to be highly repeatable, only the axis attached to the body segment of interest. For example, the shoulder abduction axis may not be sufficiently repeatable because this rotation has no off-axis articular or ligamentous constraints. Certainly, inter-subject reproducibility of the

abduction axis should be very poor. However, humeral axial rotation might be considerably more repeatable relative to the humerus, and both axes can be expected to intersect at the humeral head center. Thus, if only a humeral segment CS is required, then a modified version of the Motion-Derived method may be useful. This same logic can be applied to the knee, hip and wrist. Also, it is not necessary that the intersection of the rotation axes be precise, only that the nearby intersection be repeatable. If the intended purpose is to measure kinematics, then it is also important that these be suitably reproducible among subjects.

The valgus angulations measured using Motion-Derived CS did not decrease towards 0º at 90º of flexion which, from contemporary studies of carrying angle, has become a commonly accepted characteristic (Van Roy *et al.*, 2005; Zampagni *et al.*, 2008b). This can be explained by differences in coordinate system definitions. As our focus was on kinematics, our reference (humerus) coordinate system was aligned with the flexion axis. In contrast, studies of carrying angle have tended to use the humeral long axis as reference, which is consistent with clinical radiographic measurements (Paraskevas *et al.*, 2004; Park and Kim, 2009; Yilmaz *et al.*, 2005; Zampagni *et al.*, 2008a). Thus, our reported valgus angulations were not intended to specifically represent the carrying angle. A study by An *et al.* (1984) addressed the controversies and inconsistencies regarding carrying angle results of previous studies, by using a theoretical analysis of three popular measurement methods (An *et al.*, 1984). One of the methods evaluated was a Eularian angle analysis consistent with the method used to calculate valgus angulation in this study. They found that the carrying angle remains essentially constant throughout flexion when the humeral shaft is nearly perpendicular to the flexion axis. This condition is equivalent to our humeral coordinate system definition which has a humeral deviation angle of zero. Using An's evaluation of the Eularian analysis with this condition, it is clear that the carrying angle remains constant and equal to the ulnar deviation angle, which is precisely the behaviour of our results.

An *et al.* also found that the various methods of measuring carrying angle produce equal results at full extension (An *et al.*, 1984). Thus the relatively constant valgus angulation can be compared with the carrying angle measured at full extension. Various

studies have reported this to be between 11º and 20º (Paraskevas *et al*., 2004; Park and Kim, 2009; Yilmaz *et al*., 2005; Zampagni *et al*., 2008a; Van Roy *et al*., 2005). In order to compare our valgus angulation to a carrying angle measurement, the humeral deviation angle is added, which ranges from 1º to 14º (Keats *et al.*, 1966; London, 1981). With this correction, we find that the valgus angulation of 6º in this study corresponds to a range of 7º to 20º, which is in agreement with the range of reported carrying angles. Furthermore, our valgus angle of 6º is confirmed by London (1981) who found a constant carrying angle of 12º (range 9º-14º) and a humeral deviation range of 4º to 8º. Thus, subtracting London's midrange humeral deviation of 6º from his carrying angle of 12º precisely confirms our average valgus angulation of 6º.

In conclusion, the ease, repeatability and low inter-subject variability makes the Motion-Derived CS method a promising tool for use in biomechanical studies of the upper limb and some surgical procedures. Previous work has shown that the SDA method is highly repeatable within-subjects (Duck *et al.*, 2003; Duck *et al.*, 2004). In the current study, performing the passive motion sequence proved to be simple and reliable. The repeatability of creating the Motion-Derived CS was less than 0.5 mm and 1º for all measurements, which is a level of repeatability that is acceptable for most applications in orthopedic surgery. This Motion-Derived CS method could find applications in computer-navigated surgery of the upper limb, including registration of pre-operative plans such as ligament reconstructions or joint replacements without severe articular deformity, or where passive motion is not impacted by injury. The reduced variability amongst arms suggests that it may be possible to use contralateral Motion-Derived CS in the setting of advanced arthritis and joint destruction. However, this needs to be further studied in paired specimens.

4.5 REFERENCES

An K N, Morrey B F, Chao E Y. Carrying angle of the human elbow joint. J Orthop Res 1984; (1): 369-378.

Ball R S. The theory of screws: A study in the dynamics of a rigid body. Hodges, Foster, 1876.

Beggs J S. Kinematics. Hemisphere, Washington, D.C. 1983.

Besier T F, Sturnieks D L, Alderson J A, Lloyd D G. Repeatability of gait data using a functional hip joint centre and a mean helical knee axis. J Biomech 2003; (36): 1159-1168.

Blankevoort L, Huiskes R, de Lange A. The envelope of passive knee joint motion. J Biomech 1988; (21): 705-720.

Bottlang M, Madey S M, Steyers C M, Marsh J L, Brown T D. Assessment of elbow joint kinematics in passive motion by electromagnetic motion tracking. J Orthop Res 2000; (18): 195-202.

Bottlang M, Marsh J L, Brown T D. Factors influencing accuracy of screw displacement axis detection with a D.C.-based electromagnetic tracking system. J Biomech Eng 1998; (120): 431-435.

Brownhill J R, Ferreira L M, Pichora J E, Johnson J A, King G J. Defining the flexion-extension axis of the ulna: implications for intra-operative elbow alignment. J Biomech Eng 2009; (131): 021005.

Brownhill J R, Furukawa K, Faber K J, Johnson J A, King G J. Surgeon accuracy in the selection of the flexion-extension axis of the elbow: an in vitro study. J Shoulder Elbow Surg 2006; (15): 451-456.

Doro L C, Hughes R E, Miller J D, Schultz K F, Hallstrom B, Urquhart A G. The Reproducibility of a Kinematically-Derived Axis of the Knee versus Digitized Anatomical Landmarks using a Knee Navigation System. Open Biomed Eng J 2008; (2): 52-56.

Duck T R, Dunning C E, King G J, Johnson J A. Variability and repeatability of the flexion axis at the ulnohumeral joint. J Orthop Res 2003; (21): 399-404.

Duck T R, Ferreira L M, King G J, Johnson J A. Assessment of screw displacement axis accuracy and repeatability for joint kinematic description using an electromagnetic tracking device. J Biomech 2004; (37): 163-167.

Dunning C E, Duck T R, King G J, Johnson J A. Simulated active control produces repeatable motion pathways of the elbow in an in vitro testing system. J Biomech 2001; (34): 1039-1048.

Dunning C E, Gordon K D, King G J, Johnson J A. Development of a motion-controlled in vitro elbow testing system. J Orthop Res 2003; (21): 405-411.

Gamage S S, Lasenby J. New least squares solutions for estimating the average centre of rotation and the axis of rotation. J Biomech 2002; (35): 87-93.

Keats T E, Teeslink R, Diamond A E, Williams J H. Normal axial relationships of the major joints. Radiology 1966; (87): 904-907.

King G J, Zarzour Z D, Rath D A, Dunning C E, Patterson S D, Johnson J A. Metallic radial head arthroplasty improves valgus stability of the elbow. Clin Orthop Relat Res 1999;114-125.

London J T. Kinematics of the elbow. J Bone Joint Surg Am 1981; (63): 529-535.

Morrey B F, Tanaka S, An K N. Valgus stability of the elbow. A definition of primary and secondary constraints. Clin Orthop Relat Res 1991;187-195.

Paraskevas G, Papadopoulos A, Papaziogas B, Spanidou S, Argiriadou H, Gigis J. Study of the carrying angle of the human elbow joint in full extension: a morphometric analysis. Surg Radiol Anat 2004; (26): 19-23.

Park S, Kim E. Estimation of Carrying Angle Based on CT Images in Preoperative Surgical Planning for Cubitus Deformities. Acta Med Okayama 2009; (63): 359-365.

Piazza S J, Cavanagh P R. Measurement of the screw-home motion of the knee is sensitive to errors in axis alignment. J Biomech 2000; (33): 1029-1034.

Schache A G, Baker R, Lamoreux L W. Defining the knee joint flexion-extension axis for purposes of quantitative gait analysis: an evaluation of methods. Gait Posture 2006; (24): 100-109.

Schwartz M H, Rozumalski A. A new method for estimating joint parameters from motion data. J Biomech 2005; (38): 107-116.

Van Roy P, Baeyens J P, Fauvart D, Lanssiers R, Clarijs J P. Arthro-kinematics of the elbow: study of the carrying angle. Ergonomics 2005; (48): 1645-1656.

Veeger H E, Yu B. Orientation of axes in the elbow and forearm for biomechanical modelling. IEEE Xplore 1996;377-380.

Wu G, van der Helm F C, Veeger H E, Makhsous M, Van Roy P, Anglin C, Nagels J, Karduna A R, McQuade K, Wang X, Werner F W, Buchholz B. ISB recommendation on definitions of joint coordinate systems of various joints for the reporting of human joint motion--Part II: shoulder, elbow, wrist and hand. J Biomech 2005; (38): 981-992.

Yilmaz E, Karakurt L, Belhan O, Bulut M, Serin E, Avci M. Variation of carrying angle with age, sex, and special reference to side. Orthopedics 2005; (28): 1360-1363.

Zampagni M L, Casino D, Martelli S, Visani A, Marcacci M. A protocol for clinical evaluation of the carrying angle of the elbow by anatomic landmarks. J Shoulder Elbow Surg 2008a; (17): 106-112.

Zampagni M L, Casino D, Zaffagnini S, Visani A, Marcacci M. Trend of the carrying angle during flexion-extension of the elbow joint: a pilot study. Orthopedics 2008b; (31): 76.

CHAPTER 5 – THE EFFECT OF TRICEPS REPAIR TECHNIQUE FOLLOWING OLECRANON EXCISION ON ELBOW STABILITY AND EXTENSION STRENGTH: AN *IN-VITRO* BIOMECHANICAL STUDY

OVERVIEW: *This chapter presents the new elbow joint motion simulator and motion-based coordinate system method in the application of an in-vitro clinical study. Anterior and posterior triceps repairs following simulated olecranon excision were evaluated and compared in the setting of olecranon deficiency. The elbow motion simulator was employed to produce elbow extension in the varus and valgus positions. Motion-based coordinate systems for the humerus and ulna were used to calculate joint kinematics and quantify the effects on elbow stability. Progressive sectioning of the olecranon increased elbow laxity for both active and passive extension ($p<0.001$). There was no statistically significant difference in laxity between the repairs for either active ($p=0.2$) or passive ($p=0.1$) extension. The posterior repair provided greater extension strength than the anterior repair at all applied triceps tensions and for all olecranon resections ($p=0.01$). Both repairs reduced extension strength relative to the intact state ($p<0.01$). Sequential olecranon excision decreased extension strength ($p=0.04$). By using the new methods presented in this work, new data (active varus and valgus extension) and improved data (reduced inter-subject variability) is used by investigators to improve patient care.*[1]

1) A version of this work has been published: Ferreira LM, Bell TH, Johnson JA, King GJW. The Effect of Triceps Repair Technique Following Olecranon Excision on Elbow Stability and Extension Strength: An In-Vitro Biomechanical Study. *Journal of Orthopaedic Trauma.* In Press. 2010. (See Appendix E.3)

5.1 INTRODUCTION

Olecranon fractures are the second most common osseous injury of the elbow (Veillette and Steinmann, 2008). The majority are displaced fractures that can be successfully treated with open reduction and internal fixation (Bailey *et al.*, 2001). However, with severe comminution or significant bone loss such as in open fractures, excision of the comminuted fragments and repair of the triceps to the ulna is recommended (Bailey *et al.*, 2001; Gartsman *et al.*, 1981). The triceps can be reattached to either the anterior or posterior aspect of the ulna (Didonna *et al.*, 2003; Morrey, 1995). It is generally recommended that the triceps should be repaired to the anterior surface of the remaining olecranon to improve joint stability (Morrey, 1995). A recent biomechanical study reported that repair to the posterior surface would provide better extension strength (Didonna *et al*., 2003). However, the effect of triceps repair location on elbow stability has not been quantified.

The purpose of this study was to determine the effect of triceps repair technique on elbow stability and extension strength in the setting of olecranon deficiency using a cadaveric model. It was hypothesized that the posterior triceps repair would produce higher triceps extension strength than the anterior repair, but that the anterior repair would produce better joint stability.

5.2 MATERIALS AND METHODS

Eight previously fresh-frozen cadaveric arms amputated at mid-humerus were used (age 75 ± 11 years). A 3D ulnar surface model was generated from CT imaging using VTK (Visualization Toolkit, Kitware Inc., Clifton Park, NY) and a pre-op plan determined cutting planes corresponding to sequential levels of olecranon resection. The orientation of the cutting planes was determined using the greater sigmoid notch and the posterior aspect of the proximal ulna. The plane containing the ridge of the greater sigmoid notch was calculated with a least-squares algorithm, and the vector normal to this plane was oriented medial-lateral. Another plane was created using three points that

were digitized on the posterior aspect, and the vector normal to this plane was oriented anterior-posterior. The cross product of the two vectors was oriented proximal-distal and it served as the vector normal to the cut planes. The olecranon was sectioned in 25% increments. Olecranon resections of 0% and 100% were defined at the most proximal and distal aspects (respectively) of the greater sigmoid notch. The pre-op plan was registered to the specimen anatomy using an Iterative Closest Point algorithm, providing real-time 3D navigation of the olecranon resection (Cao *et al.*, 2004; Popescu *et al.*, 2003).

Muscle tendons (biceps, brachialis, brachioradialis and triceps) were sutured to the actuators of an elbow motion simulator using a locking Krackow repair (Howard *et al.*, 1997). A Steinmann pin was inserted transversely through the radius and ulna, approximately 3 cm proximal to the DRUJ to secure the forearm in neutral rotation. Another Steinmann pin was inserted through the long finger metacarpal into the distal radius to secure the wrist in neutral flexion. The simulator could be rotated into the varus and valgus positions in order to generate gravity loaded varus or valgus extension. Active elbow extension was simulated by applying physiologic loads to the tendons (Johnson *et al.*, 2000). Passive elbow extension was performed by manually moving the arm. An electromagnetic tracking system (Flock Of Birds™, Ascension Technology Corp., Burlington, VT) recorded active and passive extension kinematics at eight joint angles from 15 to 120º at 15º intervals. Joint laxity was calculated as the difference in valgus angulation between the varus and valgus positions, at corresponding angles of flexion.

Using a 0.4 mm oscillating saw, serial resections of the olecranon were performed at 25% increments using the aforementioned image guidance system (Figure 5.1). Resections began at the most proximal aspect of the greater sigmoid notch and continued to 100% at the most distal aspect. The triceps was advanced and repaired to the remaining olecranon using either an anterior or posterior repair to the remaining olecranon (Figure 5.2). The triceps sutures were passed through two transosseous tunnels adjacent to the articular surface (anterior repair) or adjacent to the subcutaneous border of the ulna (posterior repair). The free suture ends were clamped to allow for repeated testing without the need to resuture the tendon for each resection. The order of the repairs was randomized for each resection level.

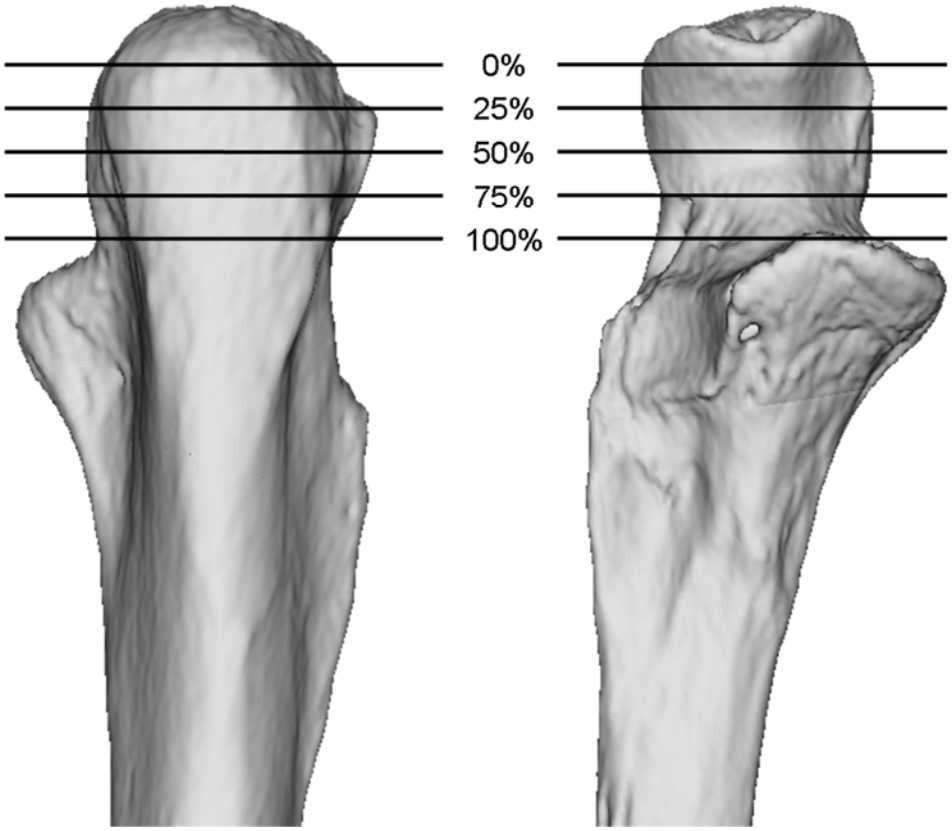

Figure 5.1: Simulated Olecranon Fracture Levels

Three-dimensional surface model of the ulna created from CT imaging. Olecranon resection levels in 25% increments begin at the most proximal aspect of the greater sigmoid notch and continue to 100% at the most distal aspect.

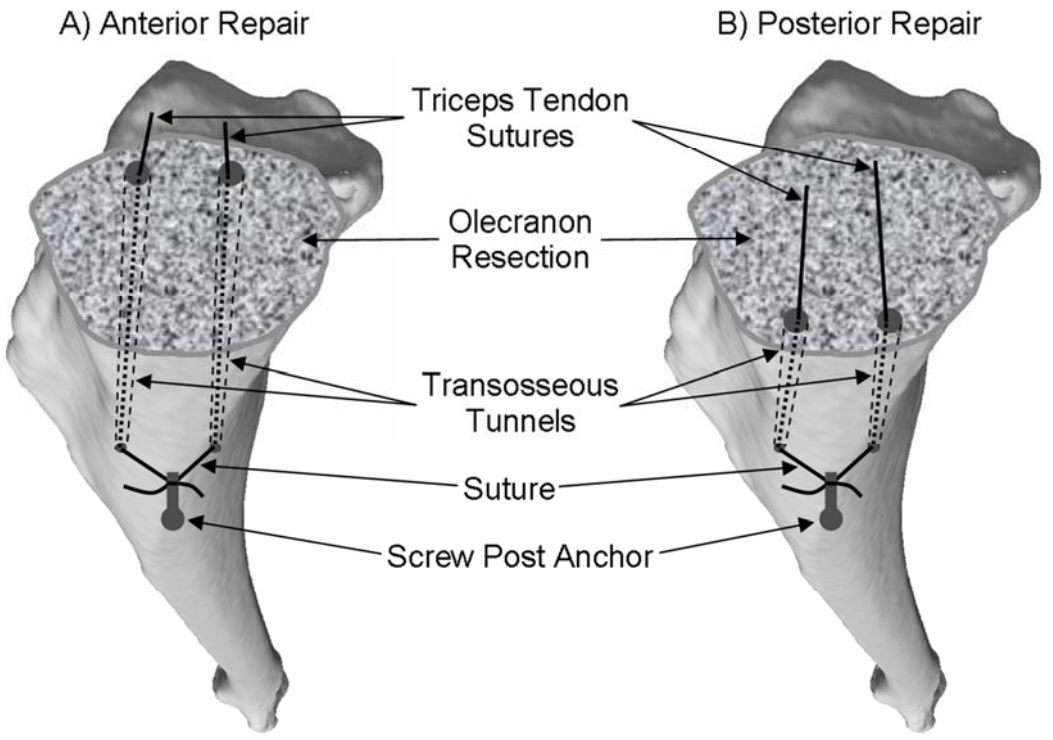

Figure 5.2: Anterior and Posterior Triceps Repairs

Proximal-Posterior views of the ulna showing (A) the Anterior Repair and (B) the Posterior repair. Transosseous tunnels were drilled through the olecranon resection and exited through the posterior aspect of the ulna. Free ends of the suture were tied to a screw post anchor. Left arm shown.

Triceps extension strength was defined as the reaction force at the distal ulnar styloid as a function of triceps tension. This was quantified in the vertical position with the elbow at 90º of flexion using a force transducer located at the distal ulnar styloid (Figure 5.3). The motion simulator was used to increase triceps tension from 25 to 200 N of static load while the transducer recorded the reaction force. This protocol was performed in the intact elbow and repeated at each stage of olecranon resection.

Outcome variables included varus-valgus elbow laxity and triceps extension strength. A comparison of elbow laxity between the repairs was evaluated with a three-way repeated measures ANOVA 2×5×8 design: 2 repair methods, 5 resection levels, and 8 joint angles. The intact state was not included in the comparison between repairs because it did not involve a triceps repair. In order to compare laxity of the intact state to subsequent olecranon resections, and between active and passive flexion modes; a three-way repeated measures ANOVA was performed for each repair with the intact state included as a resection level, for a 2×6×8 design: 2 extension modes, 6 resection levels, and 8 joint angles. A comparison of triceps extension strength between the repairs was evaluated with a three-way repeated measures ANOVA 2×5×8 design: 2 repair methods, 5 resection levels, and 8 triceps tensions. In order to compare extension strength of the intact state to subsequent olecranon resections, a two-way repeated measures ANOVA was performed for each repair with the intact state included as a resection level, for a 6×8 design: 6 resection levels and 8 triceps tensions. When Mauchly's test for sphericity was violated ($p < 0.05$), the degrees-of-freedom for the main effect was corrected using the Greenhouse-Geisser procedure when $\varepsilon < 0.75$. For significant main effects, pairwise comparisons were performed between levels using t-tests with a modified Bonferroni procedure. Significance was set at $p < 0.05$.

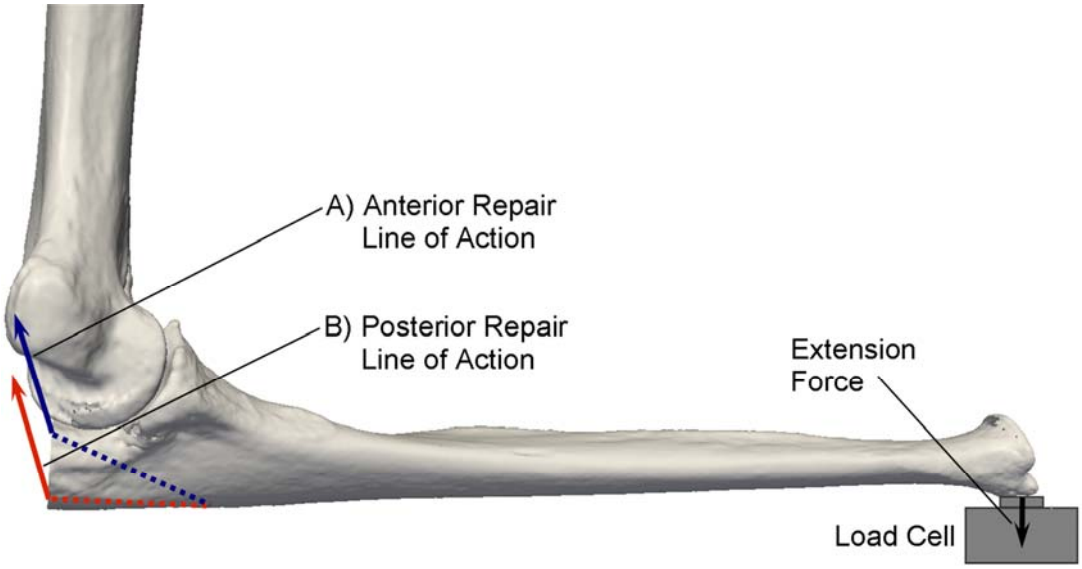

Figure 5.3: Triceps Extension Strength Test

Triceps extension strength test setup showing (A) the Anterior Repair and (B) the Posterior Repair. Applied triceps tension levels were 25 to 200 N. Transosseous tunnels (dashed blue and red lines) and approximate triceps tendon lines of action (solid blue and red lines) are also shown for (A) the Anterior Repair (blue) and (B) the Posterior Repair (red). Left arm shown.

5.3 RESULTS

Progressive sectioning of the olecranon from the initial (0%) resection level increased elbow laxity for both active and passive extension (Figure 5.4) ($p < 0.001$). Although the posterior repair resulted in greater laxity than the anterior repair for all but the 50% resection, this difference was small (less than 3º) and not statistically significant for either active ($p = 0.2$) or passive ($p = 0.1$) extension. Both repairs increased elbow laxity relative to the intact state ($p < 0.05$). Active extension produced less joint laxity than passive extension for both the anterior ($p = 0.007$) and posterior ($p = 0.001$) repairs.

The posterior repair provided greater extension strength than the anterior repair at all applied triceps tensions and for all olecranon resections (Figure 5.5) ($p = 0.01$). The anterior repair produced 93% of the extension strength of the posterior repair. Progressive sectioning of the olecranon from the initial (0%) resection level caused a reduction in extension strength ($p = 0.04$). However, there were no significant differences between resection levels ($p > 0.05$). Compared to the intact state with native olecranon and triceps, the anterior repair reduced extension strength for every resection level by 30.6% (2.7±0.4 N) to 34.5% (3.1±0.5 N) ($p < 0.01$). For the posterior repair, a reduction of 13.0% (1.1±0.3 N) with the initial (0%) resection was not significant ($p = 0.21$), but subsequent resections reduced extension strength by 25.5% (2.2±0.4 N) to 28.5% (2.4±0.3 N) compared to the intact state ($p < 0.01$). The loss of extension strength from the intact state, throughout the 25 to 200 N range of applied triceps tensions, was on average 24% for the posterior and 30% for the anterior repair.

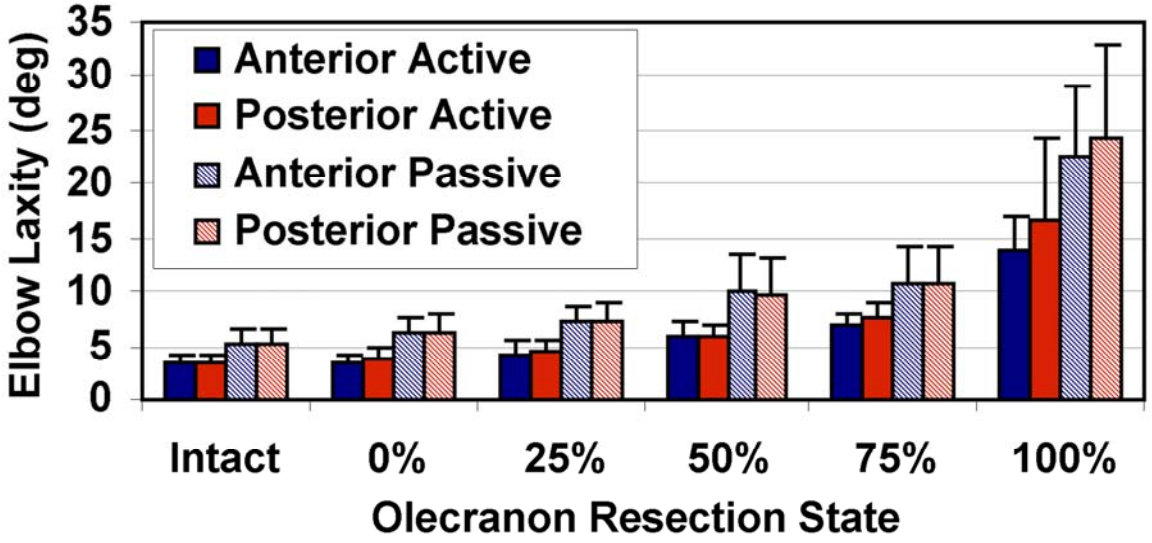

Figure 5.4: Elbow Joint Laxity *vs*. Olecranon Resection

Laxity increased with progressive resections ($p < 0.001$). Laxity was greater for passive than active extension ($p < 0.01$). There was no difference in laxity between the anterior and posterior repairs for either active ($p = 0.2$) or passive ($p = 0.1$) extension.

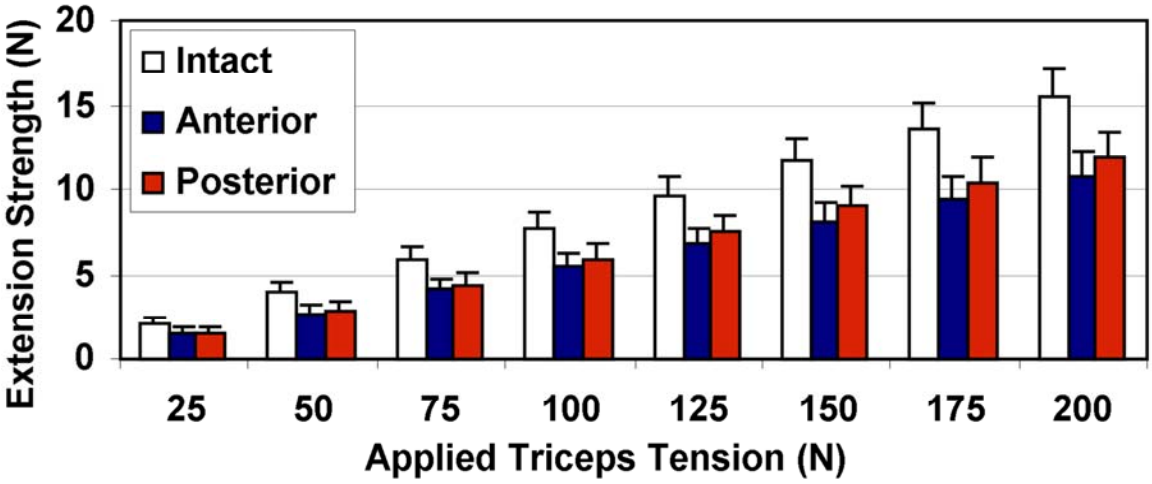

Figure 5.5: Extension Strength *vs*. Triceps Muscle Tension

The posterior repair resulted in greater extension strength than the anterior repair ($p = 0.01$). Extension strength was reduced by both repairs compared to the intact state ($p < 0.01$). Plotted results are the average of all resection levels.

5.4 DISCUSSION

Joint laxity increased with increasing olecranon resections, which agrees with previous studies (An *et al.*, 1986; Kamineni *et al.*, 2003). Laxity was greater for passive compared to active motion, suggesting that post-surgical therapy should employ active motion to optimize joint tracking and avoid undue stress on the olecranon repair. With a 100% olecranon resection, the posterior repair produced slightly more joint laxity (3º) than the anterior repair. However, this was not statistically significant, and performance at the other resection levels was virtually identical for both repairs. Thus, even for large olecranon fractures, the choice of triceps repair technique may not have significant impact on joint stability.

Triceps extension strength was higher for the posterior repair as has previously been reported by DiDonna and coworkers (Didonna *et al.*, 2003). This is likely due to the greater distance of the posterior repair to the joint rotation center, thus providing a greater moment arm for increased mechanical advantage of the triceps. Extension strength was reduced by progressive olecranon resections, although there were no significant differences between resection levels. Olecranon resection reduced extension strength from the intact state by an average of 24% and 30% for the posterior and anterior repairs respectively, with the elbow at 90º. The 30% loss of extension strength for the anterior repair agrees precisely with the results of Gartsman *et al*. (1981) and DiDonna *et al*. (2003) who reported a loss of 29% and 30% respectively (Didonna *et al.*, 2003; Gartsman *et al.*, 1981). DiDonna *et al*. reported that the posterior repair lost 18% of the intact strength whereas we recorded a 24% loss. The source of this difference is not clear, but the conclusion is the same: that the anterior repair resulted in a greater loss of extension strength than the posterior repair.

The fact that progressive olecranon resections had little effect on extension strength may be due to wrapping of the triceps tendon around the posterior trochlea, which may result in the tendon having an “angle of attack” that is more in line with the ulnar long axis. Thus, loss of the olecranon in the distal axial direction would have little impact on the effective moment arm of the triceps tendon, at least with the elbow at 90º.

Conversely, the difference in location of the anterior versus posterior repairs is perpendicular to the direction of olecranon loss. The anterior repair brings the triceps insertion much closer to the joint rotation center, thus reducing the moment arm.

This investigation had a number of strengths. To our knowledge, it is the first to quantify joint laxity during elbow extension as a function of olecranon loss, with either an anterior or posterior triceps repair. The active motion simulator replicated *in-vivo* elbow extension, which allowed us to more accurately model elbow kinematics. The use of simulated muscle activation was an advance over previous studies, as the muscles crossing the joint are now recognized as integral secondary elbow stabilizers (Dunning *et al.*, 2001; Mathew *et al.*, 2009; O'Driscoll *et al.*, 2001). This muscle activation caused the observed decrease in joint laxity compared to manual passive motion, and thus should be considered when performing similar biomechanical studies in order to replicate *in-vivo* joint tracking. Three-dimensional image-guidance removed the need for an unobstructed view of the greater sigmoid notch. This allowed us to minimize damage to soft tissues such as elbow stabilizers, while ensuring accurate olecranon resections. The protocol included randomization of the repair order following each level of olecranon resection. This avoided any potential bias between the repairs in terms of strength or longevity due to unforeseen progressive tissue damage or other unrealized phenomena, which may otherwise have occurred with a constant repair order.

This study has some limitations. First, soft tissue and osseous injuries that are often concurrent with olecranon fractures were not modeled since the focus was to quantify the contribution of the olecranon to elbow stability. Second, this investigation was performed in elderly cadaveric specimens. Younger, more active patients may be less tolerant to the loss of strength which occurs with the olecranon resections tested in this study. Third, as this was an *in-vitro* study, active extension was simulated using an elbow testing system and passive extension did not include muscle tone loads. These methods likely do not produce precisely the elbow kinematics experienced *in-vivo*. While there was a statistically significant difference in strength between the two repairs, it is not clear whether this difference is clinically relevant. The triceps extension strength was quantified only at 90º of static elbow flexion. At this joint angle, there is some wrapping

of the triceps tendon around the posterior distal humerus, especially for increased levels of olecranon excision. This may have caused the triceps tendon line of action to be similar for both repairs. The posterior repair insertion site is further from the joint center than the anterior repair, which would likely generate a greater moment arm for the posterior repair at joint angles with a less prominent tendon wrapping effect. Thus, future work should include a comparison of extension strength of both repairs at joint angles between 90º and full extension.

In conclusion, there was no significant difference in elbow stability between the anterior and posterior triceps repairs following sequential excision of the olecranon in this *in-vitro* study. However, the posterior repair produced significantly greater triceps extension strength than the anterior repair. Thus, the authors favour posterior repair of the triceps after excision of the olecranon. Clinical studies are needed to confirm these experimental *in-vitro* observations.

5.5 REFERENCES

An K N, Morrey B F, Chao E Y. The effect of partial removal of proximal ulna on elbow constraint. Clin Orthop Relat Res 1986;270-279.

Bailey C S, MacDermid J, Patterson S D, King G J. Outcome of plate fixation of olecranon fractures. J Orthop Trauma 2001; (15): 542-548.

Cao Z, Pan S, Li R, Balachandran R, Fitzpatrick J M, Chapman W C, Dawant B M. Registration of medical images using an interpolated closest point transform: method and validation. Med Image Anal 2004; (8): 421-427.

Didonna M L, Fernandez J J, Lim T H, Hastings H, Cohen M S. Partial olecranon excision: the relationship between triceps insertion site and extension strength of the elbow. J Hand Surg Am 2003; (28): 117-122.

Dunning C E, Zarzour Z D, Patterson S D, Johnson J A, King G J. Muscle forces and pronation stabilize the lateral ligament deficient elbow. Clin Orthop Relat Res 2001;118-124.

Gartsman G M, Sculco T P, Otis J C. Operative treatment of olecranon fractures. Excision or open reduction with internal fixation. J Bone Joint Surg Am 1981; (63): 718-721.

Howard R F, Ondrovic L, Greenwald D P. Biomechanical analysis of four-strand extensor tendon repair techniques. J Hand Surg Am 1997; (22): 838-842.

Johnson J A, Rath D A, Dunning C E, Roth S E, King G J. Simulation of elbow and forearm motion in vitro using a load controlled testing apparatus. J Biomech 2000; (33): 635-639.

Kamineni S, Hirahara H, Pomianowski S, Neale P G, O'Driscoll S W, ElAttrache N, An K N, Morrey B F. Partial posteromedial olecranon resection: a kinematic study. J Bone Joint Surg Am 2003; (85-A): 1005-1011.

Mathew P K, Athwal G S, King G J. Terrible triad injury of the elbow: current concepts. J Am Acad Orthop Surg 2009; (17): 137-151.

Morrey B F. Current concepts in the treatment of fractures of the radial head, the olecranon, and the coronoid. Instr Course Lect 1995; (44): 175-185.

O'Driscoll S W, Jupiter J B, King G J, Hotchkiss R N, Morrey B F. The unstable elbow. Instr Course Lect 2001; (50): 89-102.

Popescu F, Viceconti M, Grazi E, Cappello A. A new method to compare planned and achieved position of an orthopaedic implant. Comput Methods Programs Biomed 2003; (71): 117-127.

Veillette C J, Steinmann S P. Olecranon fractures. Orthop Clin North Am 2008; (39): 229-36, vii.

CHAPTER 6 – GENERAL DISCUSSION AND CONCLUSIONS

OVERVIEW: *This chapter briefly revisits each of the objectives and hypotheses identified at the outset of this research. The developmental work that was performed to achieve those objectives, and the investigations undertaken to address those hypotheses are summarized and discussed. The strengths and limitations of the methods used to simulate elbow joint motion, and to evaluate its performance are reviewed and discussed. Forthcoming applications of the simulator and its associated methods are presented, and future directions of this research are explored.*

6.1 SUMMARY

The assessment of joint kinematics and stability in a controlled laboratory setting is essential in order to gain an improved understanding of normal joint function, and the aberrations that can occur with injury or disease. Furthermore, *in-vitro* testing allows treatment options to be evaluated and optimized before they are applied to patients. Simulated active elbow motion has been shown to produce more reproducible joint kinematics compared to passive motion. Of greatest significance is the reduction of joint laxity when using active simulation. However, *in-vitro* simulation of elbow motion has not enjoyed significant development, especially in positions other than vertical (gravity dependent). By studying elbow motion in the four principal positions, important information regarding joint kinematics and dynamics, including soft tissue loads, can be deduced for a variety of common upper extremity activities. In light of the foregoing, this research was undertaken to develop an accurate and reliable *in-vitro* elbow motion simulator capable of generating elbow flexion and extension in the horizontal, varus and valgus positions, as well as the vertical position. To support the development of this system, studies were conducted to evaluate its performance.

The first phase of this work was to develop and evaluate a closed-loop muscle tension controller using a servo-motor actuator with a custom force feedback transducer (Appendix B). This muscle tensioning system was found to have sufficient accuracy (within 7 N, 7% of setpoint) and speed under very rigorous square wave testing conditions. Through an evaluation of its performance and operating speed, it was determined that the tension controller would serve as a modular component within the overall real-time flexion controller system.

The second phase of this work (Objective 1, Chapter 2) was to generate controlled elbow flexion in the varus, valgus and horizontal positions. This was accomplished by developing a set of transfer functions for the four principal positions, and for pronated and supinated flexion, for a total of eight conditions. A transfer function for each muscle was defined, and depending on the muscle and on the condition, the transfer function inputs were a mixture of joint angle and 'prime mover' load. The output was either muscle tension or velocity. In order to address the challenges of the horizontal position in particular, biceps and triceps transfer functions used the current elbow joint angle feedback as input. Valgus angulations were calculated as a measure of simulator performance during active and passive flexion. Valgus angulations were significantly more repeatable for active flexion, and joint laxity was significantly decreased for pronated (26%) and supinated (29%) active flexion when compared to passive flexion. Thus Objective 2 was satisfied, as it was shown that the combination of system components (hardware and software) could reliably achieve horizontal as well as varus and valgus active elbow flexion.

The next phase of this work, Objectives 2 and 3, described in Chapter 3, was to develop an algorithm capable of simultaneous muscle tension and elbow joint angle control using closed-loop feedback of muscle load and joint angle. Simultaneous tension control for multiple muscles, and variable numbers of muscles, was also supported. Additionally, transfer functions for feedforward control were also developed. This overall control scheme was incorporated into a system (hardware and software) capable of real-time execution of the tension/flexion controller while recording muscle forces and motion data as a function of elbow joint angle. The complete system was dubbed the Hand and

Upper Limb Centre Multiple Orientation Simulator for the Elbow (HULC MOSE), henceforth referred to as MOSE.

Objective 4 was to achieve constant elbow flexion and extension rate using MOSE in the varus, valgus and horizontal positions. Motion controller development was presented, and its accuracy was investigated in Chapter 3. In that study of seven specimens, the largest absolute joint angle error was 5.3 ± 2.4º for flexion and 4.5 ± 2.8º for extension. In the horizontal position, root mean square error was 2.7º and 2.9º for pronated and supinated flexion, and 3.0º and 2.7º for pronated and supinated extension. Thus, real-time flexion-extension was achieved with near-constant angle control in the horizontal, varus, valgus and vertical positions using MOSE.

Objective 5 was achieved in Chapter 4 with the development of motion-derived coordinate systems for the humerus and ulna. As coordinate systems are a requirement for kinematic data, this work focussed on the development of an easier and more practical way to create them. Unlike traditional anatomy-based methods which require access to bony anatomy, the new technique creates coordinate frames non-invasively. Motion-derived coordinate systems were also shown to generate more consistent elbow kinematics among specimens. Inter-subject variability of valgus angulation kinematics was 1.0 ± 0.8° when using Motion-Derived CS, which was significantly less than the 3.8 ± 2.7° using Anatomy-Derived CS ($p < 0.05$). Inter-subject variability of internal ulnar rotation kinematics was 1.8 ± 1.6° when using Motion-Derived CS, which was also less than the 6.6 ± 5.7° calculated using Anatomy-Derived CS ($p < 0.05$). This has important implications for *in-vitro* studies, since reduced variability can increase statistical power, or provide the option to use fewer specimens. Moreover, this method is compatible with a minimally invasive approach to surgical protocols, and it could find its way into existing procedures and/or provide the efficacy for computer-navigation in others.

The final phase of this treatise (Objective 6) was to apply the developments of this work in an *in-vitro* biomechanical investigation with clinical relevance. A study of eight cadaveric upper extremity specimens was undertaken to evaluate two triceps repair techniques following simulated olecranon fracture and excision. The new MOSE simulator and coordinate system method developed in this work generated kinematic data

that was previously unattainable. With the new ability to produce elbow extension in the varus and valgus positions, we were able to conclude that laxity was greater for passive compared to active motion. This suggests that post-surgical therapy should employ active motion to optimize joint tracking and avoid undue stress on the olecranon repair. Also, when using these motions and the improved coordinate system method to compare anterior versus posterior triceps reattachments, we found that there was no statistically significant difference in laxity between the repairs. These laxity results contradict the currently held popular opinion that the anterior repair is advantageous due to its superior restoration of joint stability (Morrey, 1995), even in spite of research showing that it can reduce extension strength (DiDonna *et al., 2003*; Gartsman *et al.*, 1981). However, this view has only been supported by theory and reasoning, whereas our experimental study is the first to quantify varus-valgus laxity with simulated active extension using this surgical model. In doing so, we have shown that both repairs provide similar levels of stability. Furthermore, our extension strength results also agree with previous studies, showing that extension strength is better restored by the posterior repair (DiDonna *et al., 2003*). Thus, the new simulation and coordinate system methods have provided us with new tools to evaluate elbow joint kinematics, and have led us to favour posterior repair of the triceps after olecranon excision.

6.2 STRENGTHS AND LIMITATIONS

MOSE is the first device to generate active *in-vitro* flexion and extension in the varus, valgus horizontal and vertical positions. It is also the first to achieve near-constant joint angle control in all four principal positions. MOSE presents a novel control structure that simultaneously controls elbow joint angle and muscle tension for multiple muscles. To our knowledge, this is the first time that elbow motion – or any joint motion – has been modeled with Cascade PID control. The cascade design allows the simulator to operate in real-time, while using elbow joint angle feedback from a spatial tracking system and muscle load feedback from load transducers. The scalability of the muscle tension control scheme allows for multiple and variable numbers of muscles to be

modeled using this approach. This makes the simulator practical and flexible for future biomechanical studies having different requirements for muscle control.

The ability of the MOSE Cascade PID controller to employ the relatively slow joint angle process for feedback is a defining feature of this design. It reduces the reliance on feedforward control elements, so that not all process characteristics need to be known and modeled. Moreover, the biomechanical models on which the feedforward transfer functions are based, do not need to be highly accurate. This is imperative, since it is inconceivable that such models will become so precise in the near future, or that they will be able to compensate for the wide variety of physical characteristics amongst cadaveric specimens. In working with the slow joint angle process, the cascade design also handles the slow tracking system report rate for joint angle closed-loop feedback. High control loop iteration frequency is critical for a control process such as elbow flexion. This is especially so when meeting the challenges of the horizontal position. While other, much faster transducers, such as rotation encoders and inclinometer are available, there is elegance to extracting closed-loop feedback from the same spatial tracking system that acquires 6DOF pose data for kinematic measurements. Note that, in applications where 6DOF data is not required, even an ultra fast angle transducer of any type would not reduce the joint angle time constant itself. Thus, the cascade design allows us to keep the intuitive and easily tuneable PID controller, and provides a unifying control algorithm for all four principal positions. It also finally unifies the concepts of muscle position-control versus load-control, providing a physiologically consistent concept in which all muscles are simultaneously controlled along with the joint angle, using similar and continuous functions.

Thus, the conclusions of the biomechanical study comparing triceps repairs after olecranon fracture excision (Chapter 5) were strengthened by the use of the MOSE system, as well as the new motion-derived coordinate system method. It is the first study to quantify joint laxity during elbow extension in the varus and valgus position as a function of olecranon loss. MOSE active motion simulation replicated *in-vivo* elbow extension, which more accurately modeled elbow kinematics compared to passive simulation. The use of simulated muscle activation in the varus and valgus positions was

an advance over previous studies, as the muscles crossing the joint are now recognized as integral secondary elbow stabilizers. Also, the motion-derived coordinate system method reduces inter-subject kinematic variability, which improves statistical power. This may also allow the option to use fewer specimens.

The investigations presented in this work had some limitations. As with all *in-vitro* biomechanical development and investigation, these studies were performed using cadaveric specimens, many of advanced age. Thus, the strength and quality of bone, ligaments and other soft tissues may have been less than in younger donors. The impact of this on the simulator's development is likely minimal, as the robust nature of the current device would likely be able to compensate for any differences in tissue behaviours.

Active and passive motion simulation methods likely do not produce precisely the elbow kinematics and loading experienced *in-vivo*. Furthermore, only relatively slow motion (10º/s) has been simulated. Thus it is difficult to estimate the actual impact that these conclusions may have on clinical practice. Also, in comparing the performance of active motion simulation to manual passive motion, passive motion did not include muscle tone loads. It is likely that some passive joint laxity may have been reduced in the presence of tone loads.

6.3 CURRENT AND FUTURE DIRECTIONS

Now that well controlled active elbow joint angle has been established for *in-vitro* simulation, the MOSE system and its accompanying software provide an extensible platform on which future advancements can be developed. Initially, these may include the ability to generate fast, as well as resisted motions, in order to model throwing or lifting objects. While the performance of MOSE was evaluated with relatively slow (10º/s) and unresisted motion, the setpoint rate is user-selectable and an external resistance force can easily be applied. Therefore, simulation of throwing and lifting activities may require additional development, and may be the next actions to be replicated in the vertical, horizontal, varus and valgus positions.

In order to conduct studies of forearm rotation with varying elbow joint angle, the Cascade PID control algorithm could be expanded to include forearm rotation. Biceps is a strong supinator muscle, as well as being integral to flexion-extension, which confounds the task of forearm rotation during flexion-extension. Currently, forearm pronation and supination are achieved by simply applying a constant pronator teres load and biceps/brachialis load ratio, respectively. Full and continuous forearm rotation angle control could be produced with a second Cascade PID using forearm rotation angle for feedback in the primary loop, with biceps and pronator teres load feedback in the secondary tension-control loop. Since biceps would exist in both the flexion and forearm rotation processes, the biceps tension outputs would have to be merged and weighted, possibly as a function of the error ratio (*i.e.* ratio of flexion error to forearm rotation error).

An important future goal could be the development and implementation of an auto-tuning algorithm for the muscle tension controller. Once all muscles are connected to their actuators, auto-tuning of each muscle's PID controller will be executed in sequence using the online Ziegler and Nichols heuristic method for determining PID parameters (Åström and Hägglund, 2004; Hang *et al.,* 1991).

This may be achievable using a modification of the current testing protocols. After setting all of the actuators' tension control parameters, the simulator could be placed in the vertical position, and with default flexion and forearm rotation PID parameters, the simulator would perform active flexion-extension and forearm rotation in accordance with the motion-derived coordinate system method of Chapter 4. Thus, elbow joint coordinate systems would be automatically generated so that elbow joint angle and forearm rotation angle feedback could begin. Note that even without forearm rotation control, elbow joint angle feedback could still be calibrated from flexion-extension motion alone.

With either automated or user-defined elbow joint angle feedback calibrated, the joint angle control loop PID parameters could be auto-tuned at a few joint angle regions (*i.e.* full extension to 30º, 30-70º, 70-110º, 110-150º). After performing this in all four principal positions, and for a variety of flexion speeds, the resulting database of PID

parameters would be used as inputs to implement a gain scheduling transfer function for the elbow joint angle PID control loop. Auto-tuning of the muscle tension controllers may then be executed again following flexion tuning. However, rather than tuning at static positions, they could be tuned while the arm is actively flexed at a variety of speeds. The resulting database of PID parameters would be used for gain scheduling of the tension control loops as with the flexion loop.

The PID parameters in both the flexion and tension control loop gain schedules could be interpolated in real-time as a function of joint angle. This would provide continuous and gradual transitions between PID tuning regions. This concept could be extended into compound positions of the simulator. Rather than tuning the PID parameters for all possible positions, the PID parameters for the horizontal, valgus and vertical positions could be spherically interpolated in order to compensate for the gravity vector and biomechanical characteristics in the testing position. This may be achieved with Slerp (spherical linear interpolation) (Shoemake, 1985).

As well as evaluating the simulator's ability to follow a prescribed setpoint at several constant flexion-extension rates, various angular accelerations may also be evaluated. More complex setpoint curves should also be tested, including stop-and-go actions with reversals associated with many common *in-vivo* activities.

The simulator's rotary servo-motors could be updated with state-of-the-art linear servo actuators. This would eliminate the technical aspects of maintaining cable spooling under very low tension conditions, and the user error that can occur if the cable is initially wound in the wrong direction. Also, since a human operator often works in close proximity to the simulator, there is a risk of fingers getting wound up in the spooling action. Safety covers are installed, but these tend to get discarded when the cables must be manually respooled.

The custom instrumented motor mounts developed in this work could be replaced with 1DOF commercially available load cells. While the custom motor mounts served their purpose in the development of the muscle tension controller, they do present innate limitations. First, the weight of the actuator must be subtracted from the load measurement. Since the motor mount is instrumented to measure a bending moment in

one particular direction (cable tension direction), the apparent actuator weight, as sensed by the mount, will vary depending on the flexion position. This requires either user input to inform the software of the current simulator position, or some sort of automatic input from an attitude sensor or limit switch, or possibly from the tracking system (requires an extra tracking sensor). Second, the actuators must be carefully guarded, since if a cable or other object rests against the actuator, this will also disrupt the load measurement. A 1DOF load cell mounted to the linear actuators end shaft would solve these shortcomings.

All pneumatic actuators could also be replaced with servo linear actuators with 1DOF load cells. While pneumatic actuation is simple and inexpensive, it has significant performance limits. Due to static friction and the compressibility of air, fine position adjustments are difficult to achieve. An all-servo actuator simulator would provide the generality and flexibility needed to apply the current muscle tension controller to all muscles.

The newly simulated motions presented here will provide the opportunities to develop new protocols to study rehabilitation methods in the horizontal, varus and valgus positions. The complex interactions between osseous, ligamentous and muscle stabilizers will be further elucidated. There is the potential for introducing *in-situ* transducers to measure osseous and tissue loads, and articular contact areas and pressures. Future implant designs will benefit from the data collected in these positions with muscle activation. The MOSE system with the motion-derived coordinate system method will serve as a platform for any number of biomechanical investigations requiring generalized and reliable replication of elbow motion.

6.4 SIGNIFICANCE

Simulated active elbow flexion and extension has been achieved in the horizontal, varus and valgus positions. With MOSE, biomechanical investigations are no longer relegated to manual passive motion in these positions. This is a marked improvement since it is known that passive motion generates significantly different kinematics than active motion. Of course, passive motion will continue to be of interest because it

provides insight into post-surgery passive rehabilitative methods. In the past, comparison of active and passive kinematics from the vertical position has been very useful to evaluate the optimal therapy following elbow injuries and surgical repairs. With this new MOSE system, it is now possible to extend that comparison into the other principal positions as well.

The active kinematic data that can be collected from this simulator, and from the new motion-derived coordinate systems, will allow for new *in-vitro* studies to better understand elbow disorders and to develop new treatments. It will serve as a platform for the addition of other load measuring devices to measure elbow motion dynamics, including joint and soft tissue loads in various flexion-extension positions. These data will provide greater insight into the effects of injuries and the pathology of diseases like arthritis, and contribute to the design of future elbow joint implants and other implantable and external orthopaedic devices. MOSE will also provide a means to evaluate surgical techniques and their effects on elbow motion during many common daily activities.

The motion-derived coordinate system method could play a part, not only in the laboratory setting for *in-vitro* investigations, but also in the operating room. This method has the potential to introduce computer-assistance to some minimally invasive surgical protocols, and to improve the accuracy of joint implant alignment. These measures may reduce surgical complications and the incidence of revision surgeries, which are a major economic burden on the health care system. The efficacy of this method in joints other than the elbow will depend on the repeatability of rotation axes and the intersection of those axes. Where only one body segment coordinate system is required, only the axis attached to the body segment of interest need to be highly repeatable. Thus, the motion-derived method may be useful in the knee, hip and wrist.

The new experimental approaches presented in this dissertation may contribute to the betterment of patient outcomes and improved quality of life. This becomes more significant as the baby boomer population ages, and the needs and demands for improved outcomes from joint injuries and degenerative disorders mandates a better understanding of surgical reconstruction and rehabilitation of the elbow.

6.5 REFERENCES

Åström,K.J., Hägglund,T. (2004) Revisiting the Ziegler–Nichols step response method for PID control. *Journal of Process Control*. (14): 635-650.

Didonna,M.L., Fernandez,J.J., Lim,T.H., Hastings,H., and Cohen,M.S. (2003) Partial olecranon excision: the relationship between triceps insertion site and extension strength of the elbow. *J.Hand Surg.Am.* (28): 117-122.

Gartsman,G.M., Sculco,T.P., and Otis,J.C. (1981) Operative treatment of olecranon fractures. Excision or open reduction with internal fixation. *J.Bone Joint Surg.Am.* (63): 718-721.

Hang,C.C. Åström,K.J., Ho,W.K. (1991) Refinements of the Ziegler-Nichols tuning formula. *Control Theory and Applications, IEEE Proceedings D*. (138): 111-118.

Morrey,B.F. (1995) Current concepts in the treatment of fractures of the radial head, the olecranon, and the coronoid. *Instr.Course Lect.* (44): 175-185.

Shoemake,K. (1985) Animating rotation with quaternion curves. *ACM SIGGRAPH Computer Graphics*. (19).

APPENDIX A – GLOSSARY

Anatomic	Pertaining to the anatomy
Anatomic axis	See flexion-extension axis
Anterior	Situated at or directed toward the front; opposite of posterior
Anteroposterior	Extending along an axis from front to back
Arthritis	Acute or chronic inflammation of a joint that is often accompanied by pain and structural changes
Arthroplasty	Surgical repair of a joint; the operative formation or restoration of a joint
Articular	Pertaining to a joint
Articular cartilage	A specialized, fibrous connective tissue lining the articular surface of synovial joints
Articular surface	The end of a bone that forms a synovial joint
Articulate	To divide into or to unite so as to form a joint
Articulation	A joint; the place of union or junction between two or more bones of the skeleton
Axial	Towards the central axis of an extremity
Biceps	Muscle which flexes and supinates the forearm
Brachialis	The largest of the muscles that act to flex the elbow
Brachioradialis	A muscle that acts to flex the elbow
Capitellum	The distal and lateral end of the humerus, which articulates with the radial head
Carrying angle	The angle between the long axis of the humerus and long axis of the ulna with the elbow in full extension
Cartilage	A specialized, fibrous connective tissue present in adults, and forming the temporary skeleton in the embryo, providing a model in which the bones develop, and constituting a part of the organism's joint mechanism

CAS	Computer-assisted surgery
Collinear	Lying in the same straight line
Comminuted	Broken into fragments
Computer-assisted orthopaedic surgery	The application of computer-assisted surgery techniques in the field of orthopaedics
Computer-assisted surgery	The utilization of modern technology (computer software and / or medical imaging) to assist the surgeon in performing a procedure
Congruity	Coinciding
Contact area	The amount of articular surface in contact with an adjacent bone
Contralateral	Relating to the opposite side
Coordinate	Real number denoting a component of location along an axis
Coordinate space	Assembly of three coordinate axes
Coordinate system	See coordinate space
Coronal plane	A vertical plane, at right angles to the sagittal plane, dividing the body into anterior and posterior portions
Coronoid	The anterior-most aspect of the proximal ulna forming part of the greater sigmoid notch
Cortical	Hard or compact bone
Current	The flow of electric charge
Digitization	The act of physically acquiring the three-dimensional location of several points on an object's surface
Discritize	To convert a continuous function into an equivalent discrete range to facilitate storage or calculation
Distal	Further from the beginning; opposite to proximal
Distraction	Separation of joint surfaces without rupture of their binding ligaments and without displacement; surgical separation of the two parts of a bone after the bone is transected

Epicondylar axis	An axis defined by the medial and lateral epicondyles
Epicondyle	A projection or boss upon a bone; above its condyle
Euclidean distance	The distance between two points in three-dimensional space
Excision	To remove by cutting
Extension	The movement by which the two ends of any jointed part drawn away from each other; the bringing of the member of a limb into or toward a straight condition
Extensor	Any muscle that extends a joint
External rotation	Rotation about the longitudinal axis laterally
Extremity	A bodily limb or appendage
Flexion	Elevation in the sagittal plane of the body
Flexion-extension axis	The axis about which primary elbow motion (flexion and extension) occurs
Flexor	Any muscle that flexes a joint
Forearm	The structure on the upper limb between the elbow and wrist
Fossa (fossae)	In anatomy, a hollow or depressed area
Frontal plane	See coronal plane
Global	The coordinate system by which the pose of all others is referenced
Greater sigmoid notch	An aspect of the proximal ulna which articulates with the trochlea of the humerus
Guiding ridge	Divides the articulation of the greater sigmoid notch into medial and lateral facets
Humeroulnar	Pertaining to the ulna and humerus
Humerus	Long bone of the upper arm
Inferior	Situated below, or directed downward; in anatomy, used in reference to the lower surface of a structure, or to the lower of the two (or more) similar structures; opposite of superior

Instability	A pathologic condition in which the there is an inability to maintain the normal relationship of the distal humeral articular surface with the proximal articular surfaces of the ulna and radius
Internal rotation	Rotation about the longitudinal axis medially
Internal fixation	The fixation of screws and/or plates underneath the soft tissue to facilitate healing
Intra-operative	During surgery
In-vitro	Latin: “in-death”, referring to within cadaveric tissue
In-vivo	Latin: “in-life”, referring to within a live subject
In-silico	“in-artificial”, referring to within a computational model
Ipsilateral	Relating to the same side
Joint	A location at which two or more bones make contact
Joint capsule	The saclike envelope enclosing the cavity of a synovial joint
Kinematics	The study of motion of one body with respect to another
Kinematic axis	The flexion-extension axis, as defined by the motion pattern of the ulna relative to the humerus
Landmarks	Readily identifiable features of a bone
Lateral	Denoting a position farther from the median plane or midline of the body or a structure
Laxity	The quality or state of being loose
Ligament	A band of fibrous tissue connecting bones or cartilages, serving to support and strengthen joints
Local	The coordinate system that is specific to a rigid body
Medial	Situated toward the midline of the body or a structure
Medial-lateral	Extending along an axis from left to right or vice versa
Modular	A self-contained unit that can be combined or interchanged to create a different design. Modularity, (noun).
Morphology	The study of the form or shape of a structure

Muscle	An organ which by contraction produces movement of an animal organism
Muscle moment arm	The perpendicular distance from the muscle insertion to the rotation axis
Normal vector	A vector indicating direction of perpendicularity
Normalize	To set vector length to magnitude one
Olecranon	The large point on the upper end of the ulna that projects behind the elbow joint and forms the point of the elbow; the body projection of the ulna at the elbow
Orthogonal	Relating to or composed of right angles
Orthonormal	Mutually perpendicular unit or normal vectors
Orthonormal basis	Three orthonormal vectors forming the basis for a coordinate system
Orthopaedics	The branch of surgery dealing with the preservation and restoration of the function of the skeletal system, its articulations, and associated structures
Osseous	Consisting of bone
Osteoarthritis (OA)	A non-inflammatory degenerative joint disease of the skeletal system, its articulations, and associated structures
Osteopenic	A generalized reduction in bone mass
Osteoporosis	A disorder in which the bones become increasing porous or brittle
Outlier	A value far from most of the others in a set of data
Pathology	The science of the origin of diseases
Physiological	Normal, not pathologic
Posterior	Directed towards, or situated at the back; opposite of anterior
Post-operative	After surgery
Pre-operative planning	Employing medical imaging to determine device placement and/or surgical cutting paths before surgery

Pose (6DOF)	Three translations and three rotations which completely define the position and orientation of a rigid body relative to a reference coordinate system
Position vector	A set of (x, y, z) coordinates that defines location
Post-traumatic	Occurring after physical trauma
Pronation	Applied to the hand, the act of turning or placing the palm backward (posteriorly) or downward, performed by a medial rotation of the forearm; the position assumed by such a limb
Prosthesis	An artificial component that replaces a missing or injured body part
Proximal	Nearest to the point of reference, as to a centre or median line or to the point of attachment or origin
RMS	Root mean square – a statistical measure of the magnitude of a varying quantity
Radial dish	A circular concave dish of the radial head surrounded by cartilage that articulates with the capitellum
Radial head	An anatomical structure resembling a cylinder that forms the proximal end of the radius, and articulates with the capitellum of the humerus and the lesser sigmoid notch of the ulna
Radial neck	A narrow region of the proximal radius just distal to the radial head
Radioulnar	Pertaining to the radius and ulna
Radius	A long, slightly curved bone that lies to the lateral side of the forearm when in the anatomical position; it is the shorter and thicker of the two bones found in the forearm
Range of motion	Amount of motion attained during an activity
Real-time	Responding to events or signals as they happen
Reference frame	See coordinate frame

Render	To convert from a file into visual form on a video display
Resection	The excision of all or part of an organ or tissue
Residual error	The difference between the approximate result and the true result
Resolution	The measure of how closely two adjacent objects can be resolved in an image
Resorption	The destruction, disappearance, or dissolution of a tissue
Rheumatoid arthritis (RA)	A chronic, inflammatory disease of the body most prominent in joints leading to joint pain, stiffness and deformity
Rigid-body	An idealization of a solid body in which deformation is neglected
Rotation	An angular rotation
Rotation axis	Vector about which rotation occurs
Sagittal Plane	A vertical plane that divides the body into left and right sides
Segmentation	The process of partitioning an image into multiple regions in order to simplify or change the representation of the image
Soft tissue	Tissues that connect, support or surround other structures of the body (muscles, tendons, ligaments)
Stylus	A pen-like object that traces the surface of an object. The three-dimensional coordinates of each point are then recorded with respect to a tracking system
Superimposed	To lay or place on or over something else
Superior	Situated above, or directed upwards; opposite of inferior
Supination	The act of turning the palm forward or upward; the position assumed by such a limb
Supinator	A flat muscle, shaped like a rhomboid, which is found in the forearm and acts to position the forearm in supination
Supinator Crest	A bone prominence located on the lateral aspect of the proximal ulna that serves as an insertion site for the lateral

	ulnar collateral ligament of the elbow
Supracondylar	Situated above a condyle or condyles
Surface model	A reconstructed computer model of the external surface of an object, consisting of points and cells
Surgical intervention	The process of performing a surgery
Tendon	A fibrous cord of connective tissue continuous with the fibres of a muscle and attaching the muscle to bone or cartilage
Thoracic	Relating to or near the thorax
TEA	Total elbow arthroplasty
Translation	A finite linear displacement
Transmitter	The origin of a tracking system
Transverse	Extending from side to side; at right angles to the long axis
Transverse plane	Horizontal plane passing through the body at right angles to the frontal and sagittal planes, dividing the body into superior and inferior segments
Trauma	A body wound or shock produced by a sudden physical injury
Triceps	A large three-headed muscle running along the back of the upper arm and serving to extend the forearm
Trochlea	An anatomical structure, resembling a pulley, found at the distal end of the humerus that articulates with the ulna
Trochlear sulcus	A narrow groove that divides the trochlea into medial and lateral regions; articulating with the guiding ridge of the proximal ulna
Ulna	The bone extending from the elbow to the wrist on the side opposite to the thumb; the inner and larger bone of the forearm
Uniaxial	Relating to one axis

Unit vector	A vector with a length of one
Upper limb	Relating to the arm
Valgus	Bent out, twisted; denoting a deformity in which the angulation is away from the mid-line of the body
Varus	Bend inward; denoting a deformity in which the angulation of the part is toward the midline of the body

APPENDIX B – MUSCLE TENSION CONTROL

B.1 INTRODUCTION

Tension control of each muscle/tendon construct is an integral part of the overall simulator. A muscle tension control system was designed to control muscle loads applied by the servo-motors. There were three servo-motors, each actuating the biceps, brachialis and triceps tendons. Load feedback in previous simulators from our laboratory used an inline tension load cell that was interposed in the 'prime mover' (brachialis) cable (Dunning *et al.*, 2003; Johnson *et al.*, 2000). This design was suitable for flexion in the vertical position. However, in the horizontal, varus and valgus positions, the suspended load cells tended to 'bounce' perpendicular to the cables. This 'bounce' causes an oscillatory load feedback, which could either cause or exacerbate oscillations in the PID load control loop. Furthermore, each load cell's electrical wire tended to impart undue tension as the load cell moved with the tendon cable. Thus, tension feedback in the current simulator needed to be removed from the cables, seamlessly integrated with the actuators, and fast enough to be part of the real-time flexion-extension simulator. This was achieved by developing strain-gauge instrumented motor mounts.

The tension controller is implemented as a PID (Proportional Integral Derivative) loop. The PID algorithm has two inputs and one output. The tension input (process variable) is the current tension level, reported by a force transducer. The tension setpoint is the desired tension, either a constant or varying value specified manually by the user or automatically by a commanding program. The process output represents an incremental change in the tension actuator. The PID algorithm adjusts the actual tension until the input reaches the desired tension setpoint. The incremental change in the process output is affected by the settings of the PID algorithm. The P (Proportional), I (Integral), and D (Derivative) values determine how quickly the process variable reaches the setpoint, and the magnitude of overshoot past the setpoint.

B.2 METHODS

The hardware components of the muscle tension controller consist of the force transducers, and muscle tension actuators (Figure B.1). Muscle/tendon tension for biceps, brachialis, and triceps is provided by servo-motors (SmartMotor™ SM2315, Animatics, Santa Clara, CA). Each servo-motor is mated with an inline planetary reduction gearhead. Gearheads for biceps and brachialis had 10:1 reduction ratios, while triceps had a 20:1 ratio in order to support the comparatively higher triceps loads. The output shaft of the gearhead has a deep groove pulley. A braided stainless steel cable is attached to and wound around the pulley.

Custom aluminum motor mounts were instrumented with strain gauges in order to produce an integrated force transducer. The force transducer was designed as a full Wheatstone bridge to measure bending moment with temperature and Poisson strain compensation. The instrumented mount itself is a 90º angle configuration with the motor mounted on the instrumented arm. Thus, the cantilever geometry of the mount converts tension in the tendon cable into a bending moment which is measured by the Wheatstone bridge. All three motor mounts were calibrated with 0 – 150 N and displayed high linearity ($R^2 = 1.000$).

The muscle tension control algorithm was implemented entirely in software (LabVIEW 7™ Express, National Instruments Corp., Austin, TX). The servo-motors were set to operate in displacement mode, implying that they interpret incoming numeric values as encoder counts in the positive or negative rotational directions. For example, sending the motor a displacement of 30 causes it to rotate 30 shaft increments in the positive direction (clockwise looking at the motor shaft).

The system dead time was determined by measuring the time taken for a motor to move in response to a displacement command. Using a chain of three motors, consistent with this application; first, the time to send and receive a shaft position report was measured (5±0.5 ms). Then the time to send and receive a displacement command followed by a position report was measured (11±0.5 ms). These were calculated with 100 sequential commands. The position report subsequent to a displacement command always

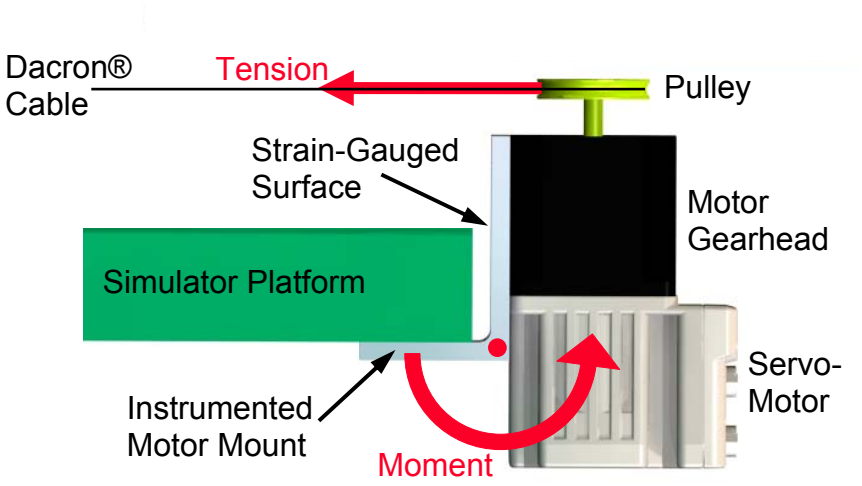

Figure B.1: Servo-Motor Actuator and Instrumented Motor Mount

Servo-motors are mounted on 90º aluminum angle. The vertical arm of the angle is instrumented with a full Wheatstone bridge strain gauge configuration. Tension in the muscle cable is converted to a bending moment (acting about the axis out of the page) which is measured by the motor mount.

showed a change in shaft position, confirming that the shaft had rotated before the subsequent position report had been processed by the motor. Thus, the time measured for the position report alone was subtracted from the time taken for the displacement command plus position report, leaving 6.0±0.5 ms. This revealed the time needed to send, process, and receive the displacement command. This was halved (3.0±0.5 ms) since the report return time is not part of the system dead time. All three motors were tested in this manner. However, the daisy chain architecture of the RS232 protocol means that communications must pass through each motor sequentially. Thus as expected, the measured dead time was identical for all motors. Since a SmartMotor™ servo rate is 4 kHz, and since according to the manufacturer's literature, a command can take 1-6 servo cycles to be executed, no more than 6/4000 s can be added for execution of the subsequent position report command, for a maximum dead time of 4.5±0.5 ms.

A triceps tendon construct was used for the PID tuning process. Both the proximal and distal ends of a triceps tendon were sutured using a Krackow stitch (Howard *et al.*, 1997) with Dacron® cable. The distal end was fixed to the simulator, and the proximal end was attached to the servo-motor. Since specimen tissue was used, the system remained 'online' while tuned using a typical manual 'online' method (Datta *et al.*, 2000; Silva *et al.*, 2005; Bolton, 2004). With (P,I,D) parameters set to (1,0,0), first the proportional term was increased until the muscle tension began to oscillate, then set to half of that value for a 'quarter wave decay' response. Then the integral term was increased until any offset error was corrected to less than 1 N as quickly as possible, without causing oscillations. The derivative term was left at zero, which is generally recommended for a fast process with a small time constant (Datta *et al.*, 2000) as determined in the preliminary dead time calculations above. The rationale for this is described in the discussion (Section B.4). The resulting PID values were P=7.00, I=0.05, D=0.00 for biceps and brachialis. For triceps, they were P=20.00, I=0.05, D=0.00.

The performance of the tuned force controller was tested on the same tendon specimen. Beginning with an initial setpoint of 5 N, the setpoint was instantly increased to 100 N until the process error settled to less than 1 N. Then the setpoint was instantly decreased to 5 N.

B.3 RESULTS

The load verses time performance curve is shown for a change in setpoint from 5-100 N (Figure B.2): The actual tendon tension reached the 100 N setpoint in 1.3 s, overshooting by 6.8 N (7% of setpoint). The error decreased to 5% and 1% at 2 s and 7 s respectively. When the setpoint was decreased from 100 N to 5 N, the actual tension reached the 5 N setpoint in 1.4 s, overshooting by 0.4 N (8% of setpoint).

B.4 DISCUSSION

An immediate setpoint change of 95 N, tested here, is an exceedingly aggressive test for a muscle tension application. In practice, a setpoint step would never be so high. In the context of the current simulator, the setpoint of this tension controller is calculated by a higher level PID controlling the joint angle. Since PID process output is continuous, the muscle tension setpoint will only change gradually and continuously, without discontinuities. The results of this test show that the tension controller is able to produce accurate and rapid corrections of large errors in muscle tension, with very little overshoot and no oscillations.

Servo motors cannot generate a desired torque directly. This is because the complex stator and rotor configurations of these devices, which are designed to achieve a desired position, results in varying distances between the rotor and stator magnetic fields as the shaft rotates. Since magnetic field strength is a function of this distance, the shaft output torque becomes a function of rotor position and velocity, as well as applied current. Thus, an external force transducer was necessary in order to monitor the tension generated by the motor.

While tendon tissue can undergo stress relaxation, this is a relatively slow process compared to a real-time process on the order of milliseconds. Since there are no other time dependent components governing the biomechanical properties of a tendon already under tension, any change in length is coupled by a nearly instantaneous change in tension. Therefore, the tendon tension process has a single process time constant (Smith, 2009). That is the process dead time constant; the time needed for the load to

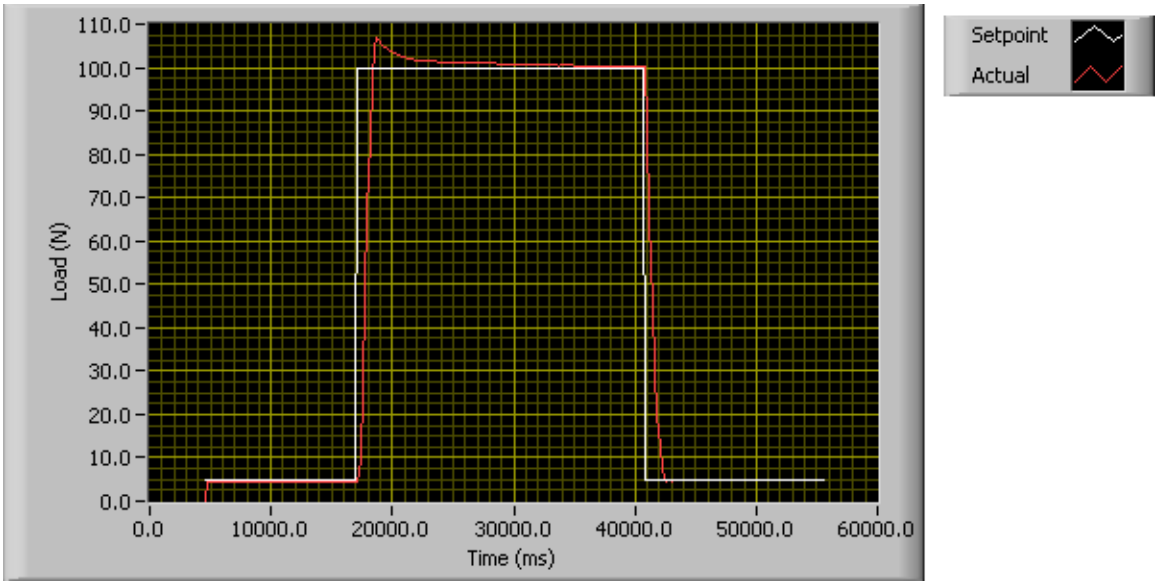

Figure B.2: Load *vs.* Time Performance Curve

The performance of one motor applying tension load to a fixed triceps tendon. The setpoint is a square wave from 5 to 100 N. Rising from 5 to 100 N: The actual load crosses 100 N at 1.3 s and overshoots by 6.8 N. Error is 5% at 2 s, and 1% at 7 s. Setpoint decreasing from 100 to 5 N: The actual load crosses 5 N at 1.4 s with less than 1 N overshoot, and less than 1% error.

respond to a change in controller output. Since tension in the tendon changes instantly with length change, the process dead time could be calculated as the time needed for a motor displacement command update from the PID to be executed by the motor. This was shown to be no more than 4.5±0.5 ms, assuming a maximum of 6 servo cycles and that the position report command may have been received before the shaft began to move. Of course the position must have been achieved before the report was executed, since new positions were always reflected in the position report. Thus, 6 servo cycles is a highly conservative estimate. Regardless, this analysis determined that the tension control process is a very fast one.

The derivative term was kept at zero because it is generally not recommended for a fast process. This is because the derivative (*i.e.* slope) of a quickly changing error term (or process variable) can be large, which can destabilize the system (Datta *et al.*, 2000). The derivative term provides no benefit when the process is described by a single time constant, as is the case in this application (Smith, 2009). Furthermore, if the derivative time is increased beyond the smallest time constant (4.5 ms at most) then controller performance suffers (Smith, 2009). Therefore, this tendon tension application is clearly suited for a zero derivative term.

To summarize, this appendix presents a classic tension control loop implemented in software with a servo-motor and strain-gauge based tension feedback. These results serve as proof of concept that this system can fulfil the requirements of muscle tension control with no risk of over tensioning to unsafe levels. This tension control prototype was evaluated for viability as a muscle tension controller in a real-time environment, and serves as a modular building block for the completed simulator control scheme, as implemented in Chapters 3-5.

B.5 REFERENCES

Bolton,W. (2004) Instrumentation and control systems. Elsevier Ltd. London.

Datta,A., Ho,M.T., Bhattacharyya,S.P. (2000) Advances in Industrial Control: Structure and synthesis of PID controllers. Springer-Verlag. London

Dunning,C.E., Gordon,K.D., King,G.J., and Johnson,J.A. (2003) Development of a motion-controlled in vitro elbow testing system. *J.Orthop.Res.* (21): 405-411.

Howard,R.F., Ondrovic,L., and Greenwald,D.P. (1997) Biomechanical analysis of four-strand extensor tendon repair techniques. *J.Hand Surg.Am.* (22): 838-842.

Johnson,J.A., Rath,D.A., Dunning,C.E., Roth,S.E., and King,G.J. (2000) Simulation of elbow and forearm motion in vitro using a load controlled testing apparatus. *J.Biomech.* (33): 635-639.

Silva,G.J., Datta,A., Bhattacharyya,S.P. (2005) PID controllers for time-delay systems. Birkhäuser. Boston.

Smith,C.L., (2009) Practical Process Control: Tuning and Troubleshooting. John Wiley & Sons Inc. New Jersey.

APPENDIX C – MOTION-DERIVED COORDINATE SYSTEM RESULTS IN THE VARUS, VALGUS AND HORIZONTAL POSITIONS

Chapter 4 presented a method for generating bone segment coordinate systems (CS) from the motions of elbow flexion and forearm rotation. Performance of the Motion-Derived CS was compared to traditional Anatomy-Derived CS in terms of inter-subject variability of kinematics. Dependent variables were the variability of elbow joint valgus angulation, and internal rotation of the ulna relative to the humerus. Inter-subject variability of the kinematic pathway was also analyzed using box plots. In Chapter 4, only results of the vertical flexion were reported for the purpose of publication of the associated manuscript. The results of the horizontal, varus and valgus positions are presented in this appendix. The vertical results are repeated to facilitate comparison. (Please refer to Chapter 4 for a description of the testing protocol and statistical analysis.)

Inter-subject variability and the median and maximum kinematic pathways are summarized for valgus angulation and internal rotation in Table C.1 and Table C.2, respectively. The results of inter-subject variability as a function of flexion angle are shown for valgus angulation (Figures C.1A through C.4A) and internal rotation (Figures C.1B through C.4B). The box plots of kinematic pathway are shown valgus angulation and internal rotation in Figures C.5 and C.6, respectively.

	Motion-Derived CS			Anatomy-Derived CS		
	Variability	Median	Maximum	Variability	Median	Maximum
Vertical	1.0 ± 0.8°	0.8°	3.3°	3.8 ± 2.7°	3.4°	9.2°
Horizontal	1.1 ± 0.8°	1.0°	3.4°	3.7 ± 2.7°	3.5°	9.0°
Varus	1.6 ± 0.8°	1.7°	3.7°	3.3 ± 2.5°	2.6°	8.8°
Valgus	0.8 ± 0.6°	0.8°	2.5°	4.0 ± 2.8°	3.7°	10.4°

Table C.1: Summary of Kinematic Variability for Valgus Angulation

Inter-subject variability, median and maximum values are shown for Motion-Derived and Anatomy-Derived CS in the four positions, and over a flexion range of 20° to 120°.

	Motion-Derived CS			Anatomy-Derived CS		
	Variability	Median	Maximum	Variability	Median	Maximum
Vertical	1.8 ± 1.6°	1.2°	5.9°	6.6 ± 5.7°	4.8°	21.6°
Horizontal	1.8 ± 1.7°	1.3°	6.6°	6.5 ± 5.7°	4.4°	21.3°
Varus	1.5 ± 1.4°	1.0°	5.4°	6.8 ± 5.8°	4.8°	21.7°
Valgus	1.5 ± 1.3°	0.9°	4.9°	6.9 ± 5.9°	5.0°	21.3°

Table C.2: Summary of Kinematic Variability for Internal Rotation

Inter-subject variability, median and maximum values are shown for Motion-Derived and Anatomy-Derived CS in the four positions, and over a flexion range of 20° to 120°.

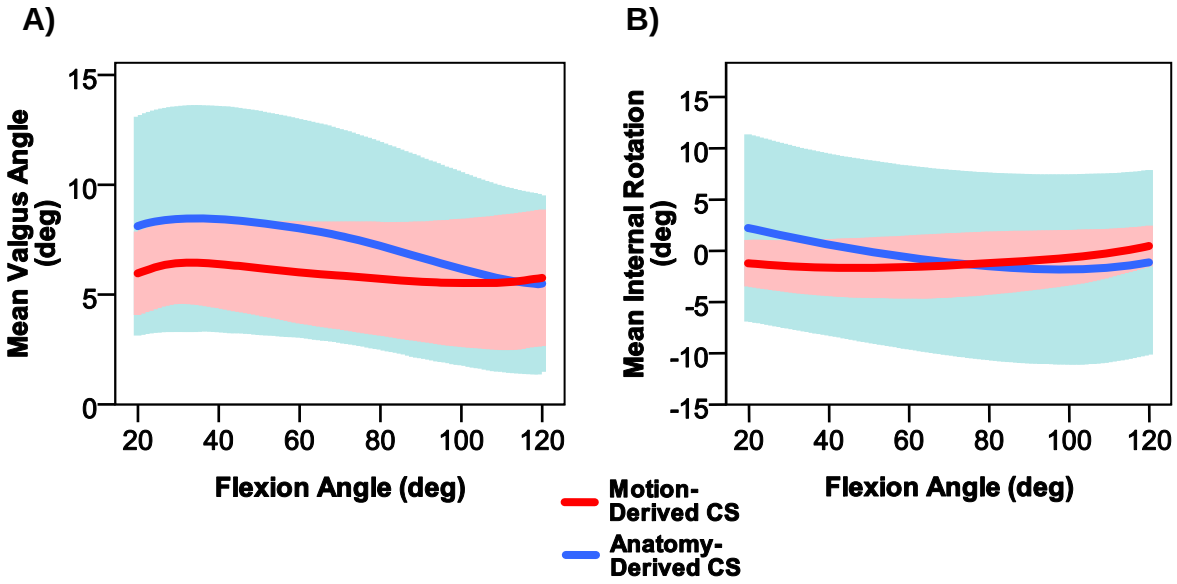

Figure C.1: Kinematic pathways in the Vertical Position

Kinematic pathways for (A) valgus angulation and (B) internal rotation are shown in the vertical position. Ulna relative to the humerus as a function of flexion angle. Solid lines represent the mean of 10 specimens. Translucent areas represent +/-1SD.

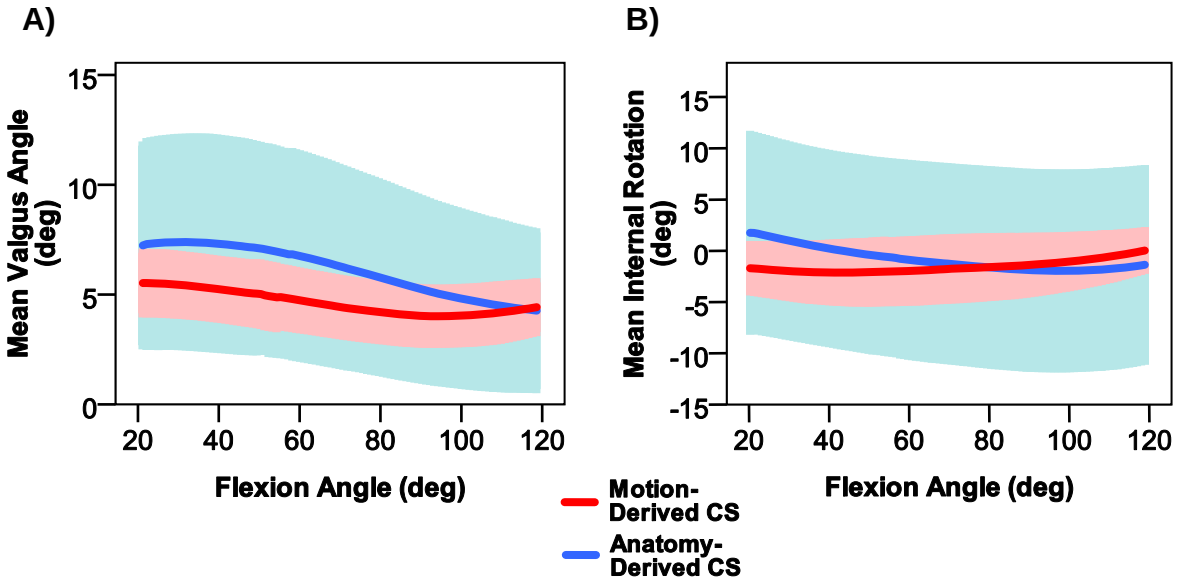

Figure C.2: Kinematic pathways in the Horizontal Position

Kinematic pathways for (A) valgus angulation and (B) internal rotation are shown in the horizontal position. Ulna relative to the humerus as a function of flexion angle. Solid lines represent the mean of 10 specimens. Translucent areas represent +/-1SD.

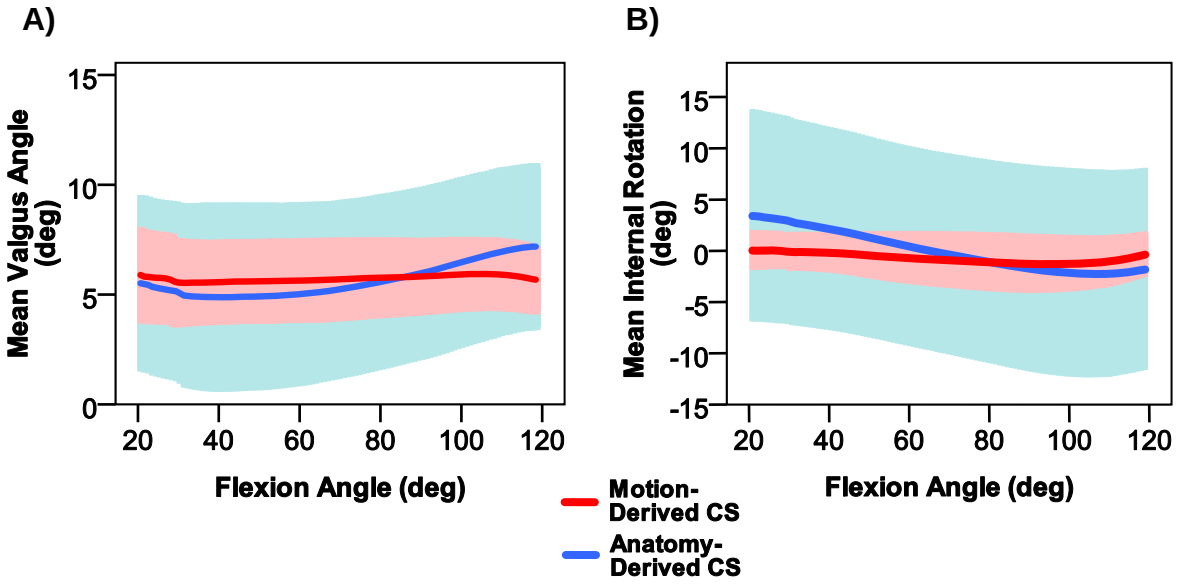

Figure C.3: Kinematic pathways in the Varus Position

Kinematic pathways for (A) valgus angulation and (B) internal rotation are shown in the varus position. Ulna relative to the humerus as a function of flexion angle. Solid lines represent the mean of 10 specimens. Translucent areas represent +/-1SD.

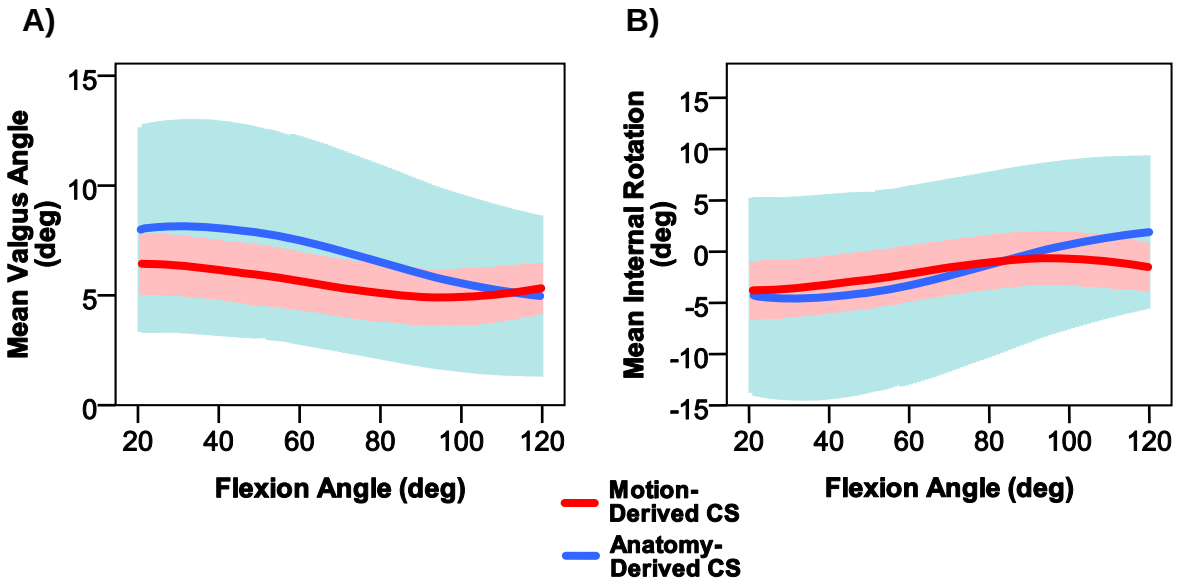

Figure C.4: Kinematic pathways in the Valgus Position

Kinematic pathways for (A) valgus angulation and (B) internal rotation are shown in the valgus position. Ulna relative to the humerus as a function of flexion angle. Solid lines represent the mean of 10 specimens. Translucent areas represent +/-1SD.

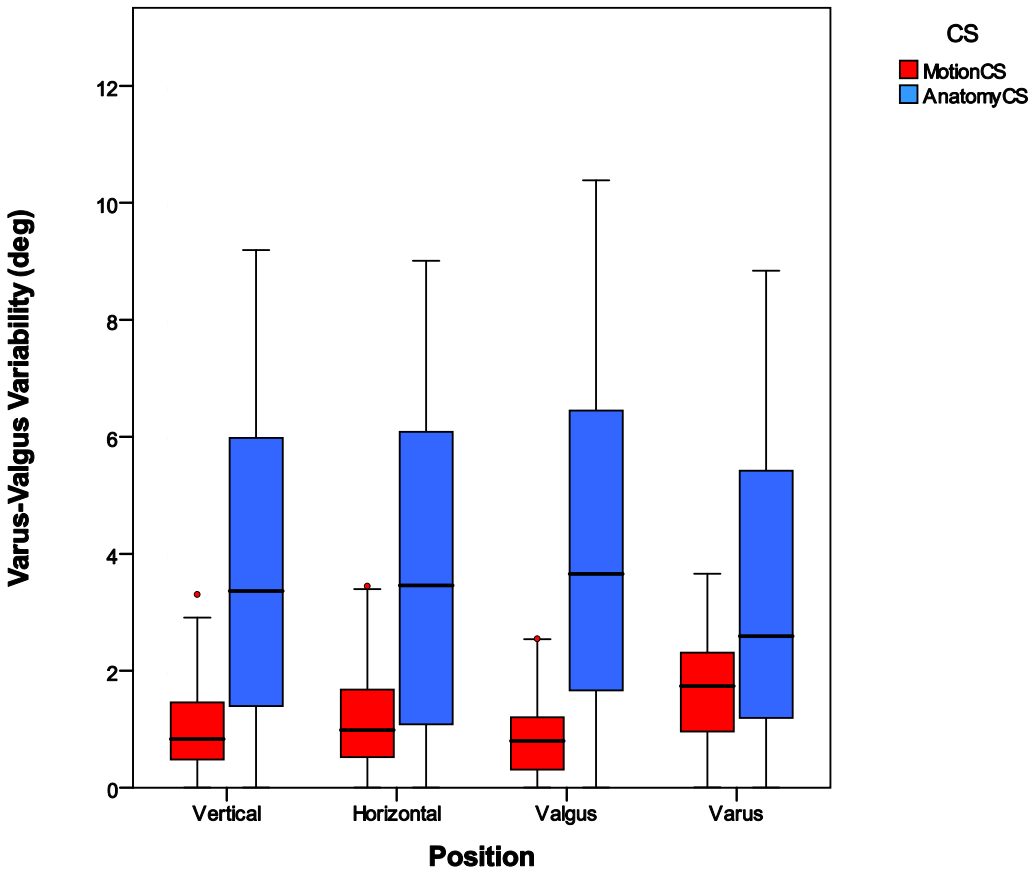

Figure C.5: Inter-Subject Variability of Valgus Angulation

Ulna relative to the humerus. Shown are the median, minimum, maximum, first quartile, third quartile, and inner fences of 10 specimens over a flexion range of 20° to 120°.

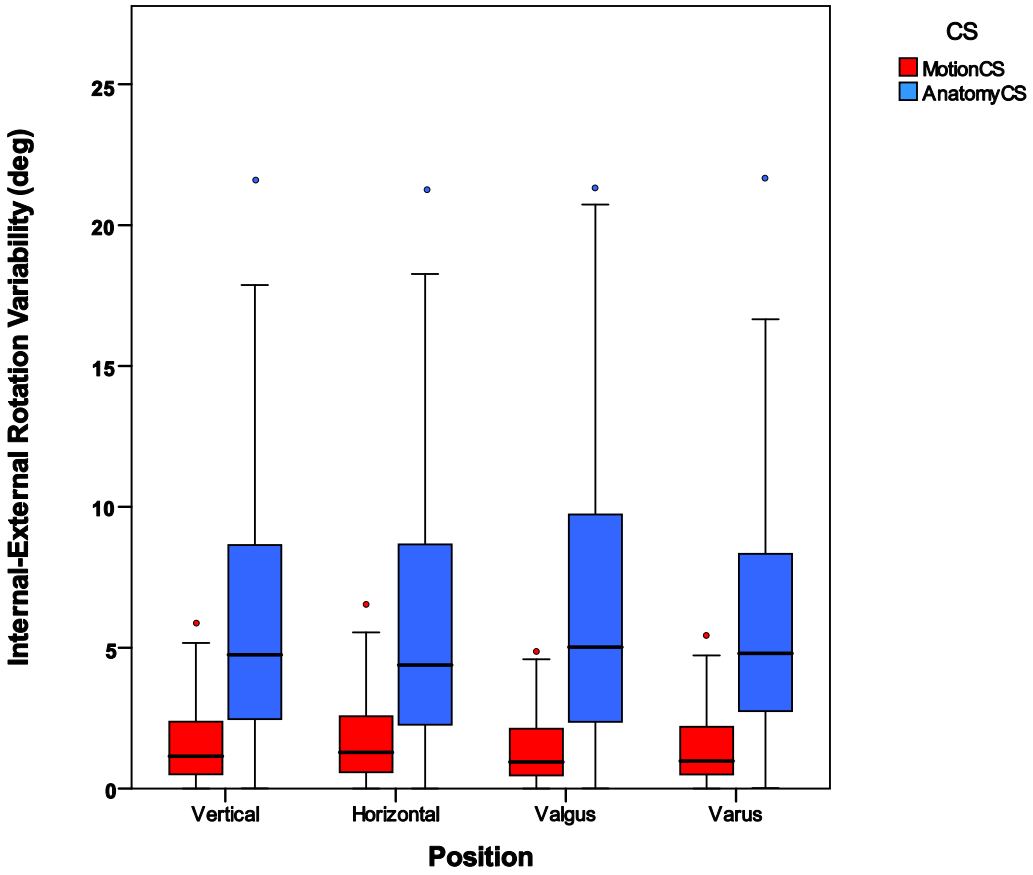

Figure C.6: Inter-Subject Variability of Internal Rotation

Ulna relative to the humerus. Shown are the median, minimum, maximum, first quartile, third quartile, and inner fences of 10 specimens over a flexion range of 20° to 120°.

APPENDIX D – MOTOR COMMUNICATION

The servo-motors for biceps, brachialis and triceps control communicate on an RS-232 serial comm link. Thus, motor displacements must be converted to ASCII strings and addressed to each motor specifically. Besides motor displacements, there are other types of motor commands, such as E-STOP (emergency stop) and status requests. The software developed in this work is highly parallel in order to maintain real-time execution. Thus, motor status and E-STOP commands can originate from several sources. This leads to a common computer resource problem. The motor comm channel is the resource that must be shared. However, if all programs that have access to the motor comm channel are allowed to send commands whenever they want, then collisions can occur. At best, a collision may cause a motor displacement to be missed. At worst, a collision may cause an E-STOP command to be missed. Therefore, motor comm channel resource management is also a safety issue.

When the simulator is running, the motor comm channel is continuously transferring motor displacement commands, making the likelihood of motor command collisions very high during this critical phase. Thus, comm channel management is not merely academic, but quite necessary.

The motor server software developed in this work is based on a client/server design. Only one component of the motor server has direct ownership of the motor comm channel, and all motor commands pass through it. For a program to access the motor server, it must acquire permission, and this is done using a semaphore model of resource allocation. In computer science, a semaphore is a protected variable or reference that provides a simple but useful abstraction for controlling access by multiple processes to a common resource in a parallel programming environment.(Dijkstra, 1965) In this case, only one program can possess the semaphore at any one time, and the semaphore will not be granted if another program is in possession.

The block diagram in Figure D.1 illustrates how motor comm allocation is implemented for motor displacement commands. The motor server, and most of the

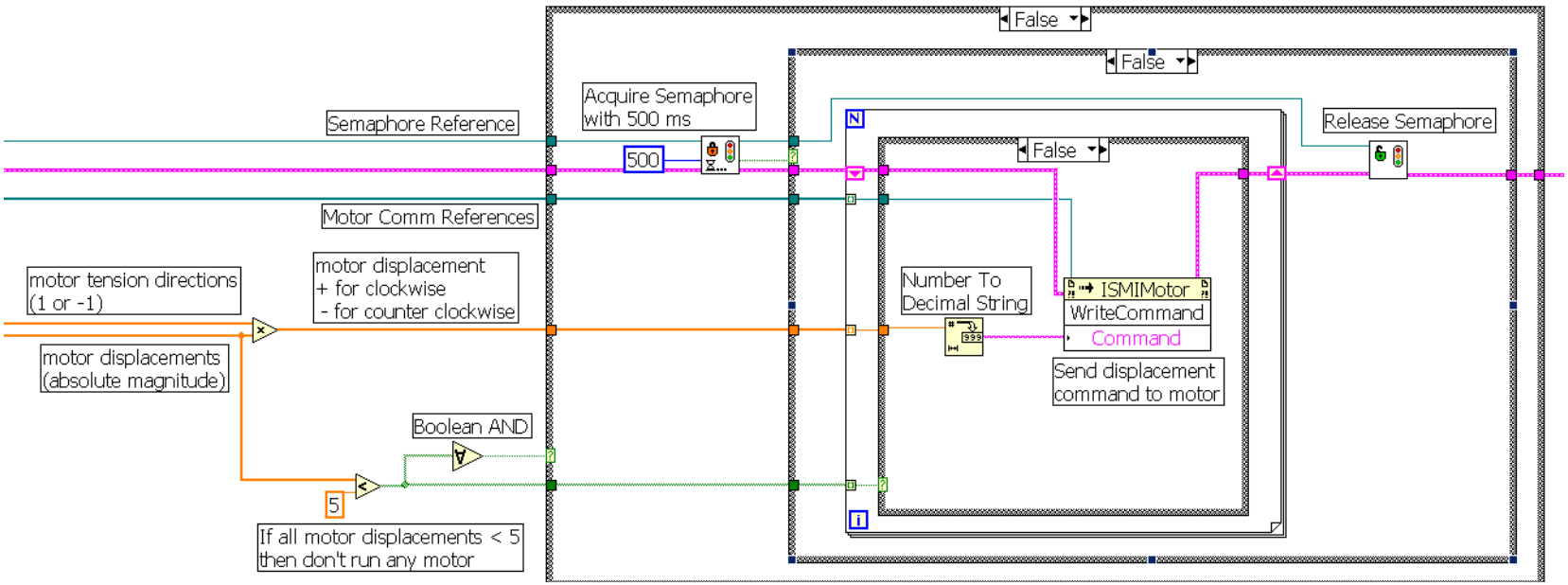

Figure D.1: Scalable Motor Displacement Server with Resource Allocation

Motor displacements are corrected for shaft rotation direction, and then sent to the motors through a serial comm link. Displacements less than 5 shaft increments are not sent in order to save bandwidth. A semaphore is acquired before transmitting the displacements, and then released.

simulator software, is designed to be scalable. Scalability means that different numbers of motors or other actuators, and even trackers and force transducers can be operated without needing to change the software. Scalability makes it possible to add actuators for more muscles, or to use more or even fewer transducers. Given that the entire software suite is very large and complex, scalability can greatly facilitate development. In this example, scalability is implemented with arrays. N motors are identified by N motor reference numbers in an array. A corresponding N number of displacements and motor tension directions also exist in arrays. When the software suite is initialized, N is set to the number of muscles that will be actuated by servo-motors, and all such arrays are initialized to size N. This architecture takes advantage of a computer's innate abilities to allocate memory spaces for arrays, and to rapidly index and traverse array structures in real-time.

Calculations on array elements are all performed simultaneously. For example, the multiplication and logical tests in this example are performed on all elements of the arrays at once (at the program execution level). This highly parallel design also takes advantage of scalability and rapid array traversal by indexing all the arrays simultaneously at the For Loop. Since there is only one motor comm channel, the motors cannot be commanded in parallel. However, this limitation does not slow performance because the RS232 link is the slowest component, and sending the motor commands individually easily keeps up with the serial link speed.

Motor displacements (shaft increments) which have been calculated, first get corrected for shaft rotation direction (clockwise: 1, counter clockwise: -1). This is the direction in which the motor can apply muscle tension. Clockwise indicates that the cable is spooled around the motor spool in a counter clockwise direction, so that clockwise motor displacements increase muscle tension. Before transmitting the displacements, a motor comm channel semaphore is requested. If any other program is communicating with the motors, then this program must wait. Since all motor commands are very short, wait times are generally less than 5 ms. If the wait period takes more than 500 ms, then and error is generated which propagates through the entire system, causing a safety shut down.

Displacements that are less than 5 increments are not transmitted to the motor. If all the displacements in the array are less than 5, then no communication is attempted and no semaphore is requested, thus avoiding unnecessary usage of comm channel bandwidth. Since the RS232 serial comm link is the bottle neck of most any system, it is important to avoid extra comm traffic. Also, motor displacements for all motors are sent with one semaphore, rather than acquiring and releasing N semaphores for N motors. This is logical since the motor displacements are synchronized and need update the motors simultaneously. If the semaphore was released after sending the motor displacement for motor 1, then another program might acquire the semaphore, causing a delay in displacement commands for motors 2 and 3. Thus the current design ensures motor synchronization.

D.1 REFERENCES

Dijkstra,E.W. (1965) Cooperating sequential processes. Technological University, Eindhoven, The Netherlands.

APPENDIX E – COPYRIGHT RELEASES

E.1 CHAPTER 2 COPYRIGHT RELEASE

ELSEVIER LICENSE
TERMS AND CONDITIONS
Oct 22, 2010

This is a License Agreement between Louis M Ferreira ("You") and Elsevier ("Elsevier") provided by Copyright Clearance Center ("CCC"). The license consists of your order details, the terms and conditions provided by Elsevier, and the payment terms and conditions.

All payments must be made in full to CCC. For payment instructions, please see information listed at the bottom of this form.

Supplier	Elsevier Limited The Boulevard,Langford Lane Kidlington,Oxford,OX5 1GB,UK
Registered Company Number	1982084
Customer name	Louis M Ferreira
Customer address	268 Grosvenor st. London, ON N6A 4V2
License number	2534370642739
License date	Oct 22, 2010
Licensed content publisher	Elsevier
Licensed content publication	Journal of Biomechanics
Licensed content title	Development of an active elbow flexion simulator to evaluate joint kinematics with the humerus in the horizontal position
Licensed content author	Louis M. Ferreira, James A. Johnson, Graham J.W. King
Licensed content date	10 August 2010
Licensed content volume number	43
Licensed content	11

issue number	
Number of pages	6
Type of Use	reuse in a thesis/dissertation
Portion	full article
Format	both print and electronic
Are you the author of this Elsevier article?	Yes
Will you be translating?	No
Order reference number	
Title of your thesis/dissertation	DEVELOPMENT OF AN ACTIVE ELBOW MOTION SIMULATOR AND COORDINATE SYSTEMS TO EVALUATE KINEMATICS IN MULTIPLE POSITIONS
Expected completion date	Nov 2010
Estimated size (number of pages)	270
Elsevier VAT number	GB 494 6272 12

Terms and Conditions

INTRODUCTION

1. The publisher for this copyrighted material is Elsevier. By clicking "accept" in connection with completing this licensing transaction, you agree that the following terms and conditions apply to this transaction (along with the Billing and Payment terms and conditions established by Copyright Clearance Center, Inc. ("CCC"), at the time that you opened your Rightslink account and that are available at any time at http://myaccount.copyright.com).

GENERAL TERMS

2. Elsevier hereby grants you permission to reproduce the aforementioned material subject to the terms and conditions indicated.

3. Acknowledgement: If any part of the material to be used (for example, figures) has appeared in our publication with credit or acknowledgement to another source, permission must also be sought from that source. If such permission is not obtained then that material may not be included in your publication/copies. Suitable acknowledgement to the source must be made, either as a footnote or in a reference list at the end of your

publication, as follows:

“Reprinted from Publication title, Vol /edition number, Author(s), Title of article / title of chapter, Pages No., Copyright (Year), with permission from Elsevier [OR APPLICABLE SOCIETY COPYRIGHT OWNER].” Also Lancet special credit - “Reprinted from The Lancet, Vol. number, Author(s), Title of article, Pages No., Copyright (Year), with permission from Elsevier.”

4. Reproduction of this material is confined to the purpose and/or media for which permission is hereby given.

5. Altering/Modifying Material: Not Permitted. However figures and illustrations may be altered/adapted minimally to serve your work. Any other abbreviations, additions, deletions and/or any other alterations shall be made only with prior written authorization of Elsevier Ltd. (Please contact Elsevier at permissions@elsevier.com)

6. If the permission fee for the requested use of our material is waived in this instance, please be advised that your future requests for Elsevier materials may attract a fee.

7. Reservation of Rights: Publisher reserves all rights not specifically granted in the combination of (i) the license details provided by you and accepted in the course of this licensing transaction, (ii) these terms and conditions and (iii) CCC's Billing and Payment terms and conditions.

8. License Contingent Upon Payment: While you may exercise the rights licensed immediately upon issuance of the license at the end of the licensing process for the transaction, provided that you have disclosed complete and accurate details of your proposed use, no license is finally effective unless and until full payment is received from you (either by publisher or by CCC) as provided in CCC's Billing and Payment terms and conditions. If full payment is not received on a timely basis, then any license preliminarily granted shall be deemed automatically revoked and shall be void as if never granted. Further, in the event that you breach any of these terms and conditions or any of CCC's Billing and Payment terms and conditions, the license is automatically revoked and shall be void as if never granted. Use of materials as described in a revoked license, as well as any use of the materials beyond the scope of an unrevoked license, may constitute copyright infringement and publisher reserves the right to take any and all action to protect its copyright in the materials.

9. Warranties: Publisher makes no representations or warranties with respect to the licensed material.

10. Indemnity: You hereby indemnify and agree to hold harmless publisher and CCC, and their respective officers, directors, employees and agents, from and against any and all claims arising out of your use of the licensed material other than as specifically

authorized pursuant to this license.

11. No Transfer of License: This license is personal to you and may not be sublicensed, assigned, or transferred by you to any other person without publisher's written permission.

12. No Amendment Except in Writing: This license may not be amended except in a writing signed by both parties (or, in the case of publisher, by CCC on publisher's behalf).

13. Objection to Contrary Terms: Publisher hereby objects to any terms contained in any purchase order, acknowledgment, check endorsement or other writing prepared by you, which terms are inconsistent with these terms and conditions or CCC's Billing and Payment terms and conditions. These terms and conditions, together with CCC's Billing and Payment terms and conditions (which are incorporated herein), comprise the entire agreement between you and publisher (and CCC) concerning this licensing transaction. In the event of any conflict between your obligations established by these terms and conditions and those established by CCC's Billing and Payment terms and conditions, these terms and conditions shall control.

14. Revocation: Elsevier or Copyright Clearance Center may deny the permissions described in this License at their sole discretion, for any reason or no reason, with a full refund payable to you. Notice of such denial will be made using the contact information provided by you. Failure to receive such notice will not alter or invalidate the denial. In no event will Elsevier or Copyright Clearance Center be responsible or liable for any costs, expenses or damage incurred by you as a result of a denial of your permission request, other than a refund of the amount(s) paid by you to Elsevier and/or Copyright Clearance Center for denied permissions.

LIMITED LICENSE

The following terms and conditions apply only to specific license types:

15. **Translation**: This permission is granted for non-exclusive world **English** rights only unless your license was granted for translation rights. If you licensed translation rights you may only translate this content into the languages you requested. A professional translator must perform all translations and reproduce the content word for word preserving the integrity of the article. If this license is to re-use 1 or 2 figures then permission is granted for non-exclusive world rights in all languages.

16. **Website**: The following terms and conditions apply to electronic reserve and author websites:
Electronic reserve: If licensed material is to be posted to website, the web site is to be password-protected and made available only to bona fide students registered on a

relevant course if:
This license was made in connection with a course,
This permission is granted for 1 year only. You may obtain a license for future website posting,
All content posted to the web site must maintain the copyright information line on the bottom of each image,
A hyper-text must be included to the Homepage of the journal from which you are licensing at http://www.sciencedirect.com/science/journal/xxxxx or the Elsevier homepage for books at http://www.elsevier.com , and
Central Storage: This license does not include permission for a scanned version of the material to be stored in a central repository such as that provided by Heron/XanEdu.

17. **Author website** for journals with the following additional clauses:

All content posted to the web site must maintain the copyright information line on the bottom of each image, and
he permission granted is limited to the personal version of your paper. You are not allowed to download and post the published electronic version of your article (whether PDF or HTML, proof or final version), nor may you scan the printed edition to create an electronic version,
A hyper-text must be included to the Homepage of the journal from which you are licensing at http://www.sciencedirect.com/science/journal/xxxxx , As part of our normal production process, you will receive an e-mail notice when your article appears on Elsevier's online service ScienceDirect (www.sciencedirect.com). That e-mail will include the article's Digital Object Identifier (DOI). This number provides the electronic link to the published article and should be included in the posting of your personal version. We ask that you wait until you receive this e-mail and have the DOI to do any posting.
Central Storage: This license does not include permission for a scanned version of the material to be stored in a central repository such as that provided by Heron/XanEdu.

18. **Author website** for books with the following additional clauses:
Authors are permitted to place a brief summary of their work online only.
A hyper-text must be included to the Elsevier homepage at http://www.elsevier.com

All content posted to the web site must maintain the copyright information line on the bottom of each image
You are not allowed to download and post the published electronic version of your chapter, nor may you scan the printed edition to create an electronic version.
Central Storage: This license does not include permission for a scanned version of the material to be stored in a central repository such as that provided by Heron/XanEdu.

19. **Website** (regular and for author): A hyper-text must be included to the Homepage of the journal from which you are licensing at

http://www.sciencedirect.com/science/journal/xxxxx. or for books to the Elsevier homepage at http://www.elsevier.com

20. **Thesis/Dissertation**: If your license is for use in a thesis/dissertation your thesis may be submitted to your institution in either print or electronic form. Should your thesis be published commercially, please reapply for permission. These requirements include permission for the Library and Archives of Canada to supply single copies, on demand, of the complete thesis and include permission for UMI to supply single copies, on demand, of the complete thesis. Should your thesis be published commercially, please reapply for permission.

21. **Other Conditions**:

v1.6

E.2 CHAPTER 4 COPYRIGHT RELEASE

JOHN WILEY AND SONS LICENSE
TERMS AND CONDITIONS
Oct 22, 2010

This is a License Agreement between Louis M Ferreira ("You") and John Wiley and Sons ("John Wiley and Sons") provided by Copyright Clearance Center ("CCC"). The license consists of your order details, the terms and conditions provided by John Wiley and Sons, and the payment terms and conditions.

All payments must be made in full to CCC. For payment instructions, please see information listed at the bottom of this form.

License Number	2534350780486
License date	Oct 22, 2010
Licensed content publisher	John Wiley and Sons

Licensed content publication	Journal of Orthopaedic Research
Licensed content title	Motion-derived coordinate systems reduce inter-subject variability of elbow flexion kinematics
Licensed content author	Louis M. Ferreira,Graham J. W. King,James A. Johnson
Licensed content date	Jan 1, 2010
Start page	n/a
End page	n/a
Type of use	Dissertation/Thesis
Requestor type	Author of this Wiley article
Format	Print and electronic
Portion	Full article
Will you be translating?	No
Order reference number	
Total	0.00 USD

Terms and Conditions

TERMS AND CONDITIONS

This copyrighted material is owned by or exclusively licensed to John Wiley & Sons, Inc. or one if its group companies (each a “Wiley Company”) or a society for whom a Wiley Company has exclusive publishing rights in relation to a particular journal (collectively “WILEY”). By clicking “accept” in connection with completing this licensing transaction, you agree that the following terms and conditions apply to this transaction (along with the billing and payment terms and conditions established by the Copyright Clearance Center Inc., (“CCC’s Billing and Payment terms and conditions”), at the time that you opened your Rightslink account (these are available at any time at http://myaccount.copyright.com).

Terms and Conditions

1. The materials you have requested permission to reproduce (the "Materials") are protected by copyright.

2. You are hereby granted a personal, non-exclusive, non-sublicensable, non-transferable, worldwide, limited license to reproduce the Materials for the purpose specified in the licensing process. This license is for a one-time use only with a maximum distribution equal to the number that you identified in the licensing process. Any form of republication granted by this licence must be completed within two years of the date of the grant of this licence (although copies prepared before may be distributed thereafter). Any electronic posting of the Materials is limited to one year from the date permission is granted and is on the condition that a link is placed to the journal homepage on Wiley's online journals publication platform at www.interscience.wiley.com. The Materials shall not be used in any other manner or for any other purpose. Permission is granted subject to an appropriate acknowledgement given to the author, title of the material/book/journal and the publisher and on the understanding that nowhere in the text is a previously published source acknowledged for all or part of this Material. Any third party material is expressly excluded from this permission.

3. With respect to the Materials, all rights are reserved. No part of the Materials may be copied, modified, adapted, translated, reproduced, transferred or distributed, in any form or by any means, and no derivative works may be made based on the Materials without the prior permission of the respective copyright owner. You may not alter, remove or suppress in any manner any copyright, trademark or other notices displayed by the Materials. You may not license, rent, sell, loan, lease, pledge, offer as security, transfer or assign the Materials, or any of the rights granted to you hereunder to any other person.

4. The Materials and all of the intellectual property rights therein shall at all times remain the exclusive property of John Wiley & Sons Inc or one of its related companies (WILEY) or their respective licensors, and your interest therein is only that of having possession of and the right to reproduce the Materials pursuant to Section 2 herein during the continuance of this Agreement. You agree that you own no right, title or interest in or to the Materials or any of the intellectual property rights therein. You shall have no rights hereunder other than the license as provided for above in Section 2. No right, license or interest to any trademark, trade name, service mark or other branding ("Marks") of WILEY or its licensors is granted hereunder, and you agree that you shall not assert any such right, license or interest with respect thereto.

5. WILEY DOES NOT MAKE ANY WARRANTY OR REPRESENTATION OF ANY KIND TO YOU OR ANY THIRD PARTY, EXPRESS, IMPLIED OR STATUTORY, WITH RESPECT TO THE MATERIALS OR THE ACCURACY OF ANY INFORMATION CONTAINED IN THE MATERIALS, INCLUDING, WITHOUT LIMITATION, ANY IMPLIED WARRANTY OF MERCHANTABILITY, ACCURACY, SATISFACTORY QUALITY, FITNESS FOR A PARTICULAR PURPOSE, USABILITY, INTEGRATION OR NON-INFRINGEMENT AND ALL SUCH WARRANTIES ARE HEREBY EXCLUDED BY WILEY AND WAIVED BY YOU.

6. WILEY shall have the right to terminate this Agreement immediately upon breach of this

Agreement by you.

7. You shall indemnify, defend and hold harmless WILEY, its directors, officers, agents and employees, from and against any actual or threatened claims, demands, causes of action or proceedings arising from any breach of this Agreement by you.

8. IN NO EVENT SHALL WILEY BE LIABLE TO YOU OR ANY OTHER PARTY OR ANY OTHER PERSON OR ENTITY FOR ANY SPECIAL, CONSEQUENTIAL, INCIDENTAL, INDIRECT, EXEMPLARY OR PUNITIVE DAMAGES, HOWEVER CAUSED, ARISING OUT OF OR IN CONNECTION WITH THE DOWNLOADING, PROVISIONING, VIEWING OR USE OF THE MATERIALS REGARDLESS OF THE FORM OF ACTION, WHETHER FOR BREACH OF CONTRACT, BREACH OF WARRANTY, TORT, NEGLIGENCE, INFRINGEMENT OR OTHERWISE (INCLUDING, WITHOUT LIMITATION, DAMAGES BASED ON LOSS OF PROFITS, DATA, FILES, USE, BUSINESS OPPORTUNITY OR CLAIMS OF THIRD PARTIES), AND WHETHER OR NOT THE PARTY HAS BEEN ADVISED OF THE POSSIBILITY OF SUCH DAMAGES. THIS LIMITATION SHALL APPLY NOTWITHSTANDING ANY FAILURE OF ESSENTIAL PURPOSE OF ANY LIMITED REMEDY PROVIDED HEREIN.

9. Should any provision of this Agreement be held by a court of competent jurisdiction to be illegal, invalid, or unenforceable, that provision shall be deemed amended to achieve as nearly as possible the same economic effect as the original provision, and the legality, validity and enforceability of the remaining provisions of this Agreement shall not be affected or impaired thereby.

10. The failure of either party to enforce any term or condition of this Agreement shall not constitute a waiver of either party's right to enforce each and every term and condition of this Agreement. No breach under this agreement shall be deemed waived or excused by either party unless such waiver or consent is in writing signed by the party granting such waiver or consent. The waiver by or consent of a party to a breach of any provision of this Agreement shall not operate or be construed as a waiver of or consent to any other or subsequent breach by such other party.

11. This Agreement may not be assigned (including by operation of law or otherwise) by you without WILEY's prior written consent.

12. These terms and conditions together with CCC’s Billing and Payment terms and conditions (which are incorporated herein) form the entire agreement between you and WILEY concerning this licensing transaction and (in the absence of fraud) supersedes all prior agreements and representations of the parties, oral or written. This Agreement may not be amended except in a writing signed by both parties. This Agreement shall be binding upon and inure to the benefit of the parties' successors, legal representatives, and authorized assigns.

13. In the event of any conflict between your obligations established by these terms and conditions and those established by CCC's Billing and Payment terms and conditions, these terms and conditions shall prevail.

14. WILEY expressly reserves all rights not specifically granted in the combination of (i) the license details provided by you and accepted in the course of this licensing transaction, (ii) these terms and conditions and (iii) CCC's Billing and Payment terms and conditions.

15. This Agreement shall be governed by and construed in accordance with the laws of England and you agree to submit to the exclusive jurisdiction of the English courts.

16. Other Terms and Conditions:

BY CLICKING ON THE "I ACCEPT" BUTTON, YOU ACKNOWLEDGE THAT YOU HAVE READ AND FULLY UNDERSTAND EACH OF THE SECTIONS OF AND PROVISIONS SET FORTH IN THIS AGREEMENT AND THAT YOU ARE IN AGREEMENT WITH AND ARE WILLING TO ACCEPT ALL OF YOUR OBLIGATIONS AS SET FORTH IN THIS AGREEMENT.

V1.2

E.3 CHAPTER 5 COPYRIGHT RELEASE

WOLTERS KLUWER HEALTH LICENSE
TERMS AND CONDITIONS
Nov 18, 2010

This is a License Agreement between Louis M Ferreira ("You") and Wolters Kluwer Health ("Wolters Kluwer Health") provided by Copyright Clearance Center ("CCC"). The license consists of your order details, the terms and conditions provided by Wolters Kluwer Health, and the payment terms and conditions.

All payments must be made in full to CCC. For payment instructions, please see information listed at the bottom of this form.

License Number	2551981044123
License date	Nov 18, 2010

Licensed content publisher	Wolters Kluwer Health
Licensed content publication	Journal of Orthopaedic Trauma
Licensed content title	The Effect of Triceps Repair Technique Following Olecranon Excision on Elbow Stability and Extension Strength: An In Vitro Biomechanical Study.
Licensed content author	Ferreira, Louis; M BSc, BEng; Bell, Timothy; H MD, FRCSC; Johnson, James; King, Graham; J W MD, MSc
Licensed content date	Jan 1, 2010
Volume Number	Publish Ahead of Print
Type of Use	Dissertation/Thesis
Requestor type	Individual
Title of your thesis / dissertation	DEVELOPMENT OF AN ACTIVE ELBOW MOTION SIMULATOR AND COORDINATE SYSTEMS TO EVALUATE KINEMATICS IN MULTIPLE POSITIONS
Expected completion date	Nov 2010
Estimated size(pages)	270
Billing Type	Invoice
Billing Address	268 Grosvenor st. Room B2-226 London, ON N6A 4V2 Canada
Customer reference info	
Total	0.00 USD

Terms and Conditions

Terms and Conditions

1. A credit line will be prominently placed and include: for books - the author(s), title of book, editor, copyright holder, year of publication; For journals - the author(s), title of article, title of journal, volume number, issue number and inclusive pages.
2. The requestor warrants that the material shall not be used in any manner which may be considered derogatory to the title, content, or authors of the material, or to Wolters Kluwer/Lippincott, Williams & Wilkins.
3. Permission is granted for one time use only as specified in your correspondence. Rights herein do not apply to future reproductions, editions, revisions, or other derivative works. Once term has expired, permission to renew must be made in writing.
4. Permission granted is non-exclusive, and is valid throughout the world in the English language and the languages specified in your original request.
5. Wolters Kluwer Health/ Lippincott, Williams & Wilkins, cannot supply the requestor with the original artwork or a "clean copy."
6. The requestor agrees to secure written permission from the author (for book material only).
7. Permission is valid if the borrowed material is original to a LWW imprint (Lippincott-Raven Publishers, Williams & Wilkins, Lea & Febiger, Harwal, Igaku-Shoin, Rapid Science, Little Brown & Company, Harper & Row Medical, American Journal of Nursing Co, and Urban & Schwarzenberg - English Language).
8. If you opt not to use the material requested above, please notify Rightslink within 90 days of the original invoice date.
9. Other Terms and Conditions:

v1.0

CURRICULUM VITAE

Louis Miguel Ferreira

BSc (Comp Sci), BEng (Mech), PEng

Citizenship: Canadian

Date of Birth: April 2, 1974

EDUCATION

1994 – 1998	University of Western Ontario London, Ontario Bachelor of Science – Computer Science, 1998
1994 - 2000	University of Western Ontario London, Ontario Bachelor of Engineering – Mechanical, 2000
2004 - Present	University of Western Ontario London, Ontario PhD in Biomedical Engineering

EMPLOYMENT HISTORY

2000 - Present	**Senior Research Engineer**, Orthopaedic Research Hand and Upper Limb Centre St. Joseph's Health Centre London, Ontario

LICENSES

2008 - Present	Professional Engineer - Ontario License Number: 100079448 Issued under the Professional Engineers Act

PROFESSIONAL MEMBERSHIPS

2008 - Present	Association of Professional Engineers of Ontario
2009 - Present	Professional and Managerial Association of The University of Western Ontario

POST-SECONDARY TEACHING

2010	Spatial math, transformations and kinematic analyses of joints, with special interest in the upper limb. MME 4469 - Biomechanics of the Musculoskeletal System. Guest Lecture delivered to 4th year and masters level engineering students.

STUDENT SUPERVISION

Co-Op & Internship Work Education

Secondary School Co-Op

Utsav Pardasani: Thames Valley District School Board, 2002-2003. S*upervisor*

Luan Pham: Thames Valley District School Board, 2003-2004. S*upervisor*

Andrew Lyons-Uhlenbrauck: Thames Valley District School Board, 2003-2004. S*upervisor*

Ryan Theakston: Thames Valley District School Board, 2004-2005. S*upervisor*

Post-Secondary Internship

Utsav Pardasani: Department of Mechatronics Engineering, University of Waterloo, 2005. *Co-Supervisor*

Utsav Pardasani: Integration of Servo-Motors into an Elbow Joint Testing Apparatus, Department of Mechatronics Engineering, University of Waterloo, 2006. *Co-Supervisor*

Matthew Pan: MotionStation3D Development and Deployment. University of Waterloo, 2008. *Co-Supervisor*

Allan Scholz: Department of Electronic Engineering Technology, Fanshawe College, 2010. *Supervisor*

University Work Study

Nicolas Peleato: 2003. S*upervisor*

Puneet Sayal: University of Western Ontario, 2006-2007. *Co*-S*upervisor*

Truc Tran: University of Western Ontario, 2008-2009. *Co*-S*upervisor*

Jennifer Ng: NSERC Summer Student Scholarship. University of Western Ontario, 2008-2009. *Co*-S*upervisor*

Alison Pellar: NSERC Summer Student Scholarship. University of Western Ontario, 2008-2009. *Co*-S*upervisor*

Hannah Shannon: University of Western Ontario, 2008-2009. *Co*-S*upervisor*

Undergraduate Student Co-Supervision

Engineering

Muna Gharib, Vladimir Pajic, Zahir Aboumourad: Development of a non-contact digitisation probe for computer assisted surgery. Department of Mechanical and Materials Engineering, University of Western Ontario, 2004-2005. *Co*-S*upervisor*

James Ferguson, Nick Oskirko: Design of Computer Assisted Upper Extremity Instrumentation. Department of Mechanical and Materials Engineering, University of Western Ontario, 2005-2006. *Co-Supervisor*

Kristin Whitney: The effect of surface area digitizations on the prediction of spherical anatomical geometries for computer-assisted applications. Department of Mechanical and Materials Engineering, University of Western Ontario, 2005-2006. *Co-Supervisor*

Stefanie Konowalczyk: Student Exchange Program, Aachen University, Germany, 2006-2007. *Co*-S*upervisor*

Katherine Fay: Flexor Tendon Tension Measurements. Department of Mechanical and Materials Engineering MME 401, University of Western Ontario, 2006-2007. *Co-Supervisor*

Josh Giles: Program development and Implant Alignment. Department of Mechanical and Materials Engineering, University of Western Ontario, Summer, 2007. *Co-Supervisor*

Brent Biro, Josh Giles, Simon Deluce: Design and development of a device for resisting motion and static loading of a cadaveric shoulder joint. Department of Mechanical and Materials Engineering, University of Western Ontario, 2008-2009. *Co-Supervisor*

Ryan Herblum, Ryan Katchky, Rachel Oosterhuis, Laura Watts: Ergonomically optimizing the Elbow Testing Apparatus at the Hand and Upper Limb Centre. Department of Mechanical and Materials Engineering, University of Western Ontario, 2008-2009. *Co-Supervisor*

Medicine, Dentistry and Science

Ashley E. Leckie: Reproducibility and repeatability in measuring contact area and stress in the radiocapitellar joint using the Tekscan I-scan sensor system. The Department of Medical Biophysics, University of Western Ontario, 2007-2008. *Co-Supervisor*

Ranita Manocha: Diagnosing the Spinning Error in the Flock of Birds. The Department of Medical Biophysics, University of Western Ontario, 2007-2008. *Co-Supervisor*

Surgical Resident and Fellow Research Co-Supervision

Dr. April Armstrong: Isometry of the medial collateral ligament of the elbow, Division of Orthopaedic Surgery, University of Western Ontario, 2000 *Co-Supervisor*

Dr. Ryan Bicknell: Mechanical testing of rotator cuff repairs. Division of Orthopaedic Surgery, University of Western Ontario, 2002 *Co-Supervisor*

Dr. Ryan Bicknell: Computer-assisted shoulder reconstruction. Division of Orthopaedic Surgery, University of Western Ontario, 2004 *Co-Supervisor*

Dr. G Beadel: Interfragmentary Compression Across a Simulated Scaphoid Fracture – Analysis of Three Screws. Division of Orthopaedic Surgery, University of Western Ontario, 2004 *Co-Supervisor*

Dr. Richard Jenkynson: Talus Fracture Fixation. Division of Orthopaedic Surgery, University of Western Ontario, 2004 *Co-Supervisor*

Dr. Duong Nguyen: Implantation of shoulder prostheses using image-assisted techniques, Division of Orthopaedic Surgery, University of Western Ontario, 2005 *Co-Supervisor*

Dr. J Pollock: Effect of the posterior bundle of the medial collateral ligament on elbow stability. Division of Orthopaedic Surgery, University of Western Ontario, 2007 *Co-Supervisor*

Dr. Marlis Sabo: The Effect of Coronal Shear Fractures of the Distal Humerus on Elbow Kinematics and Stability: An In-Vitro Biomechanical Study. Division of Orthopaedic Surgery, University of Western Ontario, 2008 *Co-Supervisor*

Dr. Tim Bell: The Effect of Triceps Repair Technique Following Olecranon Excision on Elbow Laxity and Extension Strength: An In-Vitro Biomechanical Study. Division of Orthopaedic Surgery, University of Western Ontario, 2009 *Co-Supervisor*

Dr. Sagar Desai: The Effects of Targeted Blocking Screws on the Mechanical Stability of Distal Femur Fractures. Division of Orthopaedic Surgery, University of Western Ontario, 2009 *Co-Supervisor*

Dr. Andrew Glennie: Measuring Tensile and Compressive Forces on Underlying Glenoid Bone in Total Shoulder Arthroplasty. Division of Orthopaedic Surgery, University of Western Ontario, 2009 *Co-Supervisor*

Dr. Brent Lanting: Design, Development and Validation of an In-Vitro Testing System to Permit Controlled Loading and Motion of the Forearm. Division of Orthopaedic Surgery, University of Western Ontario, 2009 *Co-Supervisor*
Dr. Joseph Assini: Interfragmentary Compression of the acute scaphoid fracture: A cadaveric model comparing two screw systems. Division of Orthopaedic Surgery, University of Western Ontario, 2009 *Co-Supervisor*

Dr. Bashar Alolabi: Coronoid Process Replacement: Biomechanical Testing of An Anatomical and Extended Prosthesis. Division of Orthopaedic Surgery, University of Western Ontario, 2010 Co-Supervisor

PUBLICATIONS IN PEER-REVIEWED JOURNALS

1) Liew VS, Cooper IC, Ferreira LM, Johnson JA, King GJW. The Effect of Metallic Radial Head Arthroplasty on Radiocapitellar Joint Contact Area. *Clinical Biomechanics,* 2003 Feb;18(2):115-8.

2) Duck TR, Ferreira LM, King GJW, Johnson JA. Assessment of Screw Displacement Axis (SDA) Accuracy and Repeatability for Joint Kinematic Description. *Journal of Biomechanics,* 2004 Jan;37(1):163-7.

3) Armstrong AD, Ferreira LM, Dunning CE, Johnson JA, King GJW. The Medial Collateral Ligament of the Elbow is Not Isometric. *American Journal of Sports Medicine*, 2004 Jan-Feb;32(1):85-90.

4) Armstrong AD, Dunning CE, Ferreira LM, Faber KJ, Johnson JA, King GJW. A Biomechanical Comparison Of Four Reconstruction Techniques For The Medial Collateral Ligament Deficient Elbow. *J Shoulder Elbow Surg,* 2005 Mar-Apr;14(2):207-15.

5) Beadel GP, Ferreira LM, Johnson JA, King GJW. Interfragmentary Compression Across a Simulated Scaphoid Fracture – Analysis of Three Screws. *Journal of Hand Surgery,* 2004 29A:273-278.

6) Bicknell RT, Harwood C, Ferreira LM, King GJW, Johnson JA, Faber K, Drosdowech D. Cyclic Loading of Rotator Cuff Repairs: An In Vitro Biomechanical Comparison of Bioabsorbable Tacks With Transosseous Sutures. *Arthroscopy: The Journal of Arthroscopic and Related Surgery,* 2005 July.

7) Gordon KD, Kedgley AE, Ferreira LM, King GJW, Johnson JA. Design and Implementation of an Instrumented Ulnar Head Prosthesis to Measure Loads In Vitro. *Journal of Biomechanics*, 2006.

8) Gordon KD, Kedgley AE, Ferreira LM, King GJW, Johnson JA. Effect of Simulated Muscle Activity on Distal Radioulnar Joint Loading In-vitro. *Journal of Orthopaedic Research*, 2006.

9) Pichora JE, Furukawa K, Ferreira LM, Faber KJ, Johnson JA, King GJ. Initial Repair Strengths Of Two Methods For Acute Medial Collateral Ligament Injuries Of The Elbow. *J Orthop Res*, 2007 Feb 8.

10) Attiah M, Sanders DW, Valdivia G, Cooper I, Ferreira LM, MacLeod MD, Johnson JA. Comminuted Talar Neck Fractures: A Mechanical Comparison Of Fixation Techniques. *J Orthop Trauma*. 2007 Jan;21(1):47-51.

11) Nguyen D, Ferreira LM, Brownhill J, Faber K, Johnson J. Design And Development Of Computer Assisted Glenoid Implantation For Shoulder Replacement Surgery. *Computer Aided Surgery*, 2007 May;12(3):152-9.

12) Bicknell RT, Delude JA, Kedgley AE, Ferreira LM, Dunning CE, King GJ, Faber KJ, Johnson JA, Drosdowech DS. Early Experience With Computer-Assisted Shoulder Hemiarthroplasty For Fractures Of The Proximal Humerus: Development Of A Novel Technique And An In Vitro Comparison With Traditional Methods. *J Shoulder Elbow Surg,* 2007 May-Jun;16(3 Suppl):S117-25.

13) JA DeLude, RT Bicknell, GA MacKenzie, LM Ferreira, CE Dunning, GJW King, JA Johnson, DS Drosdowech. An Anthropometric Study of The Bilateral Anatomy Of The Humerus. *Journal of Shoulder and Elbow Surgery*, 2007 Jul-Aug;16(4):477-83.

14) AE Kedgley, GA Mackenzie, LM Ferreira, DS Drosdowech, GJW King, KJ Faber, JA Johnson. The Effect Of Muscle Loading On The Kinematics Of In Vitro Glenohumeral Abduction. *Journal of Biomechanics*, 2007;40(13):2953-60.

15) JE Pichora, GS Fraser, LF Ferreira, JR Brownhill, JA Johnson, GJ King. The Effect of Medial Collateral Ligament Repair Tension on Elbow Joint Kinematics and Stability. *The Journal of Hand Surgery*, 2007 Oct; Vol. 32A No. 8.

16) Kedgley AE, Mackenzie GA, Ferreira LM, Johnson JA, Faber KJ. In Vitro Kinematics Of The Shoulder Following Rotator Cuff Injury. *Clin Biomech (Bristol, Avon)*, 2007 Dec;22(10):1068-73.

17) Kedgley, AE, MacKenzie GA, Ferreira LM, Drosdowech DS, King GJW, Faber KJ, Johnson JA: Humeral Head Translation Decreases with Muscle Loading. *Journal of Shoulder and Elbow Surgery*, 2008 Jan-Feb;17(1):132-8.

18) Fraser GS, Pichora JE, Ferreira LM, Brownhill JR, Johnson JA, King GJ. Lateral Collateral Ligament Repair Restores The Initial Varus Stability Of The Elbow: An In Vitro Biomechanical Study. *J Orthop Trauma*, 2008 Oct;22(9):615-23.

19) Nguyen D, Ferreira LM, Brownhill J, King G, Drosdowech D, Faber K, Johnson J. Improved Accuracy Of Computer Assisted Glenoid Implantation In Total Shoulder Arthroplasty: An In-Vitro Randomized Controlled Trial. *J Shoulder Elbow Surg*. In Press. May 29, 2009.

20) Fraser GS, Ferreira LF, Johnson JA, King GJ. The Effect Of Multiplanar Distal Radius Fractures On Forearm Rotation: In Vitro Biomechanical Study. *J Hand Surg Am*, 2009 May-Jun;34(5):838-48.

21) Pollock JW, Pichora JE, Brownhill JR, Ferreira LF, McDonald CP, Johnson JA, King GJ. The Influence Of Type II Coronoid Fractures, Collateral Ligament Injuries, And Surgical Repair On The Kinematics And Stability Of The Elbow: An In Vitro Biomechanical Study. *J Shoulder Elbow Surg*, 2009 May-Jun;18(3):408-17.

22) Pollock JW, Brownhill JR, Ferreira LF, McDonald CP, Johnson JA, King GJ. The Effect Of Anteromedial Facet Fractures Of The Coronoid And Lateral Collateral Ligament Injury On Elbow Stability And Kinematics. *J Bone Joint Surg Am*, 2009 Jun;91(6):1448-58.

23) Whitney KD, Ferreira LM, King GJ, Johnson JA. The Effect Of Surface Area Digitizations On The Prediction Of Spherical Anatomical Geometries For Computer-Assisted Applications. *J Biomech,* 2009 May 29;42(8):1158-61. Epub 2009 Apr 18.

24) Pollock JW, Brownhill J, Ferreira LM, McDonald CP, Johnson JA, King GJ. Effect Of The Posterior Bundle Of The Medial Collateral Ligament On Elbow Stability. *J Hand Surg Am*, 2009 Jan;34(1):116-23.

25) Brownhill JR, Ferreira LM, Pichora JE, Johnson JA, King GJ. Defining The Flexion-Extension Axis Of The Ulna: Implications For Intra-Operative Elbow Alignment. *J Biomech Eng*, 2009 Feb;131(2):021005.

26) Brownhill JR, Mozzon JB, Ferreira LM, Johnson JA, King GJ. Morphologic Analysis Of The Proximal Ulna With Special Interest In Elbow Implant Sizing And Alignment. *J Shoulder Elbow Surg*, 2009 Jan-Feb;18(1):27-32.

27) Bell TH, Ferreira LM, McDonald CP, Johnson JA, King GJ. Contribution of the Olecranon to Elbow Stability: An In-vitro Biomechanical Study. *J Bone & Joint Surg.* 2010 Apr;92(4):949-57.

28) Ferreira LM, Stacpoole RA, Johnson JA, King GJW. Cementless Fixation Of Radial Head Implants Is Affected By Implant Stem Geometry: An In-Vitro Study. *J Clin Biomech*. 2010 Jun;25(5):422-6.

29) Sabo MT, Fay K, McDonald CP, Ferreira LM, Johnson JA, King GJW. Effect of coronal shear fractures of the distal humerus on elbow kinematics and stability. *J Shoulder and Elbow Surgery*, 2010 Jul;19(5):670-80.

30) Ferreira LM, Johnson JA, King GJW. Development of an Active Elbow Flexion Simulator to Evaluate Joint Kinematics with the Humerus in the Horizontal Position. *Journal of Biomechanics*, 2010 Aug 10;43(11):2114-9.

31) Ferreira LM, King GJW, Johnson JA. Motion-Derived Coordinate Systems Reduce Inter-Subject Variability of Elbow Flexion Kinematics. *Journal of Orthopedic Research*. In Press. 2010.

32) Ferreira LM, Bell TH, Johnson JA, King GJW. The Effect of Triceps Repair Technique Following Olecranon Excision on Elbow Stability and Extension Strength: An In-Vitro Biomechanical Study. *Journal of Orthopaedic Trauma.* In Press. 2010.

SUBMITTED MANUSCRIPTS FOR PUBLICATION UNDER REVIEW

1) Desai S, Sanders D, Ferreira LM, Giles J. Biomechanical Analysis of the Effects of Targeted Blocking Screws in Distal Femur Fractures. *Journal of Orthopaedic Trauma.* In Review 2010.

2) Giles JW, Boons HW, Ferreira LM, Johnson JA, Athwal GS. The Effect of the Conjoined Tendon of the Short Head of the Biceps and Coracobrachialis on Shoulder Stability & Kinematics during In-Vitro Simulation. *Journal of Biomechanics.* In Review 2010.

3) Assini J, Grewal R, Sauder D, Ferreira LM, Johnson JA, Faber KJ. A Comparison of Two Headless Compression Screws for Operative Treatment of Scaphoid Fractures. *Journal of Orthopedic Research.* In Review 2010.

4) Sabo MT, McDonald CP, Ng J, Ferreira LM, Johnson JA, King GJW. A Morphological Analysis of the Humeral Capitellum with an Interest in Prosthesis Design. *Journal of Shoulder and Elbow Surgery*. In Review 2010.

5) Sabo MT, Shannon H, Ng J, Ferreira LM, Johnson JA, King GJW. The Impact of Capitellar Arthroplasty on Elbow Contact Mechanics: Implications for Implant Design. *Journal of Clinical Biomechanics*. In Review 2010.

MANUSCRIPTS IN PREPARATION FOR SUBMISSION

1) Ferreira LM, Fay K, Lalone EA, King GJW, Johnson JA. Development of a Load Sensing Transducer to Quantify Tension in the Medial Collateral Ligament of the Elbow. 2010.

2) Ferreira LM, Fay K, Lalone EA, King GJW, Johnson JA. Effect of Brachioradialis Load on Tension in the Medial Collateral Ligament of the Elbow. 2010.

3) Ferreira LM, Fay K, Lalone EA, Johnson JA, King GJW. Does Radial Head Arthroplasty Affect Medial Collateral Ligament Tension? 2010.

4) Ferreira LM, Johnson JA, King GJW. The Development and Validation of A Novel Controller for Simultaneous Control of Flexion Angle and Muscle Tension for an Elbow Simulator. 2010.

5) Ferreira LM. Development of a Closed-Loop Servo-Actuated Tension Controller. 2010.

ABSTRACTS AND PRESENTATIONS TO PROFESSIONAL MEETINGS

1) Ferreira LM, Pollock JW, King GJW, Johnson JA: Modeling Elbow Flexion in Vitro: Are Active Flexion Simulator Necessary? *Lawson Health Research Institute Research Day,* London, Ontario, 2006. (Poster)

2) Ferreira LM, Pollock JW, King GJW, Johnson JA: Motion-Derived Joint Coordinate Systems Reduce Inter-Subject Variability of Elbow Flexion Kinematics. *55th Annual Meeting of the Orthopaedic Research Society*, Las Vegas, 2009. (Poster)

3) Ferreira LM, Pollock JW, King GJ, Johnson JA: Development of a Novel In-Vitro Simulator For Elbow Motion. *The American Society of Mechanical Engineers – Summer Bioengineering Conference*, Marco Island, Florida, June 2008. (Podium)

4) Ferreira LM, King GJ, Johnson JA: Motion-Derived Joint Coordinate Systems Reduce Inter-Subject Variability of Elbow Flexion Kinematics. *The American Society of Mechanical Engineers – Summer Bioengineering Conference*, Lake Tahoe, California. June 2009. (Podium)

5) Ferreira LM, King GJ, Johnson JA: Motion-Based Joint Coordinate Systems for the Elbow: A New Method for Reducing Variability of Flexion Kinematics. *Canadian Orthopaedic Research Society*. Whistler, British Columbia. July 2009. (Podium)

6) Ferreira LM, Bell TH, Johnson JA, King GJW: Anterior vs Posterior Triceps Repair Following Olecranon Excision: Effects on Stability and Strength on an In-Vitro Model. *44th Canadian Orthopaedic Research Society Annual Meeting*. Edmonton, Alberta. June 17, 2010. (Podium)

7) Manwell S, Ferreira LM, Cooper I, Petrie M, Chess DG, Johnson J: Non-Image Based Hip Implant Tracking. *5th Annual North American Program on Computer-Assisted Orthopaedic Surgery*, Pittsburgh, July 2001.

8) Liew V, Cooper I, Ferreira LM, Johnson JA, King GJW: The Effect of Radial Head Implant Size on Joint Contact Surfaces. *The 56th Annual Meeting of the Canadian Orthopaedic Research Society,* London, June 2001.

9) King GJW, Liew V, Johnson JA, Ferreira LM, Cooper IC: The Effect of Metallic Radial Head Arthroplasty on Radiocapitellar Joint Contact Area. *The 48th Annual Meeting of the Orthopaedic Research Society*, Dallas, February 2002.

10) Campbell LJ, Armstrong AD, Ferreira LM, King GJW, Johnson JA: Optimizing Metacarpal Component Configuration for the Development of a Total Wrist Arthroplasty. *3rd Annual Great Lakes Hand Society Program*, Hamilton, Ontario, May 2002.

11) Stacpoole RA, Johnson JA, Harwood JC, Ferreira LM, King GJW: The Effect of Radial Head Implant Stem Geometry on Initial Implant Micromotion In Vitro. *3rd Annual Great Lakes Hand Society Program*, Hamilton, Ontario, May 2002.

12) Armstrong AD, Ferreira LM, Dunning CE, Johnson JA, King GJW: The Medial Collateral Ligament of the Elbow is not Isometric: an In-Vitro Biomechanical Study. *Combined Annual Meeting of the American Orthopaedic Association and the Canadian Orthopaedic Association*, Victoria, British Columbia, June 2002.

13) Campbell LJ, Ferreira LM, Armstrong A, King GJW, Johnson JA: The Effect of Metacarpal Stem Configuration on Load Transfer to the Long-Finger Metacarpal: an In-vitro Biochemical Study. *Combined Annual Meeting of the American Ortho. Assoc. and the Canadian Ortho. Assoc.*, Victoria, British Columbia, June 2002.

14) Armstrong AD, Dunning CE, Ferreira LM, Faber KJ, Johnson JA, King GJW: A biomechanical Comparison of Four Reconstruction Techniques for the Medial Collateral Ligament Deficient Elbow. *The 49th Annual Meeting of the Orthopaedic Research Society*, New Orleans, 2003.

15) Armstrong AD, Ferreira LM, Dunning CE, Johnson JA, King GJW: The Medial Collateral Ligament of the Elbow Is Not Isometric. *The 49th Annual Meeting of the Orthopaedic Research Society*, New Orleans, 2003.

16) Stacpoole RA, Ferreira LM, Harwood JC, Johnson JA, King GJW: The Effect of Cementless Radial Head Implant Stem Geometry on Initial Implant Micromotion In-Vitro. *The 49th Annual Meeting of the Orthopaedic Research Society*, New Orleans, 2003.

17) Campbell LJ, Armstrong AD, Ferreira LM, King GJW Johnson JA: The Effect of Metacarpal Stem Configuration On Load Transfer To The Long-Finger Metacarpal: An In-Vitro Biomechanical Study. *The 49th Annual Meeting of the Orthopaedic Research Society*, New Orleans, 2003.

18) Duck TR, Ferreira LM, King GJW, Johnson JA: Accuracy of the Screw Displacement Axis Technique for Quantifying Relative Motion across a Joint. *The 49th Annual Meeting of the Orthopaedic Research Society*, New Orleans, 2003.

19) Beadel GP, Ferreira LM, Johnson JA, King GJW: Intrascaphoid Compression Generated by the Acutrak Standard, Acutrak Mini and Bold Screws: An In-Vitro Biomechanical Study. *The 58th Annual Meeting of the Canadian Orthopaedic Research Society,* Winnipeg, 2003.

20) Duck TR, Ferreira LM, King GJW, Johnson JA: Accuracy of the Screw Displacement Axis Technique for Quantifying Relative Motion Across a Joint. *The Canadian Orthopaedic Research Society,* Winnipeg, October 2003.

21) Manwell S, Ferreira LM, Johnson JA, Drosdowech D: Biomechanics of Clavicle Fracture Internal Fixation. *The Canadian Orthopaedic Research Society,* Winnipeg, October 2003.

22) Stacpoole RA, Ferreira LM, Harwood FC, Johnson JA, King GJW: The Effect of Cementless Radial Head Implant Stem Geometry on Initial Implant Micromotion In-Vitro. *The Canadian Orthopaedic Research Society,* Winnipeg, October 2003.

23) Skrinskas TV, Viskontas DG, Ferreira LM, King GJW, Johnson JA, Chess DG: The Effect of Sub-Physiologic Loading on the Medial-Lateral Load Balance Following Knee Arthroplasty: An In-Vitro Model. *Medical Imaging Computing & Computer Assisted Intervention,* Montreal, November 2003.

24) Stacpoole RA, Ferreira LM, King GJW, Johnson JA: Development of Computer Assisted Radial Head Replacement. *Medical Imaging Computing & Computer Assisted Intervention,* Montreal, November 2003.

25) Skrinskas TV, Viskontas DG, Ferreira LM, King GJW, Johnson JA, Chess DG: The Effect of Sub-Physiologic Loading on the Medial-Lateral Load Balance Following Knee Arthroplasty: An In-Vitro Model. *Canadian Arthritis Network, Annual Scientific Conference Program,* Montreal, November 2003.

26) Bicknell RT, DeLude JA, Ferreira LM, Johnson JA, Dunning CE, Drosdowech D, King GJW, Faber KJ: Computer Assisted Shoulder Hemiarthroplasty for Fracture of the Proximal Humerus. *Canadian Arthritis Network, Annual Scientific Conference Program,* Montreal, November 2003.

27) Bicknell RT, Harwood C, Ferreira LM, King GJW, Johnson JA, Faber K, Drosdowech D: Cyclic Loading of Rotator Cuff Repairs: An in vitro Biomechanical Comparison of Bioabsorbable Anchors with Transosseous Sutures. *22nd Annual Meeting Arthroscopy Association of North America,* Phoenix, April 2003.

28) Bicknell RT, Harwood C, Ferreira LM, King GJW, Johnson JA, Faber K, Drosdowech D: Cyclic Loading of Rotator Cuff Repairs: An in vitro Biomechanical Comparison of Bioabsorbable Anchors with Transosseous Sutures. *58th Meeting of The Canadian Orthopaedic Association,* Toronto, May 2003.

29) Armstrong A, Dunning C, Ferreira LM, Faber KJ, Johnson JA, King GJW: A Biomechanical Comparison of Four Reconstruction Techniques for the Medial Collateral Ligament of the Elbow. *58th Meeting of The Canadian Orthopaedic Association,* Toronto, May 2003.

30) Manwell S, Drowdowech DS, Faber KJ, Johnson JA, Ferreira LM: Biomechanics of Clavicle Fracture Internal Fixation. *58th Meeting of The Canadian Orthopaedic Association,* Toronto, May 2003.

31) Stacpoole RA, Harwood C, Ferreira LM, Johnson JA, King GJW: The Effect of Radial Head Implant Stem Geometry on Initial Implant Micromotion In-Vitro. *58th Meeting of The Canadian Orthopaedic Association and 37th Annual Meeting of The Canadian Orthopaedic Research Society,* Toronto, May 2003.

32) Duck TR, Ferreira LM, King GJW, Johnson JA: Assessment of Screw Displacement axis (SDA) Accuracy for Describing Joint Kinematics. *58th Meeting of The Canadian Orthopaedic Association and 37th Annual Meeting of The Canadian Orthopaedic Research Society,* Toronto, May 2003.

33) Beadel GP, Ferreira LM, Johnson JA, King GJW: Intrascaphoid Compression Generated by the Acutrak Standard, Acutrak Mini and Bold Screws – An In-Vitro Biomechanical Study. *58th Meeting of The Canadian Orthopaedic Association and 37th Annual Meeting of The Canadian Orthopaedic Research Society,* Toronto, May 2003.

34) Brownhill JR, Johnson JA, King GJW: Anatomic Axes of the Distal Humerus With Relevance to Elbow Implant Design. *The 50th Annual Meeting of the Orthopaedic Research Society,* San Francisco, February 2004.

35) Bicknell RT, Harwood C, Ferreira LM, King GJW, Johnson JA, Faber K, Drosdowech D: Cyclic Loading of Rotator Cuff Repairs: An in vitro Biomechanical Comparison of Bioabsorbable Anchors with Transosseous Sutures. *50th Annual Meeting of the Orthopaedic Research Society,* San Francisco, February 2004.

36) Skrinskas TV, Viskontas DG, Ferreira LM, King GJ, Johnson, JA, Chess DG: The Effect of Sub-Physiologic Loading On The Medial-Lateral Load Balance Following Knee Arthroplasty: An In-Vitro Model. *50th Annual Meeting of the Orthopaedic Research Society,* San Francisco, February 2004.

37) Bicknell RT, Harwood JC, Ferreira LM, King GJW, Johnson JA, Faber KJ, Drosdowech D: Cyclic Loading of Rotator Cuff Repairs: An In-vitro Biomechanical Comparison of Bioabsorbable Anchors with Transosseous Sutures. *The 9th International Congress on Surgery of the Shoulder,* Washington, May 2004.

38) DeLude JA, Ferreira LM, King GJW, Johnson JA, Faber KJ, Drosdowech D: Computer-assisted Shoulder Hemiarthroplasty for Fractures of the Proximal Humerus. *The 59th Annual Meeting of the Canadian Orthopaedic Society*, Calgary, June 2004.

39) Gordon KD, Kedgley AE, Ferreira LM, King GJW, Johnson JA: Development of an Instrumented Ulnar Head Prothesis to Quantify Load Transfer In Vitro. *The 59th Annual Meeting of the Canadian Orthopaedic Society*, Calgary, June, 2004.

40) Gordon KD, Kedgley AE, Ferreira LM, King GJW, Johnson JA: Development of an Instrumented Ulnar Head Prosthesis to Quantify Load Transfer In-vitro. *The 59th Annual Meeting of the Canadian Orthopaedic Society*, Calgary, June 2004.

41) Bicknell RT, DeLude JA, Ferreira LM, Dunning CE, Johnson JA, King GJW, Faber KJ, Drosdowech DS: Computer-assisted Shoulder Hemiarthroplasty for Fracture of the Proximal Humerus. *The 59th Annual Meeting of the Canadian Orthopaedic Society*, Calgary, June 2004.

42) Bicknell RT, DeLude JA, Ferreira LM, Dunning CE, King GJW, Johnson JA, Faber KJ, Drosdowech D: Computer-assisted Shoulder Hemiarthroplasty for Fractures of the Proximal Humerus*. 4th Annual Conference of the International Society for Computer Assisted Orthopaedic Surgery*, Chicago, June 2004.

43) Bicknell RT, Harwood JC, Ferreira LM, King GJW, Johnson JA, Faber KJ, Drosdowech D: Cyclic Loading of Rotator Cuff Repairs: An In-vitro Biomechanical Comparison of Bioabsorbable Anchors with Transosseous Sutures. *The 11th Meeting of the Combined Orthopaedic Associations*, Sydney, October 2004.

44) Bicknell RT, DeLude JA, Ferreira LM, King GJW, Johnson JA, Faber KJ, Drosdowech D: Computer-assisted Shoulder Hemiarthroplasty for Fractures of the Proximal Humerus. *The 11th Meeting of the Combined Orthopaedic Associations*, Sydney, October 2004.

45) Gordon K, Kedgley A, Ferreira LM, King GJ, Johnson JA: Effect of Simulated Muscle Loads on Distal Radioulnar Joint Reaction Forces In-Vitro. *51st Annual Meeting of the Orthopaedic Research Society,* Washington, DC, February 2005.

46) Gordon K, Kedgley A, Ferreira LM, King GJ, Johnson JA: Design and Implementaiton of An Instrumented Ulnar Head Prosthesis to Measure Loads In-Vitro. *51st Annual Meeting of the Orthopaedic Research Society,* Washington, DC, February 2005.

47) Kedgley AE, Mackenzie GA, Ferreira LM, Drosdowech DS, King GJ, Faber KJ, Johnson JA: The Effect of Variable Muscle Loading Ratios on the Kinematics of Glenohumeral Abduction. *51st Annual Meeting of the Orthopaedic Research Society,* Washington, DC, February 2005.

48) DeLude JA, Bicknell RT, Mackenzie GA, Ferreira LM, Dunning CE, King GJ, Johnson JA, Drosdowech DS: An Anthropometric Study of the Bilateral Anatomy of the Humerus. *51st Annual Meeting of the Orthopaedic Research Society,* Washington, DC, February 2005.

49) Kedgley AE, Mackenzie GA, Ferreira LM, Drosdowech DS, King GJ, Johnson JA: Kinematics of the Shoulder Following Rotator Cuff Injury: An In-Vitro Biomechanical Study. *51st Annual Meeting of the Orthopaedic Research Society,* Washington, DC, February 2005.

50) Guerra SM, Ferreira LM, Pichora JE, King GJ, Johnson JA: Design and Development of A Total Elbow Prosthesis To Quantify Ulnohumeral Load Transfer In-Vitro. *51st Annual Meeting of the Orthopaedic Research Society,* Washington, DC, February 2005.

51) Pichora JE, Furukawa K, Ferreira LM, Faber KJ, Johnson JA: A Biomechanical Evaluation of the Initial Strength of Repair Methods for Acute Medial Collateral Ligament Injuries of the Elbow. *51st Annual Meeting of the Orthopaedic Research Society,* Washington, DC, February 2005.

52) Bicknell RT, DeLude JA, Kedgley AE, Ferreira LM, Dunning CE, King GJW, Johnson JA, Faber KJ, Drosdowech D: Computer Assisted Shoulder Hemiarthroplasty for Fractures of the Proximal Humerus: Development of a Novel Method and an In Vitro Comparison with Traditional Methods. *21st Annual Open Meeting of the American Shoulder and Elbow Surgeons*, Washington, DC, February 2005.

53) Furukawa K, Pichora JE, Ferreira LM, Steinmann SP, Faber KJ, Johnson JA: Efficacy of the Interference Screw and Double Docking Methods Using Palmaris Longus and Graft Jacket for Medial Collateral Elbow Ligament Reconstruction. *51st Annual Meeting of the Orthopaedic Research Society,* Washington, DC, February 2005.

54) Nguyen D, Ferreira LM, Brownhill J, Kedgley A, MacDermid JC, King GJW, Drosdowech D, Johnson JA, Faber KJ: Total Shoulder Arthroplasty: Comparison of Three Methods of Version Measurement. *60th Annual Meeting of The Canadian Orthopaedic Association and 39th Annual Meeting of The Canadian Orthopaedic Research Society,* Montreal, June 2005.

55) Stacpoole RA, Guerra SM, Ferreira LM, Johnson JA, King GJW: The Effect of Radial Head Implant Head Position on Forearm Kinematics In-Vitro. *60th Annual Meeting of The Canadian Orthopaedic Association and 39th Annual Meeting of The Canadian Orthopaedic Research Society,* Montreal, June 2005.

56) Pichora J, Furukawa K, Ferreira LM, Faber KJ, Johnson JA, King GJW: The Initial Strength of Repair Methods for Acute Medial Collateral Ligament Injuries of the Elbow. *60th Annual Meeting of The Canadian Orthopaedic Association and 39th Annual Meeting of The Canadian Orthopaedic Research Society,* Montreal, June 2005.

57) Gordon K, Kedgley AE, Ferreira LM, Johnson JA, King GJW: The Effect of Muscle Loads on Distal Radioulnar Joint Reaction Forces In-Vitro. *The 60th Annual Meeting of the Canadian Orthopaedic Research Society*, Montreal, Quebec, June 2005.

58) Gordon K, Kedgley AE, Ferreira LM, King GJW, Johnson JA: The Joint Reaction Force in the Distal Radioulnar Joint During In-Vitro Forearm Rotation. *The Canadian Society for Surgery of the Hand Annual Scientific Program*, Montreal, Quebec, June 2005.

59) Guerra SM, Ferreira LM, King GJW, Johnson JA: Design and Development of an Adjustable Elbow Prosthesis to Investigate the Effects of Implant Position on Elbow Kinematics. *60th Annual Meeting of The Canadian Orthopaedic Association and 39th Annual Meeting of The Canadian Orthopaedic Research Society,* Montreal, June 2005.

60) Kedgley AE, Mackenzie GA, Ferreira LM, Drosdowech DS, King GJW, Faber KJ, Johnson JA: The Effect of Variable Muscle Loading Ratios on the Kinematics of Glenohumeral Abduction. *60th Annual Meeting of The Canadian Orthopaedic Association and 39th Annual Meeting of The Canadian Orthopaedic Research Society,* Montreal, June 2005.

61) Kedgley AE, Mackenzie GA, Ferreira LM, Drosdowech DS, King GJW, Faber KJ, Johnson JA: Kinematics of the Shoulder Following Rotator Cuff Injury: An In-Vitro Biomechanical Study. *60th Annual Meeting of The Canadian Orthopaedic Association and 39th Annual Meeting of The Canadian Orthopaedic Research Society,* Montreal, June 2005.

62) Pichora JE, Furukawa K, Ferreira LM, Steinmann SP, Faber KJ, Johnson JA, King GJW: Efficacy of the Interference Screw and Double Docking Methods Using Palmaris Longus and Graft Jacket for Medial Collateral Elbow Ligament Reconstruction. *60th Annual Meeting of The Canadian Orthopaedic Association and 39th Annual Meeting of The Canadian Orthopaedic Research Society,* Montreal, June 2005.

63) Guerra SM, Ferreira LM, King GJ, Johnson JA: Effect of Implant Position on Ulnohumeral Load Transfer in Total elbow Arthroplasty. *60th Annual Meeting of The Canadian Orthopaedic Association and 39th Annual Meeting of The Canadian Orthopaedic Research Society,* Montreal, June 2005.

64) Kedgley AE, Gordon K, Ferreira LM, Johnson JA, King GJW: The Effect of Muscle Loads on Dital Radioulnar Joint Reaction Forces In-Vitro. *60th Annual Meeting of The Canadian Orthopaedic Association and 39th Annual Meeting of The Canadian Orthopaedic Research Society,* Montreal, June 2005.

65) Kedgley AE, Mackenzie GA, Ferreira LM, Drosdowech DS, King GJW, Faber KJ, Johnson JA: The Effect of Active Loading on Translation of the Humeral Head During Glenohumeral Abduction. *60th Annual Meeting of The Canadian Orthopaedic Association and 39th Annual Meeting of The Canadian Orthopaedic Research Society,* Montreal, June 2005.

66) Gordon KD, Kedgley A, Ferreira LM, King GJW, Johnson JA: Effect of Simulated Muscle Loads on Distal Radioulnar Joint Reaction Forces In-Vitro. *Joint Annual Meeting of the American Society for Surgery of the Hand and the American Society for Hand Therapists*, San Antonio, Texas, September 2005.

67) Pichora J, Furakawa K, Ferreira LM, Steinmann S, Faber KJ, Johnson JA, King GJW: Efficacy of Interference Screw and Double Docking Methods Using Palmaris Longus and Graft Jacket for Medial Collateral Ligament Reconstruction. *Joint Annual Meeting of the American Society for Surgery of the Hand and the American Society for Hand Therapists*, San Antonio, Texas, September 2005.

68) Pichora J, Ferreira LM, Johnson JA, King GJW: The Initial Strength of Repair Methods for Acute Medial Collateral Ligament Injuries of the Elbow. *Joint Annual Meeting of the American Society for Surgery of the Hand and the American Society for Hand Therapists*, San Antonio, Texas, September 2005.

69) Brownhill JR, Ferreira LM, King GJW, Johnson JA: The Flexion Axis of the ulna: Implications for Intraoperative Alignment. *52nd Annual Meeting of the Orthopaedic Research Society,* Chicago, 2006.

70) Nguyen D, Ferreira LM, Brownhill JR, Kedgley A, Mozzon JB, Garvin G, MacDermid J, King GJW, Johnson JA, Drosdowech D, Faber KJ: Improved Accuracy and Reliability of Computer Assisted Glenoid Implantation: A Randomized Controlled Study. *52nd Annual Meeting of the Orthopaedic Research Society*, Chicago, 2006.

71) Nguyen D, Ferreira LM, Kedgley A, MacDermid JC, King GJW, Drosdowech DS, Johnson JA, Faber KJ: Computer-Assisted Total Shoulder Arthroplasty. *Sister Mary Doyle Research Day, Lawson Research Institute*, London, Ontario, March 2006.

72) Nguyen D, Ferreira LM, Kedgley A, MacDermid JC, King GJW, Drosdowech DS, Johnson JA, Faber KJ: Computer-Assisted Total Shoulder Arthroplasty. *52nd Annual Orthopaedic Research Society*, Chicago, Illinois, March 2006.

73) Nguyen D, Brownhill J, Drosdowech DS, Faber KJ, Ferreira LM, Garvin G, Johnson J, Kedgley A, King G, Macdermid J, Mozzon J: Improved accuracy of computer-assisted glenoid implantation: A randomized controlled trial. *CAOS meeting*, Montreal, Quebec, June 2006.

74) Nguyen D, Ferreira LM, Brownhill J, MacDermid J, King G, Johnson J, Drosdowech DS, Faber K: Computer Assisted total Shoulder Arthroplasty: Design & Validation of an Intraoperative Glenoid Tracking System. Computer Aided Surgery. *SN Residents Research Competition*, Memphis, Tennessee, August 2006.

75) Pichora JE, Fraser GS, Ferreira LM, Brownhill JR, Johnson JA, King GJW: The Effect of MCL Repair Tension on Elbow Joint Stability. *52nd Annual Meeting of the Orthopaedic Research Society,* Chicago, 2006.

76) Mozzon JB, Brownhill JR, Ferreira LM, Johnson JA, King GJW: Morphologic Analysis of the Proximal Ulna With Special Interest in Elbow Implant Sizing and Alignment. *52nd Annual Meeting of the Ortho. Research Society,* Chicago, 2006.

77) Brownhill JR, Ferreira LM, Guerra SM, King GJW, Johnson JA: Computer-Assisted Surgical Alignment for Total Elbow Arthroplasty. *52nd Annual Meeting of the Orthopaedic Research Society,* Chicago, 2006.

78) McDonald CP, Ferreira LM, Brownhill JR, King GJW, Peters TM, Johnson JA: Surface Morphology of the Capitellum: Implications for Computer-Assisted Surgery. *52nd Annual Meeting of the Orthopaedic Research Society,* Chicago, 2006.

79) Whitney KD, Ferreira LM, King GJW, Johnson JA: The Effect of Surface Area Digitizations on The Prediction Of Spherical Anatomical Geometries For Computer Assisted Applications. *52nd Annual Meeting of the Orthopaedic Research Society,* Chicago, 2006.

80) Kedgley AE, Bicknell RT, DeLude JA, Ferreira LM, Dunning CE, King GJW, Faber KJ, Drosdowech DS, Johnson JA: Assessment of Humeral Head Position During Glenohumeral Abduction With Computer-Assisted Shoulder Hemiarthroplasy. *52nd Annual Orthopaedic Research Society*, Chicago, 2006.

81) Brownhill JR, Ferreira LM, Pichora JE, King GJW, Johnson JA: The Flexion Axis of the Ulna: Implications for Intraoperative Alignment. *40th Annual Canadian Orthopaedic Research Society*, Toronto, Ontario, 2006.

82) Whitney KD, Ferreira LM, King GJW, Johnson JA: The Effect of Surface Area Digitizations on the Prediction of Spherical Anatomical Geometries Anatomical Geometries for Computer Assisted Applications. *40th Annual Canadian Orthopaedic Research Society*, Toronto, Ontario, 2006.

83) Kedgley AE, Bicknell RT, DeLude JA, Ferreira LM, Dunning CE, King GJW, Faber KJ, Drosdowech DS, Johnson JA: Computer-Assisted Shoulder Hemiarthroplasty Improves Humeral Head Position. *40th Annual Canadian Orthopaedic Research Society*, Toronto, Ontario, 2006.

84) Nguyen D, Ferreira LM, Brownhill JR, Kedgley A, Mozzon J, Garvin G, MacDermid J, King GJW, Johnson JA, Drosdowech D, Faber KJ: Improved Accuracy and Reliability of Computer Assisted Glenoid Implantation: A Randomized Controlled Study. *61st Annual Canadian Orthopaedic Association*, Toronto, Ontario, 2006.

85) Brownhill JR, Ferreira LM, Pichora JE, King GJW, Johnson JA: The Flexion Axis of the Ulna: Implications for Intraoperative Alignment. *Lawson Health Research Institute Research Day*, London, Ontario, 2006.

86) Fraser GS, Ferreira LM, Pichora JE, Johnson JA, King GJW: Development of a Testing System to Simulate Wrist Fractures in vitro. *Lawson Health Research Institute Research Day*, London, Ontario, 2006.

87) Kedgley AE, Bicknell RT, DeLude JA, Ferreira LM, Dunning CE, King GJW, Faber KJ, Drosdowech DS, Johnson JA: Assessment of Humeral Head Position During Glenohumeral Abduction With Computer-Assisted Shoulder Hemiarthroplasy. *Lawson Health Research Institute Research Day*, London, Ontario, 2006.

88) Nguyen D, Ferreira LM, Brownhill JR, Kedgley A, Mozzon J, Garvin G, MacDermid J, King GJW, Johnson JA, Drosdowech D, Faber KJ: Improved Accuracy and Reliability of Computer Assisted Glenoid Implantation: A Randomized Controlled Study. *Lawson Health Research Institute Research Day,* London, Ontario, 2006.

89) McDonald CP, Ferreira LM, Brownhill JR, King GJW, Peters TM, Johnson JA: Surface Morphology of the Capitellum: Implications for Computer-Assisted Surgery. *40th Annual Meeting of The Canadian Orthopaedic Research Society*, Toronto, June 2006.

90) Whitney KD, Ferreira LM, King GJW, Johnson JA: The Effect of Surface Area Digitizations on the Prediction of Spherical Anatomical Geometries Anatomical Geometries for Computer Assisted Applications. *40th Annual Meeting of The Canadian Orthopaedic Research Society*, Toronto, June 2006.

91) Mozzon JB, Brownhill JR, Ferreira LM, Johnson JA, King GJW: Morphologic Analysis of the Proximal Ulna With Special Interest in Elbow Implant Sizing and Alignment. *40th Annual Meeting of The Canadian Orthopaedic Research Society*, Toronto, June 2006.

92) Brownhill JR, Ferreira LM, Pichora JM, King GJW, Johnson JA: The Flexion Axis of the Ulna: Implications for Intraoperative Alignment. *40th Annual Meeting of The Canadian Orthopaedic Research Society*, Toronto, June 2006.

93) Pichora JE, Fraser GS, Ferreira LM, Brownhill JR, Johnson JA, King GJW: The Effect of MCL Repair Tension on Elbow Joint Stability. *61st Annual Meeting of The Canadian Orthopaedic Association*, Toronto, June 2006.

94) Mozzon JB, Brownhill JR, Ferreira LM, Johnson JA, King GJW: Morphologic Analysis of the Proximal Ulna With Special Interest in Elbow Implant Sizing and Alignment. *61st Annual Meeting of The American Society For Surgery Of The Hand*, Washington, September 2006.

95) Fraser GS, Ferreira LM, Pichora JE, Johnson JA, King GJW: Effect of Distal Radius Fractures On Forearm Rotation. *MANUS Canada Annual Scientific Meeting*, Quebec City, Quebec, June 16, 2006.

96) Yazdani A, Stacpoole R, Ferreira LM, Chinchalkar S, Ross D: A Comparison of Distal Zone II Flexor Tendon Superficialis Repair Techniques. *MANUS Canada Annual Scientific Meeting*, Quebec City, Quebec, June 16, 2006.

97) Brownhill J, Ferreira LM, Pichora J, King G, Johnson J: Defining The Flexion-Extension Axis Of The Ulna: Implications For Computer-Assisted Intraoperative Elbow Alignment. *ASME Summer Bioengineering Conference*, Amelia Island, Florida, June 23, 2006.

98) Nguyen D, Ferreira LM, Brownhill J, MacDermid J, King G, Johnson J, Drosdowech DS, Faber K: Computer Assisted total Shoulder Arthroplasty: Design & Validation of an Intraoperative Glenoid Tracking System for Computer Aided Surgery. *Canadian Orthopaedic Association Annual Meeting*, Toronto, June 2006.

99) Kedgley A, Mackenzie G, Ferreira LM, Drosdowech D, King G, Faber K, Johnson J: Kinematics Of The Shoulder Following Rotator Cuff Injury: An In-Vitro Biomechanical Study. *ASME Summer Bioengineering Conference*, Amelia Island, Florida, June 23, 2006.

100) McDonald C, Ferreira LM, Brownhill J, King G, Peters T, Johnson J: Surface Morphology Of The Capitellum: Implications For Computer-Assisted Surgery. *ASME Summer Bioengineering Conference*, Amelia Island, Florida, June 22, 2006.

101) Fraser G, Pichora J, Ferreira LM, Brownhill J, Johnson J, King G: Lateral Collateral Ligament Repair of the Elbow Using Transosseous Sutures Restores Joint Kinematics and Stability. *Lawson Health Research Institute Research Day,* London, Ontario, 2006.

102) Pichora J, Fraser G, Ferreira LM, Brownhill J, Johnson J, King G: The Effect of MCL Repair Tension On Elbow Joint Stability. *53rd Annual Orthopaedic Research Society*, San Diego, 2007.

103) Nguyen D, Ferreira LM, Brownhill J, Kedgley A, Mozzon J, Gavin G, MacDermid J, King G, Johnson J, Drosdowech D, Faber K: Improved Accuracy of Computer Assisted Glenoid Implantation: A Randomized Controlled Trial. *The American Academy of Orthopaedic Surgeons 2007 Annual Meeting*, San Diego, 2007.

104) Nguyen D, Ferreira LM, Brownhill J, King GJK, Johnson J, Faber K, Drosdowech DS, MacDermid JC: Improved accuracy of computer assisted glenoid implantation: A randomized controlled trial. American *Academy of Orthopaedic Surgery Annual Meeting*, San Diego, February 2007.

105) Fraser G, Ferreira LM, Johnson JA, King GJW: Effect of Distal Radius Fracture Alignment on Forearm Rotation. *The 41st Annual Meeting of the Canadian Orthopaedic Research Society*, Halifax, Nova Scotia, June 2007.

106) Fraser G, Pichora J, Brownhill JR, Ferreira LM, Johnson JA, King GJW: Lateral Collateral Ligament Repair of the Elbow using Transosseous Sutures Restores Joint Kinematics and Stability. *The 41st Annual Meeting of the Canadian Orthopaedic Research Society*, Halifax, Nova Scotia, June 2007.

107) Fraser G, Pichora J, Brownhill JR, Ferreira LM, Johnson JA, King GJW: Lateral Collateral Ligament Repair of the Elbow using Transosseous Sutures Restores Joint Kinematics and Stability. *MANUS* , Halifax, Nova Scotia, June 2007.

108) Brownhill JR, Pollock J, Ferreira LM, Johnson JA, King GJW: Influence of the Radial Head on the Stability and Loading of the Latitude Total Elbow Arthroplasty. *MANUS,* Halifax, Nova Scotia, June 2007.

109) Fraser GS, Pichora JE, Ferreira LM, Brownhill JR, Johnson JA, King GJ: Lateral Collateral Ligament Repair of the Elbow Using Transosseous Sutures Restores Joint Kinematics and Stability. *62nd Annual Meeting of the American Society for Surgery of the Hand*, Seattle, Washington, September 2007.

110) Pollock JW, Pichora JE, Ferreira LM, Brownhill J, Johnson JA, King GJ: Effectiveness of Internal Fixation of Type 2 Coronoid Fractures on Elbow Kinematics and Stability with and without Collateral Ligament Repair. *54th Annual Orthopaedic Research Society*, San Francisco, 2008.

111) Brownhill JR, Pollock JW, Ferreira LM, Johnson JA, King GJ: The Effect of Implant Constraint, Ligament Sectioning and Radial Head Management on Joint Loading in Total Elbow Arthroplasty. *54th Annual Orthopaedic Research Society*, San Francisco, 2008.

112) Brownhill JR, Pollock JW, Ferreira LM, Johnson JA, King GJ: The Effect of Humeral Component Malalignment on the Loading of Total Elbow Arthroplasty: An In-Vitro Study. *54th Annual Orthopaedic Research Society*, San Francisco, 2008.

113) Pollock JW, Ferreira LM, Johnson JA, King GJW, Brownhill JR: The Effect of Humeral Component Malalignment on the Loading of Total Elbow Arthroplasty: An In-Vitro Study. *The American Academy of Orthopaedic Surgeons - 75th Annual Meeting*, San Francisco, 2008.

114) Pollock JW, Ferreira LM, Johnson JA, King GJW, Brownhill JR: The Influence of Type-II Coronoid Fractures, Collateral Ligament injuries and Surgical Repair on the Kinematics and Stability of the Elbow: An In-vitro Biomechanical study. *6th Biennial AAOS/ASES Shoulder and Elbow Meeting*, Orlando, Florida, April 2008.

115) Fraser GS, Pichora JE, Ferreira LM, Brownhill JR, Johnson JA, King GJ: Lateral Collateral Ligament Repair of the Elbow Using Transosseous Sutures Restores Joint Kinematics and Stability. *American Shoulder and Elbow Surgeons - 2008 Open Meeting*, San Francisco, California, March 2008.

116) Pollock JW, Pichora J, Ferreira LM, Brownhill J, Johnson JA, King GJ: Effectiveness of Internal Fixation of Type 2 Coronoid Fractures on Elbow Kinematics and Stability with and without Ligament Repair. *Canadian Orthopaedics Association*, Quebec, June 2008.

117) Pollock JW, Pichora J, Ferreira LM, Brownhill J, Johnson JA, King GJ: Effectiveness of Internal Fixation of Type 2 Coronoid Fractures on Elbow Kinematics and Stability with and without Collateral Ligament Repair. *54th Annual Meeting of the Orthopaedic Research Society*, San Francisco, 2008.

118) Brownhill JR, Pollock JW, Ferreira LM, Johnson JA, King GJW: The Effect of Implant Linkage, Collateral Ligament Sectioning and Radial Head Management on the Kinematics and Loading in Total Elbow Arthroplasty. *Canadian Orthopaedics Association*, Quebec, June 2008.

119) Brownhill JR, Pollock JW, Ferreira LM, Johnson JA, King GJW: The Effect of Humeral Component Alignment on the Loading of Total Elbow Arthroplasty: An In-Vitro Study. *Canadian Orthopaedics Association*, Quebec, June 2008.

120) Brownhill JR, Ferreira LM, McDonald CP, Pollock JW, Johnson JA, King GJW: The Development and Validation of Computer Assisted Total Elbow Arthroplasty. *Canadian Orthopaedics Association*, Quebec, June 2008.

121) Nguyen D, Ferreira LM, Browhnill J, King GJW, Johnson JA, Faber KE, Drosdowech D, MacDermid J: Improved Accuracy and Reliability of Computer Assisted Glenoid Implantation in Total Shoulder Arthroplasty: A Randomized Controlled Trial. *American Shoulder and Elbow Surgeons - 2008 Open Meeting*, San Francisco, March 2008.

122) Fraser, Ferreira, Johnson, King: The Influence of Distal Radius Fracture Alignment on Forearm Rotation. *55th Annual Meeting of the Orthopaedic Research Society*, Las Vegas, 2009.

123) Sabo M, Fay K, Ferreira LM, McDonald CP, Johnson JA, King GJW: Osteochondral Lesions of the Capitellum do not Affect Elbow Kinematics and Stability. *55th Annual Meeting of the Orthopaedic Research Society*, Las Vegas, 2009.

124) Sabo M, Fay K, Ferreira LM, McDonald CP, Johnson JA, King GJW: The Effect of Coronal Shear Fractures of the Distal Humerus on Elbow Kinematics and Stability. *55th Annual Meeting of the Orthopaedic Research Society*, Las Vegas, 2009.

125) Pollock JW, Brownhill JR, Ferreira LM, Johnson JA, King GJW: The Effect of the Posterior Bundle of the Medial Collateral Ligament on Elbow Stability. *55th Annual Meeting of the Orthopaedic Research Society*, Las Vegas, 2009.

126) Bell T, King GJW, Ferreira LM, McDonald CP, Johnson JA: Contribution of the Olecranon to Elbow Stability: An In-Vitro Biomechanical Study. *Annual Meeting of the American Academy of Orthopaedic Surgeons*, Las Vegas, 2009.

127) Sabo M, Fay K, Ferreira LM, McDonald C, Johnson JA, King GJW: Osteochondral Lesions of the Capitellum Do Not Affect Elbow Kinematics and Stability. *Canadian Orthopaedic Research Society*, Whistler, British Columbia, July 2009.

128) Sabo M, Fay K, Ferreira LM, McDonald C, Johnson JA, King GJW: Effect of Coronal Shear Fractures of the Distal Humerus on Elbow Kinematics and Stability. *Canadian Orthopaedic Research Society*, Whistler, British Columbia, July 2009.

129) Whitcomb J, Pollock J, Browhill JR, Ferreira LM, McDonald CP, Johnson JA, King GJW: The Effect of the Posterior Bundle of the Medial Collateral Ligament on Elbow Stability. *Canadian Orthopaedic Research Society*, Whistler, British Columbia, July 2009.

130) Bell TH, King GJW, Johnson JA, Ferreira LM, McDonald CP: Contribution of the Olecranon to Elbow Stability: An In-vitro Biomechanical Study. *Canadian Orthopaedic Research Society*, Whistler, British Columbia, July 2009.

131) Grewal R, Sauder D, Assini J, Ferreira LM, Johnson J, Faber KJ: Interfragmentary Compression of the Acute Scaphoid Fracture: A Cadaveric Model Comparing 2 Screw Systems. *Canadian Orthopaedic Research Society*, Whistler, British Columbia, July 2009.

132) Assini J, Grewal R, Sauder D, Ferreira LM, Johnson JA, Faber KJ: Interfragmentary Compression of the Acute Scaphoid Fracture: A Cadaveric Model Studying Two Screw Systems. *The 37th Annual Orthopaedic Surgery Residents' Research Day*, London, Ontario, October 6, 2009.

133) Bell T, Ferreira LM, Johnson JA, King GJW: The Effect of Triceps Repair Technique Following Olecranon Excision on Elbow Laxity and Extension Strength: An In-Vitro Biomechanical Study. *The 37th Annual Orthopaedic Surgery Residents' Research Day*, London, Ontario, October 6, 2009.

134) Glennie RA, Giles JW, Ferreira LF, Athwal G, Johnson JA, Faber KJ: Measuring Tensile and Compressive Forces on Underlying Glenoid Bone in Total Shoulder Arthroplasty. *The 37th Annual Orthopaedic Surgery Residents' Research Day,* London, Ontario, October 6, 2009.

135) Lanting B, Pellar A, Ferreira LM, Johnson JA, King GWJ: Design, Development and Validation of an In-Vitro Testing System to Permit Controlled Loading and Motion of the Forearm. *The 37th Annual Orthopaedic Surgery Residents' Research Day*, London, Ontario, October 6, 2009.

136) Sabo M, Shannon H, Ng J, Ferreira LM, Johnson JA, King GWJ: Radiocapitellar Contact Mechanics of the Elbow: Implications for Implant Design. *The 37th Annual Orthopaedic Surgery Residents' Research Day*, London, Ontario, October 6, 2009.

137) Desai S, Ferreira LM, Giles J, Johnson JA: The Effects of Targeted Blocking Screws on the Mechanical Stability of Distal Femur Fractures. *The 37th Annual Orthopaedic Surgery Residents' Research Day*, London, Ontario, October 6, 2009.

138) Sabo M, Fay K, Ferreira LM, McDonald CP, Johnson JA, King GJW: Effect of Coronal Shear Fractures of the Distal Humerus on Elbow Kinematics and Stability. *64th Annual Meeting of the American Society for Surgery of the Hand,* San Francisco, 2009.

139) Fay KE, Lalone EA, Ferreira LM, Johnson JA, King GJW: Quantification of Medial Collateral Ligament Tension in the Elbow. 56th Annual Meeting of the Orthopaedic Research Society, New Orleans, March 6, 2010.

140) Ferreira LM, Bell TH, Johnson JA, King GJW: The Effect of Triceps Repair Technique Following Olecranon Excision on Elbow Laxity and Extension Strength: An In-Vitro Biomechanical Study. 56th Annual Meeting of the Orthopaedic Research Society, New Orleans, March 6, 2010.

141) Giles JW, Glennie A, Ferreira LF, Athwal G, Faber KJ, Johnson JA: Mechanisms of Load Transfer between a Polyethylene Glenoid Implant and Bone: Implications for Loosening in Total Shoulder Arthroplasty. 56th Annual Meeting of the Orthopaedic Research Society, New Orleans, March 6, 2010.

142) Lalone EA, McDonald CP, Ferreira LF, King GJ, Johnson JA: Image-Based Proximity Mapping to Determine Joint Surface Interactions at the Elbow. 56th Annual Meeting of the Orthopaedic Research Society, New Orleans, March 6, 2010.

143) Lalone EA, McDonald CP, Ferreira LF, King GJ, Johnson JA: Visualization of 3D Elbow Kinematics Using Reconstructed Surfaces. 56th Annual Meeting of the Orthopaedic Research Society, New Orleans, March 6, 2010.

144) Sabo MT, Fay K, Ferreira LM, McDonald CP, Johnson JA, King GJW: The Trochlea is an Important Stabilizer of Both the Ulnohumeral and Radiocapitellar Joints. American Association of Orthopaedic Surgeons Annual Meeting, New Orleans, March 9 2010.

145) Ferreira LM, Bell TH, Johnson JA, King GJW: The Effect of Triceps Repair Technique Following Olecranon Excision on Elbow Laxity and Extension Strength: An In-Vitro Biomechanical Study. Lawson Health Research Institute Research Day, London ON, 2010.

146) Glennie RA, Giles JW, Ferreira LM, Athway GS, Johnson JA, Faber K: Strain in Glenoid Bone in Total Shoulder Arthroplasty: an *in-vitro* study. 65th Canadian Orthopaedic Association Annual Meeting. Edmonton, June 17, 2010. *(podium)*

147) Fay KE, Lalone EA, Ferreira LM, Johnson JA, King GJW: The Measurement of Tension in the Medial Collateral Ligament of the Elbow. 44th Canadian Orthopaedic Research Society Annual Meeting. Edmonton, June 17, 2010. *(podium)*

148) Giles JW, Glennie A, Ferreira LM, Athwal G, Faber KJ, Johnson JA: Interface Distraction and Loosening of the Polyethylene Glenoid Implant for Various Joint Loading Modalities: Implications for Failure in Total Shoulder Arthroplasty. 44th Canadian Orthopaedic Research Society Annual Meeting. Edmonton, June 17, 2010. *(podium)*

149) King GJW, Greeley GS, Beaton BJ, Ferreira LM, Johnson JA: Distal Ulnar Load With Simulated Colles Fractures. 44th Canadian Orthopaedic Research Society Annual Meeting. Edmonton, June 17, 2010. *(podium)*

150) Ng J, Lalone EA, McDonald CP, Ferreira LM, King GJW, Johnson JA: Determination of the Centre of the Capitellum for Elbow Reconstructive Procedures: The Effect of Digitization Protocols. 44th Canadian Orthopaedic Research Society Annual Meeting. Edmonton, June 17, 2010. *(podium)*

151) Lalone EA, McDonald CP, Ferreira LM, King GJW, Johnson JA: Image-based Proximity Mapping to Determine Joint Surface Interactions at the Elbow. 44th Canadian Orthopaedic Research Society Annual Meeting. Edmonton, June 17, 2010.

152) Lalone EA, McDonald CP, Ferreira LM, King GJW, Johnson JA: Visualization of 3D Elbow Kinematics Using Reconstructed Surfaces. 44th Canadian Orthopaedic Research Society Annual Meeting. Edmonton, June 17, 2010. *(podium)*

153) Sanders DW, Desai S, Ferreira LM, Giles JW, Johnson JA: The Mechanical Effect of Locking and Blocking Screws in Distal Femur Fractures. 65th Canadian Orthopaedic Association Annual Meeting. Edmonton, June 17, 2010. *(podium)*

154) Alolabi B, Gray A, Ferreira LM, Johnson JA, Athwal GS, King GJW: Coronoid Process Replacement: Biomechanical Testing of an Anatomical and Extended Prosthesis. *The 38th Annual Orthopaedic Surgery Residents' Research Day*, London, Ontario, October 13, 2010. *(podium)*

155) Lanting B, Athwal GS, Ferreira LM, Johnson JA, King GJW: The Effect of Radial Head Prosthesis Size on the Mechanics of Forearm Load Transfer. *The 38th Annual Orthopaedic Surgery Residents' Research Day*, London, October 13, 2010. *(podium)*

156) Glennie RA, Giles J, Ferreira LM, Athwal GS, Johnson JA, Faber K: The Effect of Cement Technique on Load Transfer and Fixation of the Glenoid Component in Total Shoulder Arthroplasty. *The 38th Annual Orthopaedic Surgery Residents' Research Day*, London, Ontario, October 13, 2010. *(podium)*

157) Alolabi B, Gray A, Ferreira LM, Johnson JA, Athwal GS, King GJW: Reconstruction Of The Coronoid Using An Anatomic And Augmented Prosthesis: An In-Vitro Biomechanical Study. *Meeting of the American Shoulder and Elbow Surgeons*. San Diego, CA. October 22, 2010.

158) Alolabi B, Gray A, Ferreira LM, Johnson JA, Athwal GS, King GJW: Reconstruction Of The Coronoid Using An Anatomic And Augmented Prosthesis: An In-Vitro Biomechanical Study. *Meeting of the American Shoulder and Elbow Surgeons*. Scottsdale, AZ . February 19, 2011.

INVITED TALKS

1) Computer-Assisted Surgery. The Canadian Medical Hall of Fame / Pfizer Canada Discovery Day in Health Sciences. The University of Western Ontario and Fanshawe College. May 9, 2008. (Demonstration)

2) Computer-Assisted Surgery. The Canadian Medical Hall of Fame / Pfizer Canada Discovery Day in Health Sciences. The University of Western Ontario and Fanshawe College, London, Ontario. December 9, 2009. (Demonstration)

3) St. Joseph's Cornerstone Society Donor Reception. Research presentation to financial donors. St. Joseph's Health Care, London, Ontario. November 4, 2010. (Podium)

PROFESSIONAL MEETINGS ATTENDED

(Since 2001)

1) The 5th Annual North American Program on Computer-Assisted Orthopaedic Surgery, Pittsburgh, July 2001.

2) The 35th Annual Meeting of the Canadian Orthopaedic Research Society, London, Ontario, June 2001.

3) The 48th Annual Meeting of the Orthopaedic Research Society, Dallas, February 2002.

4) The 3rd Annual Great Lakes Hand Society Program, Hamilton, Ontario, May 2002.

5) The 70th Annual Meeting of the American Academy of Orthopaedic Surgeons, New Orleans, February 2003.

6) The 37th Annual Meeting of the Canadian Orthopaedic Research Society, Winnipeg, October 2003.

7) The Annual Scientific Conference of the Canadian Arthritis Network, Montreal, November 2003.

8) The 71st Annual Meeting of the American Academy of Orthopaedic Surgeons, San Francisco, March 2004.

9) The 59th Annual Meeting of the Canadian Orthopaedic Research Society, Calgary, June 2004.

10) American Society for Surgery of the Hand, New York, September 2004.

11) The 51st Annual Meeting of the Orthopaedic Research Society, Washington, DC, February 2005.

12) The 60th Annual Meeting of The Canadian Orthopaedic Association and 39th Annual Meeting of The Canadian Orthopaedic Research Society, Montreal, June 2005.

13) The 52nd Annual Orthopaedic Research Society, Chicago, 2006.

14) The 61st Annual Meeting of The Canadian Orthopaedic Association and 40th Annual Meeting of The Canadian Orthopaedic Research Society, Toronto, June 2006.

15) The American Society of Mechanical Engineers 2006 Summer Bioengineering Conference, Amelia Island, Florida, 2006.

16) The 53rd Annual Orthopaedic Research Society, San Diego, 2007.

17) The 41st Annual Meeting of the Canadian Orthopaedic Research Society, Halifax, Nova Scotia, June 2007.

18) The American Society of Mechanical Engineers – Summer Bioengineering Conference, Marco Island, Florida, June 2008.

19) The 54th Annual Orthopaedic Research Society, San Francisco, 2008.

20) The 55th Annual Orthopaedic Research Society, Las Vegas, 2009.

21) The American Society of Mechanical Engineers – Summer Bioengineering Conference, Lake Tahoe, California, June 2009.

22) 43rd Canadian Orthopaedic Research Society, Whistler, BC, July 2009.

23) 56th Annual Meeting of the Orthopaedic Research Society, New Orleans, March 6, 2010.

24) 44th Canadian Orthopaedic Research Society Annual Meeting. Edmonton, June 17, 2010.

HONOURS AND AWARDS

2000	Dean's Honour List – For achieving an average of 80% or more in the September to April session. Faculty of Engineering Undergraduate Program University of Western Ontario
2000	Certificate of Merit for Fourth Year Thesis Computerized Hip Implant Positioning in the Operating Theatre Faculty of Engineering University of Western Ontario
2009	2nd Place: Solids, Design, and Rehab PhD Competition Podium Division. ASME Bioengineering Conference, 2009.

AWARDS BY CO-AUTHORS

(* indicates chief recipient)

2000 1st Prize, Basic Science Category
Manwell S*, Ferreira LM, Cooper I, King G, Chess D, Johnson J
Computerized Total Hip Arthroplasty
28th Clinical Seminar in Orthopaedic Surgery
University of Western Ontario. *(Co-Author)*

2003 Best Poster – Applied Research
Skrinskas T, DG Viskontas*, Ferreira LM, Chess DG, Johnson JA
Application of an Intra-operative Load Measuring System for Knee Replacement Surgery
Canadian Arthritis Network, Annual Scientific Conference
Montreal, Quebec. *(Co-Author)*

2003 Physician Services Incorporated (PSI) Foundation Resident Research Prize – Ryan Bicknell. *(Co- Supervisor and Co-Author)*

2004 Best Research Poster- Guerra SA*, Ferreira LM, King GJW, Johnson JA. Development of an Adjustable Elbow Implant to Quantify Joint Loading. Margaret Moffat Research Day, Faculty University of Western Ontario, May 2004. *(Co-Author*)

2005 Winner of the W. Harvey Bailey Award for Best Basic Science Presentation.
Nguyen D*, Ferreira LM, Brownhill JR, Kedgley A, Mozzon JB, Garvin G, MacDermid J, King GJW, Johnson JA, Drosdowech D, Faber KJ: Improved Accuracy and Reliability of Computer Assisted Glenoid Implantation: A Randomized Controlled Study.
33rd Clinical Seminar in Orthopaedic Surgery
University of Western Ontario. *(Co- Supervisor and Co-Author)*

2008 Winner of the W. Harvey Bailey Award for Best Basic Science Presentation.
Sabo M*, Shannon H, Ng J, Ferreira LM, Johnson JA, King GWJ: Radiocapitellar Contact Mechanics of the Elbow: Implications for Implant Design. The 37th Annual Orthopaedic Surgery Residents' Research Day, London, Ontario, 2008.
University of Western Ontario. *(Co- Supervisor and Co-Author)*

2008 Nominated for the Charles S. Neer Research Excellence Award by the American Shoulder & Elbow Surgeons society.
Nguyen D*, Ferreira LM, Brownhill JR, King GJW, Johnson JA: Computer Assisted Shoulder Surgery. *(Co- Supervisor and Co-Author)*

2010 Best poster in the Shoulder and Elbow classification at the 2010 AAOS American Association of Orthopaedic Surgeons Annual Meeting.
Sabo MT*, Fay K, Ferreira LM, McDonald CP, Johnson JA, King GJW: The Trochlea is an Important Stabilizer of Both the Ulnohumeral and Radiocapitellar Joints. *(Co- Supervisor and Co-Author)*

2010 1st Prize Podium Sister Mary Doyle Award at the Lawson Research Day
Sabo MT*, Shannon H, Ng J, Ferreira LM, Johnson JA, King GJW: Radiocapitellar Contact Mechanics of the Elbow: Implications for Implant Design. *(Co- Supervisor and Co-Author)*

2010 Runner-up to the Dr. H. Bailey Award at The 38th Annual Orthopaedic Surgery Residents' Research Day.
Alolabi B*, Gray A, Ferreira LM, Johnson JA, Athwal GS, King GJW. Coronoid Process Replacement: Biomechanical Testing of an Anatomical and Extended Prosthesis. *(Co- Supervisor and Co-Author)*